Investigating the role of age-related intestinal barrier dysfunction and microbial translocation in driving immunesenescence

by

Jessica Conway

A thesis submitted to the University of Birmingham for the degree of
DOCTOR OF PHILOSOPHY

Institute of Inflammation and Ageing
College of Medical and Dental Sciences
University of Birmingham
September 2023

Abstract

The human gut is populated by millions of microorganisms and the intestinal epithelium functions as a dynamic barrier against microbes and the environment. The gut microbiota and its metabolites play a vital role in host functional homeostasis, including immune responses. Advancing age is accompanied by alterations in the gut microbiome composition and metabolite profile. Concurrently, ageing is accompanied by remodelling of the immune system, termed immunesenescence, which exerts negative effects on aged host health. However, the precise impact of microbiome changes on immunity are poorly understudied. This thesis aims to improve our understanding of the intricate relationship between the ageing gut microbiome, intestinal barrier dysfunction and immunesenescence.

In this thesis, we identified associations between intestinal barrier dysfunction and features of thymic involution and accelerated T cell ageing in older adults and confirmed a causal relationship between microbial translocation and thymic ageing using an aged germ-free mice model. Next, we linked the age-related loss of core commensals (*Lactobacillus* and *Bifidobacterium*) and reduced bioavailability of immunomodulatory microbial metabolites (short-chain fatty acids and secondary bile acids) with an unhealthy immune system and low influenza vaccine immunogenicity in old age. Lastly, we explored the potential for dietary patterns, such as the Mediterranean diet and multi-vitamin supplementation, as a strategy to promote healthy immune ageing. These novel findings extend our understanding of the consequences of age-related changes in the microbial-immune-metabolic axis and provide evidence for designing future microbiome-targeted interventions that restore immune homeostasis and promote healthy ageing in older adults.

Acknowledgements

First and foremost, I would like to thank my supervisors Dr Niharika Arora Duggal and Professor Claudio Mauro for providing me with the opportunity to do this PhD with them. I would especially like to thank Dr Niharika Arora Duggal for her support, guidance and encouragement throughout the duration of this PhD. I could have not asked for a better supervisor, and I have truly enjoyed working with you. Special thanks must also go to my second supervisor Professor Claudio Mauro for his constant involvement and technical advice. I would also like to express my gratitude to the MRC-Versus Arthritis Centre for Musculoskeletal Ageing Research for funding this PhD and to all the volunteers for taking an interest in my research and making this project possible.

Next, I would to like to thank Professor Dawn ME Bowdish and Erica DeJong for providing me with mouse samples. I must also thank Professor Graham Anderson, Dr Andrea J White and Dr Sonia M Parnell for their thymus expertise. On a similar note, I would like to thank Dr Animesh Acharjee and Dr Archana Sharma-Oates for their bioinformatical support. Additionally, I would like to extend my thanks to members of the Duggal and Mauro groups, especially Nia Rees Paddison, Ben Dugan, Dr Jennifer Niven and Dr Michelangelo Certo for their contribution to this project. A very special thanks must also go to Dr Jon Hazeldine for his constant mentorship and words of wisdom throughout this PhD. Thanks to everyone in Lab 1 for their help and for keeping me sane during long lab days making long lab days more enjoyable. Finally, I would like to thank my parents for their endless love, support and encouragement throughout my many years of education. Mom and dad, I owe all my accomplishments to you.

For Mom and Dad

Table of Contents

List of Figures

Chapter 1: Introduction

Chapter 2: Materials and methods

Chapter 3: Age-related intestinal permeability and microbial translocation play an integral role in thymic involution and T cell ageing

Chapter 4: Links between microbial dysbiosis, immunesenescence and influenza vaccine immunogenicity in older adults

List of Tables

Chapter 2: Materials and methods

Chapter 3: Age-related intestinal permeability and microbial translocation play an integral role in thymic involution and T cell ageing

Abbreviations

Ab	Antibody
ABC	Age-associated B cell
AhR	Aryl-hydrocarbon receptor
AIM2	Absent in melanoma 2
AIRE	Autoimmune regulator
ALCAM	Activated leukocyte cell adhesion molecule
AMICA1	Adhesion molecule interacting with CXADR antigen 1
AMP	Antimicrobial peptide
ANOVA	Analysis of variance
ATG7	Autophagy related 7
ATM	Ataxia telangiectasia mutated
BAX	B cell lymphoma 2 associated X
BCL2	B cell lymphoma 2
BCL6	B cell lymphoma 6
BCR	B cell receptor
BID	BH3 interacting-domain death agonist
BLNK	B cell linker
BMI	Body mass index
Bregs	Regulatory B cell
BSA	Bovine serum albumin
CASP3	Caspase 3
CASP8	Caspase 8
CCL25	Chemokine ligand 25
CCR7	C-C motif chemokine receptor 7
CLEC6A	C-type lectin domain containing 6A

CM	Central memory
CMJ	Corticomedullary junction
CMV	Cytomegalovirus
CR1	Complement C3b/C4b receptor 1
CR2	Complement C3d receptor 2
CRP	C-reactive protein
CSR	Class switch recombination
cTEC	Cortical thymic epithelial cells
CVD	Cardiovascular disease
DAMP	Damage-associated molecular pattern
DC	Dendritic cell
DCA	Deoxycholic acid
ddH_2O	Double-distilled water
DMSO	Dimethyl sulfoxide
DN	Double negative
DNA	Deoxyribonucleic acid
DP	Double positive
DQI	Diet Quality Index
DUSP	Dual specific phosphatase
EC	Epithelial cell
EDTA	Ethylenediaminetetraacetic acid
ELISA	Enzyme-linked immunosorbent assay
ELISpot	Enzyme-linked immunosorbent spot
EM	Effector memory
EMRA	Effector memory re-expressing CD45RA
ERG1	Early growth response 1

ERK	Extracellular signal-regulated kinase
ETP	Early thymocyte progenitor
FCS	Foetal calf serum
FETA	FFQ EPIC Tool for Analysis
FFQ	Food Frequency Questionnaire
FMT	Faecal microbiota transplantation
FOS	Fos proto-oncogene AP-1 transcription factor subunit
FS-A	Forward scatter-area
FSC	Forward scatter
FXR	Farnesoid X receptor
G6PD	Glucose-6-phosphate dehydrogenase
GC	Germinal centre
GDCA	Glycodeoxycholic acid
GM-CSF	Granulocyte macrophage colony-stimulating factor
GPCR	G-protein coupled receptor
H&E	Haematoxylin and eosin
HADS	Hospital Anxiety and Depression Scale
HAI	Haemagglutination inhibition
HAVCR2	Hepatitis A virus cellular receptor 2
HDAC	Histone deacetylase
HDCA	Hyodeoxycholic acid
HiFCS	Heat-inactivated foetal calf serum
HLA-DRB4	Major histocompatibility complex class II DR beta 4
HMGB1	High mobility group box 1 protein
HSC	Haematopoietic stem cell
IBD	Inflammatory bowel disease

ICOS	Inducible T cell costimulatory
IEC	Intestinal epithelial cell
IFN	Interferon
Ig	Immunoglobulin
IL	Interleukin
IL12RB	Interleukin 12 receptor subunit beta
IL18R1	Interleukin 18 receptor 1
IMM-AGE	Immunological age
IRF5	Interferon regulatory factor 5
KLRG1	Killer cell lectin-like receptor G1
LAMP1	Lysosomal associated membrane protein 1
LBP	Lipopolysaccharide binding protein
LC	Liquid chromatography
LC-MS	Liquid chromatography-mass spectrometry
LCA	Lithocholic acid
LILRB2	Leukocyte immunoglobulin like receptor B2
LPS	Lipopolysaccharide
LRRN3	Leucine rich repeat neuronal 3
MAF	Mucosa-associated fungi
MAMP	Microbe-associated molecular pattern
MAPK	Mitogen-activated protein kinase
MDS	Mediterranean diet score
MedDiet	Mediterranean diet
MEFV	Mediterranean fever
MFGE8	Milk fat globule-epidermal growth factor-factor 8
MFI	Mean fluorescence intensity

MHC	Major histocompatibility complex
MIP	Macrophage inflammatory protein
MT	Microbial translocation
mTEC	Medullary thymic epithelial cell
mTOR	Mammalian target of rapamycin
mtROS	Mitochondrial reactive oxygen species
MUFA	Monounsaturated fatty acid
MyD88	Myeloid differentiation primary response 88
NEFL	Neurofilament light polypeptide
NET	Neutrophil extracellular trap
NF-κB	Nuclear factor kappa B
NGS	Normal goat serum
NK	Natural killer
NKCC	Natural killer cell cytotoxicity
NLRP3	NLR family pyrin domain containing 3
NT5E	5’-nucleotidase ecto
OCT	Optimal cutting temperature
OMV	Outer membrane vesicle
OTU	Operational taxonomic unit
PBMC	Peripheral blood mononuclear cell
PBS	Phosphate buffered saline
PBST	Phosphate buffered saline with Tween® 20
PCR	Polymerase chain reaction
PD1	Programmed cell death protein 1
PI3K	Phosphoinositide 3-kinase
PKA	Protein kinase A

PMA	Phorbol 12-myristate 13-acetate
POU2AF1	POU class 2 homeobox associating factor 1
PRR	Pattern recognition receptor
PSQI	Pittsburgh Sleep Quality Index
PTGS2	Prostaglandin-endoperoxide synthase 2
PTK7	Protein tyrosine kinase 7
PUFA	Polyunsaturated fatty acid
PXR	Pregnane X receptor
RA	Rheumatoid arthritis
RBC	Red blood cell
RDE	Receptor-destroying enzyme
RNA	Ribonucleic acid
RORA	RAR related orphan receptor A
RORγ	Retinoic acid-related orphan receptor-gamma
ROS	Reactive oxygen species
rRNA	Ribosomal RNA
RT	Room temperature
RT-qPCR	Real-time quantitative polymerase chain reaction
RTE	Recent thymic emigrant
SAA	Serum amyloid A
SASP	Senescence-associated secretory phenotype
SBA	Secondary bile acid
sCD14	Soluble CD14
sCD25	Soluble CD25
SCFA	Short-chain fatty acid
SF-12	12-item short-form

SFB	Segmented filamentous bacteria
sIgA	Secretory IgA
SP	Single positive
SSC	Side scatter
SSC-A	Side scatter-area
TBE	Tris-borate-ethylenediaminetetraacetic
TBST	Tris-buffered saline with Tween® 20
TCR	T cell receptor
TEC	Thymic epithelial cell
Tfh	T follicular helper
TGFβ	Tumour growth factor beta
TGR5	Transmembrane G-protein coupled receptor 5
Th	T helper
TLR	Toll-like receptor
TMAO	Trimethylamine N-oxide
TMB	3,3’,5,5’-Tetramethylbenzidine
TNFRSF13B	TNF receptor superfamily member 13B
TNFα	Tumour necrosis factor alpha
TRA	Tissue-restricted antigen
TREC	T cell receptor excision circle
Treg	Regulatory T cell
TXNIP	Thioredoxin interacting protein
UDCA	Ursodeoxycholic acid
ZAP70	Zeta chain of T cell receptor-associated protein kinase 70

Chapter 1: Introduction

This chapter contains text written by Jessica Conway and edited by Dr Niharika A Duggal from the following publications.

Conway J, A Duggal N. Ageing of the gut microbiome: Potential influences on immune senescence and inflammageing. *Ageing Res Rev*. 2021; 68:101323.

Conway J, Rees NP, Duggal NA. Ageing of the Gut Microbiome and Its Potential Contribution Towards Immunesenescence and Inflammaging. In: Marotta, F. (eds) Gut Microbiota in Aging and Chronic Diseases. *Healthy Ageing and Longevity*. 2023; p.41-63.

1.1 Population ageing

Human life expectancy has risen drastically over the last 200 years following improvements in public health and standard medical care [1] .This coupled with steady declining early-life mortality rates has led to an increase in the number of older adults in many developed and developing countries. According to the Office for National Statistics, in 2020 people aged 65 and over constituted 19% of the UK's total population [2]. However, with demographic trends likely to persist, it is projected that 25.1% of the UK's population will be aged ≥65, while 5% will be of the 'oldest old' group (≥85 years) [2]. Although increasing longevity is positive news, health span has not kept pace with increases in lifespan. Between the period of 2009-11 and 2018-18, healthy life expectancy decreased by 0.2 years for women and increased by 0.4 years for men, while life expectancy for both sexes rose by 0.6 years and 0.8 years, respectively (Figure 1.1) [3]. Evidently, older adults are spending additional years of life in ill-health and states of dependency.

Advancing age is a complex multifactorial process driven by the accumulation of molecular damage, resulting in an array of physiological, epigenetic, metabolic and immunological alterations that promote functional deterioration across multiple systems, including the gut microbiome and the immune system [4]. Together, these deficits culminate in an increased susceptibility to infection [5] and a greater risk of developing chronic diseases, such as autoimmunity [6], cancer [7], type 2 diabetes [8], cardiovascular disease (CVD) [9], gastrointestinal infections [10] and Alzheimer's disease [11]. Multimorbidity, defined as suffering from two or more diseases simultaneously, also becomes more prevalent with increasing age, affecting more than

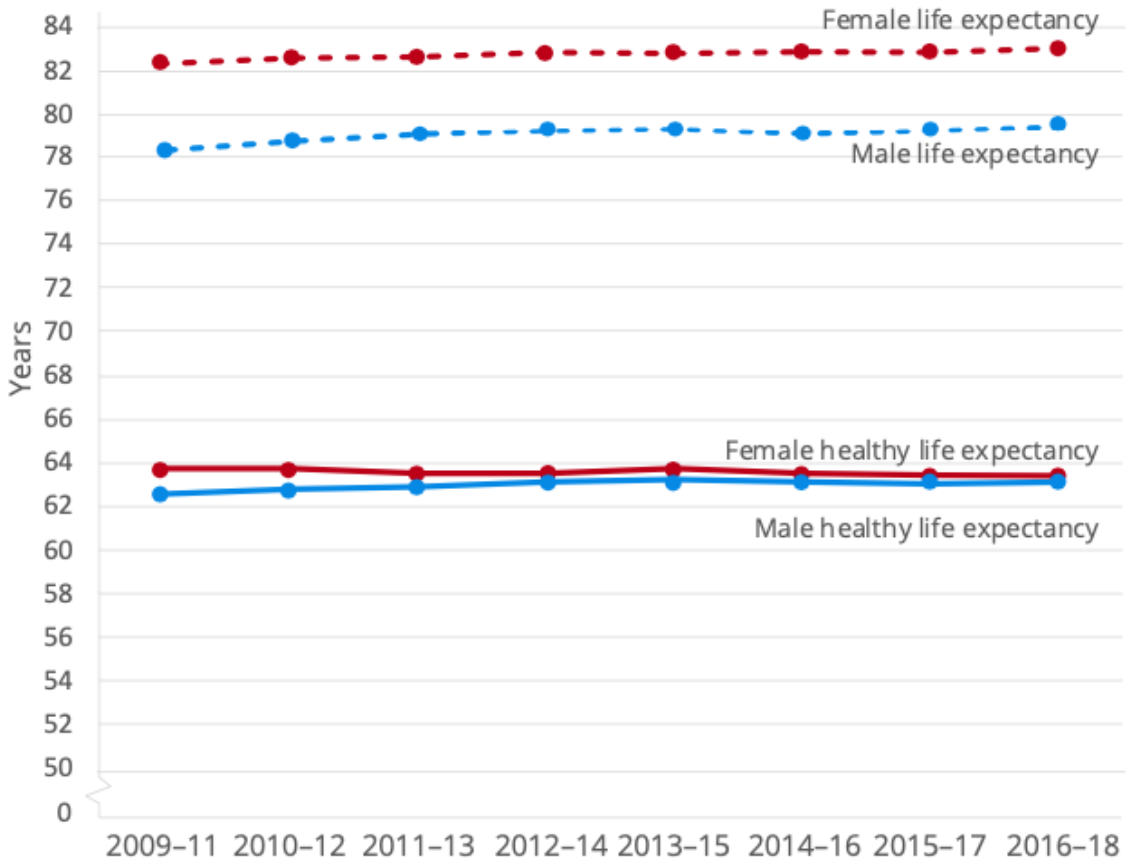

Figure 1.1 Life expectancy and healthy life expectancy gains for men and women in the UK between the period of 2009-11 and 2016-18. Over recent decades, medical and technological advances have led to an increase in human life expectancy in the UK with women typically living longer than men. From the period of 2009-11 to 2016-18, life expectancy at birth rose from 78.5 years to 79.3 years for men and from 82.3 years to 82.9 years for women. A similar trend has been observed for healthy life expectancy for men, though increasing at a much slower rate compared to life expectancy at birth. In contrast, healthy life expectancy for women has declined since the period of 2009-11, which contributed towards the decrease in healthy life expectancy for both sexes combined. Figure taken from [3].

half of the UK's ageing population [12]. Given that the prevalence of multimorbidity is likely to increase in coming decades, population ageing poses a significant global health care challenge. Thus, current ageing research aims to develop strategies that delay age-related dysfunction to extend health span and improve the quality of life of older people.

1.2 Immunesenescence and inflammageing

The immune system is arguably the most important protective system in humans since it is equipped with a multitude of defences for pathogen elimination and the preservation of homeostasis. However, ageing is accompanied by remodelling of the immune system that leads to a state of immune incompetence, termed immunesenescence, impairing the host's ability to mount robust immune responses [13]. Clinically, immunesenescence manifests as an increased vulnerability to bacterial and viral infections [5], autoimmunity [14], malignancies and poor responses to vaccination due to impaired antimicrobial activity [15,16]. Most importantly, recent animal studies have brought to light a causal role of immunesenescence in driving systemic ageing in non-lymphoid organs [17,18].

Haematopoietic stem cells (HSCs) are multipotent, self-renewing precursors found in blood and bone marrow that give rise to immune cells through the myelopoietic or lymphopoietic pathway. Although ageing leads to an increase in the number of HSCs [19], aged HSCs exhibit a reduced regenerative potential, impaired homing capability and myeloid-biased differentiation [19-21]. HSC ageing is driven by a combination of intrinsic and extrinsic factors including the accumulation of DNA damage [22], epigenetic reprogramming [23], reactive oxygen species (ROS) signalling [24],

impaired autophagy/mitophagy [25,26], cellular senescence [27], loss of polarity and microenvironment-derived cytokines and chemokines [28,29]. Together, these age-related changes lead to a decline in lymphopoiesis, thereby contributing towards adaptive immunesenescence in older adults [30].

Another universal feature of ageing is the presence of basal low-grade systemic inflammation, termed inflammageing, that is characterised by high serum levels of pro-inflammatory cytokines (e.g. interleukin (IL) 6, tumour necrosis factor alpha (TNFα) and C reactive protein (CRP)) [31]. Elevated baseline circulating levels of anti-inflammatory cytokines (e.g. IL4, IL10 and tumour growth factor beta (TGFβ)) have also been found in older adults [32], though this has been challenged by a study that reported an age-related decline in IL10 serum levels [33]. Inflammageing promotes cellular senescence and heightens pro-inflammatory innate immune responses, while suppressing adaptive responses [34]. This not only exacerbates inflammation but also accelerates immune ageing, creating a vicious feedback loop in which inflammageing and immunesenescence drive each other [34] (Figure 1.2). Inflammageing, like immunesenescence, increases the risk of mortality in late life by contributing towards increased frailty [35], cognitive defects and the pathogenesis of age-related diseases, such as type 2 diabetes [13,36]. Potential contributing factors towards inflammageing include lifelong antigenic load, increased DNA damage, the accumulation of senescent cells, increased central adiposity, altered endocrine signalling, physical inactivity, immunesenescence and microbial dysbiosis [34,37].

Cytomegalovirus (CMV) is a prevalent β-herpesvirus carried by 60-90% of the world's population that establishes lifelong persistence [38]. Despite being asymptomatic in healthy individuals, CMV infection can perturb immune function and promote morbidity

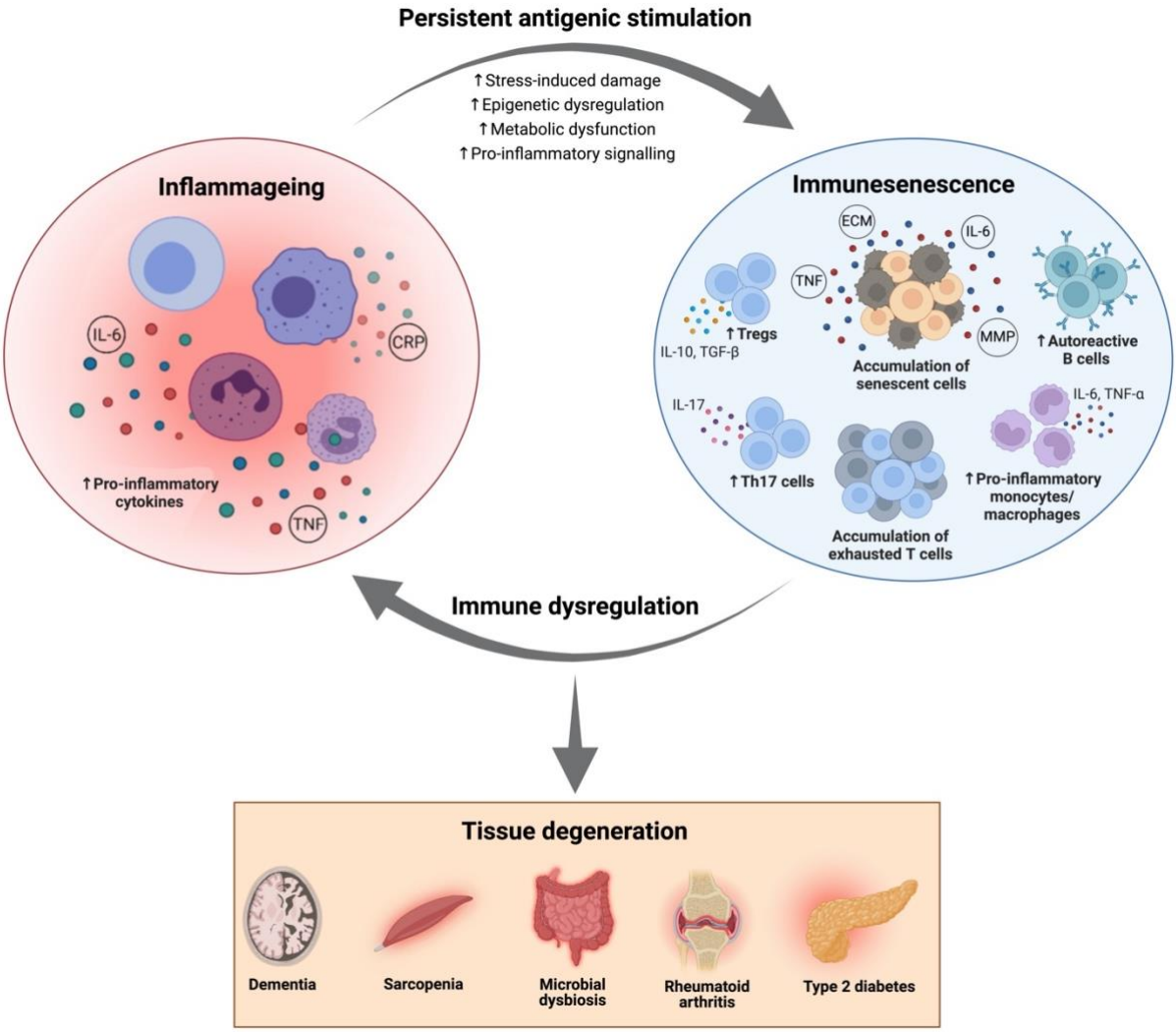

Figure 1.2 The positive feedback circuit between immunesenescence and inflammageing. Lifelong accumulation of molecular and cellular damage causes the gradual decline in immune function, known as immunesenescence. Heightened pro-inflammatory immune responses and the accumulation of senescent cells with a senescence-associated secretory phenotype alongside the lack of anti-inflammatory modulators promote chronic low-grade systemic inflammation, termed inflammageing. Elevated circulating levels of pro-inflammatory cytokines further exacerbate immunesenescence through persistent antigenic stimulation. This gives rise to stress-induced damage and activation of pro-inflammatory signalling pathways, creating a positive feedback loop between immunesenescence and inflammageing that eventually triggers tissue degeneration and increases the risk of age-related diseases. Abbreviations: ECM, extracellular matrix proteins; MMP, matrix metalloproteinases; Th17, T helper cell 17; Treg, regulatory T cell.

in those who are immunocompromised [39,40]. CMV seropositivity prevalence increases with age and was previously thought to be a major driver of immunesenescence and inflammageing due to its association with low vaccine efficacy [41-43]. However, this has recently been contested by studies that have shown no effect of CMV seropositivity on antibody titres following influenza vaccination and T cell responses to viral infection [44,45]. Further, CMV infection did not impact the level of circulating pro- and anti-inflammatory cytokines (IL6, IL10, TNFα and CRP) in a 10-year longitudinal study of older adults [33].

1.3 Age-associated changes in the innate immune system

The innate immune system plays a pivotal role in host protection by providing rapid and robust immune responses against foreign antigens. However, ageing is accompanied by marked phenotypical and functional alterations in monocytes, macrophages, neutrophils, natural killer (NK) cells and dendritic cells (DCs) (Figure 1.3) [46].

1.3.1 Monocytes and macrophages

Monocytes and macrophages play a critical role in early immune responses through the phagocytosis of pathogens and apoptotic cells, antigen-presentation and the secretion of inflammatory mediators. Additionally, monocytes support adaptive immune responses by serving as essential precursors to macrophages and DCs in tissues [47]. Monocytes can be categorised into three functionally distinct subsets on the basis of CD14 and Fc receptor CD16 surface expression: $CD14^{+ve}CD16^{-ve}$ classical monocytes (~90%), $CD14^{+ve}CD16^{+ve}$ intermediate monocytes and $CD14^{+ve}CD16^{++ve}$ non-classical monocytes [48]. Functionally, classical monocytes are highly phagocytic

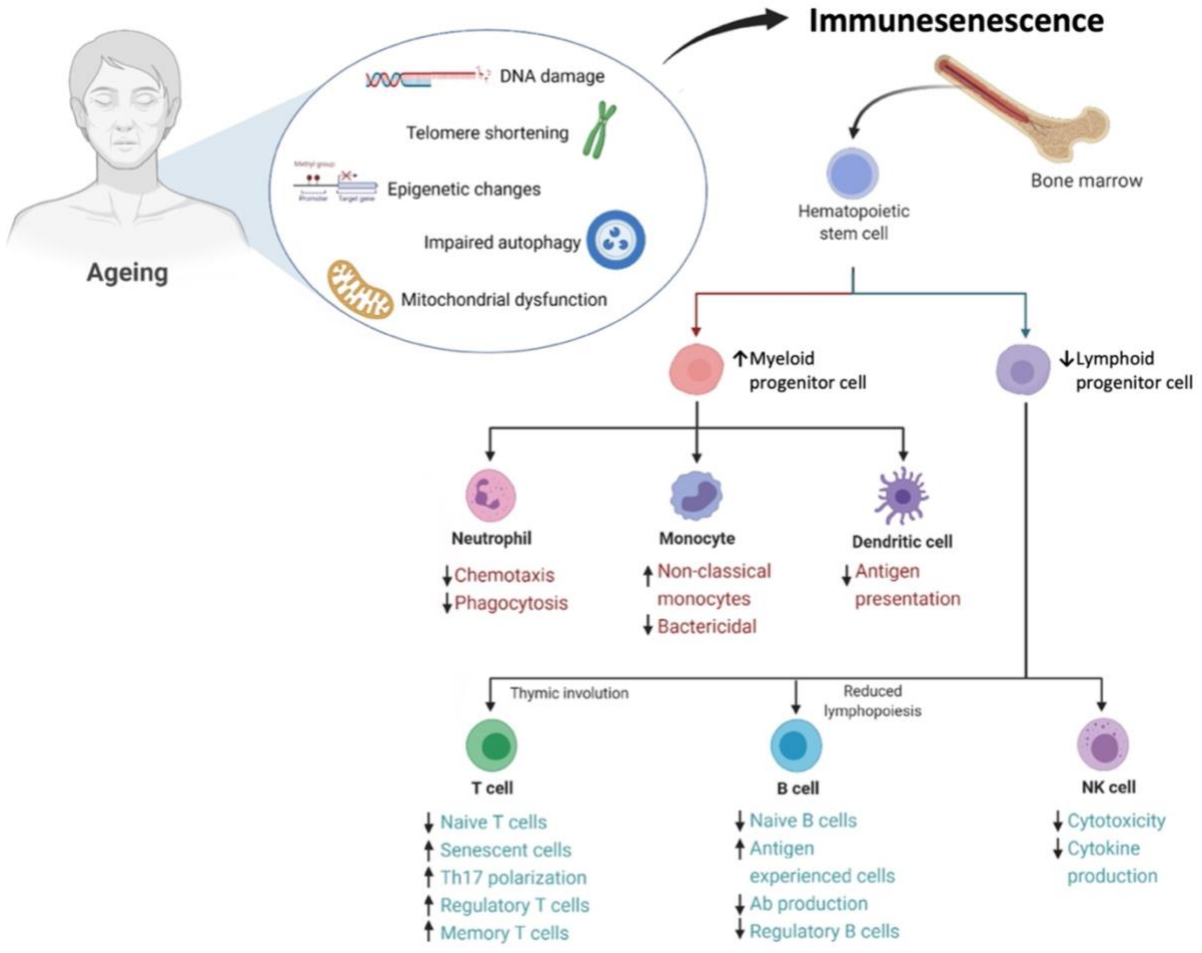

Figure 1.3 Ageing of the innate and adaptive immune systems. Haematopoietic ageing in the bone marrow leads to myeloid-biased differentiation at the expense of lymphocyte specificity and function. Despite an increase in myelopoiesis, ageing results in dysregulated innate immune responses that are characterised by reduced phagocytic activity, impaired antigen presentation and altered neutrophil chemotaxis. On the other hand, age-related changes in the bone marrow and thymic involution lead to a decline in adaptive immunity, which is characterised by decreased NK cell cytotoxicity, a reduced naïve/memory T cell and B cell ratio, the accumulation of senescent T cells, increased regulatory T cells and B cells and reduced antibody production by plasma cells. Abbreviations: Ab, antibody; Th17, T helper 17. Figure adapted from [49].

scavenger cells that produce large amounts of ROS and anti-inflammatory cytokine IL10 in response to toll-like receptor (TLR) stimulation, whereas intermediate and non-classical monocytes produce high levels of pro-inflammatory cytokines (e.g. IL1β, IL6, IL8 and TNFα) following viral challenge [48,50,51].

Advancing age does not affect the percentage and/or absolute number of circulating monocytes [52]. However, there is a significant shift in the distribution of monocyte subsets towards an increased frequency of intermediate and non-classical monocytes in older adults [53-55]. Interestingly, non-classical monocytes from older people exhibit high levels of miR-146α and a senescence-associated secretory phenotype (SASP), which contributes towards inflammageing [56,57]. Increased myelopoiesis with age raises macrophage counts in the spleen and bone marrow of aged mice [58]. Yet, the proportion of $CD68^{+ve}$ myeloid precursors is significantly decreased due to reduced HSC proliferation as a result of replicative senescence [59,60].

Elevated circulating levels of TNFα promote early egression of monocytes from the bone marrow. Consequently, immature monocytes are more readily recruited to sites of inflammation in old age [61]. Monocyte chemotaxis is reduced in older adults and is associated with decreased surface expression of adhesion molecules, such as CD62L and CX3CR1, with age [55,62]. Together, these defects contribute to impaired pathogen clearance in older people.

Monocytes and macrophages from older adults exhibit a decline in pathogen phagocytosis and reduced ROS production, which result in delayed pathogen clearance [55,63,64]. In contrast, studies conducted on rodents have found monocyte and macrophage phagocytosis and ROS production to be increased or unaltered with

age [65-67]. These conflicting findings most likely reflect differences in experimental conditions and stimuli used as well as the tissue microenvironment in which the cells reside. Interestingly, macrophages from aged germ-free mice show improved bactericidal activity against *Streptococcus pneumoniae* compared to those from aged wild-type mice [68]. This suggests that microbial dysbiosis is a key driver of age-related macrophage dysfunction. Aged macrophages are also less efficient at phagocytosing apoptotic cells, contributing to the build-up of apoptotic bodies that may aggravate immunesenescence. This impairment is linked with the age-related decline in the expression of T cell immunoglobulin mucin receptor 4, which is a receptor expressed by macrophages that recognises and binds apoptotic bodies for their removal [69-71].

Monocytes and macrophages also have a reduced potential for antigen presentation with age due to reduced major histocompatibility complex (MHC) II surface expression [72,73]. This is evidenced by the age-associated expansion of $CD14^{+ve}HLA\text{-}DR^{low/neg}$ immunosuppressive monocytes, which have a diminished capacity for antigen presentation as a result [74]. Moreover, ageing is accompanied by reduced expression of costimulatory molecule CD80 but not CD86 [75]. Conversely, another study reported an age-related defect in TLR-mediated upregulation of CD80 and CD86 that was correlated with poor responses to influenza vaccination in older adults [76].

Monocytes regulate effector functions of other immune cells via the secretion of a range of cytokines. Monocytes from older adults exhibit increased secretion of basal cytokines, such as IL1β and IL6 [51,55]. However, an age-related decrease in IL6 and TNFα production following TLR1/2 receptor ligation has also been reported [77,78]. Additionally, macrophages from aged mice and humans have been shown to downregulate IL1β, IL6, IL12, IL23, TNFα and interferon (IFN) production and

upregulate IL8 in response to TLR and absent in melanoma 2 (AIM2) agonists [51,52,78-81]. This contrasts with a recent study that demonstrated that aged peritoneal macrophages secrete higher levels of IL6 and TNFα upon lipopolysaccharide (LPS) and *S. pneumoniae* treatment [68]. Furthermore, ageing leads to an increase the production of immunosuppressive mediators, such as prostaglandin E2, in macrophages due to upregulated expression of cyclooxygenase 2 [82,83].

These defects in cytokine production have been attributed to reduced surface expression and aberrant signalling of TLR1, TLR2 and TLR4 with age [52,53,55,77]. Macrophages from old donors also exhibit reduced expression of the pattern recognition receptor (PRR) AIM2, which recognises cytosolic double-stranded DNA from bacteria and viruses [84,85]. Perturbations in signal transduction pathways downstream of these receptors are known to drive dysregulated cytokine production in aged monocytes and macrophages. These include reduced expression of c-Fos [86], enhanced activation of phosphoinositide 3-kinase (PI3K) and decreased activation of mitogen-activated protein kinases (MAPKs) p38, extracellular signal-regulated kinase (ERK) and c-Jun N-terminal kinase [53,79,87,88].

1.3.2 Neutrophils

Despite being relatively short-lived, neutrophils are the most abundant leukocyte in peripheral blood and the first immune cell to arrive at sites of bacterial and fungal infection [89,90]. Neutrophils are equipped with several defence mechanisms for the elimination of infectious agents, including phagocytosis, ROS generation and neutrophil extracellular trap (NET) formation [91]. Previous studies have reported no effect of ageing on the frequency and/or absolute number of total circulating

neutrophils [54,92]. However, during chronic infection, older adults can mount an increase in neutrophil production (neutrophilia).

Neutrophils can be categorised into three subsets based on differential surface expression of CD16 and CD62L: $CD16^{dim}CD62L^{bright}$ immature, $CD16^{bright}CD62L^{dim}$ immunosuppressive and $CD16^{bright}CD62L^{bright}$ mature neutrophils [93]. An expansion of $CD16^{bright}CD62L^{dim}$ immunosuppressive neutrophils has been reported in older adults [94]. Ageing is accompanied by impaired neutrophil chemotaxis (directional migration) towards chemotactic agents due to constitutive activation of PI3K, while neutrophil chemokinesis (non-directional movement) remains unaltered [95]. Reduced directional accuracy blunts neutrophil trafficking to sites of inflammation, and thus contributes to delayed wound healing [96], excessive neutrophil-mediated inflammation and increased tissue damage in old age [95,97].

Neutrophils from older adults also display reduced phagocytic activity towards complement and immunoglobulin (Ig) G-coated bacteria [92,98,99], but not non-opsonised microbes [100]. This defect has been attributed to loss of Fc receptor CD16 surface expression with age, restricting Fc-mediated phagocytosis [99]. Although aged neutrophils generate higher basal levels of ROS [101,102], ageing leads to a significant decline in ROS production by stimulated neutrophils possibly due to alterations in the lipid membrane composition [92,94,103,104]. NETs are extracellular fibre meshes composed of granule-derived proteins and enzymes bound to a DNA backbone that entrap and neutralise microbes in a process known as NETosis [105,106]. Ageing is accompanied by impaired NET formation, possibly due to a decline in ROS production by primed neutrophils [107,108]. Further, NETs from aged neutrophils show lower

antimicrobial activity due to age-related structural modifications in their DNA threads [109].

Although advancing age does not affect the expression of TLRs on neutrophils, neutrophil ageing is driven by aberrant receptor signalling [104]. In aged neutrophils, the recruitment of receptors (TLR4 and triggering receptor expressed on myeloid cell-1) and downstream signalling proteins (myeloid differentiation primary response 88 (MyD88) and IL1 receptor-associated kinase 1) into lipid rafts is drastically reduced following LPS stimulation, thereby hindering downstream effector functions [104,110,111]. Additionally, age-related changes in neutrophil calcium homeostasis have been shown to negatively impact ROS generation and chemotaxis [92,112].

1.3.3 Natural killer cells

NK cells are cytotoxic innate immune cells that play a crucial role in the early recognition and elimination of virus-infected cells and tumour cells [113]. NK cells can be categorised into two subsets based on CD56 expression: $CD56^{dim}$ cytotoxic NK cells and $CD56^{bright}$ immunomodulatory NK cells [114,115]. Advancing age leads to an increase in the percentage and/or absolute number of total NK cells due to the expansion of $CD56^{dim}$ NK cells [116-118]. This is accompanied by an age-related decrease in the frequency of $CD56^{bright}$ NK cells, which secrete regulatory cytokines and chemokines [116,117,119]. Further, NK cells from older adults, particularly $CD56^{dim}$ NK cells, exhibit increased surface expression of the maturation maker CD57 [117,120], which is associated with cellular senescence in aged T cells [121,122]. Thus, the loss of non-senescent $CD56^{dim}$ NK cells with age perturbs intercellular signalling and leukocyte recruitment [118].

NK cells express an array of activating (e.g. NKp30, NKp44 and NKp46) and inhibitory receptors that tightly regulate their cytotoxic and secretory functions. NK cell activation requires synergistic activation of receptor pairs to overcome inhibitory signals, ensuring restrained natural killer cell cytotoxicity (NKCC) [123,124]. The impact of ageing on the NK cell repertoire is controversial. Whilst some studies have reported an age-related decline in the proportion of NK cells expressing NKp30 and NKp46 [125,126], others have observed no effect for age [119]. Similarly, it is unclear whether inhibitory killer-cell immunoglobulin-like receptor expression levels increase or remain stable with age [125,127]. More consistent findings have been reported for activating receptors NKG2D and CD16, whose expression levels are unaltered by advancing age [119,126]. On the other hand, NK cells from older adults exhibit reduced surface expression of inhibitory receptors KLRG1, NKG2A and CD94 [126-128].

Ageing is accompanied by a decline in NKCC at the single cell level due to reduced perforin secretion and impaired lytic granule polarization towards the immunological synapse that forms at the NK-target cell interface [126]. NK cells play a pivotal role in the removal of senescent cells [129]. Thus, impaired granule exocytosis could drive the accumulation of senescent cells in aged tissues. Low NKCC activity is also associated with high infection rates, an increased risk of infection-related death and low antibody titres post vaccination in the elderly [130,131]. In contrast, antibody-dependent cellular cytotoxicity, which involves the recognition of antibody-coated targets through the Fc receptor CD16, remains unaffected with advancing age [128].

NK cells are immunomodulatory and secrete a wide variety of cytokines and chemokines. However, stimulated NK cells from older adults produce less IL8, IFNγ and macrophage inflammatory protein (MIP)-1α compared to young individuals [132-

134]. This reduction in cytokine production may be due to a decrease in the frequency of $CD56^{bright}$ NK cells with age since they are the main producers of NK cell-derived inflammatory mediators [126]. Whilst the effect of age on NK cell migration in humans is unknown, several studies have reported an age-related decline in the expression of the IL8 chemokine receptor CXCR1 [132].

1.3.4 Dendritic cells (DCs)

DCs are a rare population of antigen presenting cells that compromise less than 1% of circulating leukocytes. DCs can be categorised into two major subsets: $CD11c^{+ve}CD123^{-ve}$ myeloid DCs and $CD11c^{-ve}CD123^{+ve}$ plasmacytoid DCs [135]. Despite having low phagocytic capacity, plasmacytoid DCs produce large amounts of IFN I and III following TLR7 and TLR9 receptor ligation [136,137], and thus are essential for maintaining antiviral immunity. In contrast, myeloid DCs secrete immunomodulatory cytokines and are primarily responsible for initiating adaptive immune responses through naïve T cell priming [138,139].

Ageing is accompanied by a reduction in the frequency and/or absolute number of plasmacytoid DCs [140,141]. In contrast, the proportion and/or frequency of myeloid DCs is unaltered by advancing age [140,142]. Advancing age results in a reduced number of Langerhans cells that have a limited migratory potential when stimulated [143,144]. Since Langerhans cells are specialised DCs present in the skin and mucosa, loss of these cells might contribute to weakened intestinal mucosal immunity and poor wound healing in older people.

Age-associated alterations in DC phenotype include a decline in MHC class II expression and unaltered CD40 and CD80 expression [142,145,146]. The impact of

age on the expression of CD86 remains controversial with some groups suggesting its expression increases with age [142,146], while others report comparable expression levels between young and old adults [145]. Nevertheless, DCs from older adults display a more mature phenotype characterised by increased surface expression of the maturation marker CD83 [145]. Cross-presentation of endocytosed foreign antigens is essential for mounting efficient CD8 T cell responses. However, ageing is accompanied by impaired antigen processing and presentation by DCs, which limits CD4 and CD8 T cell activation [147,148]. Moreover, DCs from older adults exhibit enhanced basal activation and are more reactive to self-antigens released from apoptotic cells [149,150]. This not only leads to the loss of central tolerance but also increases the risk of systemic inflammation and autoimmunity in older adults.

Migration of DCs to lymphoid and secondary lymphoid organs is also reduced in older adults and aged mice in response to chemokines (MIP-3β and stromal cell-derived factor 1) [142,151]. DCs from older adults secrete higher levels of pro-inflammatory cytokines IL6 and TNFα at baseline and in response to TLR4 stimulation [142,149]. However, IL12 production by aged DCs is significantly lower upon TLR engagement [145,152]. In contrast, DCs from young and old adults secrete comparable levels of IL10 following stimulation [145]. Plasmacytoid DCs from older adults also secrete less IFN I and IFN III [52,140,147], which may be due to an age-related decrease in TLR7 and TLR9 expression and impaired phosphorylation of interferon regulatory factor 7 [140,146,147]. Secretion of IFNs by DCs is important for maintaining viral immunity. Thus, an age-related reduction in IFN I and IFN III production is associated with poor vaccination responses and may be a contributing factor towards the increased burden of viral infections in older people [152].

1.4 Age-associated changes in the adaptive immune system

Advanced ageing is accompanied by age-associated remodelling of the adaptive immune system and the key changes are summarised in Figure 1.3.

1.4.1 T cells

T cells express a diverse range of T cell receptors (TCRs) for the recognition of pathogenic and tumour-derived antigens displayed by antigen presenting cells. Following antigen stimulation, naïve T cells differentiate into short-lived effector T cells that secrete immunomodulatory cytokines and cytotoxic molecules and long-lived memory T cells that provide long-lasting immune protection [153]. T cells can be separated into two main lineages: $CD4^{+ve}$ T cells which are predominantly T helper (Th) cells and cytotoxic $CD8^{+ve}$ T cells.

1.4.1.1 Thymic involution

The thymus is a specialised lymphoid organ responsible for the development and maturation of self-tolerant T cells. The thymus is divided into two lobes comprised of an outer cortex and inner medullary regions, which are separated by a network of blood vessels known as the corticomedullary junction (CMJ) [154]. T cell development is mainly driven by thymic epithelial cells (TECs), which consist of $CD205^{+ve}$ cortical TECs (cTECs) and $ERTR5^{+ve}$ medullary TECs (mTECs) [155,156]. cTECs control T cell lineage commitment and positive selection by secreting thymostimulatory cytokines, such as IL7 [157-159], while mTECs facilitate negative selection [160] (Figure 1.4). Autoimmune regulator (AIRE) is a transcription factor expressed by mature mTECs that maintains central immune tolerance through the induction of

tissue-restricted antigens (TRAs) expressed by mTECs, which promote the generation of self-tolerant T cells and the clearance of autoreactive T cells [161,162].

The thymus undergoes progressive shrinkage (involution) with advancing age that begins as early as 1 year of age in humans, deteriorating further after puberty [16]. By age 65, thymic architecture is compromised due to the expansion of perivascular spaces and subsequent contraction of epithelial regions, the loss of a definitive CMJ [163], fibroblast infiltration [164], increased adiposity and the accumulation of senescent cells [165-167] (Figure 1.4). Age-related thymic involution impairs TEC proliferation and reduces mTEC cellularity in mice, promoting the expansion of the cTEC population [168-170]. Furthermore, aged TECs display an inflammageing transcriptome signature [170], have a diminished capacity for antigen presentation and produce less thymopoiesis-stimulating cytokines, like IL7 [169,171]. The thymic frequency of $AIRE^{+ve}$ mTECs and TRA expression levels also decline with age [170,172,173], perturbing negative selection and increasing the incidence of autoimmunity in old age [174]. Aberrations in TEC function promote an altered thymic microenvironment that is characterised by elevated levels of thymopoiesis-suppressing cytokines (IL6 and leukaemia inhibitory factor) and low levels of thymopoieis-stimulating molecules (IL7, ghrelin and keratin growth factor) [163,175,176].

Together, HSC ageing and thymic microenvironment alterations disrupt early thymic progenitor (ETP) differentiation [163,177], resulting in fewer double negative (DN) ($CD4^{-ve}CD8^{-ve}$) and double positive (DP) ($CD4^{+ve}CD8^{+ve}$) thymocytes [171,178]. Thymocyte maturation is also attenuated during ageing as indicated by downregulated CD3 expression on aged DP thymocytes and single positive (SP) ($CD4^{+ve}$ or $CD8^{+ve}$)

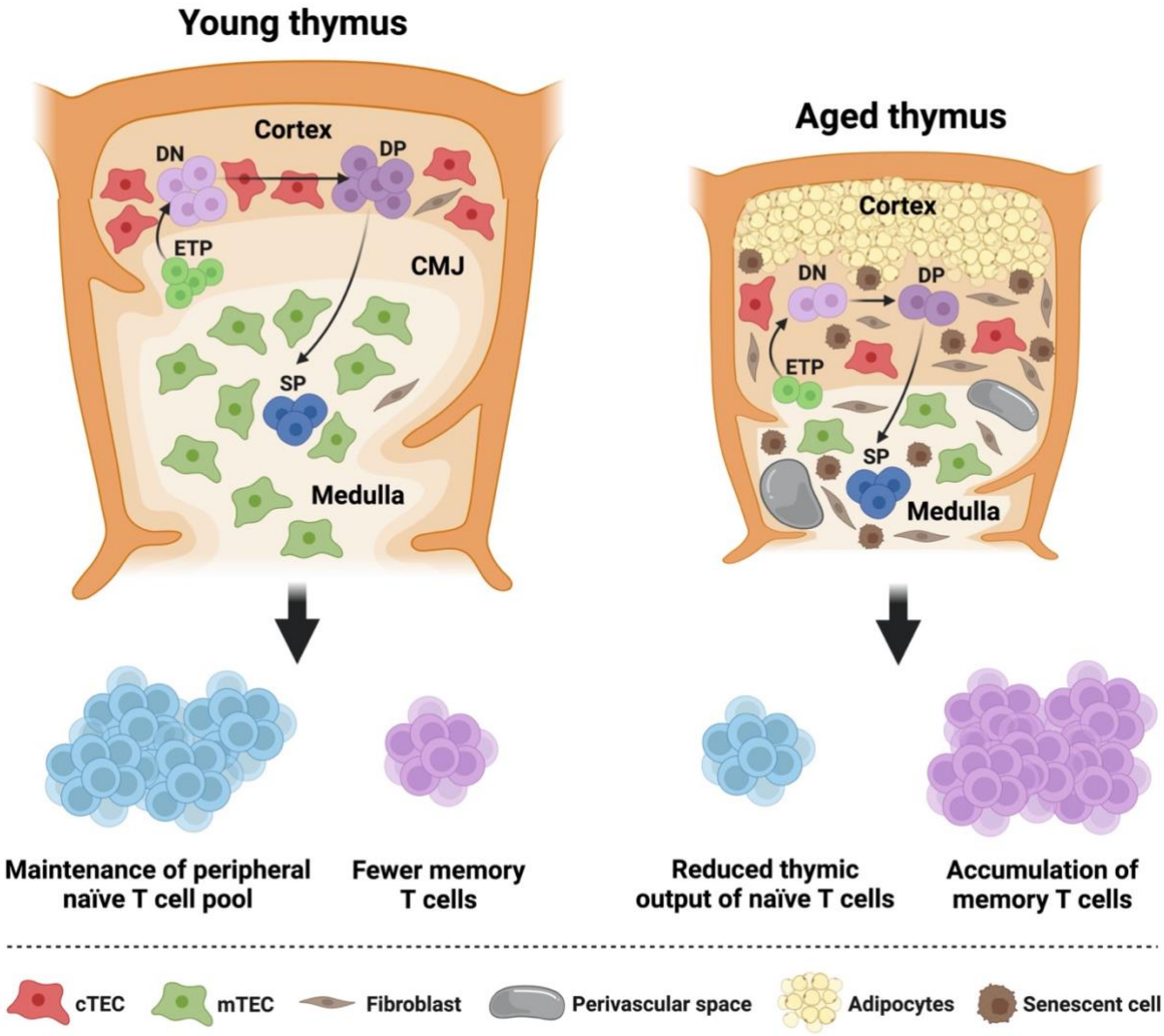

Figure 1.4 Age-related thymic involution. Early thymic progenitors (ETPs) originating from the bone marrow enter the thymus through the CMJ, migrating outwardly towards the cortex in response to chemokines secreted by cTECs. ETPs differentiate into double negative (DN) ($CD4^{-ve}CD8^{-ve}$) thymocytes, which eventually give rise to double positive (DP) ($CD4^{+ve}CD8^{+ve}$) thymocytes. Positively selected DP thymocytes mature into single positive (SP) ($CD4^{+ve}$ or $CD8^{+ve}$) T cells, which undergo negative selection facilitated by mTECs before exiting into the periphery. The thymus shrinks progressively with advancing age, resulting in reduced thymic cellularity and an altered thymic stromal cell microenvironment that is characterised by medullary shrinkage and cortical expansion, CMJ disruption, the emergence of perivascular spaces, fewer cTECs and mTECs, adipocyte and fibroblast infiltration and senescent cell accumulation. These architectural changes ultimately reduce the frequency of ETPs, DN thymocytes and DP thymocytes, thereby compromising thymopoeisis and decreasing thymic output of naïve T cells.

T cells [179,180], which could hamper TCR-dependent stimulation [181]. These changes culminate in a reduced thymic output of naïve T cells in aged mice [182] (Figure 1.4). A similar decline in thymic output has been reported in humans using TCR excision circle (TREC) markers [183]. Moreover, loss of functional recent thymic emigrants (RTEs) is a major contributor to the increased incidence of infections, autoimmunity and cancers in older adults [16,184].

1.4.1.2 T cell subset changes with age

The age-associated decline in naïve T cell production significantly reduces TCR repertoire diversity and is accompanied by the homeostatic expansion and accumulation of memory T cells [185,186]. CD4 and CD8 memory T cells can be categorised into three phenotypically and functionally distinct subsets: ($CD45^{-ve}CCR7^{+ve}$) central memory (CM) T cells, ($CD45^{-ve}CCR7^{-ve}$) effector memory (EM) T cells and ($CD45^{+ve}CCR7^{-ve}$) effector memory re-expressing CD45RA (EMRA) T cells [187,188]. CM T cells play a central role in the immunosurveillance of secondary lymphoid organs [189], while EM T cells traffic through various tissue compartments in the periphery [190]. Advancing age is accompanied by the accumulation of CM and EM cells in the CD4 and CD8 T cell compartments [186,187,191]. Additionally, older adults have a greater proportion of terminally differentiated EMRA T cells compared to young individuals [192]. EMRA T cells exhibit several features of cellular senescence, including increased DNA damage, reduced telomerase activity, mitochondrial dysfunction, low proliferative capacity and a SASP [193,194].

Adaptive immunesenescence is accompanied by the expansion of senescent T cells displaying loss of CD28 and gain of CD57 expression [121]. Costimulatory molecule CD28 is critical for effector T cell activation and reduced expression is associated with

a more restricted TCR repertoire and cellular senescence. The age-related accumulation of senescent $CD28^{-ve}CD57^{+ve}$ T cells is correlated with poor SARS-CoV-2 and influenza vaccination outcomes in aged individuals [195,196]. This is partially due to their limited proliferative potential, which prevents senescent T cells from undergoing clonal expansion in response to novel antigens. Chronic lifelong antigenic stimulation induces cellular senescence in T cells, leading to the progressive loss of T cell effector functions (exhaustion) [197-200].

Exhausted T cells are characterised by high expression levels of inhibitory receptors, such as programmed cell death protein 1 (PD1), lymphocyte-activation gene, cytotoxic T-lymphocyte associated protein 4 and killer-cell lectin-like receptor G1 (KLRG1) [201,202]. Like senescent T cells, exhausted T cells accumulate with age and exhibit several hallmarks of ageing, including DNA damage, mitochondrial dysfunction and telomere attrition [199,200,203,204]. Although exhausted T cells have a reduced capacity to secrete immunomodulatory cytokines, exhausted T cells express high levels of granzyme K following TCR stimulation [205]. This together with the SASP displayed by senescent T cells can exacerbate systemic inflammation in older adults.

1.4.1.3 CD4 T helper cell polarisation and function with age

Upon activation, naïve CD4 T cells differentiate into a variety of functionally distinct T helper cell subsets, including T-bet^{+ve} Th1, $GATA3^{+ve}$ Th2, $ROR\gamma^{+ve}$ Th17 and $Foxp3^{+ve}$ regulatory T cells (Tregs). T helper cells help facilitate adaptive immune responses by secreting immunomodulatory cytokines that can activate cytotoxic T cells, induce B cell maturation, promote B cell antibody production and dampen inflammation. Ageing is accompanied by a decline in T helper cell activity that is attributed to reduced CD40L

expression on aged naïve CD4 T cells [206,207]. This results in impaired antigen-specific B cell responses in older adults [206,207].

The of impact ageing on the prevalence of Th1 and Th2 cells is conflicting. Whilst some studies observed an age-related increase in Th1 and Th2 polarisation [208,209], others reported skewing from Th1 responses (TNFα and IFNγ) towards Th2 cytokine production (IL4 and IL10) in older individuals [210,211]. Moreover, advancing age promotes the expansion of pro-inflammatory Th17 cells and anti-inflammatory Tregs [203,212,213], the latter of which most likely serves as a compensatory mechanism to counterbalance excessive inflammation. However, there is a lack of consensus with regards to whether aged Tregs have an enhanced suppressive capacity or are functionally comparable to those from young individuals [214,215].

There is also an age-related decline in the systemic frequency of ($CXCR5^{+ve}BCL6^{+ve}$) T follicular helper (Tfh) cells [216-219], which are required for germinal centre (GC) formation, affinity maturation and the generation of memory B cells and antibody-producing plasma cells [220]. Aged Tfh cells produce higher levels of IL10 and display defects in antigen-specific B cell stimulation, resulting in poor B cell class switching and reduced antibody production [217,221,222]. Interestingly, defective TCR-induced ERK signalling in aged naïve CD4 T cells triggered by enhanced dual specific phosphatase 6 (DUSP6) activity has been identified as a contributor towards poor vaccine effectiveness in older adults [223].

1.4.2 B cells

B cells are antigen presenting cells that facilitate humoral immune responses through the secretion of high-affinity antibodies, which form the basis of immunological

memory. B cells are generated from HSCs and undergo development in the bone marrow prior to maturation in secondary lymphoid organs. Advancing age is accompanied by a decline in B cell lymphopoiesis due to alterations in the architecture and microenvironment of the bone marrow. These include decreased cellularity [59], increased marrow adiposity [224-226], HSC ageing [227], high levels of pro-inflammatory cytokines (e.g. IL6 and TNF) and low levels of IL7 which promotes B cell development [187,228,229]. Disruption of the bone marrow niche as well as cell-intrinsic defects, such as impaired V(D)J recombination, lead to decreased production of B cell progenitors and myeloid-bias differentiation in older adults [230,231]. Consequently, the number of naïve B cells declines with age, while memory B cells expand in the periphery [232].

Like T cells, ageing reduces the B cell receptor (BCR) repertoire diversity and increases pro-inflammatory cytokine production in resting memory B cells [233,234]. Memory B cells can be divided into three main subpopulations: IgM memory B cells ($IgD^{+ve}CD27^{+ve}$), switched memory B cells ($IgD^{-ve}CD27^{+ve}$) and late/exhausted memory B cells ($IgD^{-ve}CD27^{-ve}$). IgM memory B cells respond rapidly to bacterial polysaccharides, and thus provide robust protection against mucosal infections [235]. Upon antigen recognition, IgM memory B cells undergo class switch recombination (CSR), resulting in a switch from IgM and IgD expression to the expression of IgG, IgE or IgA [236].

Older adults possess significantly fewer IgM memory and switched memory B cells compared to young individuals, rendering them susceptible to bacterial infections [237-239]. Aged memory B cells have a reduced ability to generate Ig due to defective CSR caused by an age-related decline in the expression of activation-induced cytidine

deaminase and E47 [237,238,240]. In contrast, late/exhausted memory B cells, which display a SASP and are refractory to CSR, accumulate with age, and thus are implicated in inflammageing [241]. This is further exacerbated by the age-related decline in the number and suppressive function of regulatory B cells (Bregs) ($CD24^{++ve}CD38^{++ve}$) [242].

An increased proportion of age-associated B cells (ABCs) has also been described in older adults [243,244]. ABCs contribute to autoimmunity in aged individuals by producing high IgG autoantibody titres [244]. Moreover, age-dependent intrinsic defects in B cells and reduced plasma cell differentiation contribute to reduced production of high-affinity antibodies in older adults [245,246].

1.5 The gut microbiome and health

The human gastrointestinal tract is colonised by a diverse microbial community comprised of over 1,000 species of bacteria, viruses, fungi and archaea that are involved in maintaining host health. Many of these microbes are involved in a variety of physiological processes, including the digestion and absorption of nutrients and minerals [247], biosynthesis of vitamins and amino acids [248,249], carbohydrate fermentation [250], development of the central nervous system and induction of host immune responses [251,252]. The composition of the gut microbiota varies substantially between individuals and is influenced by genetics and numerous lifestyle factors, including diet [253], physical activity [254], smoking [255], sleep quality [256], mental health and medication [257,258]. In healthy adults, the gut microbiota is dominated by bacteria, specifically members of the Actinobacteria (*Bifidobacterium*), Bacteroidetes (*Bacteroides* and *Prevotella*), Firmicutes (*Clostridium,*

Faecalibacterium, Lactobacillus and *Ruminococcus*), Proteobacteria (*Escherichia, Helicobacter* and *Shigella*) and Verrucomicrobia (*Akkermansia*) phyla. Bacteroidetes and Firmicutes are the most abundant, representing over 90% of gut microbes [259].

1.5.1 Interactions between gut microbiota and the immune system

In recent years, the gut microbiome has gained considerable recognition for its role in shaping intestinal and systemic immune responses during health (summarised in Figure 1.5). Studies in germ-free and antibiotic-treated animals have provided direct evidence of the importance of the gut microbiota in macrophage and neutrophil microbicidal activities [260,261], the maturation of antigen presenting cells and the development of GCs [262,263]. Most evidence that supports a relationship between the microbiome and immune system in humans comes from dietary probiotic intervention studies that have found that *Lactobacillus* strains, such as *L. reuteri*, exhibit anti-inflammatory properties. *L. reuteri* has been shown to induce distinct cytokine profiles in monocytes and DCs, resulting in the generation of IL10-producing Tregs and Th1 polarisation [264]. Other studies have reported a beneficial effect of *Bifidobacterium lactis* and *Lactobacillus rhamnosus* supplementation on granulocyte phagocytosis and NKCC in older adults [265,266].

Moreover, certain bacterial species exert effects on specific T helper cell subsets; for example, segmented filamentous bacteria (SFB) induce Th17 polarisation in the gut [267]. On the other hand, *Bacteroides fragilis, Bifidobacterium bifidum* and *Bifidobacterium infantis* promote IL10 secretion by colonic CD4 T cells [268], induce the generation of Tregs and enhance Th1 differentiation [269,270]. SFB also promote Peyer's patch GC responses for the generation of secretory IgA (sIgA)-producing plasma cells [271]. sIgA antibodies serve as the first line of defence against

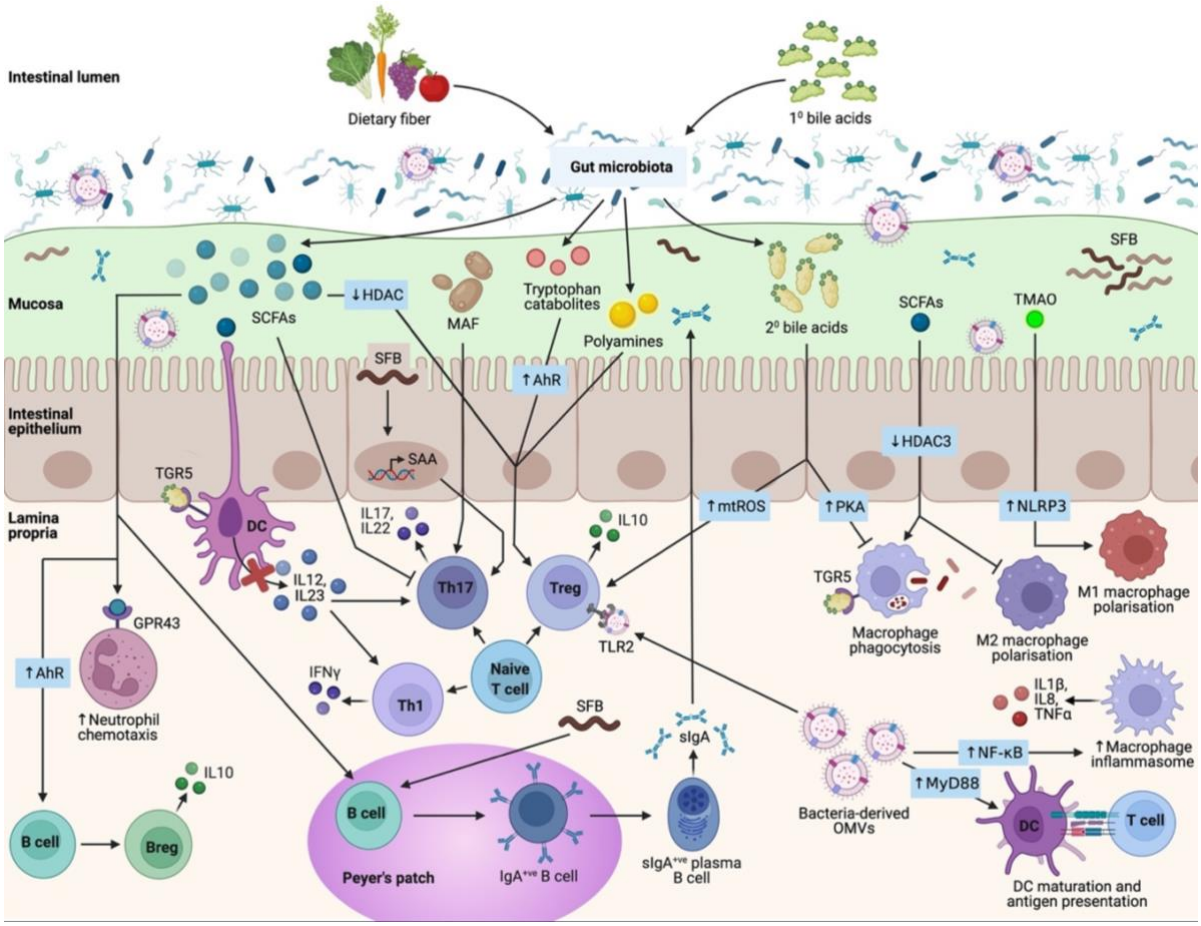

Figure 1.5 Dissecting interactions between gut microbiota and the immune system. Indigestible dietary fibres are fermented by gut microbiota to produce short-chain fatty acids (SCFAs) that possess multiple immunomodulatory properties. Additionally, primary (1^0) bile acids synthesised by the liver are metabolised by microbiota, generating secondary (2^0) bile acids that maintain the Treg/Th17 balance. Other immunoregulatory microbial metabolites include polyamines, tryptophan catabolites and trimethylamine N-oxide (TMAO). Moreover, bacterial-derived outer membrane vesicles (OMVs) have recently been found to exert immunomodulatory effects on macrophages and DCs. Abbreviations: AhR, aryl-hydrocarbon receptor; GPR43, G-protein coupled receptor 43; HDAC, histone deacetylase; MAF, mucosa-associated fungi; mtROS, mitochondrial ROS; NF-κB, nuclear factor kappa B; NLRP3, NLR family pyrin domain containing 3; PKA, protein kinase A; SAA, serum amyloid A; SFB, segmented filamentous bacteria; sIgA, secretory IgA. Figure lifted from [272].

opportunistic bacteria and are therefore essential for maintaining mucosal immunity [273].

1.5.2 Mechanisms driving microbiome-immune system crosstalk

Gut microbiota influence host immune responses through the direct activation of immune cells and the release of metabolites, such as short-chain fatty acids (SCFAs) and secondary bile acids (SBAs) (Figure 1.5). Recognition of microbial molecules, termed microbe-associated molecular patterns (MAMPs), by PRRs expressed on the surface of immune cells is critical for coordinating effective inflammatory responses to infectious agents [274]. PRR signalling induced in response to MAMPs (e.g. bacterial peptidoglycan, flagellin and lipoproteins) leads to the production of antimicrobial peptides (AMPs) and mucin by secretory epithelial cells (ECs) [275,276]. This is especially important for maintaining intestinal homeostasis and regulating microbiota composition.

SCFAs, including acetate, butyrate and propionate, are the end-products of bacterial fermentation of non-digestible dietary fibres and a key source of energy for ECs [277]. SCFAs mediate communication between the host and gut microbiota, and have been shown to exert a variety of effects on different immune cells through the activation of G-protein coupled receptors (GPCRs) (e.g GPR41, GPR43 and GPR109a) and inhibition of histone deacetylases (HDACs) [278]. Butyrate, in particular, enhances macrophage antimicrobial activity and limits M2 macrophage polarisation via HDAC3 inhibition [279,280]. SCFAs also act as chemoattractants for neutrophils and play a critical role in GPR43-mediated neutrophil chemotaxis during intestinal inflammation [281,282]. On the other hand, butyrate and propionate suppress IL12 and IL23 secretion by DCs, thus modulating the polarisation of Th1 and Th17 cells [283,284].

Furthermore, SCFAs, namely butyrate, have been shown to promote the differentiation of naïve T cells into IL10-producing Tregs by HDAC inhibition at the *Foxp3* locus [285], suppress Th17 polarisation and enhance Breg differentiation via aryl-hydrocarbon receptor (Ahr) signalling [284,286,287]. SCFAs also control mucosal and systemic immunity by promoting plasma cell differentiation and IgA and IgG antibody production [288]. In contrast to butyrate and propionate, acetate has been found to have little to no impact on immune cells. Instead, acetate has been implicated in the maintenance of gut epithelial barrier integrity [289], indicating that SCFAs regulate other aspects of host physiology.

Primary bile acids (e.g. cholic acid and chenodeoxycholic acid) are cholesterol-derived molecules synthesised in the liver for the emulsification of dietary lipids, and can be altered by gut microbes to generate SBAs, such as deoxycholic acid (DCA) and lithocholic acid (LCA) [290]. Microbial-derived bile acids regulate intestinal homeostasis by binding bile acid receptors, such as the GPCR transmembrane G-protein coupled receptor 5 (TGR5), and nuclear receptors farnesoid X receptor (FXR), pregnane X receptor (PXR) and vitamin D receptor [291]. Of these four receptors, FXR is the most extensively studied and has been shown to suppress the production of pro-inflammatory cytokines and chemokines by monocytes and macrophages [292,293]. SBAs dampen gut inflammation [294,295], protect against intestinal barrier dysfunction and confer gut mucosal protection through interactions with the immune system [296,297].

In vitro studies have demonstrated that SBAs inhibit pro-inflammatory cytokine production (IL6, IL12 and TNFα) and reduce the basal phagocytic activity of macrophages via induction of TGR5 and protein kinase A (PKA) activation [298].

Conversely, elevated levels of DCA induced by a high-fat diet promote a pro-inflammatory M1 phenotype in murine macrophages [299], suggesting a dual role of SBAs that could be dependent on circulating levels. Moreover, SBA-induced TGR5 signalling suppresses classical DC activation and promotes the differentiation of IL12 hypo-producing DCs through activation of the cyclic adenosine 3',5'-monophosphate-PKA signalling pathway and nuclear factor kappa B (NF-κB) inhibition [300,301]. With regards to the adaptive immune system, LCA derivatives can increase the Treg/Th17 ratio through enhanced mitochondrial ROS (mtROS) production [302]. Furthermore, DCA and LCA have been shown to decrease Th1 development and IFNγ secretion in mice [301].

Other microbial-derived metabolites include polyamines, tryptophan catabolites and trimethylamine N-oxide (TMAO), though their effect on immune cells at the molecular level is less known. Polyamines, such as spermidine, display immunomodulatory properties, governing the ability of CD4 T cells to differentiate into T helper cell subsets while preferentially promoting the generation of Tregs [303]. Spermidine has also been reported to restore B cell function and boost vaccine responses in aged mice [304]. On the other hand, microbial tryptophan catabolites (e.g. indole, indoleacetic acid and indolepropionic acid) regulate immune responses through activation of AhR, which plays a crucial role in Treg gut homing and immunosuppression [305]. TMAO and tryptophan metabolites can also drive M1 macrophage polarisation through activation of the NLR family pyrin domain containing 3 (NLRP3) inflammasome and modulate inflammatory responses in macrophages [306,307].

Gut microbiota also exert effects on systemic immune responses by releasing outer membrane vesicles (OMVs) that carry bioactive cargo (DNA, RNA, proteins and lipids).

These components exhibit potent immunomodulatory properties that can trigger immune cell activation, and thus regulate the inflammatory response (Figure 1.5) [308]. For instance, bacterial-derived OMVs (20-400 nm) induce DC maturation via TLR activation and subsequent MyD88 signalling [309]. OMVs released by *B. fragilis* and *Akkermansia muciniphila* also dampen intestinal inflammation by reducing IL6 cytokine secretion from colonic ECs and promoting the generation of IL10-producing Tregs via the activation of tolerogenic DCs [310,311]. In contrast, pathogenic OMVs can activate inflammasome complexes in monocytes and macrophages, increasing pro-inflammatory cytokine production (IL1β, IL8 and TNFα) which can promote periodontitis [312]. Nevertheless, the potential use of OMVs for vaccine delivery is an area of growing interest, serving as a possible solution to the increased incidence of infectious diseases in the older population [313].

1.6 Age-associated microbial dysbiosis

Despite remaining relatively stable throughout adult life, the gut microbial composition changes drastically with advancing age, termed microbial dysbiosis. This shift is characterised by reduced species richness and loss of bacterial diversity [314]. Further, the abundance of core commensals, such as *Bacteroides*, *Bifidobacterium* and Firmicutes (*Lactobacillus*), is reduced in older adults [315,316]. This is accompanied by the expansion of Proteobacteria (*Escherichia*) and other opportunistic microbes, including *Fusobacterium*, *Parabacteroides* and *Ruminococcaceae*, which are present at low abundance in healthy young individuals (Figure 1.6) [317,318].

Accompanying microbial composition changes is a shift in the metabolic profile of the microbiota, affecting the bioavailability of metabolites, such as SCFAs and SBAs [319].

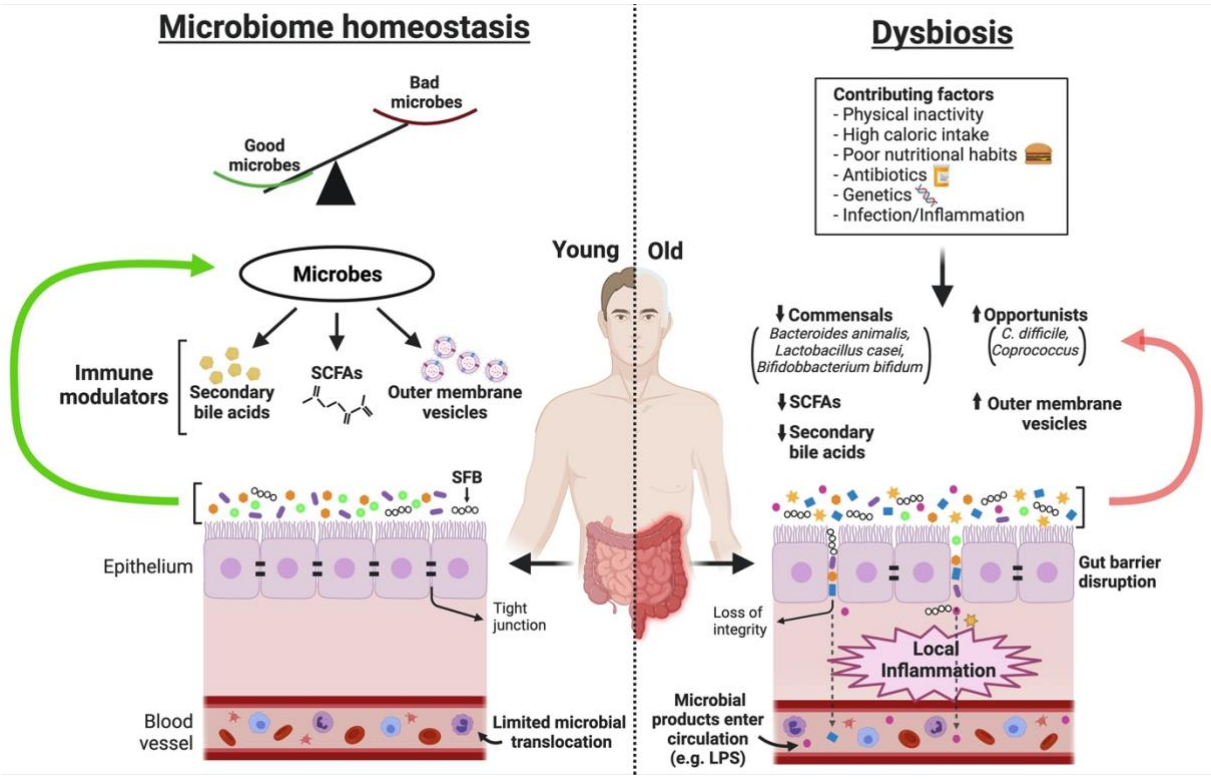

Figure 1.6 Age-associated changes in the gut microbiome and their impact on systemic inflammation. In healthy young individuals, the composition of the gut microbiota is balanced and intestinal epithelial barrier integrity is maintained, preventing the translocation of microbes and MAMPs (e.g. LPS) into the underlying lamina propria and circulation. However in old age, altered diet and lifestyle patterns cause perturbations in the gut microbiome, termed dysbiosis, that lead to the deterioration of health. Figure from [320].

Reduced SCFA and SBA levels with age are directly linked with the loss of SCFA-producing commensals, including *Clostridium*, *Bacteroides*, *Bifidobacterium* and *Roseburia*. Microbial metabolites play a key role in regulating physiological functions, such as host metabolism and immune responses, locally in the gut and in peripheral tissues [321]. Reduced metabolite production with advancing age could therefore contribute towards intestinal inflammation and the development of systemic inflammatory disorders. Factors that contribute towards age-associated microbial composition changes include an altered diet [315], physical inactivity [322], altered gut morphology and reduced intestinal functionality [323], recurrent infections, repeated hospitalisation and antibiotic usage [324].

1.6.1 Clinical implications of an ageing gut microbiome on the health of older adults

Age-related microbial dysbiosis is recognised for its profound effects on the health of the aged host (Figure 1.7). Evidence in mice suggests that reduced microbial diversity increases the risk of infection at distal mucosal sites, such as the lungs [325,326]. This is largely driven by the loss of SCFAs, which negatively impacts the host immune system.

Physical frailty is a major risk factor for disability and is associated with sarcopenia, which is characterised by the loss of skeletal muscle mass and function [327]. While sedentary behaviour and malnutrition contribute towards frailty and sarcopenia, recent evidence suggests that microbial dysbiosis promotes muscle atrophy in older adults by altering skeletal muscle metabolism, triggering frailty onset [328,329]. Studies conducted on community dwelling older adults show that frailty is associated with a lower microbiota diversity, specifically fewer butyrate-producing bacteria and

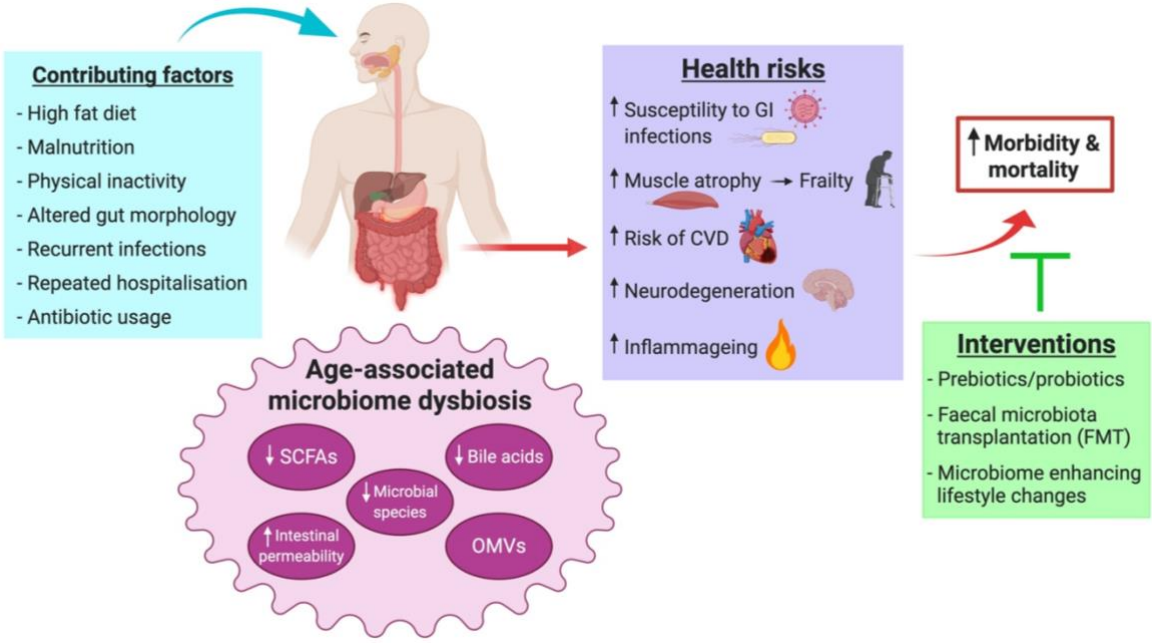

Figure 1.7 Age-related microbial dysbiosis causes health deterioration in older adults. Altered dietary patterns and lifestyle habits with advancing age can perturb microbial homeostasis (microbial dysbiosis), resulting in the loss of beneficial bacteria, blooming of pathobionts and increased gut permeability. These age-related microbial changes ultimately reduce the bioavailability of microbial metabolites, such as SCFAs and SBAs, that possess immunoregulatory properties. Consequently, older adults are at a greater risk of adverse health and mortality. Modulation of the gut microbiome through microbiome-targeted interventions has emerged as a novel therapeutic strategy for restoring the intestinal microbiota composition and potentially reducing morbidity and mortality in older adults. Figure from [320].

pathobiont (*Enterobacteriaceae*) overgrowth [330]. SCFAs produced by gut microbes provide pro-anabolic signals that induce mitochondrial biogenesis and glucose uptake in skeletal muscle cells [331]. Therefore, an age-associated decline in SCFA-producing bacteria could lead to mitochondrial dysfunction and insulin resistance, increasing intramuscular fat deposition [332].

Gut microbiota also play a role in the pathogenesis of intestinal and extraintestinal chronic inflammatory diseases such as inflammatory bowel disease (IBD) and rheumatoid arthritis (RA), both of which are associated with an increased abundance of certain pathobiont species. Although IBD is commonly diagnosed in younger people, recent data suggests there is an increasing incidence of IBD in the older population possibly due to age-related microbial composition changes [333]. IBD patients exhibit lower levels of butyrate-producing bacteria (Firmicutes and *Lachnospiraceae*) and an increased prevalence of invasive *Escherichia coli* and *Fusobacterium nucleatum* strains, resulting in reduced butyrate levels, increased intestinal permeability and gut inflammation [334].

In RA patients, taxonomical changes, namely an overabundance of *Prevotella copri* and *Eggerthella lenta*, are strongly correlated with disease status [335]. Mechanistically, microbiota dysbiosis in RA increases microbiota-mediated Th17 cell differentiation that enhances systemic GC responses, resulting in enhanced production of autoantibodies that cause joint inflammation [336]. Furthermore, gut commensals, specifically SFB, trigger autoimmune arthritis in transgenic mice by inducing Peyer's patch Tfh differentiation and egression to systemic sites [337]. Epidemiological data suggest that there is an increase in the incidence of autoimmune disorders with advancing age, which could be due to an age-related expansion of

opportunistic bacterial species including *F. nucleatum, P. copri, E. lenta* and *E. coli* [338,339].

Advancing age is associated with an increased risk of developing CVD due to vascular endothelial dysfunction and arterial stiffening [340], which could be driven by age-related microbial composition changes (Figure 1.7) [341]. Furthermore, patients with symptomatic atherosclerosis are enriched with *Collinsella*, but show reduced levels of *Roseburia*, *Eubacterium* and *Bacteroides* in the gut compared with healthy controls [342], suggesting that microbial dysbiosis may be implicated in the pathogenesis of atherosclerosis. One possible mechanism by which the gut microbiome promotes plaque formation is by increasing TMAO production, which leads to the accumulation of macrophage foam cells and endothelial dysfunction [343]. Interestingly, ageing is associated with a greater abundance of Proteobacteria species such as *Desulfovibrio*, resulting in increased plasma TMAO levels and risk of atherosclerosis [341].

Alterations in the gut microbiome can also impact the gut-brain axis and may play a pivotal role in neurodegeneration and Alzheimer's disease. Recent studies in amyloid precursor protein transgenic mice have demonstrated that microbial perturbations influence cerebral amyloid deposition by regulating innate immunity [344,345]. Thus, microbial dysbiosis-induced inflammation could be a contributing factor driving neuropathology. In support of this, examination of post-mortem brain tissues from Alzheimer's disease patients shows that LPS colocalises with amyloid plaques [346]. The intestinal microbiota composition of patients with Alzheimer's disease differs significantly from that of healthy individuals and is characterised by a decreased abundance of Firmicutes and *Bifidobacterium* and an increased abundance of Bacteroidetes [347].

Furthermore, cognitively impaired patients with brain amyloidosis have a lower proportion of anti-inflammatory *Escherichia rectale* and a greater proportion of pro-inflammatory *Escherichia-Shigella* compared to amyloid-negative patients. This coincides with higher levels of pro-inflammatory mediators (IL1β, L6, CXCL2 and NLRP3) and reduced levels of IL10, potentially contributing towards neuroinflammation and protein aggregation [348]. Similar microbial composition modifications have also been reported in healthy older adults and might be a potential contributing factor in the age-related predisposition towards cognitive impairment [349].

In contrast, super centenarians are characterised by the enrichment of allochthonous bacteria taxa (*Akkermansia*, *Bifidobacterium* and *Christensenellaceae*). Enrichment of these health-associated bacteria in the gut has been identified as a potential contributor towards reaching extreme longevity [314]. More recently, a study in centenarians from longevity villages demonstrated that centenarians also have a higher proportion of Firmicutes, *Escherichia*, *Clostridium* and *Collinsella* and a reduced proportion of Bacteroidetes, *Faecalibacterium* and *Prevotella* compared with older adults from urbanized towns. An increased abundance of these commensals was predicted to be associated with metabolic pathways that maintain immune homeostasis and a healthy microbiota ecosystem in centenarians [350].

1.7 Intestinal membrane permeability increases with age

The intestinal barrier is comprised of an overlying mucus layer, ECs and epithelium, which together physically and functionally separate the intestinal lumen from the underlying lamina propria. Intestinal ECs are interlinked by junctional complexes composed of tight junction proteins (e.g. zonulin and occludin) and junctional adhesion

molecules (e.g. cadherin and catenin). These apical junctional complexes regulate the trafficking of nutrients and essential ions, while preventing the permeation of pathogens and toxins from the lumen into the epithelium [351]. Commensal bacteria contribute to the maintenance of intestinal barrier integrity through the production of SCFAs, which strengthen intestinal barrier function [352], promote mucin production by goblet cells [353], reduce intestinal inflammation and help repair epithelial damage [354-356]. Additionally, SCFAs induce sIgA responses and AMP production (RegIIIγ and β-defensins) [357,358], which promote the clearance of toxins and pathogens via immune exclusion (involves agglutination, mucus entrapment and subsequent removal via peristalsis) [359].

However, ageing is accompanied by mucus layer thinning and remodelling of intestinal epithelial tight junction proteins [360], which increase intestinal membrane permeability, also known as 'leaky gut', in non-human primates [323,361]. Loss of intestinal barrier integrity allows the leakage of microbes, MAMPs, toxins and dietary antigens from the gut lumen into the circulation [362]. Recent evidence from animal studies suggests that microbial translocation is a contributing factor for inflammageing (Figure 1.6) [68]. This is evidenced in several inflammatory conditions, including IBD and RA [363-365].

Interestingly, aged TNFα-deficient mice, which are protected from inflammageing, do not display age-related microbiota changes [68]. This suggests that there is a potential positive feedback loop in which inflammageing promotes microbial dysbiosis. Microbial translocation has also been reported to contribute to chronic immune cell activation in human and simian immunodeficiency virus-infected primates [366,367], and is linked with increased CD8 T cell exhaustion and an increased proportion of HLA-DR-

expressing CD4 T cells [368]. Whilst many studies have reported an increase in intestinal membrane permeability with age, the mechanisms underlying these alterations and potential implications on health have yet to be fully elucidated.

1.8 Effect of diet on the gut microbiome and the immune system

Optimal dietary patterns play a significant role in influencing the composition of the gut microbiota and overall health and wellbeing [369]. For example, a high-fibre diet rich in non-digestible carbohydrates (polysaccharides) increases intestinal *Bifidobacterium* and *Lactobacillus* [370], reduces the abundance of Firmicutes and *Clostridium* and *E. coli* species and enhances the production of SCFAs [371,372]; whereas, a diet high in saturated and trans fats but low in mono and polyunsaturated fats (Western diet) has the opposite effect and is associated with adverse health outcomes, like inflammation [373,374]. Furthermore, high-intensity sweeteners and food additives, such as emulsifiers, have been shown to alter the balance and biodiversity of the gut microbiome in mice and rats [375,376].

Older adults that consume less daily volumes of food are at a greater risk of malnutrition (i.e. lower intake of calcium, iron and zinc) [377,378], which is associated with an increased risk of frailty and loss of bone mineral density [379], possibly contributing towards immunesenescence and microbial dysbiosis. Risk factors for malnutrition in older adults include difficulties with chewing and swallowing, loss of appetite, depression, reduced physical function and malabsorption of essential nutrients [380].

Several dietary interventions have been suggested for the maintenance of the gut microbial composition and reduction of age-related inflammation to promote healthier

ageing. The Mediterranean diet (MedDiet) is a well-balanced diet that features high intake of fruits, vegetables, nuts, legumes, whole grains, fish and olive oil and low consumption of meat, refined carbohydrates and sweets. The MedDiet is associated with increased longevity and reduces the risk of frailty [381], cognitive impairment [382], CVD and cancer in older adults [383,384]. High adherence to the MedDiet is linked with a lower Firmicutes/Bacteroidetes ratio, higher *Bifidobacterial* counts, a greater abundance of polysaccharide-degrading microbes and high faecal SCFA levels [385].

The MedDiet has also been shown to have an anti-inflammageing effect by reducing plasma levels of various pro-inflammatory mediators, including IL6, CRP, intercellular adhesion molecule 1 and vascular cell adhesion protein 1, in aged people [386,387]. Additionally, adoption of the MedDiet by older adults led to an increase in the proportion of $CXCL8^{+ve}$ DCs, which secreted significantly less IL1β and IL6 upon stimulation [388]. Furthermore, a significant upregulation in the expression of costimulatory molecules CD40 and CD86 by lymphocytes has been reported in older women after one-year adoption of the MedDiet supplemented with vitamin D_3, supporting the notion that the MedDiet could improve different aspects of immune ageing [389].

1.9 Hypotheses and aims

A study in young germ-free mice reported that cohousing these mice with aged wild-type mice resulted in elevated cytokine levels in young germ-free mice, suggesting a causal role of age-related dysbiosis in increasing intestinal membrane permeability and promoting inflammageing and macrophage dysfunction [68]. A recent study

involving faecal transplantation in aged mice has reported the rescue of age-associated impairments in GC reactions, which may have implications for improving vaccine responses in older adults [390]. Additionally, research comparing intestinal membrane permeability between healthy young and old adults observed elevated occludin levels in aged individuals that were positively correlated with the production of pro-inflammatory cytokine TNFα by monocytes [Niharika Duggal, University of Birmingham, personal communications]. Despite these interesting findings, the potential links between age-related microbial dysbiosis, intestinal barrier dysfunction and immunesenescence are poorly understood, and thus will be investigated in this thesis.

We hypothesis that loss of intestinal barrier integrity and depletion of SCFA- and SBA-producing commensals contribute towards features of T cell ageing possibly through hyperactivation of the immune system. Secondly, we hypothesis that adherence to a healthy diet that is fibre-rich and low in saturated fat promotes immune health in older adults possibly via maintenance of a healthy gut microbiome.

<u>The scientific objectives of this thesis are:</u>

1) To dissect the relationship between age-related intestinal barrier dysfunction and immunesenescence.
2) To identify major bacterial groups that correlate with a beneficial effect on immune ageing and good influenza vaccination outcomes in older adults.
3) To evaluate links between diet, age-associated microbial dysbiosis, gut barrier dysfunction and immune ageing.

Chapter 2: Materials and methods

This chapter contains text written by Jessica Conway and edited by Dr Niharika A Duggal from the following manuscripts.

Conway J, Dugan B, Rees Paddison N, Sharma-Oates A, Sullivan J, White AJ, Parnell SM, DeJong E, Mauro C, Anderson G, Bowdish DME, Duggal NA. Age-related intestinal barrier dysfunction and microbial translocation play an integral role in thymic involution and T cell ageing (In preparation).

Conway J, Animesh A, Duggal NA. Integrated analysis revealing novel associations between dietary patterns and the immune system in older adults (In preparation).

2.1 Media and solutions

AutoMACS® Running Buffer (Miltenyi Biotec, Germany): Phosphate buffered saline (PBS) containing 0.5% bovine serum albumin (BSA), 2 mM ethylenediaminetetraacetic acid (EDTA) and 0.09% azide.

Complete RPMI medium: 10% (volume/volume (v/v)) heat-inactivated foetal calf serum (HiFCS) (Gibco®, UK) in RPMI-1640 media (Sigma-Aldrich, UK) supplemented with 2 mM glutamine, 100 U/ml penicillin and 100 µg/ml streptomycin (Sigma-Aldrich).

Foxp3 Fixation/Permeabilisation working solution: 1 part of Foxp3 Fixation/Permeabilisation concentrate with 3 parts of Foxp3 Fixation/Permeabilisation Diluent (Foxp3 Transcription Factor Staining Buffer Set; eBiosciences™, UK).

Freezing medium: 10% (v/v) dimethyl sulfoxide (DMSO) (Sigma-Aldrich) in HiFCS (56°C for 30 minutes in a water bath).

Reagent diluent: Filtered (0.2 µm) 1% (weight/volume (w/v)) BSA in 1x PBS (pH 7.2-7.4) or filtered (0.2 µm) 5% (v/v) Tween® 20 in 1x PBS (pH 7.2-7.4), depending on the protocol.

Staining/wash buffer: 1% BSA in 1x PBS.

Stop solution (2N H_2SO_4): Sulphuric acid (H_2SO_4) diluted 18-fold in double-distilled water (ddH_2O).

Working lysing solution: 10-fold dilution of BD FACS™ lysing solution (BD Biosciences, UK) in ddH_2O.

1% Agarose/Tris-Borate-Ethylenediaminetetraacetic (TBE) gel: 0.5 g of agarose (Sigma-Aldrich) dissolved in 50 ml of 5x TBE (National Diagnostics, USA) containing 5 ul of SYBR™ Safe DNA Gel Stain (Invitrogen™, UK).

1x Citrate buffer: 10x citrate buffer (pH 6; Sigma-Aldrich) diluted 10-fold in nuclease-free water (Qiagen, Germany).

1x Permeabilisation Buffer: 10X Permeabilisation Buffer (Foxp3 Transcription Factor Staining Buffer Set) diluted 10-fold in ddH_2O.

1x PBS: One PBS tablet (Sigma-Aldrich) dissolved in 200 ml of ddH_2O.

1x PBS with Tween® 20 (PBST): 0.02% Tween® 20 in 1x PBS.

1x Tris-buffered saline with Tween ® 20 (TBST): 10x TBST (Cell Signalling Technology, USA) diluted 10-fold in nuclease-free water.

1x Wash buffer: 0.05% (v/v) Tween® 20 in 1x PBS, pH 7.2-7.4.

2.2 Study design and participants

This is an observational, cross-sectional study approved by the North Staffordshire Research Ethics Committee (IRAS reference number: 301974). Forty healthy young (aged 18-37 years) and 61 healthy old (aged ≥60 years) adults were recruited into this study, the latter of whom were enrolled from the Birmingham 1000 Elders group. The exclusion criteria included self-reported infections (e.g. cold), comorbidities (e.g. chronic inflammatory/autoimmune conditions, cancer and type 1 diabetes), use of any medication known to influence immune function (e.g. immunosuppressing and anti-inflammatory medications), antibiotic usage in the past two months, hospitalisation in the past three months and/or travelling outside of the UK in the month leading up to

recruitment. Written informed consent was obtained from all eligible participants prior to blood sampling and stool sample donation. Older adults who were eligible for an annual influenza vaccination provided a paired stool and blood sample prior to vaccination and four weeks post-vaccination. Additional participant demographics, including height, weight, body mass index (BMI), hours of TV watched and stairs climbed), sleep quality, mental health status (anxiety and depression) and diet, were gathered via self-assessed questionnaires.

2.3 Questionnaires

At the visit, subjects were asked to answer a series of questionnaires to determine demographics, medication use, medical history, health and wellness (questionnaire packs are in Appendix 1). Health behaviours (e.g. BMI, alcohol consumption, smoking and sleep quality) and mental health were assessed using general health questions, an adapted version of the 12-Item Short-Form (SF-12) Health Survey [391], the Pittsburgh Sleep Quality Index (PSQI) [392] and the Hospital Anxiety and Depression Scale (HADS) [393].

- BMI was determined using the following equation: $\mathbf{BMI} = \frac{\mathbf{kg}}{\mathbf{m}}\ \mathbf{x\ 100}$

2.4 Nutrient and food frequency assessment

All participants were sent Food Frequency Questionnaires (FFQs) via post to evaluate dietary intake and completed FFQs were brought along to the visit at the hospital. FFQs consisted of two sections, the first being a list of 130 foods with portion sizes (e.g. medium serving) grouped into 11 categories (e.g. meat and fish, bread and savoury biscuits, sweets and snacks, fruit and vegetables) and the second containing questions on fat consumption and supplement use. To complete FFQs, participants

were to select the appropriate frequency of consumption for each food listed in Part 1 and provide answers to the supplementary questions in Part 2.

FFQ data was manually inputted into an excel spreadsheet (Microsoft Windows, USA) as numeric codes taken from the Mulligan *et al*. study prior to data processing [394]. For part one, frequencies were coded as 1-9, using 1 for 'never or less than once/month' to 9 for '6+ per day'. -9 or -4 were used when frequencies were missing or more than one frequency was provided, respectively. For part two, data was numerically coded using a reference list of food codes to translate text for milk type, daily milk frequency, cereal type, type of frying fat, type of baking fat and visible fat consumption. Once the dataset was complete, numeric coding was processed using FFQ EPIC Tool for Analysis (FETA) software GPL v.2 (EPIC-Norfolk, UK) to generate a nutrient output with average daily nutrient and food group intakes for each participant [394].

2.4.1 Diet Quality Index

Diet quality was measured using the Diet Quality Index-International (DQI) tool, which considers the variety, adequacy, moderation and overall balance of nutrient and food intake [395]. A poor diet was defined as those with a DQI score of ≤60%, while a DQI score >60% indicated a good diet.

2.4.2 Mediterranean Diet Score

14-Item Mediterranean Diet Questionnaires were completed by the researchers to determine each participant's adherence and calculate the Mediterranean diet score (MDS) [396].

2.5 Blood sample collection and haematological analysis

A venous blood sample of 30 ml was collected from all participants in the morning between 9:00-11:30am in lithium heparin and anti-coagulant-free vacutainers (BD, UK) by a trained healthcare professional using standard venepuncture technique. To determine whole blood cell counts, 1 ml of blood was transferred to a 1.5 ml microcentrifuge tube and run on a Sysmex XN-1000 automated haematology analyser (Sysmex, UK). Following blood collection, anti-coagulant free vacutainers (6 ml) were positioned upright for at least 30 minutes undisturbed at room temperature (RT) to allow the blood to clot. The vacutainers were then centrifuged at 1,620 x *g* for 10 minutes at RT. Post-centrifugation, 500 µl of serum was transferred to 1.5 ml microcentrifuge tubes and stored at -80°C prior to analysis.

2.6 Serum microbial translocation and cytokine analysis

The concentration of circulating inflammatory cytokines and surrogate markers for intestinal membrane permeability and microbial translocation was measured in thawed serum samples using commercially available Enzyme-Linked Immunosorbent Assays (ELISAs) and a Human Premixed Multi-Analyte Magnetic Luminex Assay (R&D Systems, USA).

2.6.1 Enzyme-linked immunosorbent assays

Table 1.1 contains a list of ELISA kits and their respective serum dilution factors. In brief, 100 µl aliquots of serum were dispensed into the wells of a 96-well microplate pre-coated with antibodies specific for occludin, lipopolysaccharide binding protein (LBP), soluble CD14 (sCD14), IL6, IL10, TNFα, IFNγ and CRP. After a 2-hour incubation at RT, the liquid was decanted and the wells were washed three times with

400 µl of 1x wash buffer. Post-wash, 100 µl of detection antibody was added to each well and the plate was incubated for 2 hours at RT. The wells were then aspirated and rinsed three times with 400 µl of 1x wash buffer, prior to the addition of substrate solution (e.g. streptavidin-horseradish peroxidase). Following a 20-minute incubation in the dark with the substrate, 50 µl of stop solution was dispensed into each well.

The absorbance of the wells was immediately measured using wavelengths specified by the manufacturers on a BioTek EL808 spectrophotometer (BioTek, USA) using BioTek Gen5 software v1.01.14 (BioTek). Protein concentrations were extrapolated from a standard curve generated using known concentrations via GraphPad Prism software v9 (GraphPad Software Inc., USA).

ELISA kit	Catalogue number	Serum dilution factor	Manufacturer
Human Occludin (OCLN)	DL-OCLN-Hu	Undiluted	DL Develop
Human LBP DuoSet	DY870-05	Undiluted	R&D Systems
Human CD14	EHCD14	Undiluted	Invitrogen™
Human IL6 DuoSet	DY206-05	1:100	R&D Systems
Human IL10 DuoSet	DY217B-05	Undiluted	R&D Systems
Human TNFα DuoSet	DY210-05	1:50	R&D Systems
CRP	EU59131	Undiluted	IBL International GMBH

Table 1.1 Enzyme-linked immunosorbent assay (ELISA) kits.

2.6.2 Luminex

Following the manufacturer's instructions, thawed serum samples were centrifuged (16,000 x *g*, 4 minutes, RT) prior to being diluted 2-fold with calibrator diluent RD6-52. Diluted serum (50 µl) was transferred to the wells of a 96-well microplate pre-coated with analyte-specific antibodies against IL1β, IL4, IL6, IL7, IL10, IL15, IL17, TNFα, IFNγ, CXCL9 and granulocyte macrophage colony-stimulating factor (GM-CSF). Then, 50 µl of microparticle cocktail (diluted 50-fold with diluent RD2-1) was added to each well. After a 2-hour incubation in the dark at RT on a shaker (800 rpm), the plate was washed three times with 100 µl of 1x wash buffer in a Bio-Plex Pro™ magnetic wash station (Bio-Rad Laboratories, USA). Then, 50 µl of biotin-antibody cocktail (50-fold dilution with diluent RD2-1) was added to each well and the plate was incubated for 1 hour in the dark at RT on a shaker (800 rpm). Following three washes with 100 µl of 1x wash buffer, 50 µl of streptavidin-phycoerythrin (diluted 24.3-fold with 1x wash buffer) was added to each well and the plate was incubated for 30 minutes in the dark at RT on a shaker (800 rpm). The plate was then washed and incubated with 100 µl of 1x wash buffer for 2 minutes at RT on a shaker (800 rpm).

Absorbance vales were read within 5 minutes of resuspending the wells on a Bio-Plex™ 200 suspension array system (Bio-Rad Laboratories) using Bio-Plex Manager software v6.2 (Bio-Rad Laboratories). Protein concentrations were extrapolated from a standard curve created using known protein concentrations via GraphPad Prism software v9.

2.7 Detecting serum cytomegalovirus IgG

CMV IgG antibody was detected in human serum using a commercially available CMV IgG ELISA kit (Immuno-Biological Laboratories, USA). 100 µl of serum (diluted 21-fold

with sample diluent) was dispensed into each well of a 96-well microplate pre-coated with CMV antigen and the plate was incubated for 20 minutes at RT. Post-incubation, the liquid was decanted and the plate was washed three times with 300 µl of 1x wash buffer before being incubated with 100 µl of enzyme conjugate (20 minutes at RT). The wells were then aspirated and 100 µl of TMB (3,3',5,5'-Tetramethylbenzidine) substrate was added to each well. Following a 10-minute incubation at RT, the absorbances were read at 450 nm and 630 nm using a BioTek EL808 spectrophotometer within 5 minutes of adding 100 µl of stop solution.

CMV seropositive status (i.e. antibody index) was determined by dividing the optical density value of each sample by the cut-off value (0.88). Antibody indexes ≥0.9 were considered CMV positive, whereas antibody indexes <0.9 were considered CMV negative.

2.8 Monocyte and DC phenotyping

Surface staining was performed on 200 µl of whole blood using a combination of fluorochrome conjugated antibodies targeted against anti-human CD14, CD16, HLA-DR, CD11c, CD123 and lineage markers (Table 1.2) in 5 ml polypropylene FACS tubes (BD). After vortexing the tubes, the antibodies were incubated for 20 minutes in the dark at 4°C before the cells were centrifuged with 500 µl of 1x PBS (250 x *g*, 5 minutes, 4°C). The liquid was aspirated and the cells were resuspended in 2 ml of working lysing solution (BD Biosciences) to lyse red blood cells (RBCs). Following a 20-minute incubation in the dark at RT, lysed whole blood was centrifuged at 250 x *g* for 5 minutes at 4°C, after which the liquid was decanted. Cell pellets were resuspended in 400 µl of

1x PBS in preparation for flow cytometric analysis. Gating strategies are shown in Figures 2.1 and 2.2.

Antibodies	Clone	Isotype	Working concentration	Manufacturer
Cell surface markers				
CD14 efluor 450 Violet	61D3	Mouse IgG1κ	25 ng/ml	Thermo Fischer
CD16 FITC	CB16	Mouse IgG1κ	25 ng/ml	Thermo Fischer
Lineage cocktail (CD3, CD14, CD16, CD19, CD20, CD56) Pacific Blue™	UCHT1, HCD14, 3G8, HIB19, 2H7 and HCD56	Mouse IgG1κ/ Mouse IgG2bκ	N/A	Biolegend
HLA-DR PEcy7	L243	Mouse IgG2aκ	6.25 ng/ml	Thermo Fischer
CD11c FITC	3.9	Mouse IgG1κ	2 µg/ml	Biolegend
CD123 APC	6H6	Mouse IgG1κ	0.5 µg/ml	Biolegend
Intracellular cytokines				
IL6 PE	MQ2-13A5	Rat IgG1κ	62.5 ng/ml	Biolegend
IL10 APC	JES3-19F1	Rat IgG2aκ	0.1 µg/ml	Biolegend
IL12 APC	REA123	Recombinant human IgG1κ	50 ng/ml	R&D Systems
IL23 PE	727753	Mouse IgG2bκ	50 ng/ml	R&D Systems
TNFα FITC	Mab11	Mouse IgG1κ	1.25 µg/ml	BD Biosciences

Table 1.2 Anti-human fluorochrome antibodies for monocyte and dendritic cell (DC) phenotyping and cytokine analysis.

2.9 Monocyte and DC cytokine production

Whole blood (400 µl) was transferred to 5 ml polypropylene FACS tubes for stimulation with LPS isolated from *E. coli* serotype 0111:B4 (10 ng/ml) (Sigma-Aldrich) for 4 hours (37°C, 5% CO_2) in the presence of 10 µg/ml brefeldin A from *Penicllium brefeldianum* (Sigma-Aldrich). A 4-hour incubation period with 10 ng/ml LPS was used because it caused the least amount of cell death and induced greater cytokine production (Figure 2.3). Post-incubation, the cells were washed with 500 µl of 1x PBS and centrifuged at 250 x *g* for 5 minutes at 4°C. The liquid was aspirated and pelleted cells were

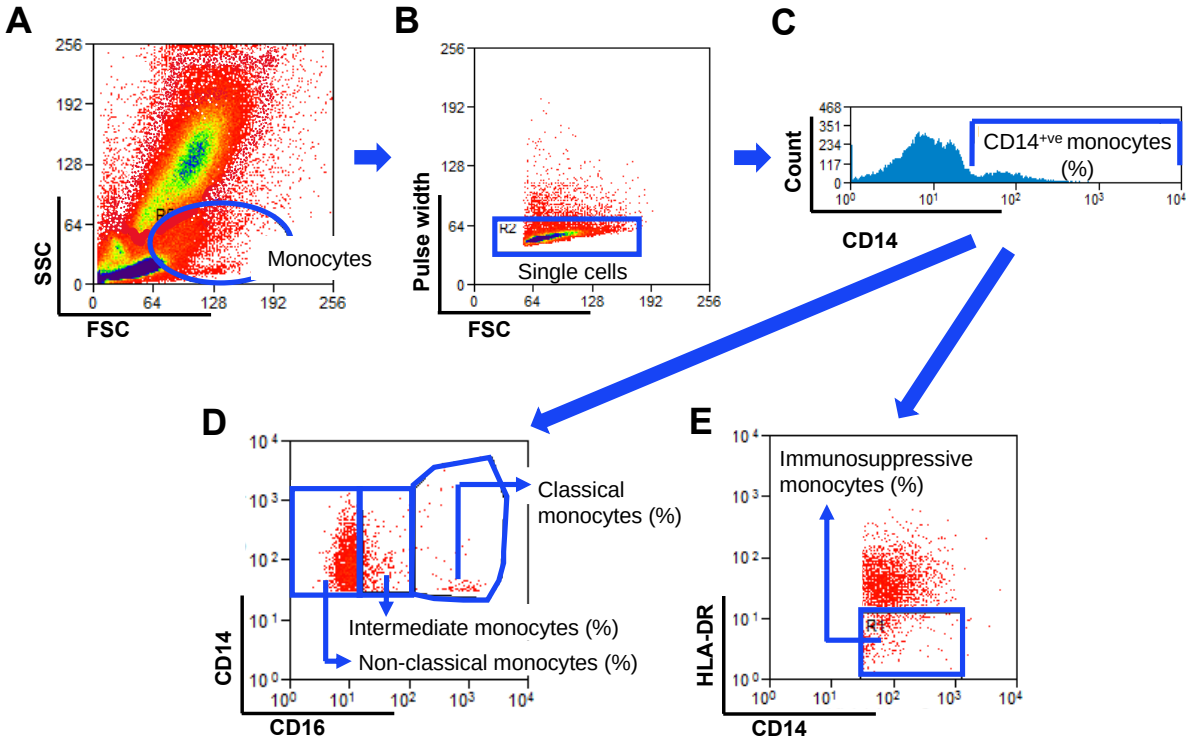

Figure 2.1 Monocyte subset gating strategy. (A) Monocytes were gated on using a forward scatter (FSC)/side scatter (SSC) flow cytometric plot, **(B)** after which doublets were excluded. **(C)** After gating on $CD14^{+ve}$ monocytes, **(D)** three monocyte subpopulations were identified based on differential expression of CD14 and CD16: $CD14^{+ve}CD16^{-ve}$ classical monocytes, $CD14^{+ve}CD16^{+ve}$ intermediate monocytes and $CD14^{+ve}CD16^{++ve}$ non-classical monocytes. **(E)** $CD14^{+ve}$ monocytes were further categorised as $CD14^{+ve}HLA\text{-}DR^{low/neg}$ immunosuppressive monocytes.

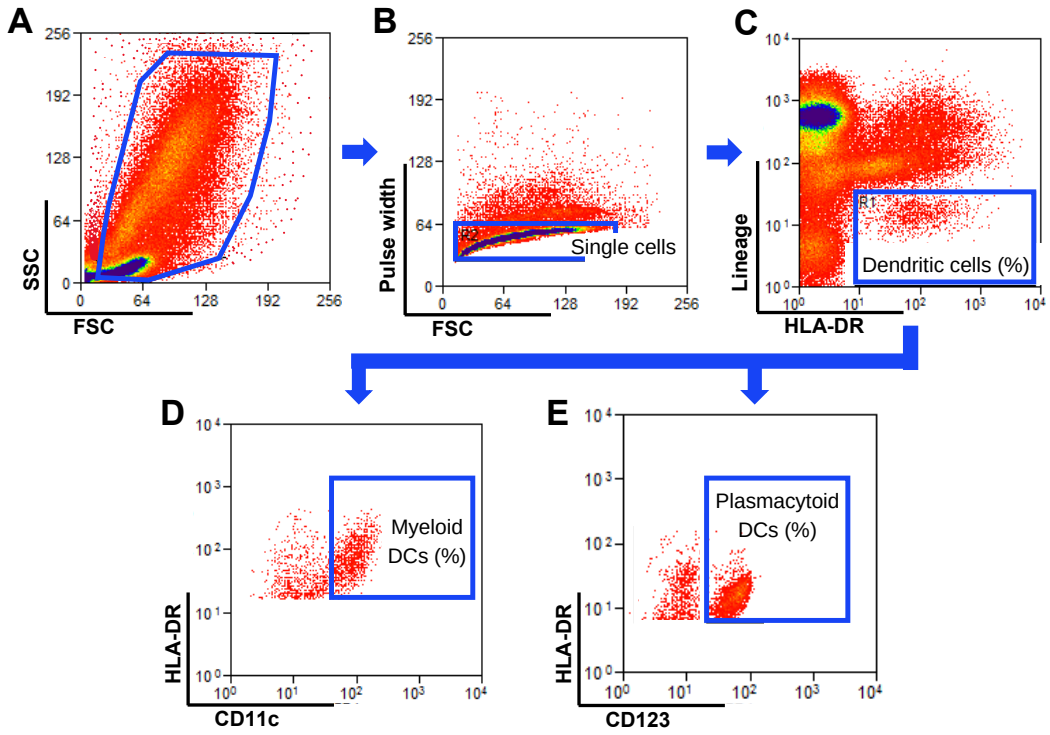

Figure 2.2 Dendritic cell (DC) subset gating strategy. (A) Granulocytes were gated on using FSC and SSC properties, **(B)** after which doublets were excluded. **(C)** Next, Lineage^{-ve}HLA-DR^{+ve} DCs were gated on and categorised into two main groups based on CD11c and CD123 surface expression: CD11c^{+ve}Lineage^{-ve}HLA-DR^{+ve} myeloid DCs **(D)** and CD123^{+ve}Lineage^{-ve}HLA-DR^{+ve} plasmacytoid DCs **(E)**.

resuspended in 1x PBS for surface staining with various fluorochrome conjugated antibodies against anti-human CD14, HLA-DR and lineage markers (Table 1.2). After a 20-minute incubation in the dark at 4°C, the cells were centrifuged (5 minutes, 250 x *g*, 4°C) and supernatants were discarded.

RBCs were lysed with 2 ml of working lysing solution for 20 minutes in the dark at 4°C. Post-lysis, the cells were centrifuged at 250 x *g* for 5 minutes at 4°C and pelleted cells were resuspended in 50 µl of permeabilization Medium B (Life Technologies, UK). The cells were intracellularly stained with monoclonal antibodies against anti-human IL6, IL10, IL12, IL23 and TNFα for 20 minutes in the dark at 4°C (see Table 1.2 for antibody details). Lastly, the cells were washed with 500 µl of 1x PBS and centrifuged at 250 x *g* for 5 minutes at 4°C, before pelleted cells were resuspended in 300 µl of 1x PBS for flow cytometric analysis.

2.10 Peripheral blood mononuclear cell (PBMC) isolation and freezing

Peripheral blood mononuclear cells (PBMCs) were isolated from whole blood using Ficoll-Paque™ density gradient centrifugation [397] (Figure 2.4). Heparinised blood (30 ml) was diluted with 10 ml of pre-warmed sterile complete RPMI medium in 50 ml falcon tubes (BD). 10 ml of diluted blood was gently layered on top of 6 ml of Ficoll-Paque™ Plus (GE Healthcare, USA) in 25 ml universal tubes (Sarstedt Ltd, UK). The tubes were spun at 420 x *g* for 30 minutes at 21°C with no break. Post-centrifugation, PBMCs residing at the plasma-Ficoll-Paque™ interface were transferred to 25 ml universal tubes containing 10 ml of autoMACS® Running Buffer using a Pasteur pipette (Sarstedt Ltd). The cells were centrifuged at 300 x *g* for 10 minutes at 21°C, after which

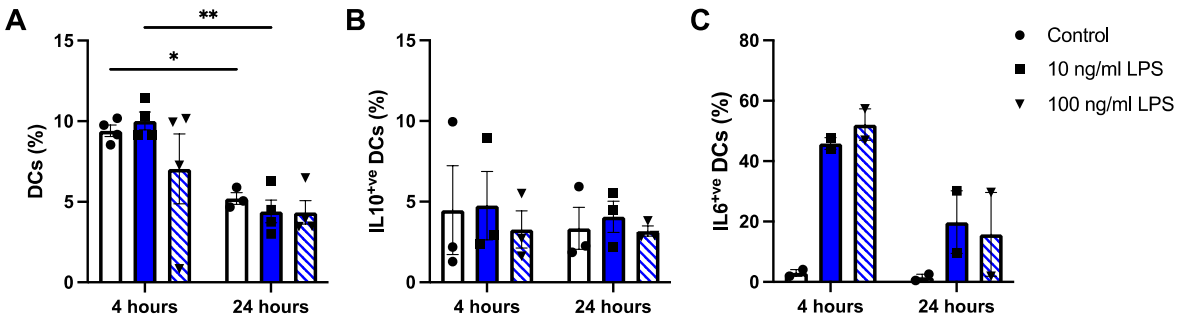

Figure 2.3 Lipopolysaccharide stimulation validation for monocyte and DC cytokine production. (A) Percentage of cytokine-secreting DCs post-stimulation with 10 ng/ml LPS and 100 ng/ml for 4 and 24 hours. Repeated measures one-way analysis of variance (ANOVA) with the Benjamin-Hochberg procedure used to calculate adjusted p-values. *p ≤0.05, ** p ≤0.01. Frequency of DCs that produce IL10 **(B)** and IL6 **(C)** following treatment with 10 ng/ml LPS and 100 ng/ml for 4 and 24 hours.

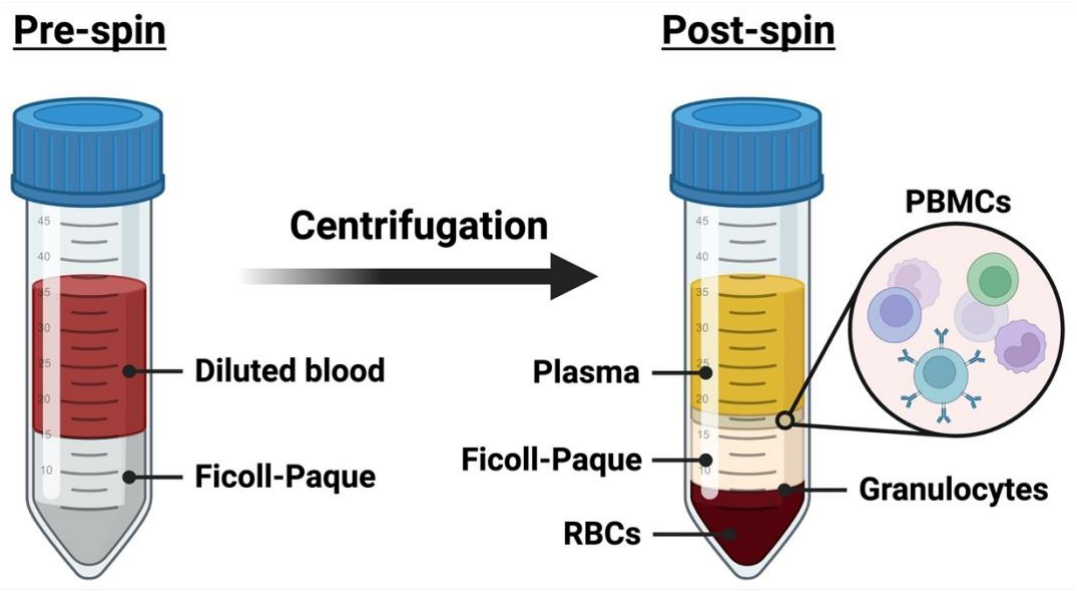

Figure 2.4 Peripheral blood mononuclear cell isolation via Ficoll-Paque density gradient centrifugation. Diluted whole blood is layered on top of Ficoll-Paque Plus density gradient medium in a conical tube. During centrifugation, the diluted blood is separated into five distinct components: plasma, PBMCs, Ficoll-Paque, granulocytes and RBCs. The PBMC fraction lying at the plasma-Ficoll-Paque interface consists of monocytes, DCs, NK cells, T cells and B cells. Post-centrifugation, PBMCs are carefully extracted, washed and counted in preparation for further experimentation.

supernatants were discarded and the pellets were resuspended in freezing medium. PBMC aliquots of 1 ml were transferred to cryovials, which were placed in a freezing container (Mr Frosty; Sigma-Aldrich) containing isopropanol (VWR International, UK). This allowed PBMC aliquots to gradually freeze at a rate of 1°C per minute before being stored at -80°C.

2.11 Surface immunostaining for T cell and B cell phenotyping

Thawed PBMCs were transferred into 20 ml universal tubes and washed with 10 ml of pre-warmed sterile complete RPMI medium (300 x *g*, 10 minutes, 4°C). Supernatants were decanted and cell pellets were resuspended in 1x PBS to a final concentration of 1 x 10^6 PBMCs/ml. 50 µl of cell suspension was transferred into 5 ml FACS tubes for staining with LIVE/DEAD™ Fixable Near-IR Dead Cell Stain (Invitrogen™) and a combination of anti-human monoclonal antibodies against CD3, CD4, PTK7, CCR7 and CD45RA for the assessment of RTEs and naïve and memory T cells. Surface staining with anti-human CD3, CD4, CD8, CD28, CD57 and PD1 antibodies was also performed for the examination of senescent and exhausted T cells. Additionally, anti-human CD69 and CD154 antibodies were used to analyse T cell activation, while anti-human CCR9 surface staining was done to assess T cell gut homing potential. Surface staining with anti-human CD19, CD24, CD27 and CD38 antibodies was carried out to analyse B cell subset distribution (antibody details are displayed in Table 1.3). Following a 20-minute incubation at 4°C in the dark, PBMCs were centrifuged with 500 µl of 1x PBS at 250 x *g* for 5 minutes at 4°C. Post-wash, the pelleted cells were resuspended in 300 µl of 1x PBS for flow cytometric analysis. Gating strategies are shown in Figures 2.5 and 2.6. Note, B cell phenotyping was carried out by Benjamin Dugan (University of Birmingham).

Antibodies	Clone	Isotype	Working concentration	Manufacturer
Cell surface markers				
CD3 PEcy7	UCHT	Mouse IgG1κ	2 µg/ml	eBiosciences™
CD4 BV421	RPA-T4	Mouse IgG1κ	2 µg/ml	BD Biosciences
CD45RA PerCP/cy5.5	HI100	Mouse IgG2bκ	3 µg/ml	Biolegend
CCR7 APCcy7	G043H7	Mouse IgG2ακ	8 µg/ml	Biolegend
PTK7 PE	188B	Mouse IgG2ακ	4.5 µg/ml	Miltenyi Biotec
CD25 APCcy7	M-A251	Mouse IgG1κ	8 µg/ml	BD Pharmingen
CXCR5 APCcy7	J252D4	Mouse IgG1κ	8 µg/ml	Biolegend
CD28 APC	CD28.2	Mouse IgG1κ	0.5 µg/ml	eBiosciences™
CD57 FITC	TB01	Mouse IgMκ	6 µg/ml	Biolegend
PD1 APCcy7	EH12.2H7	Mouse IgG1κ	4 µg/ml	Biolegend
CD69 PEcy5	FN50	Mouse IgG1κ	0.5 µg/ml	Biolegend
CD154 APCcy7	24-31	Mouse IgG1κ	16 µg/ml	Biolegend
CD19 PE	HIB19	Mouse IgG1κ	1.5 µg/ml	eBiosciences™
CD24 FITC	eBioSN3	Mouse IgG1κ	1.5 µg/ml	eBiosciences™
CD27 APC	O323	Mouse IgG1κ	1 µg/ml	eBiosciences™
CD38 PEcy7	HIT2	Mouse IgG1κ	4 µg/ml	eBiosciences™
CCR9 PE	112509	Mouse IgG2aκ	3 µg/ml	R&D Systems
Transcription factors				
BCL6 APC	BCL-UP	Mouse IgG1κ	5 ng/ml	Invitrogen
Foxp3 PE	PCH101	Rat IgG2aκ	10 ng/ml	eBiosciences™
RORγ APC	AFKJS-9	Rat IgG2aκ	4 µg/ml	eBiosciences™
Intracellular cytokines				
IL4 PE	8D4-8	Mouse IgG1κ	25 µg/ml	eBiosciences™
IL10 APC	JES3-19F1	Rat IgG2aκ	100 ng/ml	Biolegend
IL17 FITC	BL168	Mouse IgG1κ	2 µg/ml	Biolegend
IFNγ APC	4S.B3	Mouse IgG1κ	0.4 µg/ml	Biolegend
TNFα FITC	Mab11	Mouse IgG1κ	1.25 µg/ml	BD Biosciences

Table 1.3 Anti-human fluorochrome conjugated antibodies for T cell and B cell phenotyping and cytokine analysis.

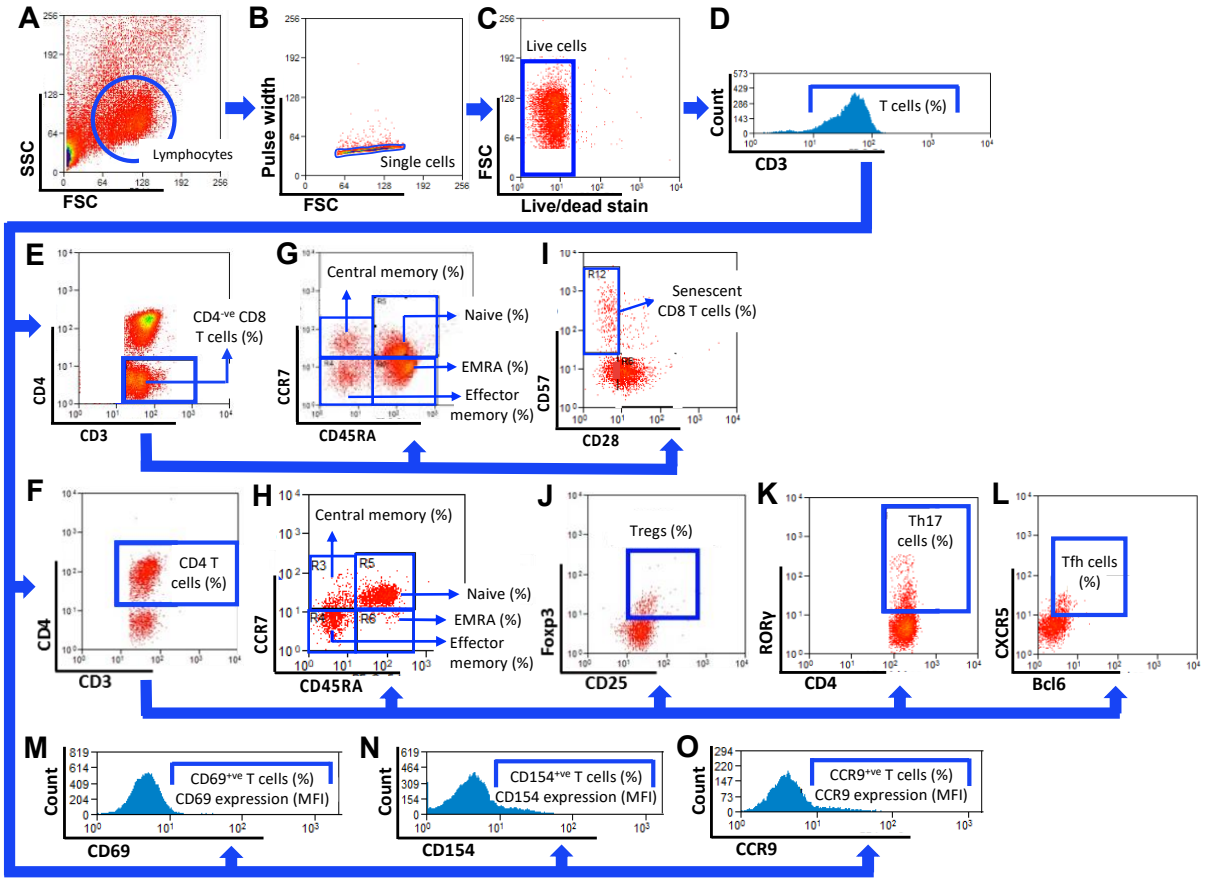

Figure 2.5 T cell subset and phenotypic expression gating strategy. (A) Lymphocytes were gated on using a FSC/SSC flow cytometric plot. After excluding double cells **(B)** and dead cells **(C)**, $CD3^{+ve}$ T cells were gated **(D)**. **(E,F)** CD4 and CD8 T cells were examined based on differential expression of CD4. **(G,H)** Naïve T cells and memory T cell subsets were identified within the CD4 and CD8 T cell pools based on differential surface expression of CCR7 and CD45RA. **(I)** Markers for CD28 and CD57 were used to identify $CD28^{-ve}CD57^{+ve}$ senescent CD8 T cells. Within the CD4 T cell pool, CD25, Foxp3 and RORγ were used to gate on $CD25^{+ve}Foxp3^{+ve}$ Tregs **(J)**, $ROR\gamma^{+ve}$ Th17 cells **(K)** and $CXCR5^{+ve}BCL6^{+ve}$ Tfh cells **(L).** Surface expression of CD69 **(M),** CD154 **(N)** and CCR9 **(O)** was assessed on all T cell subsets along with the percentage of antigen positive cells.

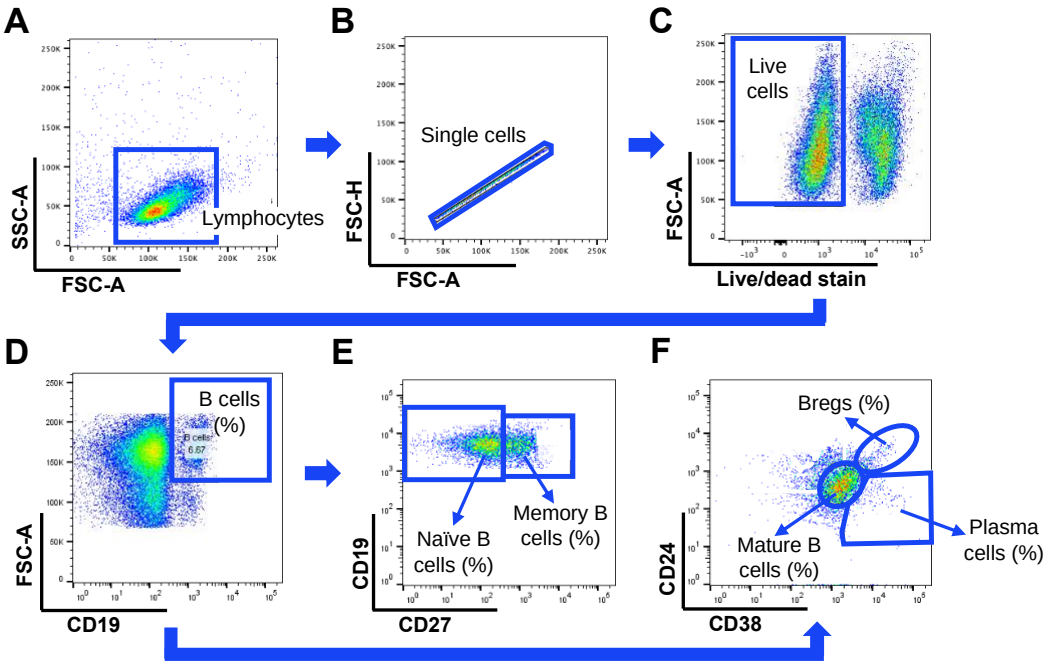

Figure 2.6 B cell subset gating strategy. (A) Lymphocytes were identified using a forward scatter-area (FSC-A)/side scatter-area (SSC-A) plot. Following the selection of single cells **(B)** and live cells **(C)**, $CD19^{+ve}$ B cells were gated **(D)**. Naïve and memory B cells were identified using markers for CD19 and CD27 **(E)**, while anti-CD24 and anti-CD38 markers were used to gate on $CD19^{+ve}CD24^{+ve}CD38^{+ve}$ mature B cells, $CD19^{+ve}CD24^{++ve}CD38^{++ve}$ Bregs and $CD19^{+ve}CD24^{-ve}CD38^{++ve}$ plasma cells **(F)**.

2.12 Intracellular staining for transcription factors in T helper cell subsets

PBMCs in 1x PBS (1 x 10^6 cells/ml) were stained with anti-human CD3-PEcy7 and anti-human CD4-BV421 antibodies for 20 minutes in the dark at 4°C. Post-incubation, the cells were washed with 1x PBS and resuspended in 1x Foxp3 Fixation/Permeabilisation working solution for 30 minutes in the dark at RT. Afterwards, the cells were centrifuged (250 x *g*, 5 minutes, 4°C) with 500 µl of 1x Foxp3 Fixation/Permeabilisation working solution prior to a 30-minute incubation with anti-human Foxp3, retinoic acid-related orphan receptor-gamma (RORγ) and B cell lymphoma 6 (BCL6) targeted antibodies diluted in 50 µl of 1x Permeabilisation Buffer (see Table 1.3 for antibody working concentrations). PBMCs were then washed (250 x *g*, 5 minutes, 4°C) with 500 µl of 1x Foxp3 Fixation/Permeabilisation working solution and the pellets were resuspended in 300 µl of 1x PBS prior to flow cytometric analysis. The percentages of $CD3^{+ve}CD4^{+ve}CD25^{+ve}Foxp3^{+ve}$ Tregs, $CD3^{+ve}CD4^{+ve}RORγ^{+ve}$ Th17 cells and $CD3^{+ve}CD4^{+ve}CXCR5^{+ve}BCL6^{+ve}$ Tfh cells were recorded and the gating strategy is displayed in Figure 2.5.

2.13 T cell functional analysis

Thawed PBMCs were incubated with 1 µl of Benzonase® Nuclease (Sigma-Aldrich) for 1 hour at 37°C in a humidified atmosphere of 5% CO_2. Post-incubation, 150 µl of PBMCs (1 x 10^6 cells/ml) was added to the wells of a 96-well U-bottom plate (Corning Inc., USA) pre-coated with 0.5 µg/ml anti-human CD3 monoclonal antibody (clone UCHT1; eBioscience™) and 5 µg/ml anti-human CD28 monoclonal antibody (clone CD28.2; eBioscience™). Following a 20-hour incubation at 37°C, 5% CO_2,10 µg/ml

brefeldin A from *P. brefeldianum*, 50 ng/ml phorbol 12-myristate 13-acetate (PMA) (Sigma-Aldrich) and 500 ng/ml ionomycin from *Streptomyces conglobatus* (Sigma-Aldrich) were added to the wells and the PBMCs were incubated for an additional 4 hours. Post-incubation, the cells were transferred to FACS tubes containing 500 µl of 1x PBS and centrifuged at 250 x *g* for 5 minutes at 4°C.

Once the supernatant was discarded, the pellets were resuspended and stained with 50 µl of LIVE/DEAD™ Fixable Near-IR Dead Cell Stain (diluted 1:50 with 1x PBS) and 2 µg/ml CD3 PEcy7 (clone UCHT1; eBioscience™) for 20 minutes in the dark at 4°C. The PBMCs were then washed with 500 µl of 1x PBS prior to being fixed and permeabilised using Reagent A and B, respectively (Life Technologies). To examine the frequency of IFNγ-producing Th1 cells, IL4-producing Th2 cells, IL17-producing Th17 cells and IL10-producing Tregs, PBMCs were intracellularly stained with anti-human monoclonal antibodies targeted against IL4, IL10, IL17A, IFNγ, TNFα, Foxp3 and RORγ for 30 minutes in the dark at RT (Table 1.3). Previously, it was reported that CD4 undergoes rapid internalisation in T cells in response to PMA treatment [398]. Thus, PBMCs were also intracellularly stained with 2 µg/ml CD4 BV421 (clone RPA-T4; BD Biosciences). Post-incubation, PBMCs were centrifuged (250 x *g*, 5 minutes, 4°C) with 500 µl of 1x PBS. After discarding the supernatant, the cell pellets were resuspended in 300 µl of 1x PBS for flow cytometric analysis.

2.14 Flow cytometry

Flow cytometric analysis of monocyte, DC and T cell subsets was performed on a CyAnADP™ benchtop flow cytometer (Beckman Coulter®, USA) using SUMMIT v4.3 software (Beckman Coulter®), while T cell function and B cell subset frequencies were

acquired on a MACSQuant Analyzer 10 benchtop flow cytometer (Miltenyi Biotec). Prior to data acquisition, fluorescence minus one controls were used to set the gates and concentration-matched isotype controls were used to monitor non-specific antibody binding (Table 1.4). Fluorescence spectral overlap was corrected via compensation during multi-colour flow cytometry. Monocyte, DC and T cell subsets were examined by gating on 5,000 $CD14^{+ve}$ monocytes, $Lin^{-ve}HLA\text{-}DR^{+ve}$ DCs, $CD3^{+ve}$ T cells and $CD19^{+ve}$ B cells based on forward scatter (FSC)/side scatter (SSC) properties (see Figures 2.1, 2.2, 2.5 and 2.6 for the gating strategies). The percentage of each subpopulation and phenotypic expression levels (mean fluorescent staining intensity (MFI)) of surface markers and intracellular cytokines were recorded for each antigen. Data files were exported and assessed using FlowJo software v10.8.1 (BD).

2.15 Calculating the immunological age (IMM-AGE) score

Eight immune cell types (T cells, naïve CD4 T cells, EM CD4 and CD8 T cells, EMRA CD8 T cells, $CD28^{-ve}$ CD8 T cells, $CD57^{+ve}$ CD8 T cells and Tregs) were selected to generate the Immunological Age (IMM-AGE) metric [399], which is a modified profile of the original 20 component scoring [400]. IMM-AGE scores were calculated by Dr Archana Sharma-Oates (University of Birmingham).

Isotype control	Clone	Manufacturer
Mouse IgG1κ efluor 450 violet	P3.6.2.8.1	eBiosciences™
Mouse IgG1κ FITC	P3.6.2.8.1	eBiosciences™
Mouse IgG1κ PE	P3.6.2.8.1	eBiosciences™
Mouse IgG1κ PEcy5	MOPC-21	Biolegend
Mouse IgG1κ PEcy7	P3.6.2.8.1	eBiosciences™
Mouse IgG1κ APC	MOPC-21	Biolegend
Mouse IgG1κ APCcy7	MOP-21	Biolegend
Mouse IgG2ακ PE	RMG2a-62	Biolegend
Mouse IgG2ακ PEcy7	104	Sigma-Aldrich
Mouse IgG2ακ APC	MOPC-173	Biolegend
Mouse IgG2ακ APCcy7	MOPC-173	Biolegend
Mouse IgG2bκ Pacific Blue™	MPC-11	Biolegend
Mouse IgG2bκ PE	MG2b-57	Biolegend
Mouse IgG2bκ PerCP/cy5.5	MPC-11	Biolegend
Mouse IgG2bκ APC	eBMG2b	eBiosciences™
Mouse IgMκ FITC	RMM-1	Biolegend
Rat IgG1κ PE	RTK2071	Biolegend
Rat IgG2aκ PE	RTK2758	Biolegend
Rat IgG2aκ APC	RTK2758	Biolegend

Table 1.4 Concentration-matched isotype controls for immunophenotyping.

2.16 NanoString nCounter® analysis

2.16.1 RNA extraction from PBMCs

RNA extractions were carried out by Benjamin Dugan (University of Birmingham) using the RNeasy Mini Isolation Kit (Qiagen). In brief, frozen PBMCs (3 x 10^6 cells/ml) were thawed on ice and transferred to 25 ml universal tubes containing 10 ml of ice-cold sterile 1x PBS prior to centrifugation at 300 x *g* for 10 minutes at RT. Post-spin, the

liquid was decanted and cell pellets were resuspended in 1 ml of ice-cold sterile 1x PBS. PBMCs were transferred to 1.5 ml nuclease-free microcentrifuge tubes (Corning Inc.) and spun at 100 x *g* for 3 minutes at RT using a benchtop centrifuge (Eppendorf, Germany) to pellet the cells and aspirate the liquid. The cells were lysed and homogenised with 350 µl of Buffer RLT containing 1% (v/v) β-mercaptoethanol (Sigma-Aldrich) for 10 minutes at RT. Then, 350 µl of 70% (v/v) ethanol was added to the PBMCs to ensure optimal binding conditions, after which 700 µl of the cell suspension was added to RNeasy Mini spin columns. Following centrifugation (8,000 x *g*, 15 seconds, 20°C), RNA bound to the spin column membrane was incubated with 80 µl of DNase I stock solution (diluted 8-fold with Buffer RDD) for 15 minutes at RT to remove residual DNA. Post-centrifugation, remaining contaminants were removed via two wash and centrifugation (8,000 x *g* for 15 seconds and 2 minutes at 20°C) steps where 350 µl of Buffer RW1 and 500 µl of Buffer RPE were added to the spin columns. Once the flow-through was discarded, 15 µl of RNase-free water was added directly to the spin column membranes and left to incubate for 5 minutes at RT. Post-incubation, the purified RNA was eluted in RNase-free water (15 µl) in 1.5 ml nuclease-free microcentrifuge tubes (centrifugation at 8,000 x *g* for 1 minute at 20°C). RNA quantity was assessed using a NanoDrop One Spectrophotometer (Thermo Fischer Scientific, USA), while the quality was determined on a 2100 Bioanalyzer (Agilent Technologies, USA) using Z100 Expert software vB.02.11.SI811 (Agilent Technologies). RNA samples were considered pure if the A260/280 and A260/230 ratios were between 1.8 and 2. Purified RNA samples were stored at -80°C prior to analysis.

2.16.2 NanoString nCounter® gene expression analysis

NanoString nCounter® was utilised for multiplex gene expression profiling in human RNA samples using the nCounter® Human PanCancer Immune Profiling Panel (Nanostring Technologies, USA). This panel consisted of 770 genes related to cytokine and chemokine signalling, cellular senescence, immune cell profiling, lymphoid cell function and innate and adaptive immune responses.

RNA hybridisation was performed by Birmingham Tissue Analytics on 80 ng of total RNA. To begin, 70 µl of hybridisation buffer (NanoString nCounter® Master Kit Prep Pack) was transferred to a tube containing 42 µl of Cancer Immune Reporter CodeSet (NanoString nCounter® XT CodeSet). The hybridisation master mix was inverted several times before the contents of the tube were spun down (400 x *g* for 8 seconds at 20°C). The hybridisation master mix (8 µl) was dispensed into each tube of a 0.2 ml nuclease-free 12-well notched strip tubes (NanoString nCounter® Master Kit Prep Pack) before 100 ng/ml RNA was added to the tubes. Afterwards, 2 µl of Cancer Immune Capture ProbeSet (NanoString nCounter® XT CodeSet) was added to each tube. The tubes were then inverted and centrifuged (400 x *g*, 8 seconds, 20°C) before being placed in a pre-heated (65°C) Eppendorf Mastercycler® nexus eco thermal cycler (Eppendorf) with a heated lid at 70°C. After an 18-hour incubation at 65°C, the hybridisation complexes were loaded onto an nCounter® Prep Station for the removal of excess reporter and capture probes. During this time, hybridised RNA-probe complexes were immobilised and aligned on a loaded nCounter® cartridge for subsequent image acquisition on a nCounter® FLEX Digital Analyser (Figure 2.7).

Data quality control and analysis were performed on nSolver™ Analysis Software v4 (NanoString). Data was normalised to a set of positive controls and housekeeping genes, after which mean expression levels and log2 fold-change were calculated for each gene. A heatmap was generated in Rstudio software v2022.12.0+353 (Posit, PBC, USA) by Dr Jack Sullivan (University of Birmingham) using log2 fold-change values to visualise differential gene expression patterns between young and old adults with low and high microbial translocation. Genes were included if p-values were statistically significant.

2.16.3 Pathway enrichment analysis

Pathway enrichment analysis was performed by Dr Jack Sullivan (University of Birmingham) on a subset of genes that were significantly differentially expressed between young adults with low microbial translocation and older adults with high microbial translocation in Rstudio software v2022.12.0+353 using the Reactome PA package v3.16 [401]. Genes were selected based on p-value and known biological relevance to adaptive immune ageing. Entrez gene IDs were obtained via the org.Hs.eg.db package v3.17 [402].

2.17 Stool sample collection and storage

All participants were sent stool collection kits containing a faecal catcher (Fe-Col®; Alpha Laboratories Ltd, UK), a faecal collection container (Sarstedt Ltd), a pair of gloves and a clear bag with instructions via post, prior to the visit at the University of Birmingham Research Labs in the QE Hospital. All participants were instructed to collect stool samples within a 24-hour window of their appointment and store it at RT before being brought along to the visit [403]. All faecal collection containers containing

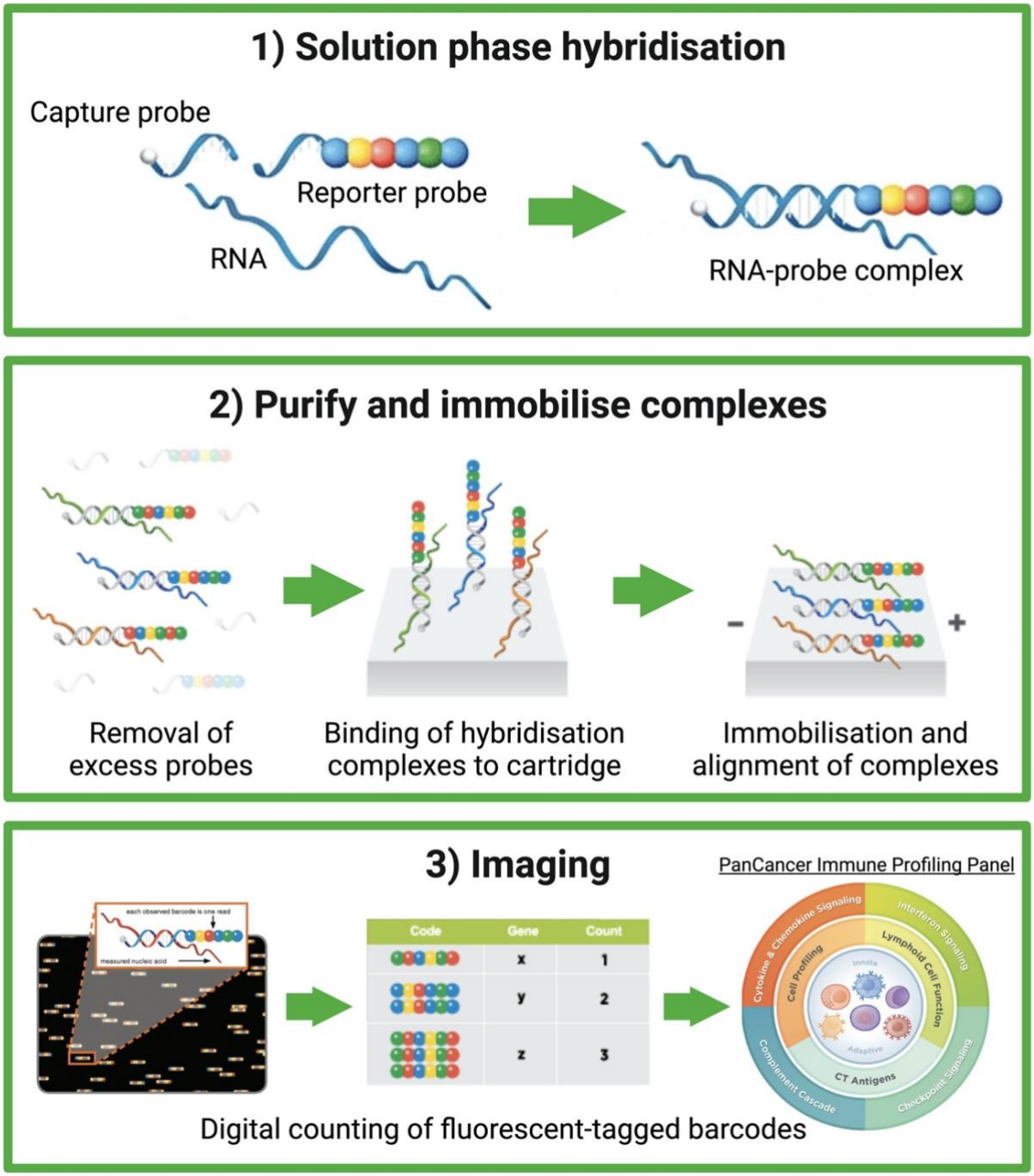

Figure 2.7 Overview of NanoString nCounter® technology. RNA is tagged with a capture probe and a reporter probe, forming an RNA-probe complex. Following hybridisation, excess probes are removed and the purified hybridisation complexes are immobilised and aligned on a nCounter® cartridge for imaging. The cartridge is then scanned by an automated fluorescence microscope, which counts fluorescent-tagged barcodes attached to the RNA-probe complexes. Each barcode represents a specific gene within the PanCancer Immune Profiling Panel, enabling digital quantification of different innate and adaptive immune cell types and genes associated with immune responses, including senescence, cytokine signalling and pathogen defence. Figure adapted from the NanoString webpage [404].

stool sample were weighed using a weighing scale and weights were recorded. Faecal samples were aliquoted into 1.5 ml microcentrifuge tubes using a stainless-steel spatula (Fischer Scientific) and stored at -80°C until analysis of faecal microbiota composition and microbial metabolite profiling [403].

2.18 Assessing the intestinal microbial metabolite profile

Faecal SCFA (acetate, butyrate and propionate) and secondary bile acid (DCA, glycodeoxycholic acid (GDCA), hyodeoxycholic acid (HDCA), LCA and ursodeoxycholic acid (UDCA)) concentrations were assessed in young and old participants via liquid chromatography-mass spectrometry (LC-MS).

2.18.1 Stool supernatant isolation

Thawed stool (100 mg) was transferred to 1.5 ml screw top tubes with O-ring screw caps (Scientific Laboratory Supplies Ltd, UK) containing 5-10 ceramic beads (VWR International). 1 ml of methanol:water (9:1, v/v) was added to the tubes; then, the stool samples were homogenised in a MaxQ™ 6000 incubated shaker (Thermo Fischer Scientific) at 500 rpm for 30 minutes at 20°C. Isolated stool supernatant (500 µl) was transferred to new 1.5 ml screw top tubes with O-ring screw caps, which were stored at -80°C prior to sample preparation by the Quadrum Institute (Norwich, UK).

Frozen stool supernatant samples were thawed and 25 µl of 40 µg/ml D4-glycocholic acid was added to each tube. Mixtures were then passed through a 10 mg capacity Oasis PriME HLB 96-well cartridge (Waters™, UK) to remove phospholipids before LC-MS.

2.18.2 Liquid chromatography-mass spectrometry

Frozen faecal samples were sent to the Quadrum Institute for the analysis of SCFAs via LC-MS. To prepare the samples, 1 ml of extraction solvent (0.5% (v/v) orthophosphoric acid) was added to each tube followed by 25 µl of 5 mg/ml D4-acetic acid and 5 mg/ml D2-proprionic acid in 0.5% (v/v) orthophosphoric acid. After adding 5-10 ceramic microbeads, the tubes were shaken at 2,500 rpm for 10 minutes at RT. The samples were centrifuged at 13,000 rpm for 10 minutes at RT, after which 400 ul of supernatant was passed through a Mini-UniPrep filter vial (0.45 µm; Whatman plc, UK).

LC-MS was carried out on purified faecal samples and stool supernatant samples alongside a set of internal standards (D4-acetic acid, D2-propionic acid and D4-glycocholic acid) using an ACQUITY ultra-high performance liquid chromatography system (Waters™) coupled to a Xevo TQ-S micro triple quadrupole mass spectrometer (Waters™). The mass spectrometer was operated in positive multiple reaction mode for SCFA quantification (Table 1.5), while negative electrospray selected ion monitoring mode was used for D4-glycocholic acid (m/z 468.2), DCA and UDCA (m/z 391.2) and LCA (m/z 375.2) during secondary bile acid analysis. For the assessment of SCFAs, 2 µl of sample was injected into a Kinetex® 1.7 µm PFP 100 Å LC column (30x2.1 mm) (Phenomenex, USA). Liquid chromatography separation was carried out by pumping solvent A (0.1% (v/v) formic acid in water) and solvent B (0.1% (v/v) formic acid in acetonitrile) at a flow rate of 0.15 ml/min with a column temperature of 35°C. Metabolites were separated using a binary gradient under the following elution conditions: 0% of solvent B at injection for 1 minute, 30% of solvent B at 2.8 minutes, 60% of solvent B at 4 minutes and 100% of solvent B from 4.1 minutes to 7 minutes.

All samples were quantified to a limit of quantification of 25 µg/ml in final solution for each targeted acid. D4-acetic acid was used as an internal standard for acetate, while D2-propionic acid was used as an internal standard for propionate and butyrate.

For the quantification of secondary bile acids, 5 µl of purified stool supernatant was injected into an Ascentis® Express C18 2.7 µm column (150x4.6 mm; Supelco, USA), which was equilibrated to initial conditions for 5 minutes. Chromatography was achieved using a binary gradient of solvent A (5 mM ammonium acetate and 0.012% (v/v) formic acid in water) and solvent B (5 mM ammonium acetate and 0.012% (v/v) formic acid in methanol) with a flow rate of 600 µl/min and a column temperature of 40°C. Sample injection was made at 50% solvent B and held for 2 minutes before being ramped to 95% solvent B at 20 minutes and held up to 24 minutes.

Metabolite	Parent ion	Fragment ion	Cone voltage	Collision energy
Acetate	61.06	43	20	8
Propionate	75.09	29	20	12
Butyrate	89.12	43	20	10
D4-acetic acid	64.06	45.9	25	10
D2-propionic acid	77.09	31	20	12

Table 1.5 Multiple reaction mode mass spectrometry conditions.

2.19 Gut microbiota composition analysis

Relative microbial abundances and microbial diversity in human faecal samples were determined via 16S ribosomal RNA (rRNA) gene sequencing of isolated stool DNA using MiSeq Illumina.

2.19.1 Stool DNA isolation

Frozen stool samples were thawed, prior to transferring 400 mg of stool to 1.5 ml nuclease-free microcentrifuge tubes. Stool aliquots were then incubated with 1 ml of DNA/RNA Shield™ (Zymo Research, USA) for 1 hour at RT to inactivate the SARS-CoV-2 virus. Post-incubation, tubes were centrifuged at 12,400 x *g* for 5 minutes at 20°C and the liquid was aspirated.

DNA was extracted from stool samples using a commercially available FastDNA™ SPIN Kit for Soil (MP Biomedicals, USA) according to the manufacturer's instructions. To begin, 500 mg of stool was transferred to 2 ml lysing matrix E tubes containing 978 µl of sodium phosphate buffer and 122 µl of MT buffer. Faecal samples were homogenised in a FastPrep-24™ 5G bead beating grinder and lysis system (MP Biomedicals) at a speed setting of 6 m/s for 40 seconds. Lysates were then centrifuged at 12,400 x *g* for 15 minutes at 20°C and the pelleted debris was discarded. Supernatants were transferred to 2 ml nuclease-free microcentrifuge tubes containing 250 µl of protein precipitation solution. After inverting the tubes 10 times to mix, the samples were centrifuged at 12,400 x *g* for 5 minutes at 20°C to pellet the precipitate. Supernatants were transferred to 15 ml falcon tubes containing 1 ml of binding matrix solution. Then, the tubes were inverted for 2 minutes and the samples were left to rest for 3 minutes at RT before 500 µl of supernatant was discarded. The binding matrix was resuspended in the remaining supernatant, after which 600 µl of the mixture was transferred to SPIN™ filter tubes. Post-centrifugation (12,400 x *g*, 1 minute, 20°C), the flow-through was decanted and the pellets were resuspended with 500 µl of prepared SEWS-M solution. After two more centrifugations at 12,400 x *g*, DNA bound to binding matrix was left to air dry for 5 minutes at RT. The purified DNA was eluted in 50 µl of

DNase/pyrogen-free water in 1.5 ml nuclease-free microcentrifuge tubes (centrifugation at 12,400 x *g* for 1 minute at 20°C).

DNA concentrations were determined on a calibrated Qubit 4 Fluorometer (Invitrogen™) using standard samples with known concentrations (Qubit™ dsDNA Broad Range Assay Kit; Invitrogen™). DNA elutes were stored at -20°C prior to PCR amplification.

2.19.2 16S ribosomal RNA (rRNA) gene amplification via real-time quantitative polymerase chain reaction (RT-qPCR)

Real-time quantitative polymerase chain reaction (RT-qPCR) was used to amplify the V4 region of the 16S rRNA gene using 515F and 806R primers (Sigma-Aldrich) to create an amplicon library. Desalted primer pairs were custom designed and primer sequences can be found in Appendix 2. RT-qPCR reagents and their volumes are described in Table 1.6. Stool DNA samples (0.16-14.48 ng/µl) were amplified in triplicate with reaction volumes of 25 µl in a hard-shell low-profile 96-well PCR plate (Bio-Rad Laboratories) under the following PCR thermocycler conditions using a SensoQuest Basic Thermal Labcycler (with gradient; Geneflow Ltd, UK): initial denaturation at 94°C for 3 minutes followed by 35 cycles of denaturation at 94°C for 45 seconds, annealing at 50°C for 60 seconds, elongation at 72°C for 90 seconds and an extended elongation step at 72°C for 10 minutes.

After pooling triplicate PCR reactions, RT-qPCR products were purified using the GeneJET PCR Purification Kit (Thermo Scientific™, USA). In brief, a 1:1 volume of binding buffer was added to each PCR mixture followed by a 1:2 volume of 100% (v/v) isopropanol. After thoroughly mixing each sample, 800 µl of solution was transferred

to GeneJET purification columns (Thermo Scientific™), which were centrifuged at 16,900 x *g* for 60 seconds at 20°C. The flow-through was discarded and 700 µl of wash buffer (Thermo Scientific™) was added to each GeneJET purification column. Post-centrifugation (16,900 x *g* for 60 seconds at 20°C), the flow-through was decanted and the empty GeneJET purification columns were spun for an additional minute to remove residual wash buffer. All GeneJET purification columns were transferred to clean 1.5 ml microcentrifuge tubes. Then, 30 µl of nuclease-free water was added to the centre of each GeneJET purification column membrane before centrifugation at 16,900 x *g* for 1 minute at 20°C. Purified PCR elutes were stored at -20°C prior to use.

Reagent	Volume per reaction (µl)
Platinum Green Hot Start PCR 2X Master Mix	10
Forward primer (10 µM)	0.5
Reverse primer (10 µM)	0.5
Stool DNA	1
Nuclease-free water	13

Table 1.6 Real-time quantitative polymerase chain reaction (RT-qPCR) reagents mixture for 16S ribosomal RNA (rRNA) gene amplification.

2.19.3 Gel electrophoresis

Purified PCR products (30 µl each) were thawed and mixed with 10 µl of 6X TriTrack DNA loading dye (Thermo Scientific™). 40 µl of each PCR mixture and 1 µl of GeneRuler 1kb Plus DNA ladder (Thermo Scientific™) were loaded onto a 1% (w/v) agarose/TBE gel, which was electrophoresed for 35 minutes at 100 V and 400 amps using an Enduro™ mini power supply (Labnet International, Inc., USA). PCR products (approximately 300-350 base pairs) were visualised with a Fastgene® Blue LED Illuminator (Geneflow Ltd). The bands were excised using single edge razor blades

(VWR International Ltd) and transferred into pre-weighed 1.5 ml microcentrifuge tubes, which were weighed again.

The excised gel slices were purified from the agarose gel using the GeneJET Gel Extraction Kit (Thermo Scientific™) according to the manufacturer's instructions. In brief, a 1:1 volume of binding buffer (Thermo Scientific™) was added to each gel slice (volume:weight). Gel mixtures were then incubated for 10 minutes at 60°C with some agitation. Post-incubation, the tubes were vortexed and gel mixtures were loaded onto columns (Thermo Scientific™). Then, one gel volume of 100% isopropanol was added to each solubilised gel solution. After thoroughly mixing the samples, 800 µl of each gel solution was transferred to separate GeneJET purification columns (Thermo Scientific™), which were centrifuged at 16,900 x *g* for 1 minute at 20°C. The flow-through was decanted and 100 µl of binding buffer was added to each GeneJET purification column. Following centrifugation (16,900 x *g*, 1 minute, 20°C), the flow-through was discarded and 700 µl of wash buffer (Thermo Scientific™) was added to each GeneJET purification column, which were centrifuged at 16,900 x *g* for 1 minute at 20°C. The empty GeneJET purification columns were then centrifuged for an additional 1 minute to remove residual wash buffer. The GeneJET purification columns were transferred to clean 1.5 ml microcentrifuge tubes and 30 µl of nuclease-free water was added to the centre of each column membrane. All tubes were centrifuged for 1 minute and the purified DNA was stored at -20°C.

The quality of the DNA library was checked via TapeStation D1000 ScreenTape® (Agilent Technologies) using TapeStation Analysis Software A.02.02 (SR1) (Agilent Technologies). The samples were pooled into a 5 ml nuclease-free microcentrifuge tube (Fischer Scientific, UK), forming a 4 nM pooled DNA library for 16S rRNA

sequencing. High-thorough 16S rRNA sequencing on the Illumina MiSeq platform (Illumina, Inc., USA) was done by Genomics Birmingham (University of Birmingham) using 5 µl of 8 pM pooled DNA library and the MiSeq v2 500 sequencing kit (Illumina, Inc.). Sequencing was performed using paired end reads (500 cycles) and custom designed primers were spiked (20% of PhiX spike).

2.19.4 16S rRNA microbial analysis

16S rRNA sequencing data was analysed on the web-based Galaxy platform (version 23.01.dev0) using the Mothur toolset according to the online-based tutorial [405-407]. Paired-end reads were merged into contigs, which were subsequently trimmed and filtered based on a quality score to remove sequences with ambiguous bases and contigs longer than 275 bases. After removing duplicate sequences, unique sequences were aligned to the SILVA v132 reference alignment to improve clustering of the operational taxonomic units (OTUs) [408], using the Needleman-Wunsch algorithm. Poorly aligned sequences and artifact sequences were removed, while near-identical sequences were clustered using a threshold of 2 mismatches per every 100 bases. Next, taxonomic classification was performed using the SILVA v132 reference taxonomy and the Bayesian classifier. Following the removal of undesired sequences (i.e. chloroplast, mitochondria, unknown, archaea and eukaryotic sequences), bacterial sequences were clustered into OTUs at the phylum level using a 97% similarity threshold. Alpha diversity metrics (Chao1 richness index, Shannon evenness index, non-parametric Shannon diversity index, ACE index and Simpson index) were calculated. The following equations were used to calculate the relative abundances (%) of each phylum and genus.

- **Relative phylum abundance (%) =** [(Sum of phylum's OTUs) / (Sum of all phylum OTU counts)] x 100
- **Relative genus abundance (%) =** [(Sum of genus' OTUs) / (Sum of all genera OTU counts within a given phylum)] x 100

2.20 Haemagglutinin inhibition assay

Antibody titres against the influenza virus were measured in serum samples from older adults at baseline and 28 days post-influenza vaccination by the Clinical Immunology Service (UK). To begin, thawed serum samples (0.5 ml) were incubated with a 3:1 volume of receptor-destroying enzyme (RDE) from *Vibrio cholera* overnight in a water-bath at 37°C. The following day, RDE-treated sera were incubated for 30 minutes in a water-bath at 56°C to inactivate any remaining RDE [409]. RDE-treated sera were then diluted 20-fold and 5-fold with 1x PBS for influenza A and influenza B viruses, respectively, in preparation for the haemagglutination and haemagglutination inhibition (HAI) assays.

Both assays were performed by adding 50 µl of 1x PBS to the wells of 96-well microtiter U-bottom and V-bottom plates (Greiner Bio-One, Austria). Then, 50 µl of RDE-treated serum was dispensed into the first well of each row. A 2-fold serial dilution of the treated antisera was performed by transferring 50 µl of solution from the first well in each column through to the last well in each column. After discarding the final 50 µl of diluted solution, 50 µl of influenza A virus subtype H3N2 (4 haemagglutination units; NIBSC, UK) was dispensed into the serially diluted antisera wells of the U-bottom plates, while 50 µl of influenza A virus subtype H1N1 (NIBSC) and influenza B viruses (NIBSC) (4 haemagglutination units each) was added to the diluted antisera wells of the V-bottom

plates. The plates were then gently agitated and incubated for 30 minutes at RT to allow virus-antibody interactions. Post-incubation, 50 µl of 1% (v/v) guinea pig RBCs (Innovative Research, USA) was added to the serum-virus mixture in the U-bottom plates, while 50 µl of 0.75% (v/v) turkey RBCs (Innovative Research) was dispensed into the wells of the V-bottom plates. Following manual agitation, U-bottom plates containing guinea pig RBCs were incubated for 30 minutes at RT, while a 60-minute incubation at RT was used for V-bottom plates containing turkey RBCs. For influenza A virus subtype H3N2, haemagglutination and HAI assays were conducted in the presence of 20 nM oseltamivir carboxylate (Sigma-Aldrich) [410]. Post-incubation, the plates were examined for RBC haemagglutination and HAI antibody titres were interpreted as the highest dilution of antiserum required to completely inhibit haemagglutination. A ≥40 HAI titre threshold was used as a correlate of seroprotection [411].

2.21 Mouse experiments and thymus cryopreservation and cryosectioning

Animal procedures were approved by McMaster University's Animal Research Ethics Board and performed by Erica DeJong (Prof Dawn Bowdish's lab group, McMaster University) under guidelines set by the Institutional Animal Care and Use Committee and the Canadian Council for Animal Care. Wild-type young (10-16 week old) and aged (20-22 month old) female and male C57BL/6J mice were purchased (The Jackson Laboratory, USA) and housed in the McMaster University Central Animal Facility prior to experimentation. Germ-free aged (20-22 month old) female and male C57BL/6J mice were housed in pathogen-free conditions in the Gnotobiotic Facility at McMaster University and pathogen-free status was constitutively monitored via faecal sampling.

All mice were subjected to a 12-hour light-dark cycle at RT and fed an ageing diet Teklad 2014 (14% protein) ad libitum with access to exercise wheels. Mice were culled via cardiac puncture from the side ribcage under terminal anaesthesia. Murine thymuses and gastrointestinal tracts were dissected and placed in separate 50 ml falcon tubes containing RPMI-1640 medium supplemented with 2% (v/v) foetal calf serum (FCS) prior to cryopreservation.

Mouse thymuses were transferred into separate plastic Tissue-Tek® cryomold moulds (15x15x5 mm) (Sakura Finetek, Netherlands) and mounted in Tissue-Tek® optimal cutting temperature (OCT) compound. Gastrointestinal tracts were separated into small and large intestines by making two cuts: one above the stomach and the other just above the caecum (Figure 2.8A). After discarding the stomachs, the faecal content was expelled from mouse gastrointestinal tracts and the surrounding adipose tissue was carefully removed. The small and large intestines were then carefully coiled in separate plastic Tissue-Tek® cryomold moulds (15x15x5 mm) and mounted in Tissue-Tek® OCT compound (Figure 2.8B). OCT-embedded tissues were snap frozen on dry ice and stored at -80°C prior to cryosectioning.

Cryosectioning was carried out in a Leica CM1950 Cryostat (Leica Biosystems, Germany) with a chamber and block temperature of -20°C at the University of Birmingham. Tissue sections were cut randomly throughout the thymus and gut at a thickness of 7 µm and 40 µm. Three tissue sections (7 µm thick) per thymus were mounted onto a slide; while one young wild-type, one aged wild-type and one aged germ-free mouse gut section (7 µm thick) were mounted per slide. All slides were stored at -80°C before immunohistochemistry. On the other hand, 40 µm thick tissue

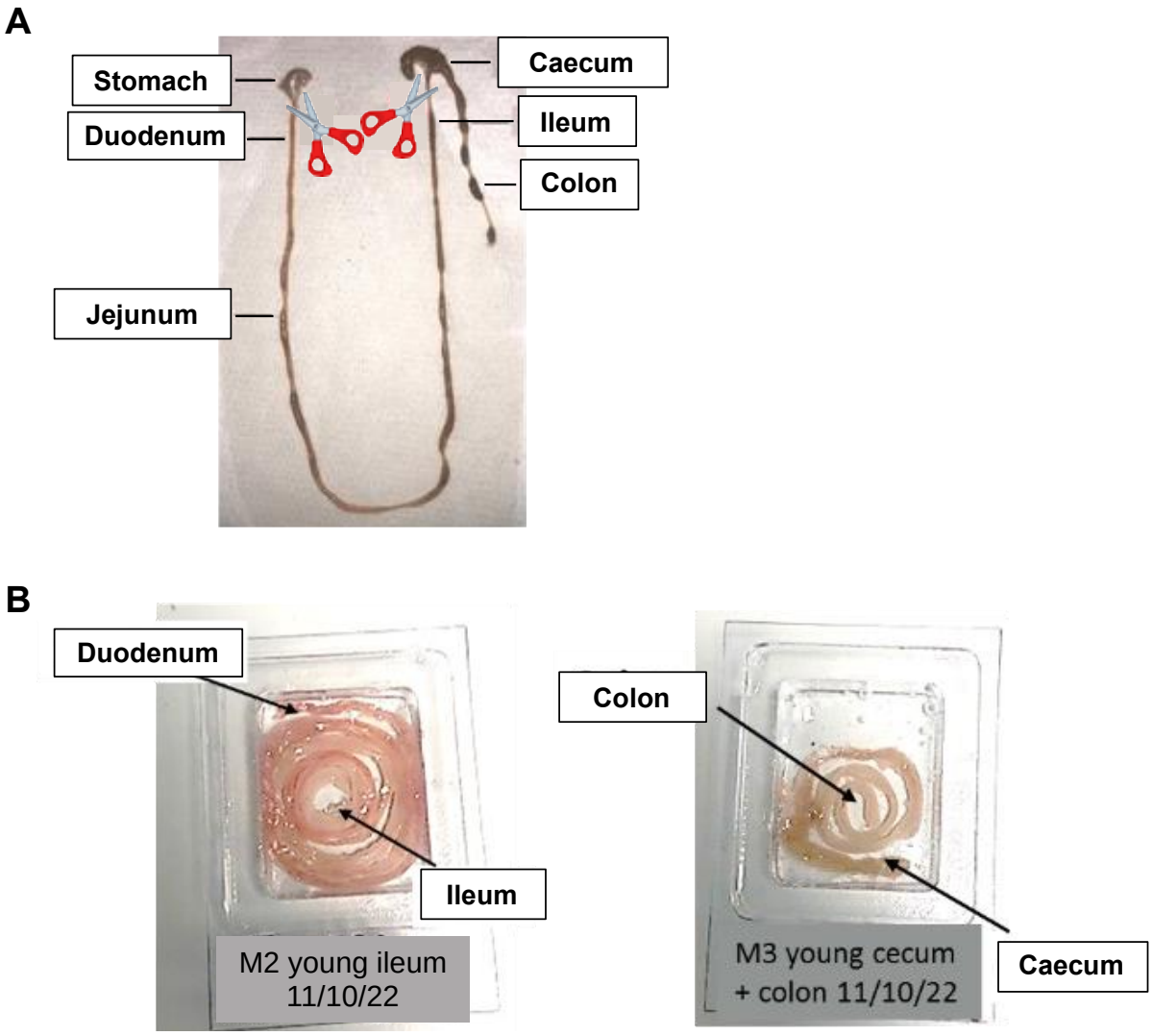

Figure 2.8 Cryopreservation of mouse intestines in OCT freezing medium. (A) Dissected mouse intestines were separated into the small and large intestines by cutting just below the stomach and above the caecum. **(B)** After removing the faecal content and the surrounding adipose tissue, the small and large intestines were carefully coiled and mounted in separate 15x15x5 mm plastic moulds containing OCT freezing medium.

sections were transferred into 1.5 ml nuclease-free microcentrifuge tubes and stored at -80°C prior to RNA isolation (Figure 2.9).

2.22 FITC-dextran trans-epithelial intestinal permeability assay

Mice were fasted (no food or water) for 4 hours prior to oral gavage of 200 µl of 80 mg/ml tracer labelled FITC-dextran (4kDa; Sigma-Aldrich) to assess *in vivo* intestinal permeability. After 4 hours, blood was collected and diluted 2-fold with 1x PBS. Fluorescent intensity was measured on a SpectraMax i3 microplate reader (Molecular Devices, USA) with an excitation wavelength of 493 nm and an emission wavelength of 518 nm by Erica DeJong (McMaster University).

2.23 Occludin staining for *ex vivo* intestinal permeability assessment

Small intestine-mounted slides were thawed at RT and fixed with ice-cold acetone (VWR International) for 10 minutes at -20°C in glass coplin staining jars (Fischer Scientific). Post-fixation, the slides were washed three times with 1x PBS (5 minutes each) and the tissues were blocked with 100 µl of 10% normal goat serum (NGS) in 1x PBS for 30 minutes at RT. The blocking solution was then decanted and the samples were incubated with 100 µl of anti-mouse occludin antibody diluted 50-fold with 1x PBST containing 1.5% NGS overnight in a humidified chamber at 4°C (Table 1.7). The following day, the slides were washed three times with 1x PBS for 5 minutes each and incubated with 100 µl of anti-mouse Alexa Fluor® 555 secondary antibody diluted 50-fold with 1x PBST containing 1.5% NGS (Table 1.8). After a 1-hour incubation in the dark at RT, the slides were washed with three changes of 1x PBS (5 minutes each) and the tissues were stained with 1 µg/ml DAPI solution (Thermo Fischer™) in 1x PBS for 10 minutes in the dark at RT. Post-incubation, the staining

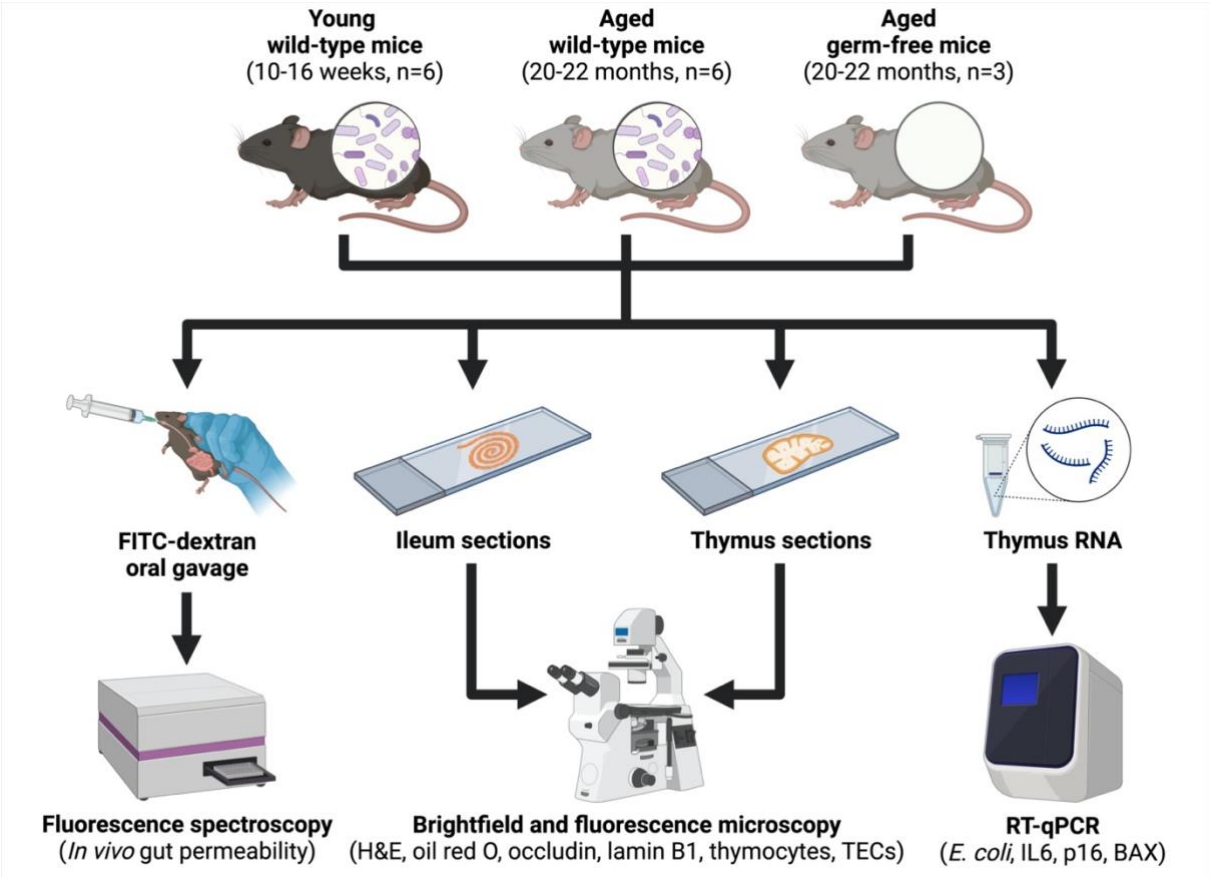

Figure 2.9 Mouse experimental design. Six young (10-16 weeks old) and six aged (20-22 months old) wild-type mice were maintained under conventional housing conditions, while three aged (20-22 months old) germ-free mice were housed under pathogen-free conditions prior to experimentation. Prior to sacrifice, FITC-dextran oral gavages were performed to assess *in vivo* intestinal permeability via fluorescence spectroscopy. Ileums and thymuses were collected from all sacrificed mice and cryosectioned. Ileum-mounted slides were examined for intestinal membrane permeability (occludin) via brightfield microscopy. Thymus-mounted slides were assessed for hallmarks of age-related thymic involution, including architectural changes (H&E), increased adiposity (oil red O), senescent cell accumulation (lamin B1) and thymocyte and TEC reduction, via a combination of brightfield, fluorescence and confocal microscopy. Additionally, RT-qPCR was performed to analyse relative mRNA expression levels of *E. coli*, pro-inflammatory cytokine IL6, senescent marker p16 and pro-apoptotic gene BAX in murine thymuses.

solution was poured off and the slides were thoroughly washed with 1x PBS. Immunoselect Antifading Mounting Medium (Dianova, Germany) followed by coverslips were applied to the slides. Once the slides had dried, clear nail varnish was applied along the perimeter of each coverslip to seal the slides prior to fluorescence microscopy.

2.24 Haematoxylin and eosin staining

Frozen microscope slides containing mouse thymus sections were thawed for 30 minutes at RT. The slides were then transferred to glass coplin staining jars and fixed with 10% (v/v) neutral buffered formalin (Sigma-Aldrich) for 10 minutes at RT prior to haematoxylin and eosin (H&E) staining. To begin, fixed slides were washed with two changes of tap water for 2 minutes each and stained with Harris Haematoxylin solution (Sigma-Aldrich) for 4 minutes at RT. The stained slides were rinsed with tap water for 2 minutes and differentiated in 1% (v/v) acid alcohol (Sigma-Aldrich) for 30 seconds at RT. After a 2-minute wash with tap water, the slides were incubated with Scott's Tap Water Substitute (Pioneer Research Chemicals Ltd, UK) for 30 seconds at RT, after which the wash step was repeated. The slides were then counterstained with eosin Y solution (Sigma-Aldrich) for 1 minute at RT and rinsed twice with tap water for 2 minutes. Finally, the tissues were dehydrated four times with absolute ethanol (VWR International) for 2 minutes each and the slides were cleared in three changes of xylene (Sigma-Aldrich) for 2 minutes. DPX mounting medium (Sigma-Aldrich) was placed on top of the tissue sections, after which glass coverslips (Fischer Scientific) were applied and left to dry overnight prior to brightfield microscopy.

2.25 Oil red O staining

Frozen microscope slides containing mouse thymus sections were thawed for 30 minutes at RT prior to staining for lipid droplets using an Oil Red O Staining Kit (Abcam). The slides were fixed with 300 µl of propylene glycol for 5 minutes at RT. After pouring off the fixative, the tissues were incubated with 300 µl of pre-heated (60°C) oil red O solution for 10 minutes at 60°C. Post-incubation, the liquid was poured off and the slides were differentiated in 300 µl of 85% (v/v) propylene glycol for 1 minute at RT. The slides were washed with two changes of distilled water for 5 minutes each prior to the addition of Immunoselect Antifading Mounting Medium and coverslips. Clear nail varnish was applied along the perimeter of each coverslip to seal the slides prior to brightfield microscopy.

2.26 Immunofluorescent staining of frozen thymus sections

Hallmarks of age-related thymic involution, including cellular senescence and the loss of thymocytes and TECs, were assessed in young and aged wild-type and aged germ-free mice via fluorescent and confocal microscopy following immunofluorescent staining of thymuses with anti-mouse antibodies against lamin B1, CD4, CD8, CD205, ERTR5 and AIRE.

2.26.1 Lamin B1 positive senescent cells

Thawed microscope slides containing mouse thymus sections were fixed with ice-cold acetone for 10 minutes at -20°C in a glass coplin staining jar and stained with 100 µl of recombinant anti-mouse lamin B1 antibody (1,000-fold dilution with 10% FCS and 0.2% triton-X 100 in 1x PBS) overnight in a humidified chamber at 4°C (Table 1.7). The following day, the slides were washed three times with 1x PBS (3 minutes each)

and incubated with 100 µl of anti-rabbit Alexa Fluor® 555 secondary antibody (300-fold dilution with 0.2% triton-X 100 in 1x PBS) for 1 hour in the dark at RT (Table 1.8). Post-incubation, the slides were washed three times with 1x PBS (3 minutes each) and the tissues were stained with 1 µg/ml DAPI in 1x PBS for 10 minutes in the dark at RT. After thoroughly washing the slides, Immunoselect Antifading Mounting Medium and coverslips were applied to the slides, which were left to dry for 30 minutes at RT. Clear nail varnish was then applied along the perimeter of each coverslip.

2.26.2 Thymocytes and thymic epithelial cells (TECs)

After thawing the slides for 30 minutes at RT, mouse thymus sections were fixed with ice-cold acetone for 10 minutes at -20°C, after which the tissues were stained with a combination of anti-mouse monoclonal antibodies against CD4, CD8α, ERTR5 and AIRE (Table 1.7). Following a 30-minute incubation in the dark at RT, the slides were washed with staining/wash buffer (three times, 3 minutes each) and incubated with several secondary antibodies (see Table 1.8) for 30 minutes in the dark at RT. The slides were washed three times with staining/wash buffer (5 minutes each) and incubated with 1 µg/ml DAPI solution in 1x PBS for 10 minutes in the dark at RT. After repeating the wash step, Immunoselect Antifading Mounting Medium and coverslips were applied, prior to the addition of nail varnish in preparation for confocal microscopy.

Primary antibody	Clone	Host/Isotype	Working concentration	Manufacturer
Occludin	E-5	Mouse IgG2bκ	4 µg/ml	Santa Cruz Biotechnology
Recombinant lamin B1	EPR22165-121	Rabbit IgGκ	0.32 µg/ml	Abcam
CD4 Alexa Fluor® 647	RM4-5	Rat IgG2aκ	2.5 µg/ml	Biolegend
CD8α biotin	53-6.7	Rat IgG2aκ	1.7 µg/ml	eBiosciences™
ERTR5	N/A	Rat IgMκ	N/A	Gifted by van Vliet *et al*. [155]
CD205 biotin	205yeka	Rat IgG2aκ	10 µg/ml	eBioscience™
AIRE Alexa Fluor™ 488	5H12	Rat IgG2acκ	10 µg/ml	Thermo Fischer Scientific
CD45 FITC	EM-05	Rat IgGκ	9.9 µg/ml	Novus Biologicals, LLC
Recombinant EpCAM Alexa Fluor® 647	EPR20533-63	Rabbit IgGκ	0.63 µg/ml	Abcam

Table 1.7 Anti-mouse primary antibodies for immunohistochemistry.

Secondary antibody	Clone	Host/Isotype	Working concentration	Manufacturer
Anti-rabbit Alexa Fluor® 555	H+L, $F(ab')_2$	Goat IgG	6.6 µg/ml	Cell Signalling Technology
Anti-mouse Alexa Fluor® 555	N/A	Goat IgG2b	40 µg/ml	Thermo Fischer Scientific
Streptavidin Alexa Fluor™ 555	N/A	N/A	2 µg/ml	Thermo Fischer Scientific
Anti-rat IgM Alexa Fluor™ 488	N/A	Goat IgG	2.5 µg/ml	Thermo Fischer Scientific
Anti-rat IgM Alexa Fluor™ 647	N/A	Goat IgG	10 µg/ml	Thermo Fischer Scientific

Table 1.8 Secondary antibodies for immunohistochemistry.

2.27 Brightfield microscopy

Brightfield microscopy was used to assess the architecture of H&E stained mouse thymuses and thymic adiposity of oil red O stained sections on a ZEISS Primovert inverted light microscope (Carl Zeiss AG, Germany). Six images were captured from multiple areas of the tissue at 4X, 10X and 40X magnification. Whole slide images of H&E stained thymuses were obtained using a ZEISS Axioscan Z1 slide scanner (Carl Zeiss AG) and the ratio of thymic cortical area to medullary area was calculated in ZEISS ZEN 2012 Blue Edition software v1.1.2.0 (Carl Zeiss AG). The number of oil red O stained lipid droplets per μm^2 was determined using ImageJ software v1.53 (National Institutes of Health, USA) [412]. To do this, oil red O stained lipid droplets were counted manually and the total number of lipid droplets was divided by the area of tissue that was analysed.

2.28 Fluorescence and confocal microscopy

Thymus samples were stained in triplicate and six images of the medullary and cortical regions were acquired on the microscope at 4X, 10X and 40X magnification. Lamin B1 stained slides were imaged on an Olympus IX71 inverted fluorescence microscope (Olympus Corporation, Japan) using Image-Pro® Plus software v7.0.1.658 (Media Cybernetics, Inc., USA), while slides stained with thymocyte and TEC markers were imaged on a ZEISS LSM 880 with Airyscan Fast confocal microscope using ZEISS ZEN 2012 SP1 Black Edition software v8.1.0.484 (Carl Zeiss AG). Prior to imaging, primary antibody only controls and secondary antibody only controls were used to detect possible non-specific binding and autofluorescence, respectively. Confocal microscope acquisition settings are described in Appendix 3. The percentage area stained and mean grey value of each antigen was calculated on ImageJ software;

mean grey value was used as a measurement of fluorescence staining intensity. First, images were spatially calibrated by setting the scale based on the embedded scale bar. Images were then converted to an 8-bit grayscale and thresholding was used to highlight antigen stained pixels and exclude background pixels.

2.29 RNA isolation from frozen mouse sections

Mouse thymus sections (40 µm thick) were weighed and homogenised with Buffer RLT (Qiagen) containing 1% (v/v) β-mercaptoethanol for 5 minutes using a 1 ml syringe (BD) and 1.5 inch needle (19 gauge; Terumo Corporations, Belgium). Lysates were centrifuged at 8,000 x *g* for 3 minutes at 20°C and supernatants were transferred to 1.5 ml RNase-free microcentrifuge tubes in preparation for RNA isolation as described in section 2.17.1. Purified RNA was eluted into 15 µl of RNase-free water, and RNA concentration and purity were determined on a NanoDrop One Spectrophotometer and a 2100 Bioanalyzer, respectively. RNA isolates were stored at -80°C for future use.

2.30 Transcriptome analysis of mouse thymuses via RT-qPCR

RT-qPCR was carried out on RNA isolated from mouse thymus samples alongside Nia Paddison Rees (University of Birmingham) using the iTaq™ Universal SYBR® Green One-Step Kit (Bio-Rad Laboratories) on a CFX384 Tough Real-Time PCR Detection System (Bio-Rad Laboratories). Primers were designed using NCBI Primer-BLAST with primer sequences shown in Table 1.9 [413]. To begin, 300 µl of RT-qPCR PCR master mix containing the reagents listed in Table 1.10 was prepared for each gene and loaded into the wells of a 384-well PCR plate (Thermo Fisher Scientific). RT-qPCR was performed in reaction volumes of 5 µl containing 5 ng/µl template RNA under the following thermocycler condition: 1) reverse transcription at 50°C for 10 minutes and

DNA polymerase activation at 95°C for 5 minutes, 2) 40 cycles of denaturation at 95°C for 10 seconds, annealing at 60°C for 30 seconds and initial elongation at 65°C for 31 seconds and 3) 60 cycles of extended elongation at 65°C for 5 seconds. All samples were assayed in triplicate and a no template control was included to monitor possible contamination and primer-dimer formation. Additionally, melting curve analysis was performed to validate primer specificity. Relative fold gene expression was calculated using the delta-delta cycle threshold ($2^{-\Delta\Delta Ct}$) method (see formulas below). Mean ΔCt values for each gene were normalised relative to mean ΔCt values for Epcam, which was used as a housekeeping gene given its high expression levels in murine thymuses and clean melting curve.

- **ΔCt =** mean Ct(gene of interest) – mean Ct(housekeeping gene)
- **ΔΔCt =** 2^-(ΔCt)
- **Relative fold gene expression =** ΔΔCt(sample) – median ΔΔCt(young wild-type mice)

Gene	NCBI reference	Forward primer sequence (5'-3')	Reverse primer sequence (3'-5')
IL6	NM_031168.1	CTGCAAGAGACTTCCATCCAG	AGTGGTATAGACAGGTCTGTTGG
p16	NM_001040654.1	TTGGCCCAAGAGCGGGGACA	GCGGGCTGAGGCCGGATTTA
BAX	NM_007527.4	AGGATGAGTCCACCAAGAAGCT	CATCTTCTTCCAGATGGTGA
Epcam	NM_008532.2	TTGCTCCAAACTGGCGTCTAA	GCAGTCGGGGTCGTACA

Table 1.9 RT-qPCR primer sequences for murine genes.

Reagent	Volume per reaction (µl)
One-step SYBR® green reaction mix	2.5
iScript reverse transcriptase	0.0624
Forward primer (20 µM)	0.1
Reverse primer (20 µM)	0.1
RNase-free water	1.236

Table 1.10 RT-qPCR reagents for transcriptional analysis of murine thymuses.

2.31 Statistical analysis

Statistical analysis was performed using a combination of GraphPad Prism® software and R software (https://www.r-project.org/). Data distribution was examined using Kolmogorov-Smirnov normality test before parametric and non-parametric tests were performed. Parametric tests were carried out on normally distributed data, while non-parametric tests were used when the data was not-normally distributed. Unpaired Student's T test (parametric test) and Mann-Whitney U test (non-parametric) were used to compare means between young and old adults. Afterwards, the Benjamini-Hochberg method was used to calculate adjusted p-values, controlling the false discovery rate at 1%. Chi-square test was used to compare categorical data, such as sex, smoking status and CMV IgG seropositivity status, between the groups. One-way analysis of variance (ANOVA) was used to compare means between young adults with low microbial translocation, old adults with low microbial translocation and old adults with high microbial translocation as well as means between young wild-type, aged wild-type and aged germ-free mice. Following one-way ANOVA, Bonferroni (parametric test) and Dunn's (non-parametric) multiple comparison tests were performed.

Spearman's correlation-based linear regression analysis was performed to determine the strength of associations between all combinations of intestinal barrier dysfunction surrogate markers, microbiota, microbial metabolites, dietary components, macro and micronutrients and hallmarks of immunesenescence with the support of Dr Animesh Acharjee (University of Birmingham) [414]. For pathway enrichment analysis, the Benjamini-Hochberg procedure was used to calculate adjusted p-values. Statistical significance was accepted as $p \leq 0.05$ for differences and correlations.

Chapter 3: Age-related intestinal permeability and microbial translocation play an integral role in thymic involution and T cell ageing

This chapter contains text written by Jessica Conway and edited by Dr Niharika A Duggal from the following manuscript.

Conway J, DeJong EN, White AJ, Dugan B, Paddison Rees N, Parnell SM, Lamberte L, Sharma-Oates A, Sullivan J, Mauro C, Willem van Schaik, Anderson G, Bowdish DME, Duggal NA. Age-related loss of intestinal barrier integrity plays an integral role in thymic involution and T cell ageing (In preparation).

3.1 Background

The gastrointestinal tract's epithelium represents the largest mucosal lining in the body that effectively limits the permeation of luminal microorganisms, antigens and toxins through its paracellular space, a process that is regulated by intercellular tight junctions [415]. Advancing age is accompanied by physiological changes to the intestine, including mucus layer thinning and remodelling of intestinal epithelial tight junction proteins, such as zonulin, which contribute towards the breakdown of intestinal barrier function in aged worms, flies, fish, rodents, non-human primates and humans [416]. Impaired intestinal barrier integrity in aged hosts creates an easy passage for commensal bacteria and their products, such as LPS, from the gut lumen into the bloodstream (referred to as a leaky gut) [362].

Age-related intestinal barrier dysfunction is closely linked to the progressive deterioration of systemic health and the gradual appearance of metabolic defects and behavioural impairments [417]. Moreover, recent evidence from animal studies indicate that microbial translocation is a major contributor to inflammageing and possibly a driver of age-related diseases [31,68,367]. Human intestinal barrier dysfunction, determined by elevated circulating LBP levels, is also associated with impaired physical function and inflammageing in healthy aged adults [418]. Therefore, it is of utmost importance that we develop a clear understanding of the relevance of intestinal barrier dysfunction in human ageing, particularly in driving chronic immune activation and cellular senescence which is still poorly understood.

Concurrently with changes to intestinal homeostasis, ageing is accompanied by remodelling of the immune system that attenuates the host's ability to mount robust

immune responses, resulting in an immunocompromised state, termed immunesenescence. One of the most striking features of immune ageing is the progressive shrinkage (involution) of the thymus that is characterised by the loss of thymocytes and TECs, expansion of perivascular spaces, increased thymic adiposity and the accumulation of senescent cells [164,166,177]. In addition to thymic architectural disorganisation, advancing age leads to alterations in the thymic stromal cell microenvironment, including elevated levels of thymopoiesis-suppressing cytokines (e.g. IL6) [163]. Together, these age-related changes compromise thymopoiesis, resulting in a reduced thymic output of naïve T cells and the homeostatic expansion of peripheral memory T cell subsets [186]. Further, chronic lifelong antigenic stimulation leads to the accumulation of senescent and exhausted T cells in the periphery [121,204], which impair tissue immunosurveillance and drive inflammageing in older adults. This is further exacerbated by the age-related expansion of pro-inflammatory Th17 cells and anti-inflammatory Tregs [203,212].

Despite these interesting findings, the relationship between intestinal barrier dysfunction and immune ageing is poorly understood. Therefore, in this chapter we aimed to identify key associations between microbial translocation and human T cell ageing. Further, we aimed to confirm a causal link between age-related gut leakage and thymic involution using an aged germ-free mouse model that is protected from intestinal membrane permeability.

3.2 Results

3.2.1 Ageing is accompanied by increased microbial translocation

Twenty-seven healthy young individuals (age range 19-37 years) and 55 community dwelling healthy old individuals (age range 63-84 years) were recruited into this study, from whom blood was collected to assess microbial translocation and immune cell profiles (Figure 3.1A). Occludin is an integral tight junction protein located on the basolateral membrane of intestinal epithelial cells (IECs), whose presence in the circulation is a biomarker of increased intestinal membrane permeability [419]. In this study, we found a significant age-associated increase in circulating occludin levels ($p < 0.0001$) (Figure 3.1B). Serum LBP is a surrogate biomarker of intestinal permeability and microbial translocation [418]. We observed elevated circulating LBP levels with age; however, this was not statistically significant ($p = 0.32$) (Figure 3.1C). sCD14 is shed from the surface of antigen-stimulated monocytes and was measured as a reactive biomarker of microbial translocation and subsequent monocyte activation in this study [420]. On assessment, we found a significant age-related increase in circulating sCD14 levels ($p = 0.01$) (Figure 3.1D).

We next investigated potential associations between markers of microbial translocation and potential drivers of increased gut permeability, including age, sex, BMI, diet, sedentary behaviour, sleep quality and mental health (Table 2.1). Interestingly, the strongest correlation that we observed in older adults was between elevated circulating LBP levels and dietary fibre intake ($R = -0.33$, $p = 0.04$) (Figure 3.1E).

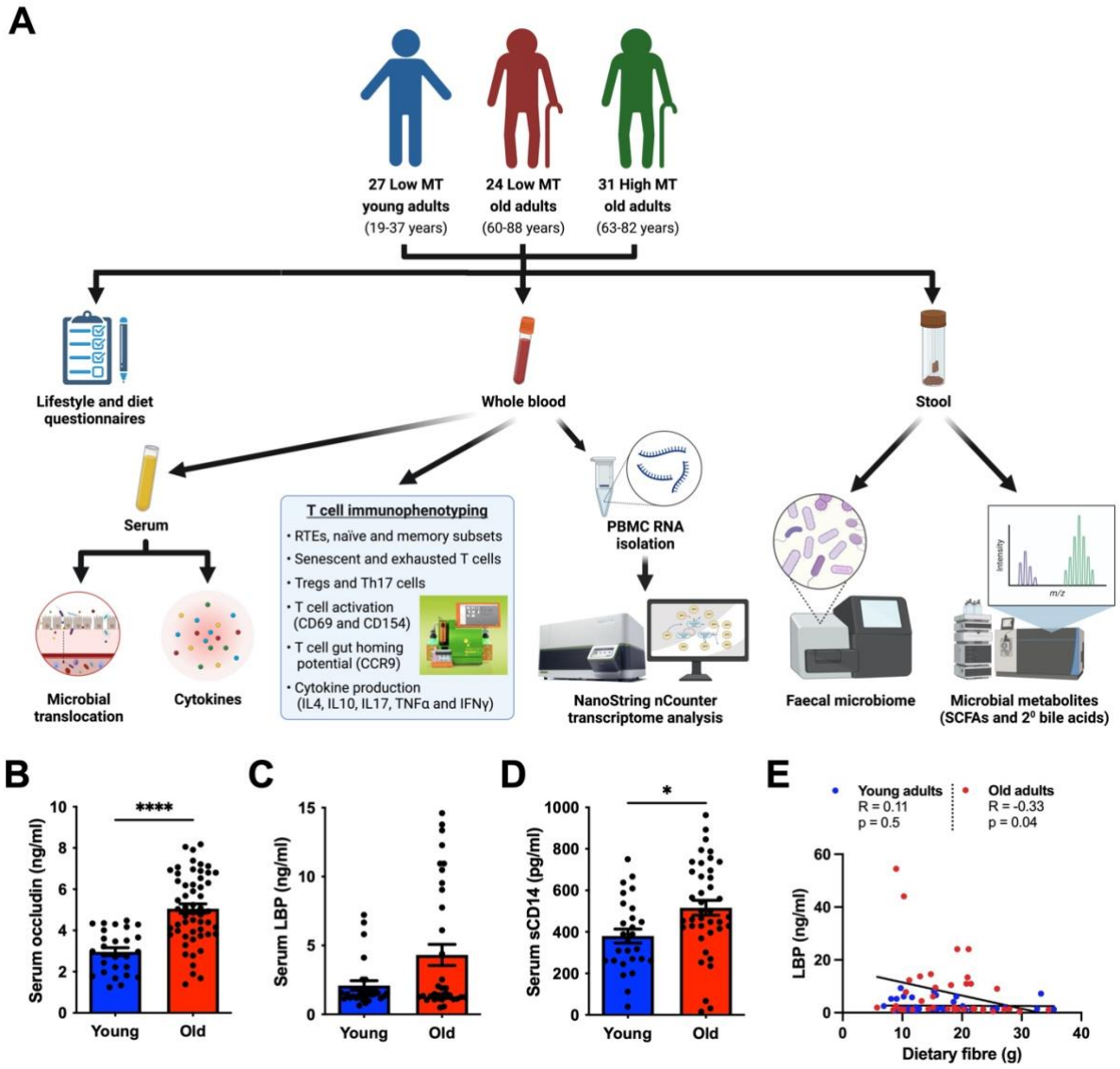

Figure 3.1 Age-related intestinal membrane permeability and microbial translocation. (A) Study design. Circulating levels of occludin **(B)**, LBP **(C)** and sCD14 **(D)** in young (n = 27) and old (n = 55) participants. Unpaired Student's T test and Mann-Whitney U test were used. *p ≤0.05, ****p ≤0.0001. **(E)** Spearman-based correlation between serum LBP levels and dietary fibre intake.

		Occludin (ng/ml)		LBP (ng/ml)		sCD14 (pg/ml)	
		R	**p**	**R**	**p**	**R**	**p**
Young adults (n = 27)	**BMI (kg/m^2)**	-0.02	0.92	**-0.4**	**0.05**	-0.12	0.59
	Sedentary TV viewing time (hrs)	-0.29	0.14	-0.35	0.08	**0.52**	**0.006**
	Sleep quality (PSQI)	-0.14	0.49	-0.11	0.57	-0.01	0.96
	HADS anxiety score	-0.08	0.68	-0.11	0.57	-0.1	0.62
	HADS depression score	-0.1	0.63	-0.12	0.56	-0.1	0.62
	MedDiet Score (MDS)	0.05	0.8	0.06	0.78	0.02	0.92
	Diet Quality Index (DQI)	-0.17	0.39	0.06	0.78	-0.22	0.27
Old adults (n = 55)	**BMI (kg/m^2)**	-0.08	0.6	-0.14	0.4	-0.04	0.79
	Sedentary TV viewing time (hrs)	-0.03	0.86	-0.19	0.24	-0.15	0.36
	Sleep quality (PSQI)	0.08	0.62	-0.2	0.21	-0.13	0.44
	HADS anxiety score	-0.25	0.13	0.14	0.4	-0.14	0.39
	HADS depression score	0.2	0.21	-0.14	0.4	-0.3	0.06
	MedDiet Score (MDS)	-0.3	0.06	0.24	0.14	0.25	0.13
	Diet Quality Index (DQI)	-0.07	0.68	-0.08	0.64	0.05	0.76

Table 2.1 Links between microbial translocation and lifestyle factors. Correlations (Spearman) between surrogate markers for microbial translocation (occludin, LBP and sCD14) lifestyle/behavioural parameters in young (n = 27) and old (n = 55) adults. Positive correlations are bold in green, while negative correlations are bold in red.

Older adults were split into two subgroups: low microbial translocation (MT) old (n = 24, age range 60-88 years) and high MT old (n = 31, age range 63-82 years) (Figure 3.1A). Low MT (similar levels to healthy young individuals) was defined as circulating occludin levels ≤4.5 ng/ml, which was the mean value observed in young participants. High MT was defined as circulating occludin levels >4.5 ng/ml. Demographic characteristics for each subgroup are shown in Table 2.2.

	Low MT young (n = 27)	**Low MT old** (n = 24)	**High MT old** (n = 31)	**P-values**		
				Low MT young vs Low MT old	**Low MT young vs High MT old**	**Low MT old vs High MT old**
Age (years)	25.8 ± 1	70.6 ± 1.6	73 ± 1	**<0.0001**	**<0.0001**	0.54
Male, n (%)	17 (37%)	11 (54%)	9 (29%)	0.22	**0.01**	0.2
BMI (kg/m^2)	26.5 ± 1.3	25.4 ± 1.4	24.4 ± 0.8	0.55	0.31	≥1
Smokers, n (%)	1 (4%)	0 (0%)	0 (0%)	0.34	0.28	≥1
Alcohol consumption (units per drink per week)	7.5 ± 1.6	8.2 ± 2.2	4.1 ± 1.2	≥1	0.22	0.29
Sedentary TV viewing time (hrs)	20.9 ± 1.8	17.4 ± 3.1	17.7 ± 2	0.52	0.38	≥1
PSQI score	4.6 ± 2.6	4.3 ± 0.5	5.1 ± 2.9	≥1	≥1	≥1
HADS anxiety score	6.2 ± 0.8	3.4 ± 0.5	2.9 ± 0.4	**0.02**	**0.0009**	≥1
HADS depression score	3 ± 0.6	1.6 ± 0.4	2.2 ± 0.5	0.76	≥1	≥1
MedDiet Score (MDS)	5 ± 0.5	7.1 ± 0.6	6.6 ± 0.5	**0.02**	**0.05**	≥1
Diet Quality Index (DQI)	62 ± 1.5	66.8 ± 1.5	64.6 ± 1.6	0.15	0.59	≥1
CMV IgG (antibody index)	0.8 ± 0.2	0.8 ± 3	0.8 ± 0.2	≥1	≥1	≥1
CMV IgG seropositivity, n (%)	10 (37%)	5 (21%)	10 (32%)	0.2	0.7	0.35

Table 2.2 Participant demographics. Data are mean ± standard error mean. One-way ANOVA with Bonferroni's multiple comparison test and Dunn's multiple comparison test along with Chi-square test were used. Significant p-values are highlighted in red.

3.2.2 Intestinal barrier dysfunction and the ageing gut microbiome

Age-related changes in microbiota composition and microbial metabolite profile are linked to intestinal barrier dysfunction in animals [68,421]. Upon assessment of the faecal microbiome, high MT older adults had a greater relative abundance of *Bifidobacterium* ($p = 0.03$) in stool compared to low MT older adults (Figure 3.2A). Interestingly, elevated circulating levels of LBP were strongly associated with the overrepresentation of *Escherichia-Shigella* ($R = 0.57$, $p = 0.0002$) (Figure 3.2B), *Peptostreptococcaceae* ($R = 0.57$, $p = 0.0002$) (Figure 3.2C) and *Paraprevotella* ($R = 0.37$, $p = 0.02$) (Figure 3.2D) in the aged faecal microbiome. Compared to young adults, older adults with low microbial translocation had decreased faecal levels of acetate and DCA, which were even lower in older adults displaying high microbial translocation ($p < 0.0001$ for all) (Figures 3.2E and 3.2F). Low faecal levels of SCFA propionate ($R = -0.37$, $p = 0.03$) and secondary bile acid GDCA ($R = -0.33$, $p = 0.04$) were strongly linked to elevated circulating levels of occludin in older adults (Figure 3.2G and 3.2H, respectively).

3.2.3 T cell immunesenescence and microbial translocation

In this study, we hypothesised that an increase in circulating microbial products would perpetuate repeated T cell activation, resulting in the accumulation of genotoxic damage, the subsequent differentiation of T cells and induction of replicative senescence, all recognised as features of T cell ageing. Therefore, we reasoned that older adults with lower levels of intestinal barrier leakage would exhibit fewer features of T cell ageing.

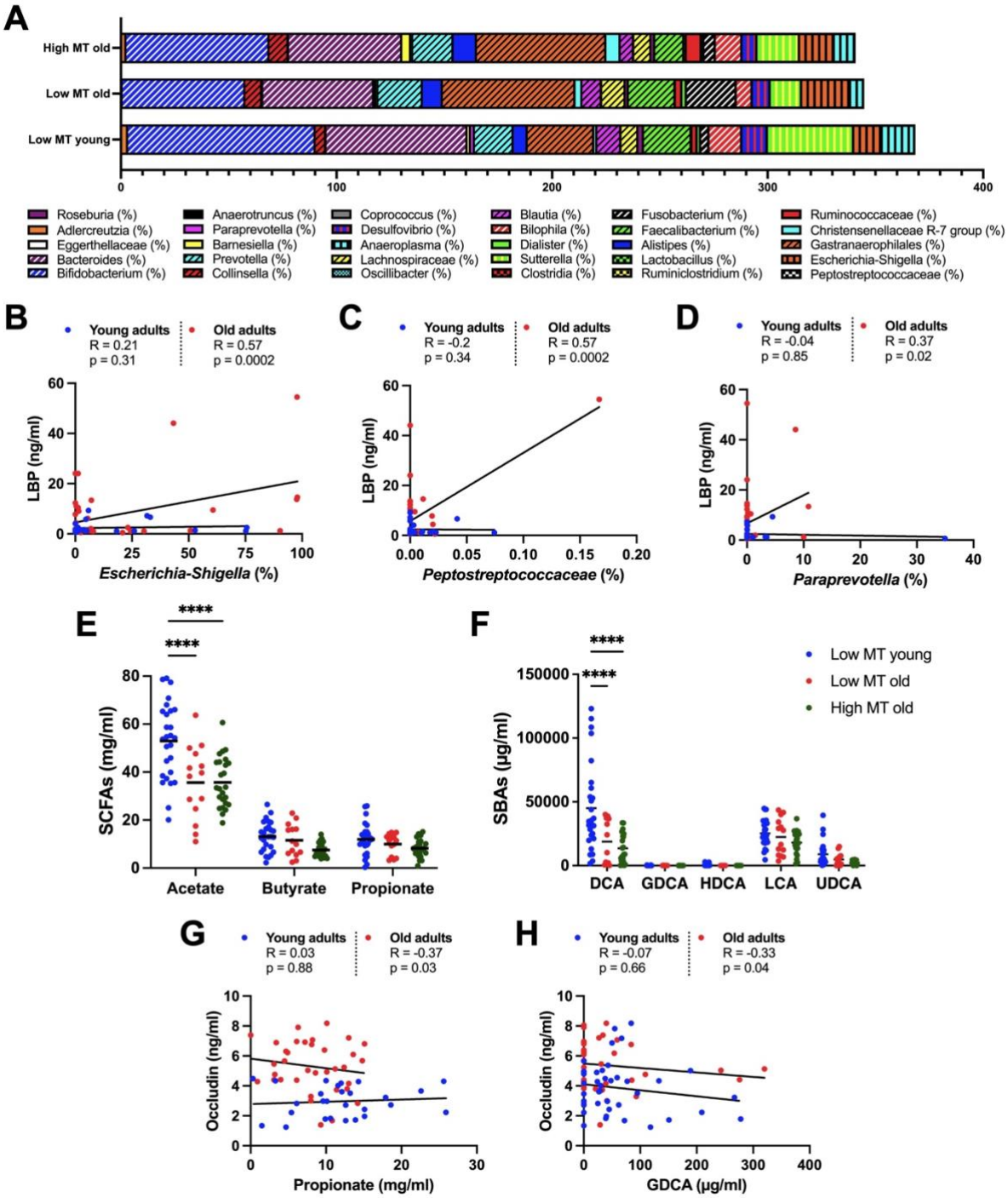

Figure 3.2 Links between age-related intestinal barrier dysfunction and the ageing gut microbiome. (A) Relative faecal abundances of bacteria expressed as percentages of each phylum in low MT young (n = 26), low MT old (n = 13) and high MT old (n = 25) adults. Spearman-based correlations between serum LBP levels and the relative abundances of *Escherichia-Shigella* **(B)**, *Peptostreptococcaceae* **(C)** and *Paraprevotella* **(D)** in the faecal microbiome. Faecal levels of SCFAs **(E)** and secondary bile acids **(F)** in low MT young (blue), low MT old (red) and high MT old (green) adults Spearman's correlations between serum occludin levels and propionate **(G)** and GDCA **(H)** levels in stool. **(E,F)** Means are shown as solid lines. One-way ANOVA with Bonferroni's multiple comparison test was used. ****p ≤0.0001.

Previous studies have reported an age-related decline in peripheral protein tyrosine kinase 7 (PTK7)$^{+ve}$CD45RA^{+ve} RTEs, which are antigenically naïve CD4 T cells that egress from the thymus into the periphery following intrathymic development and thus a surrogate marker for human thymic output [182]. Interestingly, we report that there is a significant reduction in the proportion of circulating RTEs in the presence of high microbial translocation in older adults ($p = 0.002$) compared to young participants, but not in those with low MT (Figure 3.3A). Older participants with high MT also presented with greater proportions of CM CD8 T cells ($p = 0.03$), EM CD4 and CD8 T cells ($p = 0.03$ and $p = 0.04$, respectively) (Tables 2.3 and 2.4) and terminally differentiated EMRA CD4 ($p < 0.0001$) and CD8 T cells ($p = 0.0005$) (Figures 3.3B and 3.3C, respectively), compared to low MT young individuals.

CD69 is an early activation marker expressed by activated lymphocytes [422]. Here, we observed an age-associated increase in the percentage of CD69^{+ve} CD8 T cells ($p = 0.01$), which was even greater in older adults displaying high MT ($p < 0.0001$) (Figure 3.3D), suggesting that translocated bacterial might induce polyclonal T cell activation.

Advancing age is accompanied by the loss of CD28 and the gain of CD57 expression on the surface of CD8 T cells (known markers of T cell senescence), which have low proliferative capacity and are highly pro-inflammatory [121]. In this study, we observed a significant increase in CD28^{-ve}CD57^{+ve} senescent CD8 T cells in older adults with high MT compared to old adults with low MT ($p = 0.04$) (Figures 3.3E and 3.3F). A similar increase in CD28^{-ve}CD57^{+ve} senescent CD4 T cells was seen in older adults displaying high MT relative to young adults ($p = 0.02$) (Table 2.3). Another hallmark of T cell immunesenescence is an increase in PD1^{+ve} exhausted CD8 T cells with

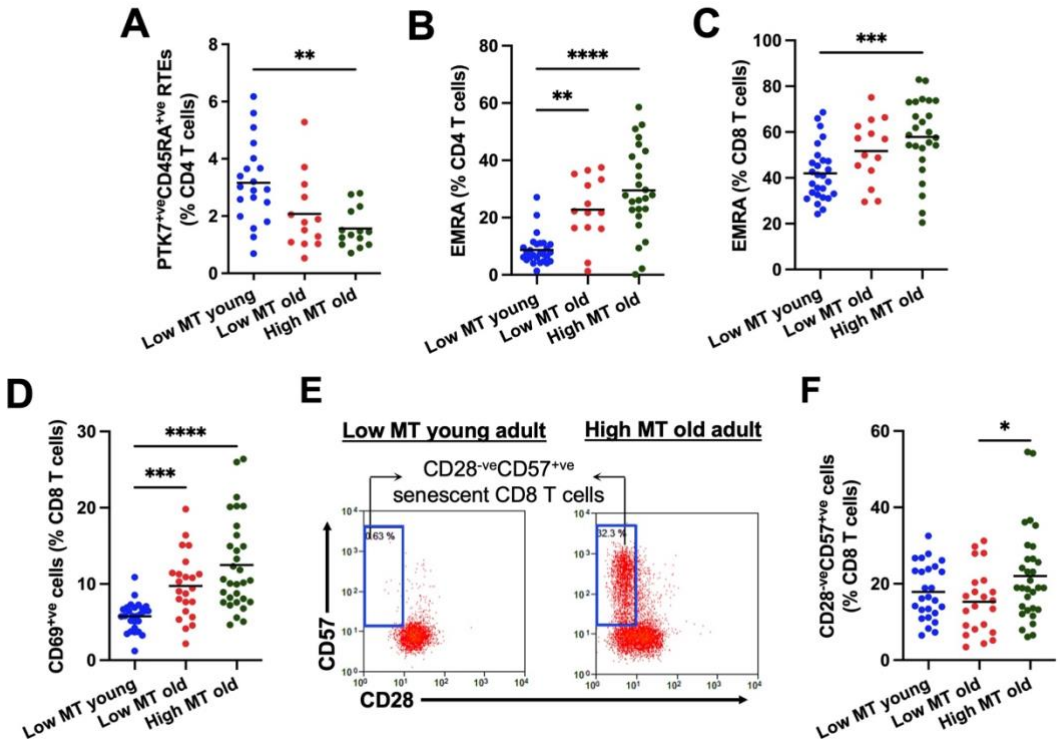

Figure 3.3 Age-related microbial translocation and T cell subset distribution. (A) The percentage of PTK7^{+ve}CD45RA^{+ve} RTEs in low MT young adults (n = 20), low MT old adults (n = 14) and high MT old adults (n = 15). The proportion of EMRA CD4 T cells **(B)**, EMRA CD8 T cells **(C)** and CD69^{+ve} CD8 T cells **(D)** in low MT young (n = 27), low MT old (n = 24) and high MT old participants (n = 31). **(E)** Representative flow cytometric plots showing CD28^{-ve}CD57^{+ve} senescent CD8 T cells in a young adult with low microbial translocation and a healthy old individual displaying high microbial translocation. **(F)** The peripheral frequency of CD28^{-ve}CD57^{+ve} senescent CD8 T cells. **(A-D,F)** Means are shown as solid lines. One-way ANOVA with Bonferroni's multiple comparison test and Dunn's multiple comparisons test were used. *p ≤0.05, ** p ≤0.01, ***p ≤0.001, ****p ≤0.0001.

	Low MT young (n = 27)	Low MT old (n = 24)	High MT old (n = 31)	P-values		
				Low MT young vs Low MT old	Low MT young vs High MT old	Low MT old vs High MT old
CD4 T cells (%)	38.9 ± 2	41.6 ± 3.3	47.6 ± 2.2	≥1	**0.02**	0.32
CD4 T cells (10^9/L)	0.5 ± 0.04	0.4 ± 0.1	0.5 ± 0.04	≥1	≥1	≥1
Naïve CD4 T cells (%)	50.9 ± 2.5	11.7 ± 2.4	18.8 ± 2.6	**<0.0001**	**<0.0001**	0.81
Naïve CD4 T cells (10^9/L)	0.3 ± 0.03	0.05 ± 0.01	0.1 ± 0.03	**<0.0001**	**<0.0001**	0.96
CM CD4 T cells (%)	16.1 ± 1.4	14.5 ± 2.9	12.3 ± 1.4	0.31	0.16	≥1
CM CD4 T cells (10^9/L)	0.08 ± 0.01	0.05 ± 0.01	0.06 ± 0.01	**<0.0001**	**<0.0001**	≥1
EM CD4 T cells (%)	27.9 ± 1.6	49.2 ± 3.1	35.7 ± 2.4	**<0.0001**	**0.03**	**0.0007**
EM CD4 T cells (10^9/L)	0.1 ± 0.01	0.2 ± 0.03	0.2 ± 0.02	**0.005**	0.14	0.39
EMRA CD4 T cells (%)	8.7 ± 1	22.8 ± 3	29.5 ± 3.1	**0.005**	**<0.0001**	0.82
EMRA CD4 T cells (10^9/L)	0.04 ± 0.002	0.1 ± 0.02	0.1 ± 0.02	**0.002**	**<0.0001**	0.4
Total memory CD4 T cells (%)	52.7 ± 2.5	86.5 ± 2.4	80.8 ± 2.4	**<0.0001**	**<0.0001**	0.87
Total memory CD4 T cells (10^9/L)	0.2 ± 0.02	0.4 ± 0.05	0.4 ± 0.04	**0.03**	**0.0006**	≥1
CD69^{+ve} CD4 T cells (%)	3.5 ± 0.4	5.7 ± 1.1	5.5 ± 0.4	0.18	**0.002**	0.91
CD154^{+ve} CD4 T cells (%)	28.3 ± 2.6	29.8 ± 2.5	31.6 ± 2.2	≥1	0.95	≥1
CD28^{-ve}CD57^{+ve} CD4 T cells (%)	12.3 ± 1.8	16.8 ± 4	27.2 ± 4.4	≥1	**0.02**	0.21
PD1^{+ve} CD4 T cells (%)	28.9 ± 2.6	32 ± 4.5	31.7 ± 2.3	≥1	0.67	≥1
Cytokine production						
IL4^{+ve} CD4 T cells (%)	6.1 ± 0.7	7.7 ± 1.7	7.7 ± 0.92	0.93	0.68	≥1
IL4 expression in CD4 T cells (MFI)	736 ± 65.2	650 ± 64.9	754.8 ± 65.4	≥1	0.42	0.25
IL10^{+ve} Tregs (%)	6.6 ± 1	10.4 ± 3.3	10.8 ± 1.6	≥1	0.2	0.14
IL10 expression in Tregs (MFI)	588.9 ± 52	507.6 ± 55.6	550.5 ± 40.3	≥1	≥1	≥1
IFNγ^{+ve} CD4 T cells (%)	15.8 ± 1.6	22.1 ± 2.4	18.8 ± 2	0.12	0.7	0.87
IFNγ expression in CD4 T cells (MFI)	1515 ± 141.1	1479 ± 178.2	1504 ± 128.4	≥1	≥1	≥1

Table 2.3 CD4 T cell subset distribution. Summary of differences in the distribution of naïve and memory CD4 T cell subsets between low MT young (n = 27), low MT old (n = 24) and high MT old (n = 31) individuals. Data are mean ± standard error mean. One-way ANOVA with Bonferroni's multiple comparison test and Dunn's multiple comparison test were used. Significant p-values are highlighted in red.

	Low MT young (n = 27)	Low MT old (n = 24)	High MT old (n = 31)	P-values		
				Low MT young vs Low MT old	Low MT young vs High MT old	Low MT old vs High MT old
CD8 T cells (%)	44.1 ± 1.6	41.9 ± 2.7	37.4 ± 1.8	≥1	**0.03**	0.41
CD8 T cells (10^9/L)	0.5 ± 0.04	0.4 ± 0.05	0.4 ± 0.03	0.47	**0.03**	≥1
Naïve CD8 T cells (%)	41.7 ± 2.5	11.8 ± 1.6	10 ± 1.1	**<0.0001**	**<0.0001**	≥1
Naïve CD8 T cells (10^9/L)	0.2 ± 0.02	0.04 ± 0.01	0.05 ± 0.01	**<0.0001**	**<0.0001**	≥1
CM CD8 T cells (%)	4.8 ± 0.6	8.8 ± 1.9	10.9 ± 1.8	0.36	**0.03**	≥1
CM CD8 T cells (10^9/L)	0.02 ± 0.01	0.03 ± 0.01	0.04 ± 0.01	≥1	0.34	≥1
EM CD8 T cells (%)	12.2 ± 1	27.5 ± 2.6	19.6 ± 2.6	**<0.0001**	**0.04**	0.06
EM CD8 T cells (10^9/L)	0.07 ± 0.01	0.09 ± 0.01	0.06 ± 0.01	0.55	≥1	0.77
EMRA CD8 T cells (%)	42 ± 2.3	51.7 ± 3.8	57.9 ± 3.3	0.11	**0.0005**	0.41
EMRA CD8 T cells (10^9/L)	0.2 ± 0.02	0.2 ± 0.03	0.2 ± 0.02	≥1	≥1	≥1
Total memory CD8 T cells (%)	61.4 ± 2.6	86 ± 1.8	89.1 ± 1.1	**<0.0001**	**<0.0001**	≥1
Total memory CD8 T cells (10^9/L)	0.3 ± 0.03	0.4 ± 0.05	0.3 ± 0.04	0.66	≥1	≥1
CD69^{+ve} CD8 T cells (%)	5.8 ± 0.4	9.7 ± 0.9	12.5 ± 1.1	**0.001**	**<0.0001**	0.56
CD154^{+ve} CD8 T cells (%)	21 ± 1.8	24.7 ± 3	26.7 ± 1.8	0.91	0.1	≥1
PD1^{+ve} CD8 T cells (%)	16 ± 1.3	25.6 ± 4.5	20.7 ± 2.2	**0.04**	0.4	0.55
Cytokine production						
IFNγ^{+ve} CD8 T cells (%)	12.3 ± 1.6	14.4 ± 2	15.1 ± 1.6	≥1	0.55	≥1
IFNγ expression in CD8 T cells (MFI)	1175 ± 110.2	1171 ± 174	1229 ± 111.3	≥1	≥1	0.79
TNFα^{+ve} CD8 T cells (%)	3.7 ± 0.4	3.7 ± 0.5	3.4 ± 0.4	≥1	≥1	≥1
TNFα expression in CD8 T cells (MFI)	441.1 ± 79.2	333 ± 56.8	424.1 ± 62.9	≥1	≥1	≥1

Table 2.4 CD8 T cell subset distribution. Summary of differences in the distribution of naïve and memory CD8 T cell subsets between low MT young (n = 27), low MT old (n = 24) and high MT old (n = 31) individuals. Data are mean ± standard error mean. One-way ANOVA with Bonferroni's multiple comparison test and Dunn's multiple comparison test were used. Significant p-values are highlighted in red.

reduced cytotoxic capability and reduced proliferative potential [204]. Older adults with low MT possessed significantly greater percentages of $PD1^{+ve}$ CD8 T cells compared to young adults ($p = 0.04$), but not older donors with high MT ($p = 0.55$) (Table 2.4).

CD4 T helper cells are important mediators of inflammatory responses, secreting effector cytokines upon activation. Retinoic acid-related orphan receptor gamma $(ROR\gamma)^{+ve}$ Th17 cells, defined by their ability to secrete IL17, are pro-inflammatory and have been associated with several autoimmune disorders [423]. Upon examination of CD4 T helper cell subsets, we observed comparable proportions of $ROR\gamma^{+ve}$ Th17 cells ($p = 0.94$) (Figure 3.4A) between the three participant groups, but older adults with increased microbial translocation had higher intracellular IL17 expression levels than young and old participants displaying low MT ($p = 0.04$ for both) (Figure 3.4B).

$CD25^{+ve}Foxp3^{+ve}$ Tregs are another subpopulation of CD4 T helper cells that maintain homeostasis and immune tolerance through the secretion of the anti-inflammatory cytokine IL10 [424]. In this study, the peripheral frequency of $CD25^{+ve}Foxp3^{+ve}$ Tregs was significantly higher in high MT older adults compared to young and old participants with low MT ($p < 0.0001$ and $p = 0.01$, respectively) (Figure 3.4C). However, the proportion of anti-inflammatory IL10-producing Tregs ($p = 0.21$) (Figure 3.4D) and intracellular IL10 expression levels (Table 2.3) were similar between the three groups. Treg expansion is thought to occur as a compensatory mechanism against a pro-inflammatory cytokine milieu, as is the case with advancing age. Interestingly, peripheral LBP levels were positively associated with the accumulation of IL10-expressing Tregs in older people ($R = 0.57$, $p = 0.0003$) (Figure 3.4E).

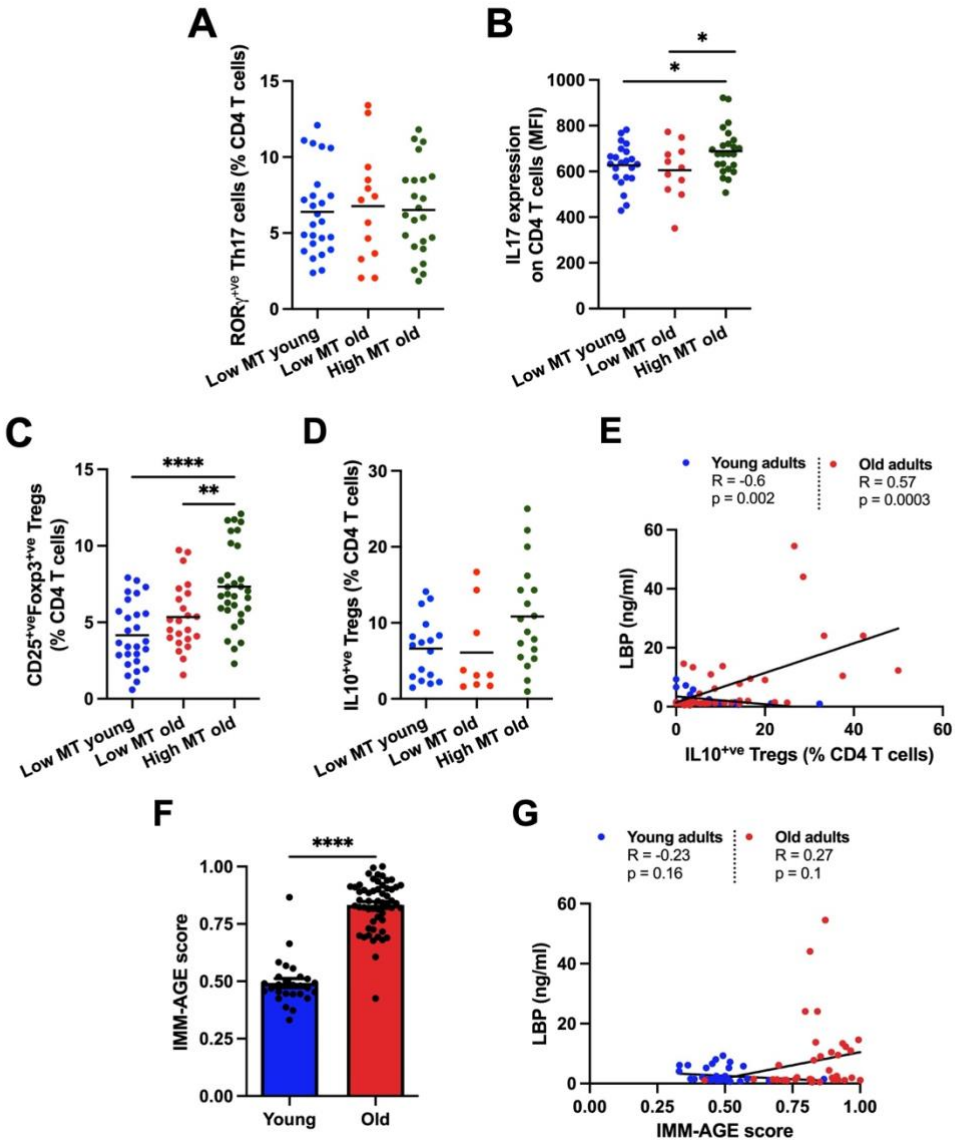

Figure 3.4 Age-related microbial translocation and T cell ageing. (A) The percentage of RORγ^{+ve} Th17 cells in low MT young adults (n = 25), low MT old adults (n = 13) and high MT old adults (n = 23). **(B)** Intracellular IL17 expression levels (MFI) in CD4 T cells. The peripheral frequency of CD25^{+ve}Foxp3^{+ve} Tregs **(C)** and IL10-expressing CD25^{+ve}Foxp3^{+ve} Tregs **(D)**. **(E)** Spearman's correlation between circulating LBP levels and the accumulation of IL10-producing Tregs in young (blue, n = 27) and old (red, n = 40) participants. **(F)** Comparison of immunological age (IMM-AGE score) between young and old volunteers using the Unpaired Student's T test. **(G)** Spearman's rank-based correlation plot depicting an association between systemic LBP levels and the IMM-AGE score. **(A-D,F)** Means are shown as solid bars. **(A-D)** One-way ANOVA with Bonferroni's multiple comparison test and Dunn's multiple comparisons test were used. *p ≤0.05, **p ≤0.01, ****p ≤0.0001.

On assessing the impact of microbial translocation on serum cytokine levels, circulating concentrations of IL1β, IL4, IL6, IL15, IL17, TNFα, CRP, IFNγ, CXCL9 and GM-CSF were unaltered by advancing age and the presence of intestinal barrier dysfunction (Table 2.5), contradicting earlier reports of elevated pro-inflammatory cytokine levels in older people [31]. Several reasons for this discrepancy are that our older participants are healthy and inflammageing typically arises in aged individuals after 80 years of age.

3.2.4 Links between microbial translocation and the IMM-AGE score

The IMM-AGE score is a recently developed metric that describes an individual's cellular immune profile in relation to their chronological age and has been recognised as a reliable predictor of all-cause mortality in older adults [400]. Here, we used a modified version that requires only eight T cell subsets: total T cells, naïve CD4 T cells, EM CD4 and CD8 T cells, EMRA CD8 T cells, $CD28^{-ve}$ CD8 T cells, $CD57^{+ve}$ CD8 T cells and Tregs [399]. This modified version was developed to minimise the number of immunological markers and is based on earlier data that shows that these eight parameters strongly influence the IMM-AGE score [399,425]. IMM-AGE scores were significantly higher in older adults relative to young controls ($p < 0.0001$) (Figure 3.4F). When investigating potential associations between the IMM-AGE score and markers of gut permeability and microbial translocation, we found that a high IMM-AGE score was positively correlated with circulating LBP levels ($R = 0.27$, $p = 0.05$) (Figure 3.4G).

	Low MT young (n = 15)	Low MT old (n = 14)	High MT old (n = 20)	P-values		
				Low MT young vs Low MT old	Low MT young vs High MT old	Low MT old vs High MT old
IL1ß (pg/ml)	7.9 ± 2.7	6 ± 3	7.6 ± 1.8	0.67	0.93	0.65
IL4 (pg/ml)	109.2 ± 25.6	72.3 ± 22.7	132.1 ± 33.1	0.94	≥1	0.38
IL6 (pg/ml)	3.6 ± 1	3.1 ± 0.7	2.2 ± 0.6	≥1	0.6	≥1
IL7 (pg/ml)	7.4 ± 1.1	9.4 ± 1.7	7.8 ± 0.8	0.33	0.79	0.35
IL10 (pg/ml)	8.6 ± 3.3	4.8 ± 2.4	7.3 ± 1.9	≥1	≥1	0.67
IL15 (pg/ml)	6.6 ± 1.4	7 ± 1.5	8.5 ± 2.5	≥1	≥1	≥1
IL17 (pg/ml)	14.7 ± 3.9	4.3 ± 1.8	1.9 ± 1.2	0.15	0.12	≥1
TNFα (pg/ml)	3.8 ± 0.7	6.9 ± 1.9	4.1 ± 0.5	0.88	≥1	≥1
CRP (µg/ml)	2.7 ± 0.7	3.1 ± 1.2	1.9 ± 0.3	≥1	0.97	≥1
IFNγ (pg/ml)	145.7 ± 48.4	186.6 ± 86	297.8 ± 123.5	≥1	≥1	≥1
CXCL9 (pg/ml)	3958 ± 897.3	2696 ± 788.6	2801 ± 656.7	0.34	≥1	≥1
GM-CSF (pg/ml)	34.2 ± 7.9	80.5 ± 25	54.6 ± 18.8	0.2	≥1	0.94

Table 2.5 Circulating inflammatory markers. Summary of differences in circulating pro- and anti-inflammatory cytokines between low MT young (n = 15), low MT old (n = 14) and high MT old (n = 20) participants. Data are mean ± standard error mean. One-way ANOVA with Bonferroni's multiple comparison test and Dunn's multiple comparison test were used. Significant p-values are highlighted in red.

3.2.5 Transcriptome signatures of older adults with low and high microbial translocation

To identify molecular signalling pathways in peripheral immune cells that might contribute towards enhanced immune ageing in older adults with high microbial translocation, we used the NanoString nCounter® gene expression assay. This allowed for the detection of 770 genes in PBMCs from healthy young individuals displaying low MT (n = 6), healthy old individuals with low MT (n = 6) and healthy old individuals displaying high MT (n = 6).

In total, 49 genes significantly differed between low MT young, low MT old and high MT old participants (Figure 3.5). Upon comparing expression levels between low MT young adults and older adults with low MT, we observed a significant downregulation in the expression of seven genes controlling cell adhesion/migration (ALCAM, p = 0.05), apoptosis (BID, p = 0.04), immune suppression (LRRN3, p = 0.05) and immune-mediated pathology (NT5E, p = 0.04; TNFRSF13B, p = 0.05) (Table 2.6). We also observed reduced expression of complement system components (CR1, CR2), irrespective of microbial translocation status (Figure 3.5), that play an important role in immunomodulation and defence against pathogens [426].

Furthermore, 27 genes were differentially expressed between young individuals and high MT older adults (Table 2.7). For instance, we observed downregulated expression of autophagy-related genes (ATG7, p = 0.05; LAMP, p = 0.03) and DNA repair machinery (ATM, p = 0.05; G6PD, p = 0.03) along with an upregulation of pro-apoptotic molecules (CASP3, p = 0.05; BID, p = 0.04) only in aged individuals with high MT (Figure 3.5). Importantly, we saw increased expression of co-stimulatory molecules expressed on activated T cells (ICOS, p = 0.05), cellular senescence markers (gain of

KLRG1, p = 0.04; loss of CD28, p = 0.05) and accelerators of cell cycle arrest (TXNIP, p = 0.05) only in older adults with high MT (Figure 3.5). It was previously reported that p53 inhibits MAPK activity by inducing phosphatases, such as DUSPs [427]. Supporting this, we observed a downregulation of MAPK3 (p = 0.04) and upregulated expression of DUSP4 (p = 0.04) and DUSP6 (p = 0.05) in older adults with high MT relative to young and aged individuals with low MT (Table 2.8). Additionally, older participants with high MT displayed increased expression of inflammatory molecules (HMBG1, p = 0.01) and T cell ageing markers (RORA, p = 0.03) compared to low MT older adults (Figure 3.5).

Gene enrichment analysis revealed that the top enriched terms in high MT olds were the intrinsic pathways for apoptosis (BCL2, BID and CD99), the cytochrome c-mediated apoptotic response (CASP3 and CASP8) and cellular senescence (CD28, DUSP4, DUSP6, KLRG1, MAPK3 and TXNIP), suggesting that these pathways might be involved in driving T cell immunesenescence during age-related intestinal barrier dysfunction.

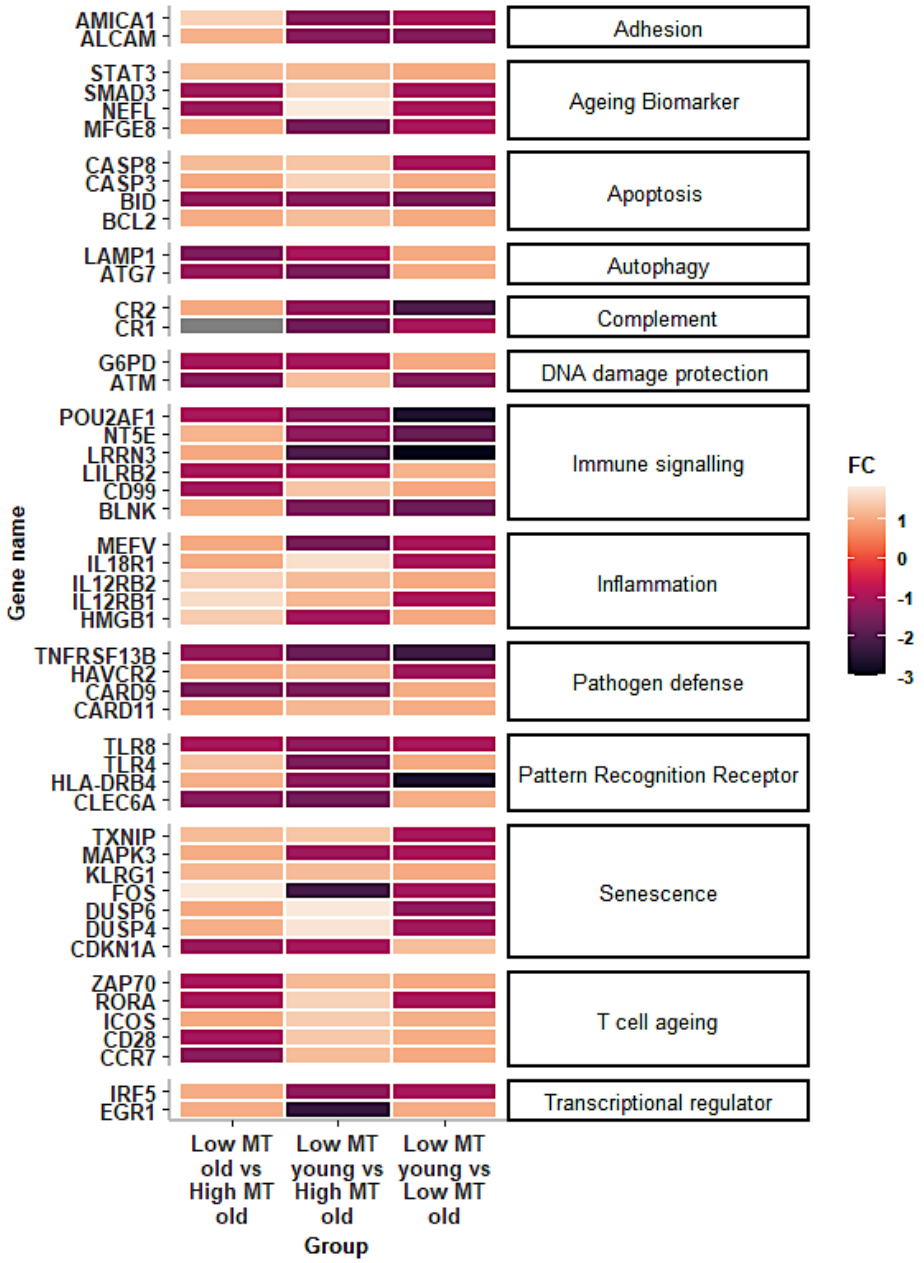

Figure 3.5 Molecular mechanisms underpinning microbial translocation-induced T cell ageing. Heat map showing fold change log(2) of differentially expressed genes in low MT young (n = 6), low MT old (n = 6) and high MT old (n = 6) participants. Figure created by Dr Jack Sullivan.

	Low MT young mean gene expression	Low MT old mean gene expression	Fold change	P-value	Gene function
Downregulated					
ALCAM	60.2	33.8	-1.43	**0.05**	Leukocyte adhesion molecule [428]
BID	46.9	26.1	-1.52	**0.04**	Pro-apoptotic molecule [429]
BLNK	57.4	27.8	-1.69	**0.03**	BCR signaling [430]
CR2	41.3	21.7	-2.04	**0.01**	Complement receptor that clears opsonized immune complexes [426]
LRRN3	71.3	20.1	-3.02	**0.05**	Biomarker for Parkinson's disease and suppressor of immune responses [431]
NT5E	41.1	23.5	-1.74	**0.04**	Immune inhibitory molecule and regulator of cellular signaling [432,433]
TNFRSF13B	49.8	20.1	-2.22	**0.05**	Controls immune-mediated pathology and enhances defense against pathogens [434]

Table 2.6 Genes differentially expressed by PBMCs from low MT young and low MT old adults. Summary of comparison of differentially expressed genes in PBMCs between low MT young (n = 6) and low MT old (n = 6). Data are expressed as mean and log2 fold change. One-way ANOVA with Bonferroni's multiple comparison test and Dunn's multiple comparison test were used. Significant p-values are highlighted in red. Abbreviations: ALCAM, activated leukocyte cell adhesion molecule; BID, BH3 interacting-domain death agonist; BLNK, B cell linker; CR2, complement C3d receptor 2; LRRN3, leucine rich repeat neuronal 3; NT5E, 5'-nucleotidase ecto; TNFRSF13B, TNF receptor superfamily member 13B.

	Low MT young mean gene expression	High MT old mean gene expression	Fold change	P-value	Gene function
Downregulated					
ALCAM	60.2	40.4	-1.39	**0.05**	Leukocyte adhesion molecule [428]
AMICA1	1089.2	724.8	-1.4	**0.04**	Leukocyte transmigration [435]
ATG7	228.1	154.5	-1.52	**0.05**	Autophagy regulator [436]
ATM	27.1	19.2	-1.28	**0.05**	DNA damage repair [437]
CCR7	211.7	184.4	-1.24	**0.05**	Chemokine receptor facilitating recruitment and retention of immune cells in lymphoid organs [438]
CD28	108.1	79.4	-1.39	**0.05**	Costimulatory receptor involved in T cell activation whose loss is a marker for cellular senescence [439]
CLEC6A	33.4	21.5	-1.63	**0.03**	Pattern recognition receptor [440]
CR1	647.3	367	-1.64	**0.05**	Complement receptor that clears opsonized immune complexes [426]
EGR1	90.8	35.2	-2.36	**0.04**	Transcriptional regulator [441]
FOS	6612.7	2861.6	-2.15	**0.04**	Regulator of proliferation and senescence onset [442,443]
IRF5	89.6	64.9	-1.28	**0.05**	Interferon regulatory transcription factor [444]
LAMP1	959.4	841	-1.02	**0.03**	Degradation of autophagic and lysosomal organelles [445]
MAPK3	243.8	199.9	-1.13	**0.04**	Regulates proliferation, differentiation and cell cycle arrest [427]
MEFV	164.7	96.7	-1.58	**0.04**	Inflammasome complex assembly and regulates inflammation [446]
PTGS2	162.9	32.6	-4.97	**0.02**	Controls prostaglandin production [447]
TLR4	313.4	195.8	-1.49	**0.05**	Pattern recognition receptor [448]
TLR8	119.5	87.5	-1.27	**0.05**	Pattern recognition receptor [449]

Upregulated					
BCL2	278.7	331.3	1.24	**0.05**	Anti-apoptotic molecule [450]
CASP3	84.1	139.1	1.52	**0.05**	Pro-apoptotic molecule [451]
CD99	1473.7	1836.2	1.34	**0.05**	Immature T cell marker, regulator of cytokine production and apoptosis inducer [452,453]
DUSP4	26.3	52.4	1.73	**0.04**	Regulates MAPKs and cellular proliferation and accelerates T cell senescence [454,455]
DUSP6	598	1456.3	1.8	**0.04**	Regulates MAPKs and cellular proliferation [454]
ICOS	91.1	132	1.44	**0.05**	Co-stimulatory molecule essential for T cell activation and proliferation [456]
KLRG1	214.9	360.8	1.23	**0.04**	Co-inhibitory receptor and cellular senescence marker [457]
NEFL	22.4	34.7	1.82	**0.04**	Blood biomarker of axonal damage [458]
RORA	420	588.4	1.51	**0.03**	Th17 polarization [459]
TXNIP	11200.8	14076.1	1.35	**0.05**	Cell cycle arrest inducer [460]

Table 2.7 Genes differentially expressed by PBMCs from low MT young and high MT old adults. Summary of comparison of differentially expressed genes in PBMCs between low MT young (n = 6) and high MT old (n = 6). Data are expressed as mean and log2 fold change. One-way ANOVA with Bonferroni's multiple comparison test and Dunn's multiple comparison test were used. Significant p-values are highlighted in red. Abbreviations: AMICA1, adhesion molecule interacting with CXADR antigen 1; ATG7, autophagy related 7; ATM, ataxia telangiectasia mutated; BCL2, B cell lymphoma 2; CASP3, caspase 3; CCR7, C-C motif chemokine receptor 7; CLEC6A, C-type lectin domain containing 6A; CR1, complement C3b/C4b receptor 1; ERG1, early growth response 1; FOS, Fos proto-oncogene AP-1 transcription factor subunit; ICOS, inducible T cell costimulatory; IRF5, interferon regulatory factor 5; LAMP1, lysosomal associated membrane protein 1; MEFV, Mediterranean fever; NEFL, neurofilament light polypeptide; PTGS2, prostaglandin-endoperoxide synthase 2; RORA, RAR related orphan receptor A; TXNIP, thioredoxin interacting protein.

	Low MT old mean gene expression	High MT old mean gene expression	Fold change	P-value	Gene function
Downregulated					
ATG7	178.5	154.5	-1.25	**0.01**	Autophagy regulator [436]
BID	26.1	23.9	-1.27	**0.04**	Pro-apoptotic molecule [429]
CD99	1444.4	1836.2	-1.09	**0.01**	Immature T cell marker, regulator of cytokine production and apoptosis inducer [452,453]
CLEC6A	55.2	21.5	-1.39	**0.003**	Pattern recognition receptor [440]
CR1	613.4	367	-2.09	**0.04**	Complement receptor that clears opsonized immune complexes [426]
G6PD	550.7	466.8	-1.04	**0.03**	Glycolytic enzyme that protects against DNA damage repair and contributes to T cell ageing [461,462]
HAVCR2	436.8	290.5	2.8	**0.05**	Cellular exhaustion inducer and negative regulator of tolerance [463]
HLA-DRB4	62.3	2290.3	-1.07	**0.05**	Antigen presenting molecule [464]
IL12RB1	171.8	151.5	-1.64	**0.01**	Receptor that binds to pro-inflammatory cytokines IL12 and IL23 [465]
IL12RB2	33.3	31.2	-1.5	**0.05**	Receptor that binds to pro-inflammatory cytokines IL12 and IL23 [465]
IRF5	95.9	64.9	-1.04	**0.05**	Interferon regulatory transcription factor [444]
LILRB2	1218.5	716.5	-3.6	**0.04**	Signal transduction via binding to MHC class I molecules on antigen-presenting cells [466]
TLR4	325.6	195.8	-1.31	**0.04**	Pattern recognition receptor [448]
Upregulated					
CASP8	940.8	1262.9	1.7	**0.04**	Pro-apoptotic molecule [467]
DUSP4	30.9	52.4	1.08	**0.04**	Regulates MAPKs and cellular proliferation and accelerates T cell senescence [454,455]

DUSP6	1031.4	1456.3	1	**0.05**	Regulates MAPKs and cellular proliferation [454]
HMGB1	423.3	521.5	1.06	**0.01**	DAMP that activates pro-inflammatory signalling pathways [468]
IL18R1	108.7	174.4	1.02	**0.04**	Receptor that binds to the pro-inflammatory cytokine IL18 [469]
MFGE8	70.3	102.3	1.31	**0.05**	Biomarker of arterial ageing [470]
POU2AF1	23.1	45.7	1.02	**0.05**	B cell transcriptional coactivator [471]
ZAP70	1168.4	1397.6	1.02	**0.05**	TCR signalling [472]

Table 2.8 Genes differentially expressed by PBMCs from low MT old and high MT old adults. Summary of comparison of differentially expressed genes in PBMCs between low MT old (n = 6) and high MT old (n = 6). Data are expressed as mean and log2 fold change. One-way ANOVA with Bonferroni's multiple comparison test and Dunn's multiple comparison test were used. Significant p-values are highlighted in red. Abbreviations: CASP8, caspase 8; DAMP, damage-associated molecular pattern; G6PD, glucose-6-phosphate dehydrogenase; HAVCR2, hepatitis A virus cellular receptor 2; HLA-DRB4, major histocompatibility complex class II DR beta 4; HMGB1, high mobility group box 1 protein; IL12RB, interleukin 12 receptor subunit beta; IL18R1, interleukin 18 receptor 1; LILRB2, leukocyte immunoglobulin like receptor B2; MFGE8, milk fat globule-epidermal growth factor-factor 8; POU2AF1, POU class 2 homeobox associating factor 1; ZAP70, zeta chain of T cell receptor associated protein kinase 70.

3.2.6 Thymic architecture, adiposity and senescence in aged germ-free mice protected from intestinal membrane permeability

To determine whether an age-related increase in circulating microbial products drives thymic involution, we used an aged germ-free mouse model that was previously shown to be protected from increased gut permeability [68]. We hypothesised that these aged germ-free mice (20-22 months) would also be protected from key features of thymic involution (Figure 2.9). The FITC-dextran assay is a well-established method for measuring *in vivo* intestinal permeability [473]. In this study, we confirmed that aged wild-type mice display enhanced translocation of FITC-dextran into the blood compared to young wild-type mice ($p = 0.004$), whereas aged germ-free mice maintained intestinal barrier function ($p = 0.14$) (Figure 3.6A). Whilst there was no

gross difference in intestinal architecture, we found that aged wild-type mice exhibit decreased expression of the tight junction protein occludin compared to young wild-type and aged germ-free mice (Figure 3.6B). Additionally, aged germ-free mice that were protected from intestinal membrane permeability displayed lower relative mRNA expression levels of *E. coli* in the thymus compared to aged wild-type mice ($p = 0.33$), which exhibited increased thymic *E. coli* mRNA expression levels relative to young mice ($p = 0.1$) (Figure 3.6C).

Age-related thymic involution disrupts the structural integrity and cellular architecture of the thymus, resulting in the shrinkage of medullary regions and impaired thymopoiesis [164,177]. Additionally, the CMJ, which separates the cortex and medulla and serves as a site for progenitor ($CD4^{-ve}CD8^{-ve}$) immigration and naïve T cell emigration [474], becomes disorganised with age and there is increased thymic adiposity [163]. In this study, morphological analysis showed medullary shrinkage, disruption of the CMJ and the emergence of vacuoles in aged wild-type mouse thymuses, but not in those from aged germ-free mice (Figure 3.6D). Oil-red O staining, which is used for the enumeration of lipid-laden tissues, also revealed an increase in the size and number of lipid deposits in the thymuses of aged wild-type mice ($p = 0.01$) compared to young mice, whereas aged germ-free mice were protected from lipid accumulation ($p = 0.06$) (Figures 3.6E and 3.6F).

Stromal components of the thymus include specialized TECs that provide signals that induce the development and functional maturation of T lymphocytes. However, the aged thymus displays an enlargement of non-cellular perivascular spaces and TEC

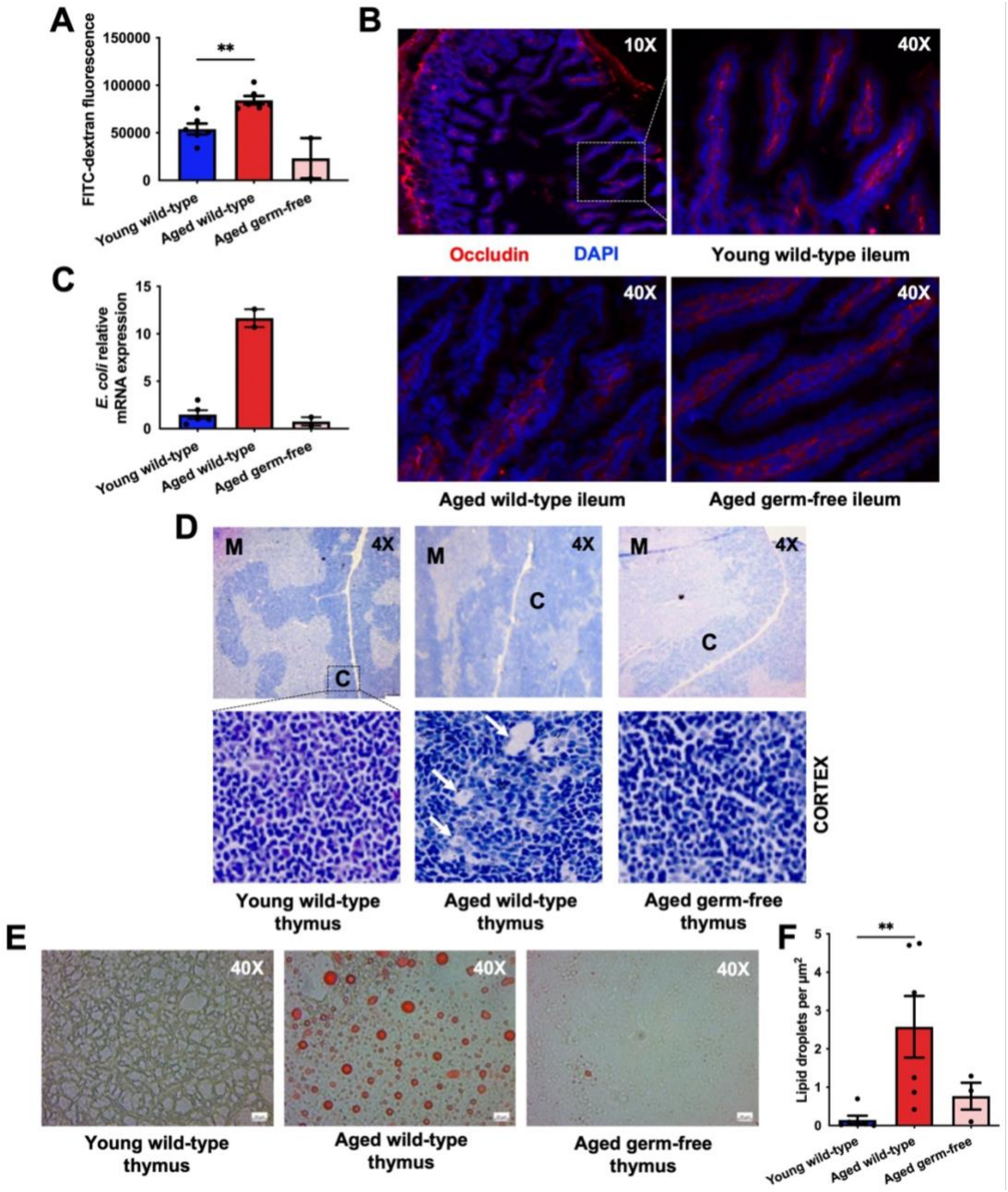

Figure 3.6 Thymic tissue organisation and adiposity in aged germ-free mice protected from intestinal barrier dysfunction. (A) Intestinal permeability in young and aged (n = 6 for both) wild-type mice and aged germ-free mice (n = 2) measured via FITC-dextran fluorescence. **(B)** Representative immunohistochemical images of tight junction protein, occludin-1 (red staining) and nuclei (blue staining) in intestinal villi of mouse ileum sections taken at 10X magnification (top row) and 40X magnification (bottom row) by Nia Paddison Rees. **(C)** Relative mRNA expression levels of *E. coli* in young (n = 5) and aged (n = 2) wild-type and aged germ-free (n = 2) mouse thymuses. **(D)** Representative H&E stained images of mouse thymus sections with medullary regions stained light purple (indicated by M) and cortical regions stained dark purple (indicated by C). Images on the top row were taken at a 4X magnification, and a higher 40X magnification was used for the cortex region shown on the bottom row. Arrows point to vacuoles. **(E)** Representative immunohistochemical images of oil red O stained mouse thymus sections at 40X magnification. **(F)** The number of lipid droplets per μm^2 in young and aged wild-type mice (n = 6 for both) and aged germ-free mice (n = 3). Statistical significance was determined using one-way ANOVA followed by Dunns' multiple comparison test. **p ≤0.01.

reductions [163,475]. Although perivascular spaces enable easy trafficking of cells and soluble proteins through the medulla, an increase in non-cellular space permits the infiltration of pro-inflammatory adipocytes and circulating senescent cells in the aged thymus [476]. Morphological analysis revealed that CD205^{+ve} cortical and ERTR5^{+ve} medullary epithelial regions become less dense with age followed by the appearance of epithelial-free areas in aged wild-type mouse thymuses, though this did not occur in aged germ-free mice (Figure 3.7A).

Next, we assessed the presence of senescent cells in the thymus of aged wild-type and germ-free mice to elucidate a potential mechanism underpinning the changes in thymus architecture. Lamin B1 is a structural protein that supports TEC development and maintains thymic architecture [167], and reduced lamin B1 expression is a marker of cellular senescence and thymic involution [477]. Aged wild-type mice exhibited tissue disorganisation and fewer lamin B1-expressing cells in the cortex compared to young mice, but these ageing features were not present in aged germ-free mice (Figure 3.7B). Further, we observed lower lamin B1 expression levels (MFI) in the cortex of aged wild-type mice ($p = 0.04$), but not in aged germ-free mice ($p = 0.57$), compared to young wild-type mice (Figure 3.7C). In contrast, lamin B1 expression levels (MFI) in the medulla were unaffected by ageing ($p = 0.22$) or microbiota composition ($p \geq 0.1$) (Figure 3.7D). Transcriptional profiling of aged wild-type mouse thymuses revealed increased mRNA expression levels of the cellular senescence marker p16 relative to young mice ($p = 0.01$), which were even lower in aged germ-free mice ($p = 0.04$) (Figure 3.7E).

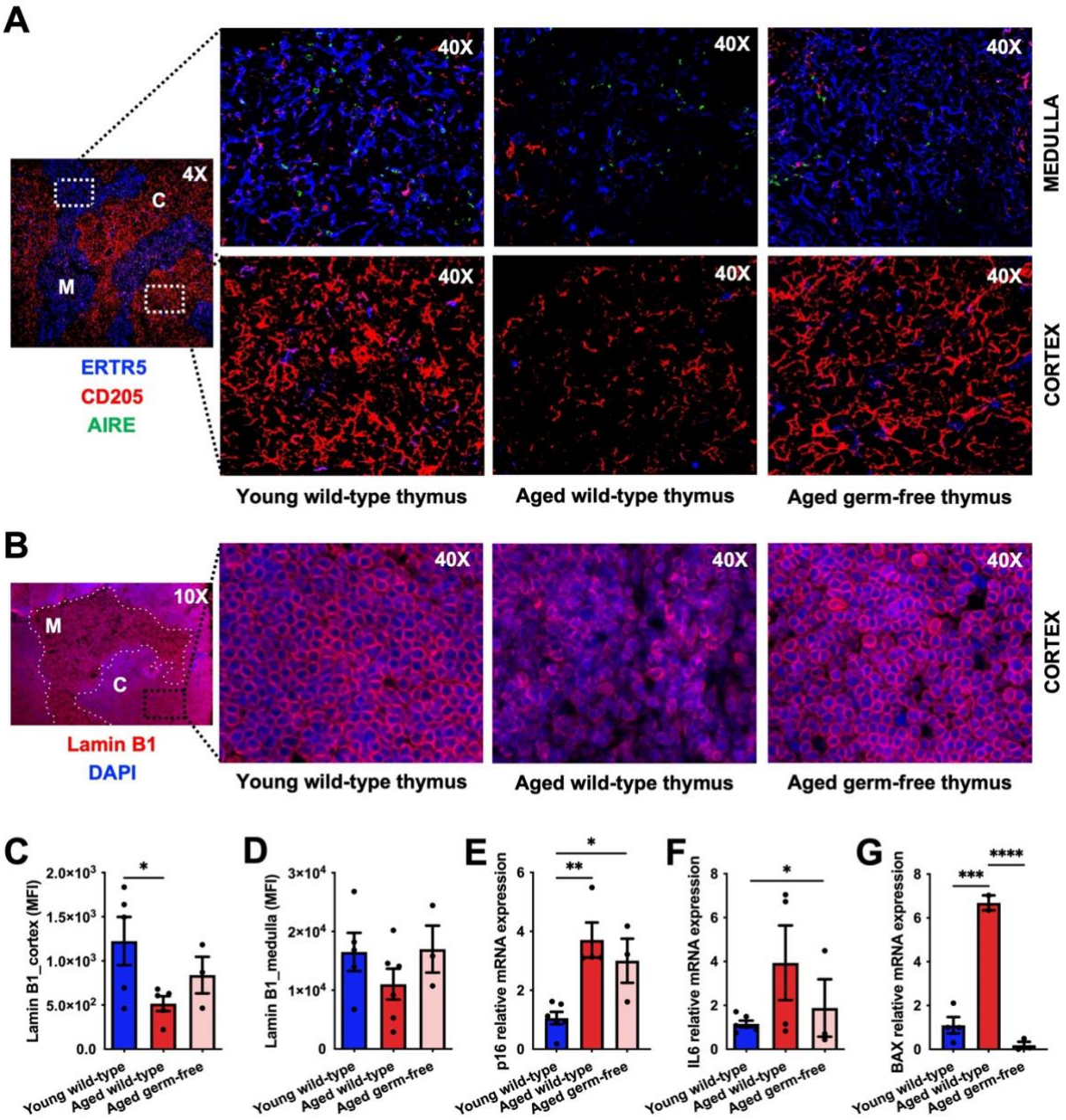

Figure 3.7 Thymic involution and underlying mechanisms in aged wild-type and aged-germ free mice. (A) Representative mouse thymus images depicting the distribution of CD205^{+ve} cTECs (red), ERTR5^{+ve} mTECs (blue) and AIRE^{+ve} mature mTECs (green) at 4X magnification (left) and 40X magnification (right). **(B)** Lamin B1 (red) and DAPI (blue) stained mouse thymus sections imaged at 4X magnification (left) and 40X magnification (right). Medullary islands are marked by 'M' and dotted lines, while cortical regions are marked by 'C'. Lamin B1 thymic expression levels (MFI) in the cortex **(C)** and medulla **(D)**. Relative mRNA expression levels of IL6 **(E)**, p16 **(F)** and BAX **(G)** in thymuses from young wild-type (n = 6), aged wild-type (n = 6) and aged germ-free (n = 3) mice. Statistical significance was determined using one-way ANOVA followed by Dunns' multiple comparison test. *p ≤0.05, ** p ≤0.01, ***p ≤0.001, ****p ≤0.0001.

Elevated IL6 levels found in the thymuses of aged mice are associated with poorer thymic function and involution [175]. However, aged germ-free mice were previously shown to be protected from inflammageing, lacking high circulating levels of IL6 [68]. Here we confirm that compared to young mice, aged wild-type mice exhibit increased IL6 mRNA expression levels in the thymus ($p = 0.05$), which were lower in aged germ-free thymuses ($p = 0.55$) (Figure 3.7F). Compared to young mice, mRNA expression levels of the apoptosis-promoting gene BCL2 associated X (BAX) were also significantly higher in aged wild-type mice ($p = 0.0001$) but not in aged germ-free mice ($p < 0.0001$) (Figure 3.7G), suggesting a possible mechanism by which increased apoptosis drives TEC loss with age.

Lastly, we examined the distribution of CD4 and CD8 thymocytes in the thymus and found that aged wild-type mice display a loss of $CD8^{+ve}$ cortical regions in the thymus (Figure 3.8). However, the cellular density of CD8 thymocytes was higher in aged germ-free mice compared to aged wild-types (Figure 3.8). A similar decline in the cellular density of CD4 thymocytes was also observed in the medulla with age, though aged germ-free mice displayed a higher cellular density of $CD4^{+ve}$ areas (Figure 3.8). In conclusion, our data demonstrate the presence of bacterial products within the aged thymus, possibly as the result of increased intestinal membrane permeability and subsequent systemic microbial translocation, that contributes towards a disrupted thymic architecture, build-up of thymic inflammation and the accumulation of senescent cells; culminating in an altered thymic microenvironment for T cell development.

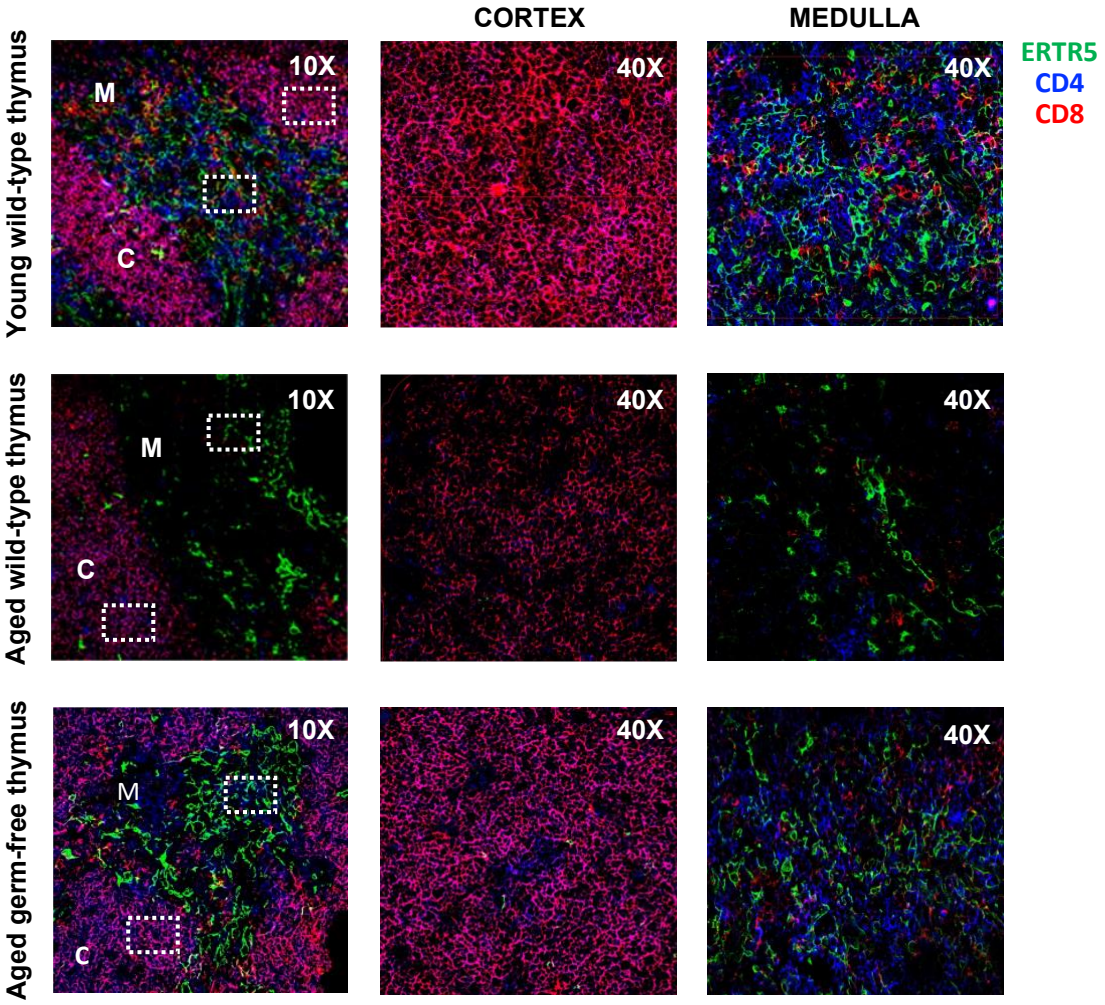

Figure 3.8 Thymocyte distribution in aged wild-type and aged germ-free mice. Mouse thymus sections stained with CD4 (blue), CD8 (red) and ERTR5 (green) to assess the distribution of thymocytes in ERTR5^{-ve} cortical (marked as 'C') and ERTR5^{+ve} medullary (marked as 'M') regions. Images on the left were taken at 10X magnification, while images on the right were taken at 40X magnification.

3.2.7 Gut homing potential of aged T cells

In this chapter, we have linked perturbations in intestinal barrier integrity with accelerated thymic involution and the accumulation of senescent T cells in old age. However, it is unclear whether increased gut permeability is a primary event or a consequence of mucosal immune ageing. Thus, we hypothesised that ageing enhances the gut homing potential of pro-inflammatory T cells, which contribute towards increased intestinal membrane permeability and enhanced microbial translocation, resulting in a feed-forward loop.

Leukocyte trafficking to the intestinal tract is a tightly controlled process mediated by a variety of chemokine and adhesion receptors expressed by immune cells [478]. Chemokine receptor CCR9 enables T cell homing by binding the chemokine ligand CCL25 expressed on IECs, leading to integrin-dependent adhesion and subsequent transendothelial migration [479-481]. Here, we observed a significant age-associated increase in the frequency of naïve CD4 and CD8 T cells expressing CCR9 ($p = 0.02$ and $p < 0.0001$, respectively) (Figures 3.9A and 3.9B). These aged naïve CD4 and CD8 T cells also had a greater CCR9 cell surface density (MFI) relative to those from young adults ($p = 0.001$ and $p < 0.0001$, respectively) (Table 2.9). Although the percentage of $CCR9^{+ve}$ memory CD4 and CD8 T cells was comparable between both age groups (Figures 3.9A and 3.9B), advancing age led to a significant increase in CCR9 surface expression on EM CD4 T cells ($p = 0.02$), CM CD8 T cells ($p = 0.03$) and EMRA CD8 T cells ($p = 0.02$) (Table 2.9).

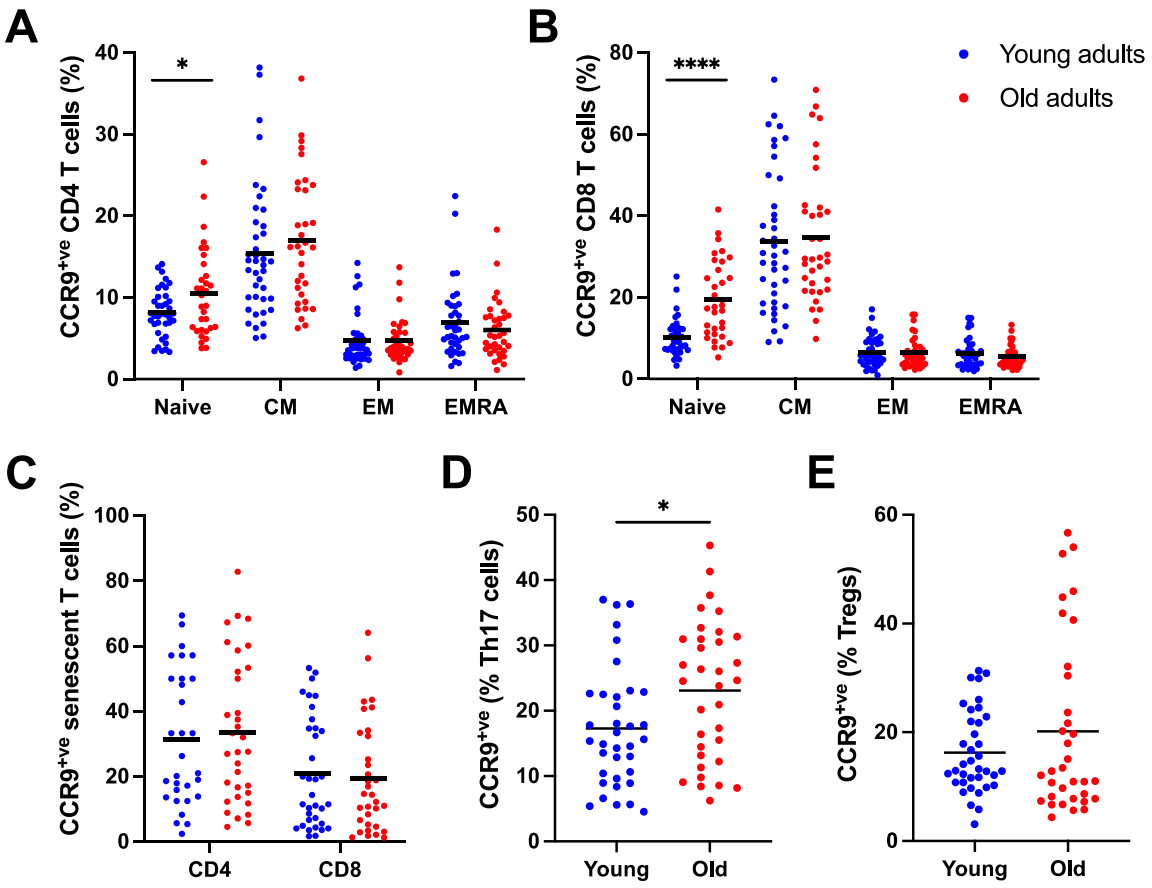

Figure 3.9 Impact of ageing on CCR9-expressing T cells. The percentage of naïve, CM, EM and EMRA CD4 **(A)** and CD8 **(B)** T cells expressing CCR9. **(C)** The frequency of CCR9^{+ve} senescent CD4 and CD8 T cells. The proportion of Th17 cells **(D)** and Tregs **(E)** expressing CCR9. Solid bars indicate that data are expressed as mean. Multiple Unpaired Student's T tests and Mann-Whitney U tests were used to determine statistical differences between young (blue, n = 40) and old (red, 40) adults. The Benjamini-Hochberg method was used to calculate adjusted p-values. *p ≤0.05, ****p ≤0.0001.

Furthermore, ageing did not affect the proportion of $CD28^{-ve}CD57^{+ve}$ senescent CD4 and CD8 T cells that expressed CCR9 (p = 0.68 for both) (Figure 3.9C), but instead significantly increased CCR9 expression levels (MFI) on $CD28^{-ve}CD57^{+ve}$ senescent CD8 T cells (p = 0.03) (Table 2.9). We also observed a significant age-related increase in the peripheral frequency of $CCR9^{+ve}$ Th17 cells compared to young adults (p = 0.02) (Figure 3.9D), whereas the percentage of Tregs expressing CCR9 was similar between young and old adults (p = 0.76) (Figure 3.9E).

	Young adults (n = 40)	**Old adults** (n = 40)	**P-value**
CCR9 expression on naïve CD4 T cells (MFI)	15.8 ± 0.7	20.5 ± 1.1	**0.001**
CCR9 expression on CM CD4 T cells (MFI)	16.1 ± 0.6	16.9 ± 0.8	0.49
CCR9 expression on EM CD4 T cells (MFI)	8.7 ± 0.2	9.8 ± 0.4	**0.02**
CCR9 expression on EMRA CD4 T cells (MFI)	8.8 ± 0.4	9.2 ± 0.5	0.69
CCR9 expression on naïve CD8 T cells (MFI)	15.2 ± 0.6	21.2 ± 1.1	**<0.0001**
CCR9 expression on CM CD8 T cells (MFI)	16.1 ± 1	19.5 ± 1.1	**0.03**
CCR9 expression on EM CD8 T cells (MFI)	10 ± 0.3	10.4 ± 0.4	0.46
CCR9 expression on EMRA CD8 T cells (MFI)	8.1 ± 0.3	9.7 ± 0.5	**0.02**
CCR9 expression on senescent CD4 T cells (MFI)	38 ± 3.3	41.5 ± 3.1	0.44
CCR9 expression on senescent CD8 T cells (MFI)	33 ± 3.2	47 ± 4	**0.03**
CCR9 expression on Th17 cells (MFI)	21.6 ± 1.6	22.4 ± 1.9	0.9
CCR9 expression on Tregs (MFI)	30.6 ± 2.7	26.8 ± 2.3	0.34

Table 2.9 Chemokine receptor CCR9 surface expression levels on T cell subsets. Data are mean ± standard error mean. Statistical significance was determined using Multiple Unpaired Student's T tests and Mann-Whitney U tests followed by the Benjamini-Hochberg correction method. Significant p-values are in bold red.

3.3 Discussion

It is becoming increasingly clear that impaired intestinal barrier integrity is a major pathophysiological feature of ageing that contributes to the decline of organismal health. Whilst recent publications have demonstrated a significant role for microbial translocation in driving chronic immune cell activation and inflammageing [68,367], the potential links between age-related intestinal barrier dysfunction and immunesenescence are still largely unknown. In this study, we demonstrate that older adults with higher levels of intestinal barrier leakage are more likely to display hallmarks of T cell ageing, contributing to high IMM-AGE scores in these individuals. Importantly, aged germ-free mice that display reduced intestinal membrane permeability and bacterial translocation preserve their thymic architecture and have an unaltered thymic microenvironment, possibly driving high thymic output in old age (Figure 3.10). These novel findings take us a step further in understanding the age-related changes in the microbiome-immune axis and provide evidence for therapeutic restoration of intestinal barrier homeostasis to preserve immune function in aged individuals.

To the best of our knowledge, this study is the first to report an age-associated increase in intestinal membrane permeability and systemic microbial translocation in healthy aged individuals in line with findings from non-human primate studies [361,482]. Dietary components play an integral role in modulating intestinal barrier integrity. For instance, there is mounting evidence that excessive consumption of dietary fats enhances intestinal membrane permeability [483], predisposing individuals to local and systemic inflammation. Interestingly, high intake of dietary fibre was inversely correlated with intestinal barrier dysfunction in this study, possibly due to the

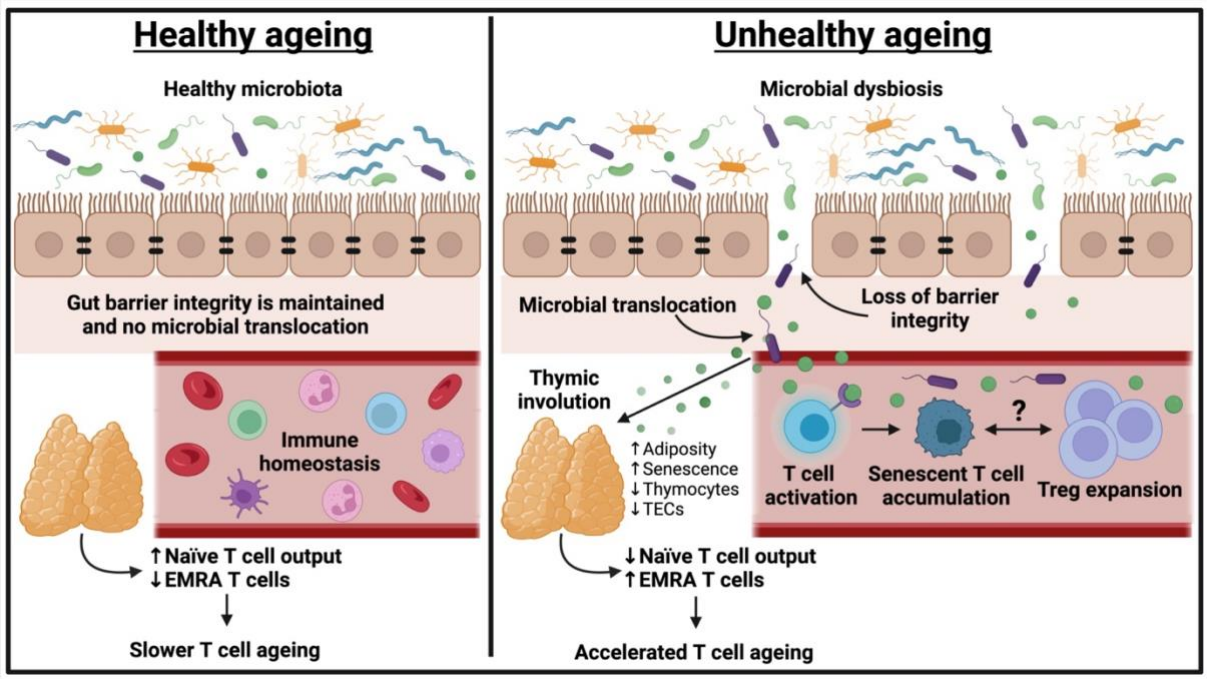

Figure 3.10 Graphical summary of the impact of age-associated gut barrier dysfunction on thymic involution and T cell ageing. Loss of intestinal barrier integrity with age permits the translocation of microbes and microbial products, such as LPS, into the circulation. These microbial products are then trafficked through the blood, contributing to persistent antigenic stimulation that leads to the accumulation of senescent T cells and possibly the compensatory expansion of peripheral Tregs. Circulating bacterial products also translocate into the thymus where they contribute towards age-related thymic involution, resulting in a reduced thymic output of RTEs. Loss of naïve T cells and chronic antigenic stimulation result in skewing towards T cell senescence, which accelerates T cell ageing in older adults.

anti-inflammatory and health-promoting properties of SCFAs, the end-products of bacterial fermentation of insoluble fibres [484,485]. This is supported by a study that demonstrated that high dietary fibre intake restores gut barrier function in non-obese diabetic mice, thereby restoring intestinal immune homeostasis (i.e. reduced gut inflammation, expansion of IL10-producing Tregs, decline in pro-inflammatory Th17 cells) [486]. However, these immune-enhancing effects have yet to be confirmed in aged humans.

Changes in gut microbiota composition with age are also closely linked with the onset of intestinal barrier leakage in mice [68]. Accordingly, intestinal barrier leakage was correlated with higher relative abundances of pro-inflammatory *Escherichia-Shigella*, *Peptostreptococcaceae* and *Paraprevotella* in stool. On the other hand, robust intestinal barrier integrity was positively associated with high faecal levels of propionate and GDCA, both of which exert immunomodulatory and anti-inflammatory effects on the immune system. These results suggest a possible role of age-related microbial dysbiosis in promoting increased gut permeability through inflammation-induced epithelial damage.

In this study, we propose that age-related microbial translocation induces a state of persistent T-cell activation. These results are supported by an earlier study that reported the loss of gut mucosa homeostasis and increased bacterial translocation in HIV patients, resulting in chronic immune system activation and systemic inflammation [366]. Therefore, we hypothesise that persistent stimulation caused by microbial translocation promotes the terminal differentiation of T cells and induces cellular senescence in aged T cells, together accelerating immune ageing. These observations are in line with those from another study reporting close links between microbial

translocation and memory T cell expansion in adult mice [487]. Furthermore, *in vitro* studies have confirmed that gut microbial secretory factors induce cellular senescence via activation of cell cycle inhibitors ($p16^{INK4a}$, $p21^{WAF1}$ and p53) and the DNA damage response, resulting in the development of a SASP [488,489].

In agreement with other ageing studies [203,490], we observed an age-related increase in the percentage of Tregs that was correlated with increased gut permeability. There is emerging evidence of a potential link between the expansion of senescent T cells and Tregs, with studies demonstrating that Tregs trigger DNA damage in effector T cells via metabolic competition during cross-talk, resulting in cellular senescence and functional exhaustion [491]. Thus, we propose that increased microbe recognition caused by enhanced bacterial translocation might contribute to dysregulated ROS production and altered glucose metabolism in aged Tregs, promoting aberrant Treg interactions and senescent cell accumulation.

Consistent with the findings discussed above, we identified several hallmarks of ageing in circulating immune cells, including upregulation of pro-inflammatory signalling markers (HMBG1), defective autophagy processes (ATG7 and LAMP), reduced DNA damage repair (ATM), increased cellular senescence (gain of KLRG1 and loss of CD28), enhanced apoptosis (BCL2, CASP3 and CASP8), loss of proliferation regulators (DUSP4 and DUSP6) and upregulation of cell-cycle arrest regulators (TXNIP), that were only present in older adults with high microbial translocation. These results are in line with those from a study that demonstrated that microbial products disrupt autophagosome formation and trigger mitochondrial dysfunction by interfering with Rab1A signalling and reducing mitochondrial coupling [289,492].

T cells are continuously produced by the thymus throughout life. However, the thymus undergoes accelerated atrophy with advancing age, resulting in a reduced thymic output of naïve T cells that limits the host's ability to respond to neoantigens [186,493]. In this study, we reported a significant age-related loss of RTEs in older adults with high microbial translocation, supporting our hypothesis that circulating bacterial products have deleterious effects on thymopoiesis. To confirm that microbial products contribute towards age-related thymic involution, we used aged germ-free mice which are protected from loss of intestinal barrier function. Here, we demonstrated for the first time that ageing is accompanied by increased thymic translocation of *E*. *coli* in wild-type mice but not in germ-free mice. Importantly, hallmarks of thymic involution, including the loss of functional thymic niches due to the depletion of TECs, adipocyte infiltration and senescent cell accumulation, were less pronounced in aged germ-free mice.

In vitro analysis reveals that LPS, found on the surface of gram-negative bacteria such as *E*. *coli*, promotes the accumulation of lipid droplets in endothelial cells [494], induces cellular senescence and enhances the SASP of senescent cells [495,496]. Thus, elevated circulating levels of microbes and microbial products, like LPS, could promote increased thymic adiposity and cellular senescence in aged hosts. Accumulation of senescent cells and adipocytes during ageing is believed to hinder thymic function through increased secretion of pro-inflammatory cytokines, such as IL6 and TNFα [167,175]. In this study, ageing was accompanied by increased thymic expression of IL6 in wild-type mice. However, aged germ-free mice exhibited comparable IL6 expression levels to those in young wild-type mice, indicating a role for microbial translocation in the age-dependent upregulation of thymopoiesis-suppressing

cytokines. Indeed, LPS treatment and *E*. *coli* enterotoxin cause thymic atrophy, leading to the loss of DN, DP and SP thymocytes [497,498]. One mechanism by which this occurs is through LPS-induced apoptosis of thymocytes [499]. Supporting this, thymic expression of the apoptotic gene BAX increased with age in wild-type mice, whereas aged germ-free mice were unaffected.

Beyond forming a physical barrier against luminal antigens, IECs engage in complex bidirectional crosstalk with mucosal immune cells, ensuring the maintenance of gut and immune homeostasis [500]. However, many questions still exist with regards to the role of mucosal immunesenescence in age-related intestinal barrier dysfunction. In this study, we report for the first time that older adults have increased frequencies of naïve CD4 and CD4 T cells and Th17 cells that express higher levels of the gut homing receptor CCR9, indicating that these cells display enhanced intestinal trafficking abilities. Additionally, we observed an age-associated increase in CCR9 cell surface densities on EMRA and senescent CD8 T cells. Importantly, CCR9 is upregulated on T cells in response to excessive inflammation [501]. Therefore, increased translocation of bacterial products into the underlying lamina propria might trigger intestinal inflammation in older adults, possibly promoting the infiltration of circulating T cells.

Recent evidence has revealed that persistently activated T cells increase paracellular permeability possibly via pro-inflammatory cytokine production, resulting in the disassembly of tight junction complexes, reduced IEC proliferation and IEC apoptosis [502]. IFNγ-secreting Th17 cells can also induce epithelial barrier disruption by downregulating tight junction proteins, particularly zonulin, indicating a potential pathogenic role in the gut [503]. Moreover, SASP components, including pro-inflammatory cytokines, growth factors and proteases, have been shown to induce

cellular senescence in bystander cells [504], initiate epithelial-to-mesenchymal transition [505], cause intestinal epithelial damage [506], increase paracellular permeability and propagate intestinal inflammation [507,508]. Based on these findings, it is highly conceivable that increased homing of senescent CD8 T cells and Th17 cells into the gut could contribute to age-related intestinal leakage, possibly through enhanced production of pro-inflammatory mediators.

Although therapeutic manipulation of the gut microbiota might improve health in aged hosts, it remains unclear how restoring intestinal barrier function possibly by targeting microbiome dysbiosis could reverse features of immune ageing. For instance, studies have reported links between microbial composition, intestinal membrane permeability and circulating cytokine levels in aged hosts, but have not investigated their impact on immune health [253]. Data from our group demonstrated that transferring healthy gut microbiota into *Clostridium difficile* infected older adults improves intestinal barrier integrity. Moreover, faecal microbiota transplantation promotes the expansion of peripheral naïve T cells and reduces the senescent T cell burden in recipients, suggesting potential anti-immunesenescence effects [509].

Microbial dysbiosis in HIV patients, characterised by the loss of beneficial *Bifidobacterium* and the overrepresentation of *Clostridium* clusters, is also alleviated in response to probiotic administration, resulting in reduced microbial translocation and improved immune cell function [510]. The appearance of opportunistic microbial communities in the aged gut is related to dietary changes, such as low consumption of fibre-rich fruits and vegetables and increased consumption of meats and processed foods [253]. Moreover, studies have reported rebalancing of the gut flora, reduced systemic inflammation and improved health status in older adults who consume a

MedDiet [381,389]. Therefore, high adherence to a MedDiet rich in fibre, polyunsaturated fats, minerals and vitamins could strengthen gut barrier function and improve immune function in older people.

3.3.1 Study limitations and future work

This study has a few limitations, the first being that the exact mechanisms linking intestinal membrane permeability to immune ageing remain to be fully elucidated. Thus, further work is required to determine the impact of individual bacterial products on immune ageing. This includes culturing T cells from young donors with different microbial products (e.g. LPS) followed by the assessment of hallmarks of T cell ageing, such as DNA damage, defective autophagy, mitochondrial dysfunction and cellular senescence [511], via flow cytometry and live-cell imaging.

Another limitation is that we did not directly assess T cell gut infiltration or the effect that this could have on the intestinal epithelium. Therefore, future studies would benefit from the utilisation of a Caco-2/T cell coculture model to mimic interactions between the gut epithelium and the mucosal immune system and assess Caco-2 permeability. Future spatial transcriptomic work is also needed to evaluate the impact of ageing on the intestinal mucosal immune system and determine whether there is an age-related influx of pro-inflammatory and senescent T cells.

3.3.2 Conclusion

In this study we propose for the first time that systemic microbial translocation due to increased intestinal barrier leakage contributes towards a reduced thymic output and the emergence of T cell ageing features (Figure 3.10). Therefore, our findings advocate for targeting intestinal barrier integrity as a novel strategy for promoting thymic

rejuvenation and combating T cell ageing in the expanding ageing population. Exploiting the restoration ability of these targets provides new opportunities to cope with lagging health span developments of individualised dietary, probiotic and postbiotic interventions.

Chapter 4: Links between microbial dysbiosis, immunesenescence and influenza vaccine immunogenicity in older adults

4.1 Background

The gut microbiota and microbiota-derived metabolites play a vital role in a range of host physiological processes, including the immune system. Advancing age is accompanied by profound microbiota compositional changes as a consequence of alterations in host health and lifestyle habits [320]. Age-related microbial dysbiosis is defined as an imbalance in gut microbiota that is characterized by decreased microbial diversity. This includes the loss of symbiotic commensals, such as *Bacteroides*, *Prevotella*, *Bifidobacterium*, *Faecalibacterium*, *Lachnospira*, *Clostridium* and *Coprococcus*, alongside an expansion of Proteobacteria and pathobionts, namely members of the *Enterobacteriaceae* family, in older adults [314,315,328]. These opportunistic bacteria generate genotoxins and carcinogenic metabolites that trigger local and systemic inflammation and disrupt intestinal barrier function [68]. Indeed, numerous autoimmune, inflammatory and metabolic diseases, including RA [512], IBD [513], type 2 diabetes and obesity [317,514], have been linked with dysbiotic bacterial signatures, signifying the importance of the microbiota in regulating immune and metabolic homeostasis.

Another feature of microbial dysbiosis is a decline in the levels of microbiota-derived metabolites, such as short-chain fatty acids (SCFAs) produced by bacteria belonging to the *Lachnospira*, *Roseburia*, *Lactobacillus* and *Bifidobacterium* genera [314,339]. Additionally, the conversion of primary to secondary bile acids (SBAs) is less efficient in the aged gut due to a decline in *Bacteroides*, *Parabacteroides* and *Odoribacter*, giving rise to low faecal levels of SBAs, including lithocholic acid (LCA), glycodeoxycholic acid (GDCA) and glycolithocholic acid (GLCA) [515,516]. SCFAs and SBAs support gut microbial diversity and maintain intestinal barrier function by

promoting IEC turnover and enhancing the expression and function of tight junction proteins, like occludin [517-519]. Further, SCFAs and SBAs exhibit potent immunomodulatory and anti-inflammatory properties, and thus represent important links between the gut microbiota and immune system [320]. Therefore, loss of metabolite-producing bacteria and low metabolite levels with age could contribute to age-related immunesenescence.

Whilst it is known that the gut microbiota is essential for inducing and shaping healthy immune responses, the relationship between age-related microbial dysbiosis and immunesenescence is still elusive. Recently, it was demonstrated that young germ-free mice transplanted with faecal microbiota from aged donors exhibit a unique 25-gene signature of immune-associated differentially expressed genes in the small intestine that is positively correlated with naïve, memory, exhausted and regulatory T cell subset gene signatures in colorectal tissues [520]. Moreover, other studies have linked microbial dysbiosis to chronic systemic T cell activation and inflammageing in aged animals and humans [315,521,522]. Nevertheless, it remains unclear which bacterial species drive immune dysfunction during ageing.

This chapter aims to identify specific gut microbiota taxa and microbial metabolites associated with a healthy immune system and higher vaccine responses in older adults.

4.2 Results

4.2.1 Microbiota diversity and compositional changes during ageing

In this study, we performed high-throughput 16S rRNA gene amplicon sequencing on stool samples collected from 37 healthy young (age range 19-37 years, 16 males) and 39 healthy old (age range 63-84 years, 17 males) participants to examine bacteria compositional differences (Figure 4.1A). All participants were Caucasian and only 3% were smokers (two young adults). Additionally, both cohorts displayed similar BMIs: mean BMI among young adults was 26.3 kg/m^2 and mean BMI among old adults was 24.5 kg/m^2.

Decreased gut microbial diversity is a key indicator of microbial dysbiosis and can be measured using alpha diversity metrics [523]. Alpha diversity calculates the diversity of species within a microbial community, taking into account species richness (i.e. the number of taxonomic groups) and/or evenness (i.e. the distribution of relative abundances amongst taxa) [524]. In our study, advancing age did not affect species richness (i.e. Chao1 richness index) ($p = 0.07$) or species evenness (i.e. Shannon evenness index) ($p = 0.18$) (Figures 4.1B and 4.1C). Additionally, non-parametric Shannon alpha diversity indices were comparable between young and old adults ($p = 0.16$) (Figure 4.1D). Similar results were obtained when other alpha diversity metrics, such as the Simpson index and the ACE index, were calculated (data not shown), demonstrating the robustness of these findings.

The faecal microbiome of healthy young and old individuals consisted of microbiota belonging to the following phyla: Actinobacteria, Bacteroidetes, Cyanobacteria, Deinoccus-Thermus, Elusimicrobia, Epsilonbacteraeota, Firmicutes, Fusobacteria,

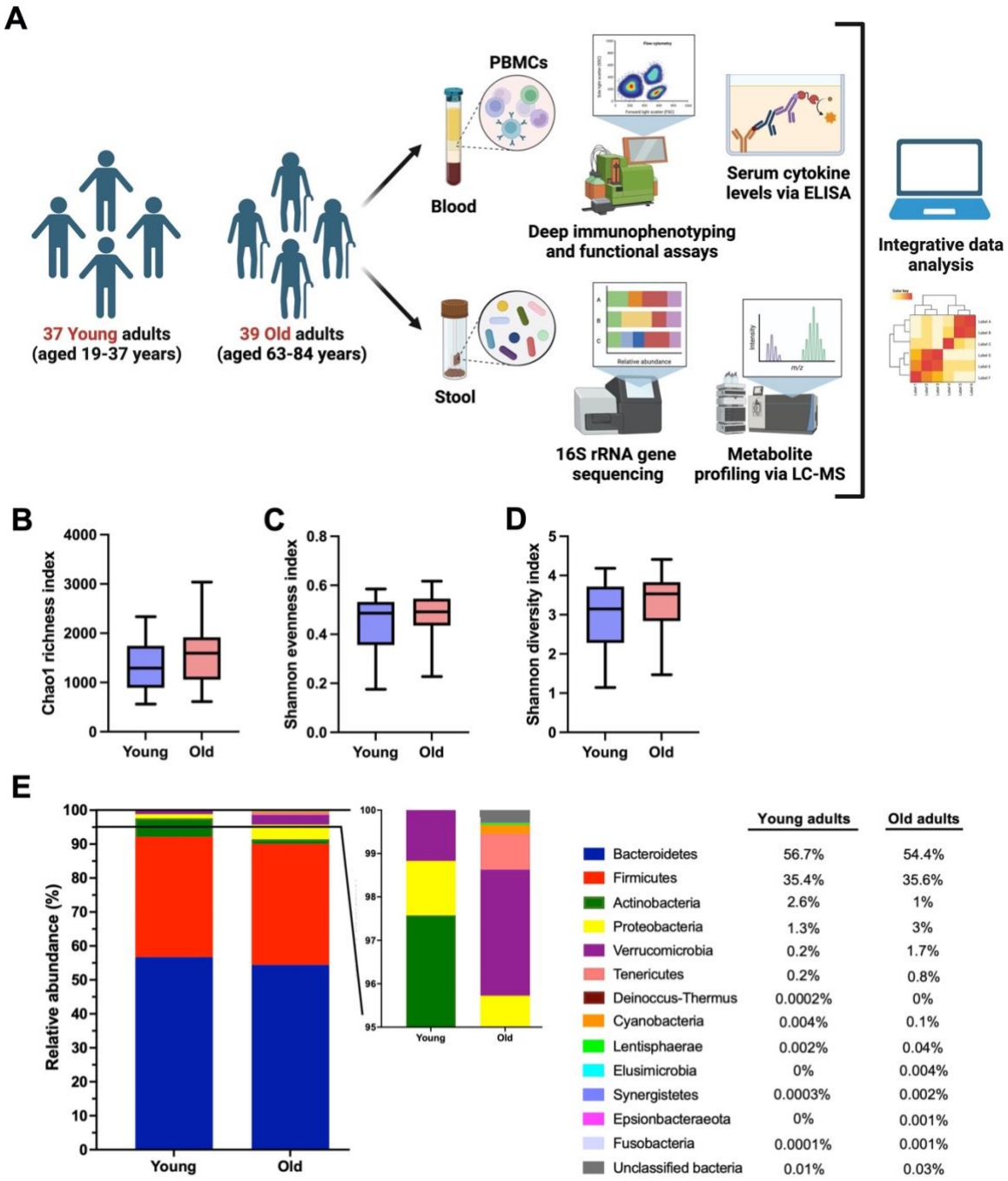

Figure 4.1 Advancing age alters gut microbial composition but not alpha diversity. (A) Study design. Box and whisker plots showing differences in the alpha diversity of faecal microbiota between healthy young (blue, n = 37) and old (red, n = 39) adults measured using the Chao1 richness index **(B)**, the Shannon evenness index **(C)** and the non-parametric Shannon diversity index **(D)**. Data are expressed as mean as indicated by the middle lines, while whisker lines represent the minimum and maximum data points. **(E)** Relative abundances of phyla in young and old participants. Colours indicate phyla with mean relative abundances (%) for each age cohort displayed (right). Statistical significance was determined via Multiple Mann-Whitney U tests and p-values were adjusted using the Benjamini-Hochberg method.

Lentisphaerae, Proteobacteria, Synergistetes, Tenericutes and Verrucomicrobia. In both age groups, the faecal microbiota was dominated by Bacteroidetes and Firmicutes with a smaller fraction of Actinobacteria and Proteobacteria (Figure 4.1E). Moreover, we observed a significant age-associated decrease in the relative abundance of Actinobacteria ($p = 0.03$) and an increase in the relative abundances of Cyanobacteria ($p = 0.0002$), Epsilonbacteraeota ($p = 0.03$), Lentisphaerae ($p < 0.0001$), Proteobacteria ($p = 0.001$), Synergistetes ($p = 0.02$), Tenericutes ($p = 0.001$), Verrucomicrobia ($p = 0.004$) and unclassified bacteria ($p = 0.05$) in stool (Figure 4.1E).

Upon assessing the impact of ageing on microbiota composition at the genus level, we found that ageing significantly increased the relative abundances of 18 bacterial taxa in stool, including *Campylobacter (*$p = 0.03$), *Gastranaerophilales* ($p = 0.01$), *VadinBE97* ($p = 0.02$) and *Victivallis* ($p = 0.03$) (Table 3.1). Additionally, there was an age-associated decrease in the faecal relative abundances of *Bifidobacterium* ($p = 0.001$), *Blautia* ($p = 0.01$), *Fusicatenibacter* ($p = 0.03$), *Lachnospiraceae* ($p = 0.02$) and *Sutterella* ($p = 0.03$) (Table 3.1).

	Young adults (n = 37)	Old adults (n = 39)	P-value
Actinobacteria			
Actinomyces	0.03 ± 0.01	0.4 ± 0.1	0.26
Adlercreutzia	3 ± 1.6	1.9 ± 0.8	0.52
Bifidobacterium	84.8 ± 3.7	64 ± 4.5	**0.001**
Collinsella	4.5 ± 1.2	8.2 ± 1.7	0.23
Eggerthellaceae	0.7 ± 0.4	0.3 ± 0.1	0.5
Bacteroidetes			
Allistipes	5.6 ± 1.1	10.1 ± 2.1	0.27
Bacteroidales	0 ± 0	0.01 ± 0.01	0.51
Bacteroides	65.8 ± 5.6	53 ± 5	0.11
Barnesiella	1.3 ± 0.3	3 ± 1.4	0.43
Butyricimonas	0.1 ± 0.02	0.2 ± 0.1	**0.01**
Coprobacter	0.1 ± 0.02	0.1 ± 0.02	0.23
Odoribacter	0.2 ± 0.04	0.3 ± 0.1	0.22
Parabacteroides	2.4 ± 0.4	2.1 ± 0.4	0.56
Paraprevotella	1.3 ± 1	0.8 ± 0.4	0.63
Prevotella	0.2 ± 0.2	2.9 ± 1.8	0.29
Prevotellaceae	1 ± 0.9	0.06 ± 0.04	0.61
Cyanobacteria			
Gastranaerophilales	21.6 ± 6.9	59 ± 8	**0.01**
Deinoccus-Thermus			
Meiothermus	2.7 ± 2.7	2.6 ± 2.6	0.8
Elusimicrobia			
Elusimicrobium	0 ± 0	7.7 ± 4.3	0.34
Epsilonbacteraeota			
Campylobacter	0 ± 0	14.8 ± 5.6	**0.03**
Firmicutes			
Anaerotruncus	0.02 ± 0.01	0.01 ± 0.003	0.38
Angelakisella	0.03 ± 0.01	0.05 ± 0.01	**0.01**
Blautia	10 ± 0.9	7 ± 1.1	**0.01**
Caproiciproducens	0.003 ± 0.002	0.002 ± 0.001	0.78
Christensenellaceae R-7 group	1.3 ± 0.3	5.3 ± 1.1	**0.03**
Clostridia	0.1 ± 0.1	0.04 ± 0.02	0.38
Clostridiales	0.3 ± 0.1	1.2 ± 0.2	**0.001**
Coprobacillus	0.0005 ± 0.0005	0.01 ± 0.01	**0.03**
Coprococcus	0.2 ± 0.02	0.2 ± 0.04	0.5
Dialister	1.8 ± 0.4	1.5 ± 0.3	0.8
Eisenbergiella	0.005 ± 0.001	0.03 ± 0.02	0.1
Enterococcus	0.003 ± 0.002	0.1 ± 0.1	0.33
Erysipelatoclostridium	0.01 ± 0.002	0.02 ± 0.005	0.31
Erysipelotrichaceae	0.004 ± 0.002	0.1 ± 0.1	0.39

Eubacterium	0 ± 0	0.003 ± 0.003	**0.05**
Faecalibacterium	22.8 ± 2.1	16.6 ± 2	0.07
Fournierella	0.05 ± 0.02	0.08 ± 0.03	0.52
Fusicatenibacter	1.9 ± 0.2	1.7 ± 0.4	**0.03**
Intestinibacter	0.1 ± 0.03	0.3 ± 0.1	0.46
Lachnospira	1.1 ± 0.2	1 ± 0.2	0.4
Lachnospiraceae	3.4 ± 0.3	2.8 ± 0.4	**0.02**
Lactobacillus	0.02 ± 0.01	0.04 ± 0.03	0.43
Oscillibacter	0.1 ± 0.02	0.1 ± 0.02	0.78
Peptostreptococcaceae	0.01 ± 0.002	0.01 ± 0.004	0.5
Phascolarctobacterium	0.5 ± 0.2	1 ± 0.3	0.26
Romboutsia	0.5 ± 0.1	0.3 ± 0.1	0.13
Roseburia	2.4 ± 0.9	1.7 ± 0.3	0.51
Ruminiclostridium	0.2 ± 0.1	0.8 ± 0.4	**0.02**
Ruminococcaceae	2.1 ± 0.7	5.5 ± 0.8	**0.001**
Sporobacter	0 ± 0	0.001 ± 0.001	0.66
Streptococcus	0.2 ± 0.1	0.4 ± 0.2	0.5
Turicibacter	0.1 ± 0.03	0.1 ± 0.01	0.43
Veillonella	0.1 ± 0.1	18.6 ± 18.3	0.29
Fusobacteria			
Fusobacterium	2.7 ± 2.7	11.1 ± 4.9	0.32
Lentisphaerae			
VadinBE97	5.8 ± 3.8	22.4 ± 5.7	**0.02**
Victivallis	15.8 ± 6	32.1 ± 6.9	**0.03**
Proteobacteria			
Bilophila	16 ± 2.9	10.1 ± 2.4	0.34
Desulfovibrio	8.6 ± 2.9	7.3 ± 2.6	0.77
Escherichia-Shigella	12.4 ± 3.5	18 ± 4.9	0.5
Haemophilus	8 ± 3.1	7 ± 2	0.51
Sutterella	35.3 ± 5.4	17.5 ± 3.1	**0.03**
Synergistetes			
Cloacibacillus	0 ± 0	21.8 ± 6.6	**0.01**
Tenericutes			
Anaeroplasma	10.6 ± 5	8.2 ± 3.7	0.54
Verrucomicrobia			
Akkermansia	97.3 ± 2.7	100 ± 0.005	0.67

Table 3.1 Relative abundances of genera at the phylum level in young and old participants. Relative abundances of key genera expressed as percentages of each phylum in healthy young (n = 37) and old (n = 39) adults. Data are mean ± standard error mean, with significant p-values highlighted in red. Multiple Mann-Whitney U tests were used to determine statistical significance and p-values were adjusted using the Benjamini-Hochberg method.

4.2.2 Microbial metabolite alterations with advancing age

Accompanying microbial composition changes, older adults displayed significantly lower faecal levels of acetate ($p < 0.0001$), butyrate ($p = 0.004$) and propionate ($p = 0.002$) compared to young participants (Figure 4.2A). Loss of SCFAs in older adults was associated with faecal blooming of *Ruminococcaceae*, *Odoribacter*, *Eisenbergiella*, *Caproiciproducens* and *Clostridia* (Figure 4.2B). In contrast, greater relative faecal abundances of *Bifidobacterium*, *Blautia*, *Faecalibacterium*, *Sutterella and Lachnospiraceae* were positively associated with higher levels of acetate, propionate and butyrate in stool from aged donors (Figure 4.2B).

Advancing age also negatively affected SBA production with older adults exhibiting lower levels of deoxycholic acid (DCA) ($p = 0.01$), hyodeoxycholic acid (HDCA) ($p = 0.001$) and ursodeoxycholic acid (UDCA) ($p = 0.01$) in stool (Figure 4.2C). This was linked to decreased relative abundances of *Blautia*, *Bilophila*, *Faecalibacterium*, *Paraprevotella* and *Lachnospiraceae* and the overrepresentation of *Ruminiclostridium*, *Eisenbergiella*, *Odoribacter*, *Oscillibacteri* and *Clostridia* in the aged faecal microbiome (Figure 4.2B).

4.2.3 Links between age-related microbial dysbiosis and innate immune ageing

Next, we sought to identify potential links between faecal microbiota, microbial metabolites and innate immunological parameters. Table 3.2 depicts the impact of ageing on monocyte and DC cytokine (IL6, IL10 and TNFα) production at baseline and in response to LPS stimulation as well as systemic levels of inflammatory mediators (IL10 and CRP). In this study, fewer $IL6^{+ve}$ and $TNF\alpha^{+ve}$ monocytes and DCs under basal conditions and/or post stimulation was correlated with higher relative

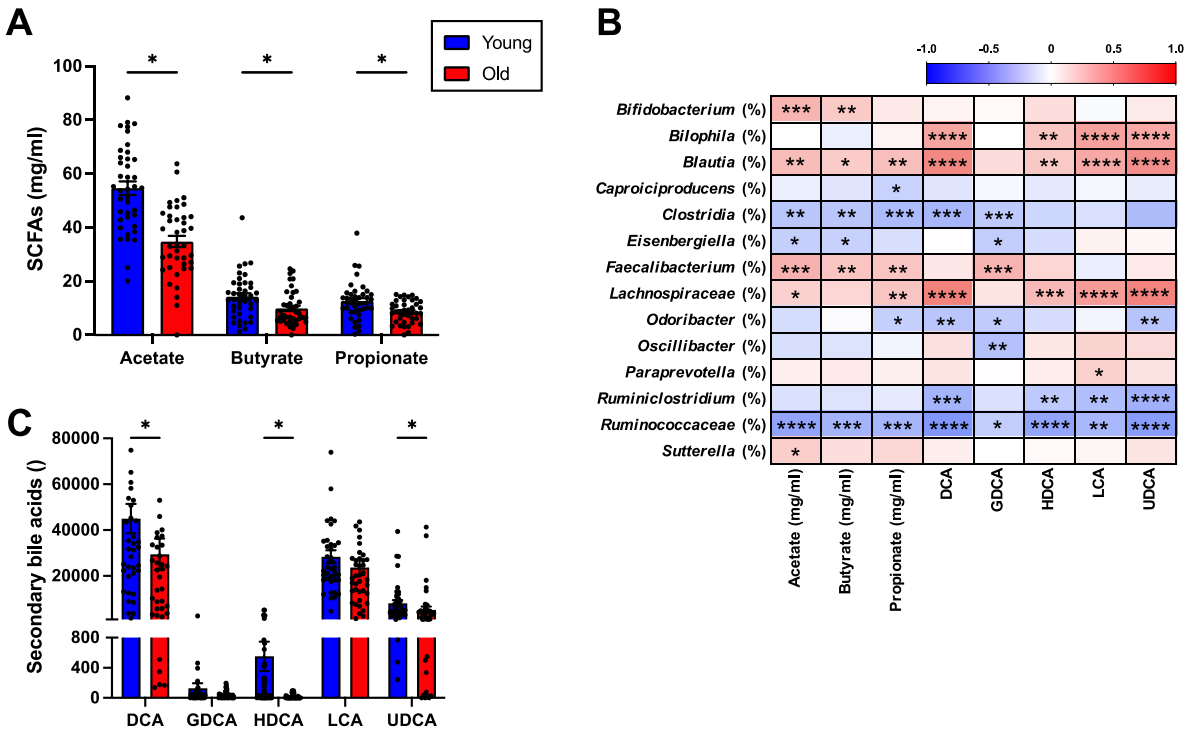

Figure 4.2 Microbial metabolite profiling and associations with microbiota in older adults. (A) Faecal levels of SCFAs (acetate, butyrate and propionate) in young (blue, n = 37) and old (red, n = 39) adults. **(B)** Correlation matrix depicting associations between the faecal concentrations of microbial metabolites and the relative abundances of bacterial genera. Red represents positive correlation coefficients, while blue denotes negative correlation coefficients as shown in the colour legend. **(C)** Faecal concentrations of SBAs (DCA, GDCA, HDCA, LCA and UDCA) in participants. Differences between both age groups were assessed via Multiple Mann-Whitney U tests. Adjusted p-values were calculated using the Benjamini and Hochberg method. *p ≤0.05, **p ≤0.01, ***p ≤0.001, ****p ≤0.0001.

	Young adults (n = 37)	Old adults (n = 39)	P-value
IL6^{+ve} monocytes_basal (%)	3.7 ± 0.7	5.7 ± 1	0.24
IL10^{+ve} monocytes_basal (%)	1.9 ± 0.2	2.6 ± 0.4	0.45
TNFα^{+ve} monocytes_basal (%)	13.5 ± 1.1	16.6 ± 1.5	0.24
IL6^{+ve} monocytes_LPS (%)	37.7 ± 4.6	50.6 ± 4.2	0.24
IL10^{+ve} monocytes_LPS (%)	5.2 ± 0.6	4.6 ± 0.4	0.52
TNFα^{+ve} monocytes_LPS (%)	28.2 ± 3.6	62 ± 10.1	0.24
IL6 expression in monocytes_basal (MFI)	10.6 ± 0.6	10.8 ± 0.7	0.77
IL10 expression in monocytes_basal (MFI)	13.2 ± 1	14.4 ± 0.9	0.2
IL6^{+ve} DCs_basal (%)	6 ± 0.6	6.4 ± 0.5	0.77
IL10^{+ve} DCs_basal (%)	3.8 ± 0.3	3.9 ± 0.3	0.67
TNFα^{+ve} DCs_basal (%)	5.7 ± 0.8	4.4 ± 0.6	0.11
IL6^{+ve} DCs_LPS (%)	39.3 ± 3	32.2 ± 2	**0.05**
IL12^{+ve} DCs_LPS (%)	5.5 ± 0.6	6.6 ± 0.7	0.56
IL6 expression in DCs_basal (MFI)	19.9 ± 2.5	15.2 ± 1.5	0.18
IL10 expression in DCs_basal (MFI)	19.2 ± 1.2	18 ± 1.2	0.48
TNFα expression in DCs_basal (MFI)	12.5 ± 1.5	14.2 ± 1.6	0.55
Serum IL10 levels (pg/ml)	3.9 ± 1.2	6 ± 1.5	0.34
Systemic CRP levels (µg/ml)	2.5 ± 0.05	2.9 ± 4.1	0.24

Table 3.2 Impact of ageing on innate immune parameters and serum inflammatory mediators. The percentage of monocytes and DCs that produce cytokines IL6, IL10, IL12 and TNFα and their cytokine expression densities (MFI) in young (n = 37) and old (n = 39) adults. Data are mean ± standard error mean. Multiple Mann-Whitney U tests were used to determine statistical significance and p-values were adjusted using the Benjamini-Hochberg method.

abundances of *Bifidobacterium* (R = -0.35, p = 0.03), *Lactobacillus* (R = -0.38, p = 0.02), *Prevotella* (R = -0.34, p = 0.04), *Lachnospiraceae* (R = -032, p = 0.05), *Terrisporobacter* (R = -0.33, p = 0.04) and *Paraprevotella* (R = -0.43, p = 0.007) and lower relative abundances of *Clostridia* (R = 0.37, p = 0.02; R = 0.33, p = 0.05), *Fournierella* (R = 0.34, p = 0.04), *Ruminococcaceae* (R = 0.48, p = 0.002; R = 0.34, p = 0.04; R = 0.35, p = 0.03; R = 0.38, p = 0.02) and *Sporobacter* (R = 0.39, p = 0.02) in stool from aged donors (Figure 4.3).

Ruminococcaceae (R = -0.42, p = 0.008; R = -0.35, p = 0.03, respectively), *Ruminiclostridium* (R = -0.38, p = 0.02; R = -0.36, p = 0.02, respectively) and *Clostridia* (R = -0.33, p = 0.04) were also positively associated with fewer IL6- and TNFα-secreting monocytes and DCs post stimulation (Figure 4.3). On the other hand, older adults with high relative abundances of *Faecalibacterium* (R = 0.49, p = 0.002), *Lachnospiraceae* (R = 0.49, p = 0.002), *Dialister* (R = -0.47, p = 0.002), *Eggerthellaceae* (R = -0.45, p = 0.005) and *Fournierella* (R = -0.5, p = 0.001) in stool displayed increased frequencies of $IL10^{+ve}$ stimulated DCs but lower IL10 surface densities (MFI) on monocytes (Figure 4.3).

Upon assessing the relationship between serum inflammatory mediator levels and faecal microbiota in older adults, we observed positive correlations between circulating IL10 levels and *Gastroenterophilales* (R = 0.42, p = 0.008), *Lachnospiraceae* (R = 0.35, p = 0.03) and *Odoribacter* (R = 0.38, p = 0.02) (Figure 4.3). Further, high relative abundances of *Akkermansia* (R = -0.33, p = 0.04), *Gastroenterophilales* (R = -0.43, p = 0.007) and *Bacteroidales* (R = -0.32, p = 0.05)

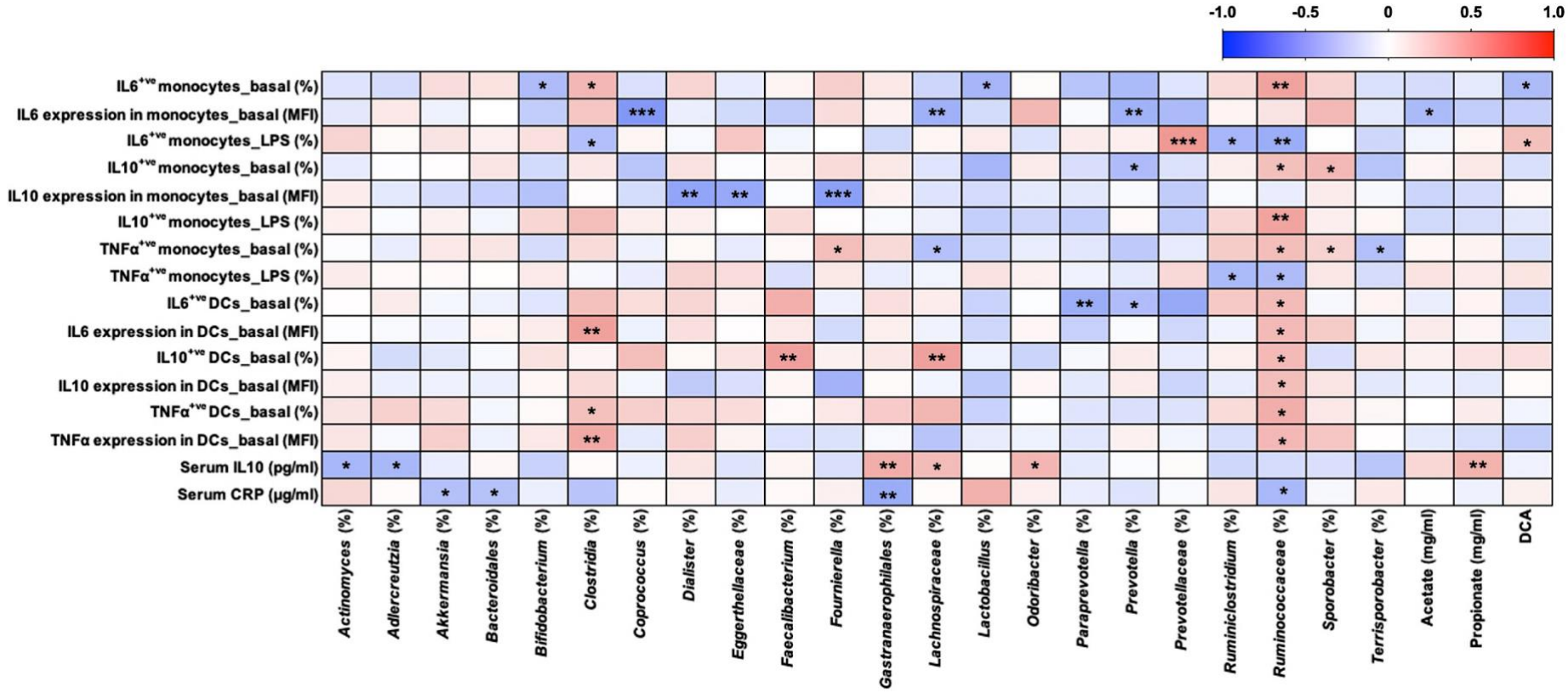

Figure 4.3 Links between key microbiota, microbial metabolites and innate immunity in older adults. Spearman's correlation matrix depicting associations between bacteria, microbial metabolites and innate immune parameters in older adults (n = 39). Red represents positive correlation coefficients, while blue denotes negative correlations. *p ≤0.05, **p ≤0.01, ***p ≤0.001.

were linked to lower serum CRP levels in old age. Among microbial metabolites, high faecal levels of acetate, propionate and DCA were strongly linked to low basal IL6 production by monocytes (R = -0.36, p = 0.02), enhanced IL6 secretion by stimulated monocytes (R = 0.32, p = 0.05) and low serum levels of IL10 (R = 0.4, p = 0.01) in older adults (Figure 4.3).

4.2.4 Links between age-related microbial dysbiosis and adaptive immune ageing

Next, we evaluated relationships between faecal microbiota, microbial metabolites and adaptive immunological parameters. Table 3.3 depicts the impact of ageing on the distribution of T cell and B cell subsets. Upon evaluating B cell subset distribution, we found that ageing significantly increased the peripheral frequency of Bregs (p = 0.03) (Table 3.3).

Among older adults, high peripheral frequencies of naïve CD4 and CD8 T cells and naïve B cells were correlated with elevated faecal butyrate levels (R = 0.47, p = 0.003) and reduced relative abundances of *Coprococcus* (R = -0.32, p = 0.05), *Collinsella* (R = 0.47, p = 0.003), *Paraprevotella* (R = 0.44, p = 0.006) and *Erysipelotrichaceae* (R = -0.45, p = 0.004) in stool (Figure 4.4). High faecal levels of butyrate and GDCA were also linked to increased proportions of CM CD4 (R = 0.55, p = 0.0004) and CD8 (R = 0.45, p = 0.005) T cells and fewer EMRA CD4 T cells (R = -0.4, p = 0.01; R = -0.35, p = 0.03) in older adults (Figure 4.4). Furthermore, we observed negative correlations between faecal *Bilophila* (R = -0.39, p = 0.02), *Blautia* (R = -0.32, p = 0.05) and *Sutterella* (R = -0.38, p = 0.02) and the accumulation of senescent CD4 and CD8 T cells in aged participants (Figure 4.4).

	Young adults (n = 37)	Old adults (n = 39)	P-value
Naïve CD4 T cells (%)	50.7 ± 1.8	16.1 ± 1.9	**<0.0001**
CM CD4 T cells (%)	17 ± 1.2	15.2 ± 1.9	**0.03**
EMRA CD4 T cells (%)	9 ± 0.8	27 ± 2.2	**<0.0001**
Naïve CD8 T cells (%)	40.6 ± 2	9.9 ± 1	**<0.0001**
CM CD8 T cells (%)	5.4 ± 0.7	10.1 ± 1.3	**0.01**
EMRA CD8 T cells (%)	42.8 ± 1.8	55.4 ± 2.5	**0.0001**
Senescent CD4 T cells (%)	0.8 ± 0.2	4.9 ± 0.9	**<0.0001**
Senescent CD8 T cells (%)	15.1 ± 1.4	42.1 ± 3.1	**<0.0001**
PD1^{+ve} exhausted CD8 T cells (%)	15 ± 1.5	23.2 ± 2.7	**0.01**
Th17 cells (%)	5 ± 0.4	6.7 ± 7.9	**0.05**
Th1 cells (%)	17.4 ± 1.4	19.6 ± 1.6	0.32
Th2 cells (%)	7.2 ± 0.8	7.6 ± 0.8	0.56
Tregs (%)	4.1 ± 0.3	7.2 ± 0.4	**<0.0001**
IL10^{+ve} Tregs (%)	6.9 ± 1	8.4 ± 1.2	0.32
IFNγ^{+ve} CD8 T cells (%)	13.1 ± 1.4	14.5 ± 1.3	0.44
Naïve B cells (%)	68.6 ± 1.5	64.6 ± 1.8	0.33
Memory B cells (%)	16 ± 1.1	19.2 ± 1.8	0.49
Bregs (%)	5.3 ± 1.4	6.9 ± 1.6	**0.03**

Table 3.3 Impact of ageing on T cell and B cell subset distribution. The proportion of T cell and B cell subsets in young (n = 37) and old (n = 39) adults. Data are mean ± standard error mean. Multiple Mann-Whitney U tests were used to determine statistical significance and p-values were adjusted using the Benjamini-Hochberg method.

Upon further assessment, we observed positive associations between relative abundances of *Anaerotruncas*, *Eisenbergiella*, *Eggerthellaceae, Erysipelotrichaceae*, *Phascolarctobacterium*, *Lactobacillus, Turicibacter*, *Phascolartobacterium* and *Bilophila* in stool from aged donors and Th1 (R = 0.38, p = 0.02; R = 0.37, p = 0.02; R = 0.33, p = 0.05), Th2 (R = 0.36, p = 0.03; R = 0.51, p = 0.001) and Th17 (R = 0.39, p = 0.02; R = 0.41, p = 0.01; R = 0.38, p = 0.02; R = -0.38, p = 0.02) polarisation (Figure 4.4). Moreover, the expansion of IL10-producing Tregs was linked to the overrepresentation of *Oscillibacter* (R = 0.38, p = 0.02), *Phascolartobacterium* (R = 0.38, p = 0.02) in the aged faecal microbiome, while Bregs were positively linked to faecal GDCA (R = 0.35, p= 0.03) and *Lactobacillus* (R = 0.45, p = 0.004) (Figure 4.4). Similarly, increased *Lactobacillus* and *Turicibacter* in stool were correlated with an increased frequency of IFNγ-secreting CD8 T cells in older people (R = 0.42, p = 0.009; R = 0.36, p = 0.03, respectively) (Figure 4.4).

Interestingly, high IMM-AGE scores were positively correlated with *Clostridiales* (R = 0.39, p = 0.0004), *Eisenbergiella* (R = 0.27, p = 0.02), *Gastranaerophilales* (R = 0.29, p = 0.01) and *Ruminococcaceae* (R = 0.54, p <0.0001) in older adults (Figure 4.4). Conversely, high relative faecal abundances of *Bifidobacterium* (R = -0.36, p = 0.002), *Blautia* (R = -0.36, p = 0.001) and *Lachnospiraceae* (R = -0.27, p = 0.02) in aged individuals were associated with lower IMM-AGE scores (Figure 4.4).

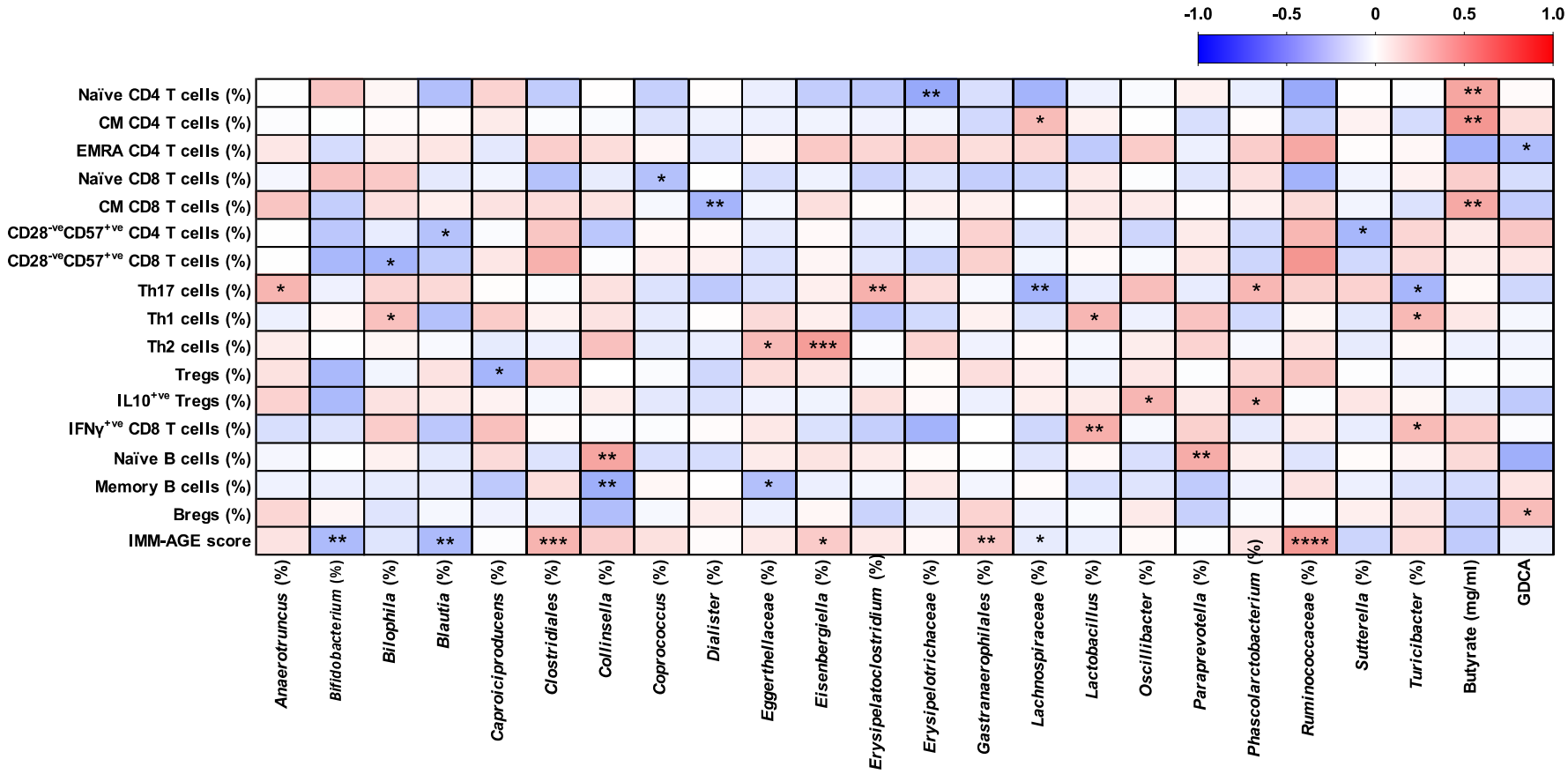

Figure 4.4 Links between key microbiota, microbial metabolites and adaptive immunity in older adults. Spearman's correlation matrix depicting associations between bacteria, microbial metabolites and adaptive immune parameters in older people (n = 39). Red represents positive correlation coefficients, while blue denotes negative correlation coefficients as shown in the colour legend. *p ≤0.05, **p ≤0.01, ***p ≤0.001, ****p ≤0.0001.

4.2.5 Impact of microbial composition on influenza vaccine responses in older adults

Serum and stool samples were collected from 27 older adults at baseline and 28 days post influenza vaccination (Figure 4.5A). The HAI assay was carried out on baseline and follow-up serum, revealing significant increases in H1N1 and B Victoria titres in older adults in response to immunization (Figure 4.5B). However, we observed no difference in H3N2 antibody titres (Figure 4.5B) or IgA ($p = 0.47$), IgG ($p = 0.92$) and IgM ($p = 0.47$) serum levels between baseline and follow-up (Figure 4.5C).

Given these results, older adults were split into two sub cohorts based on HAI H1N1 titres: low responders (n = 15, age range 68-84) and high responders (n = 12, age range 65-83). Both groups were comprised of a similar number of males (5 in each group). BMI (mean BMI among low and high responders was 23.9 kg/m^2 and 24.9 kg/m^2, respectively; $p = 0.61$), smoking status (zero low responding smokers and one high responding smoker; $p = 0.44$) and alcohol consumption (units consumed per drink per week for low and high responders were 4 and 8.6, respectively; $p = 0.72$) were also comparable between both groups.

Alpha diversity metrics, including the Chao1 richness index, the Shannon evenness index and the non-parametric Shannon diversity index ($p = 0.8$ for all) were also comparable between low and high responders (Figures 4.5D, 4.5E and 4.5F). Microbial profiling revealed comparable abundances of core phyla, including Actinobacteria, Bacteroidetes, Cyanobacteria, Deinoccus-Thermus, Elusimicrobia, Epsionbacteraeota, Firmicutes, Fusobacteria, Lentisphaerae, Proteobacteria, Synergistetes, Tenericutes and Verrucomicrobia between groups ($p \geq 1$ for all) (data not shown).

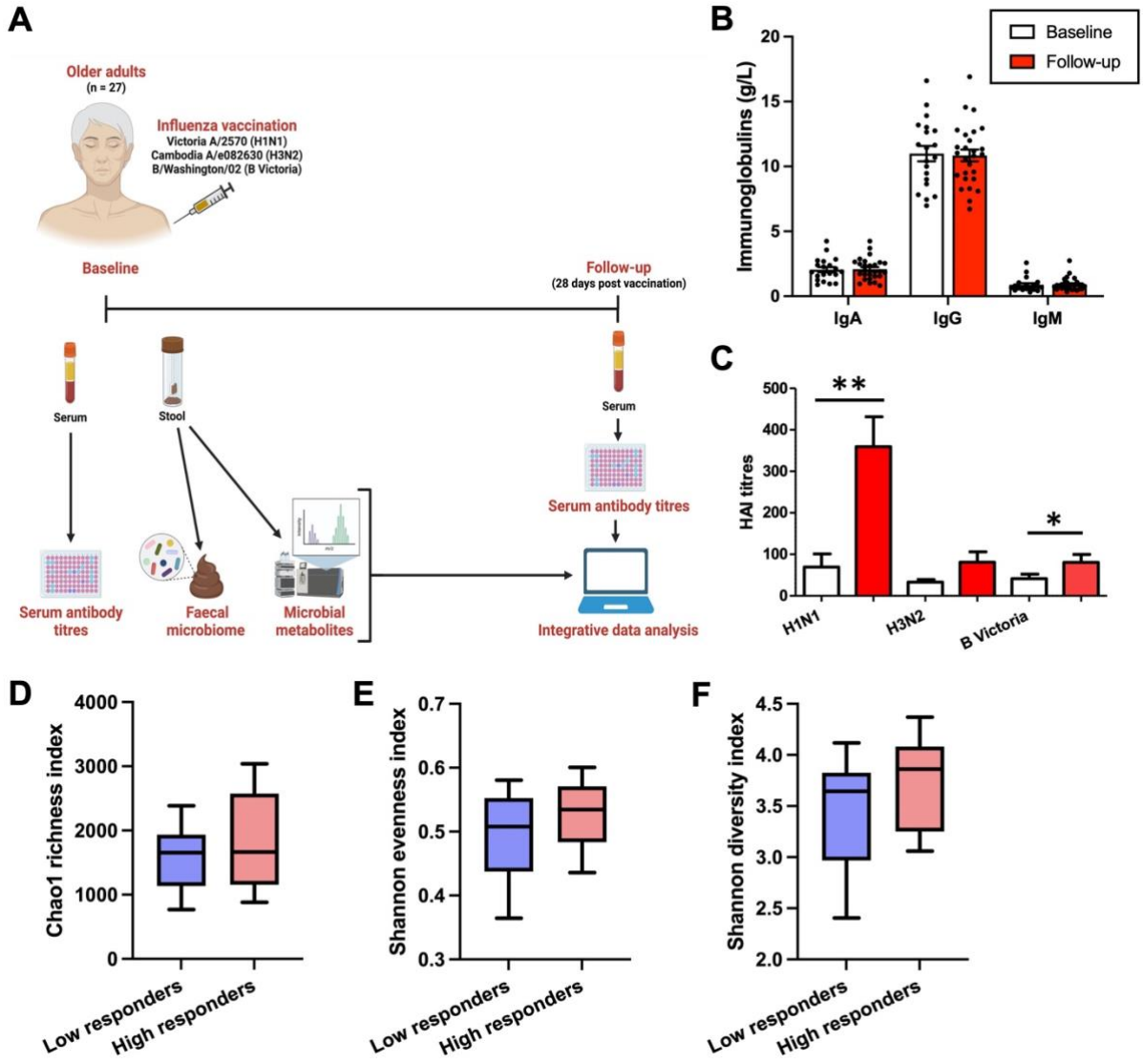

Figure 4.5 Relationship between influenza immunogenicity and microbiota diversity. (A) Vaccine sub-study design. **(B)** Serum immunoglobulin levels **(B)** and haemagglutination inhibition (HAI) titres **(C)** in older participants (n = 27) at baseline (white) and 28-days post influenza vaccination (red). Data are mean ± standard error mean. Alpha diversity of faecal microbiota from in low (blue, n = 15) and high (red, n = 12) influenza vaccine responding older adults measured using the Chao1 richness index **(D)**, the Shannon evenness index **(E)** and the non-parametric Shannon diversity index **(F)**. **(D-F)** Data are expressed as mean as indicated by the middle lines, while whisker lines represent the minimum and maximum data points. Multiple Mann-Whitney U tests were used to determine statistical significance. P-values were adjusted using the Benjamini-Hochberg method. *p ≤0.05, **p ≤0.01.

Although the relative abundances of key microbial taxa did not significantly differ between groups, high responding older adults exhibited trends for increased faecal levels of *Bifidobacterium* ($p = 0.06$) and *Lactobacillus* ($p = 0.06$) compared to low responders (Figure 4.6A). Faecal concentrations of SCFAs and SBAs were also comparable between low and high responders (Figures 4.6B and 4.6C). However, upon the assessment of links between faecal microbiota and serum antibody titres in old adults, IgA was positively correlated with several bacterial taxa, including *Adlercreutzia* ($R = 0.39$, $p = 0.04$), *Anaerotruncas* ($R = 0.44$, $p = 0.02$), *Bacteroides* ($R = 0.44$, $p = 0.02$), *Coprococcus* ($R = 0.44$, $p = 0.02$), *Flavonifractor* ($R = 0.38$, $p = 0.05$), *Lachnospiraceae* ($R = -0.5$, $p = 0.007$), *Negativibacillus* ($R = 0.38$, $p = 0.05$), *Oscillibacter* ($R = 0.45$, $p = 0.02$), *Oscillospira* ($R = 0.4$, $p = 0.04$) and *Ruminiclostridium* ($R = 0.48$, $p = 0.01$) (Figure 4.6D). We also observed a positive association between serum IgM titres and *Lachnospiraceae* in the aged faecal microbiome ($R = 0.67$, $p = 0.0001$) (Figure 4.6D). On the other hand, high serum IgA levels were negatively correlated with stool DCA ($R = -0.52$, $p = 0.02$), LCA ($R = -0.46$, $p = 0.04$) and UDCA ($R = -0.46$, $p = 0.04$) concentrations (Figure 4.6D).

Among IgG, the strongest correlations were with *Lachnospiraceae* ($R = -0.51$, $p = 0.007$), *Bifidobacterium* ($R = 0.48$, $p = 0.01$), *Alistipes* ($R = 0.4$, $p = 0.04$) and *Adlercreutzia* ($R = -0.38$, $p= 0.05$) (Figure 4.6D). Lastly, we observed positive associations between H1N1 titres and *Lactobacillus* ($R = 0.51$, $p = 0.007$), *Bifidobacterium* ($R = 0.43$, $p = 0.02$), *Intestinibacter* ($R = 0.42$, $p = 0.03$), *Enterobacteriaceae* ($R = 0.4$, $p = 0.04$) and LCA ($R = 0.47$, $p = 0.04$) in aged individuals (Figure 4.6D).

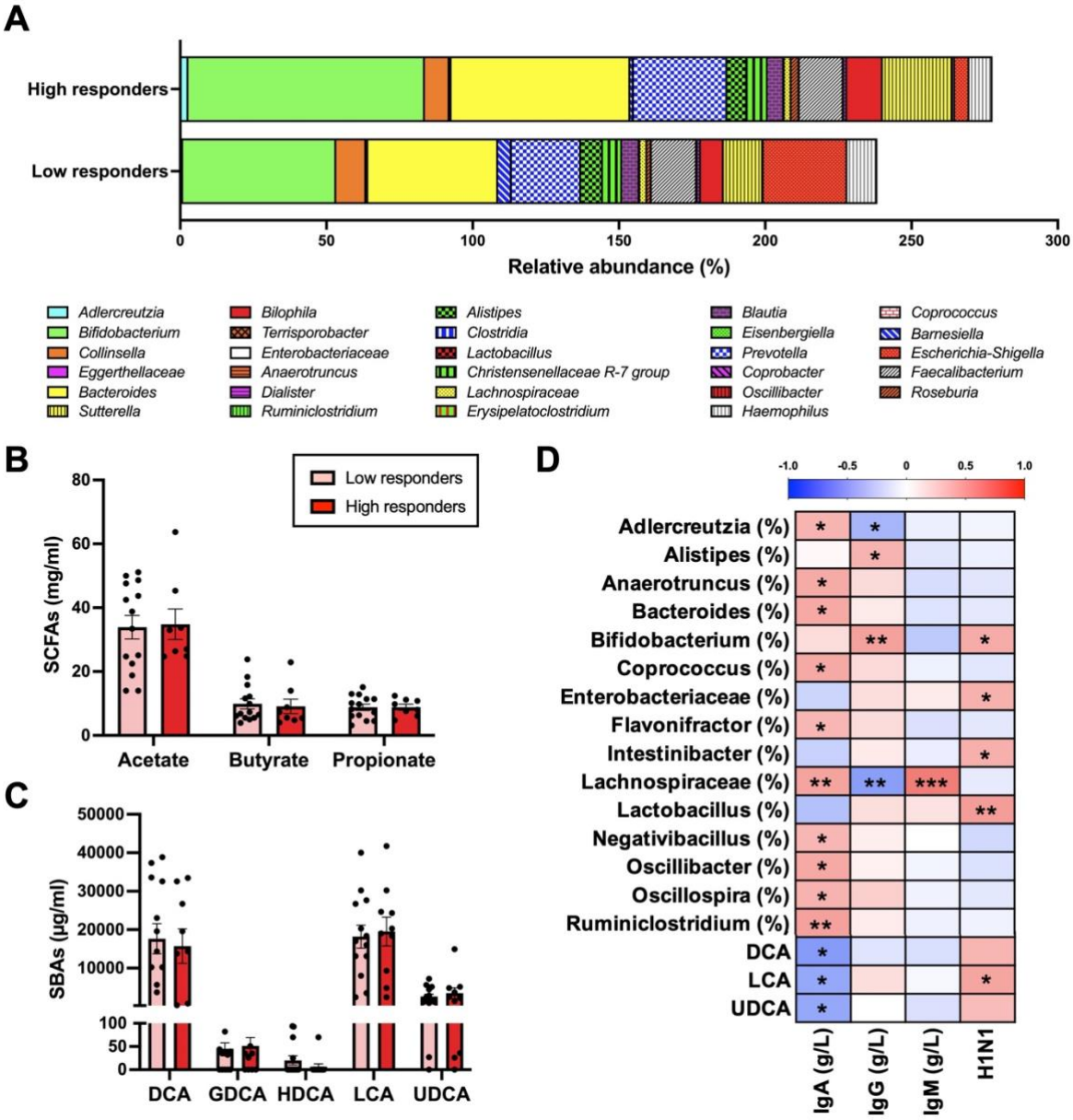

Figure 4.6 Relationship between influenza vaccine immunogenicity, microbiota composition and metabolites in older adults. (A) Relative abundances of bacteria expressed as percentages of each phylum in low (n = 15) and high (n = 12) influenza vaccine responding older adults. Faecal levels of SCFAs **(B)** and secondary bile acids **(C)** in low (pink, n = 15, pink) and high (red, n = 12) responders. Data are expressed as mean **(A)** and mean ± standard error mean. **(B,C)**. Multiple Mann-Whitney U tests were used to determine statistical significance. P-values were adjusted using the Benjamini-Hochberg method. **(D)** Correlation (Spearman's) matrix depicting links between bacteria, SBAs and serum antibody titres in older adults (n = 27). Red represents positive correlation coefficients, while blue denotes negative correlation coefficients as shown in the colour legend. *p ≤0.05, **p ≤0.01, ***p ≤0.001.

4.3 Discussion

With advancing age, the gut microbiome and immune system undergo profound compositional and functional modifications that increase the host's susceptibility to infection and morbidity, while contributing to poor immunogenicity [320]. Recent studies have indicated that age-related microbial dysbiosis plays a key role in promoting chronic immune cell activation and inflammageing [315,521,522], and thus may also drive immunesenescence. Here, we demonstrated that ageing is accompanied by commensal dysbiosis and pathobiont blooming, which are associated with several features of innate and adaptive immune ageing, possibly contributing to accelerated immunological ageing (high IMM-AGE scores). Further, we identified multiple key bacterial taxa linked with a healthy immune system and good vaccine responses in older adults, emphasizing the potential of microbiome-based interventions to delay immune ageing and improve health span.

Although, faecal microbial diversity did not decrease with age, older adults displayed distinct bacterial signatures that were characterized by the depletion of Actinobacteria and the expansion of opportunistic phyla, including Cyanobacteria, Epsilonbacteraeota, Lentisphaerae, Synergistetes, Tenericutes and Verrucomicrobia. These findings are similar to those from other studies of older adults, which demonstrated an age-related increase in enteric pathogens despite no change in alpha diversity [328,525]. One of the most well-known features of age-related microbial dysbiosis is the loss of Bacteroidetes and the expansion of Firmicutes and Proteobacteria [526,527], which reduce the bioavailability of immunomodulatory SCFAs and SBAs. Decreased SCFA and SBA levels are associated with bacterial overgrowth [528], gut barrier damage and subsequent microbial translocation

[289,529], intestinal and systemic inflammation [294], autoimmunity and immune dysfunction [287,530], highlighting the importance of these metabolites in regulating host health. Indeed, expansion of potential opportunistic taxa, such as *Ruminococcaceae*, *Ruminiclostridium*, *Anaerotruncas* and *Erysipelatoclostridum*, were linked to increased pro-inflammatory cytokine production by monocytes and DCs, Th17 cell expansion, senescent cell accumulation and fewer anti-viral IFNγ-expressing CD8 T. Furthermore, a high relative abundance of *Ruminococcaceae* was strongly correlated with higher IMM-AGE scores, suggesting that these bacteria have a deleterious effect on the immune system.

Alterations in microbiota composition and metabolic profile increase an individual's risk of immune dysregulation and chronic inflammation, predisposing them to age-related diseases [320]. Among core commensals, *Lactobacillus* and *Bifidobacterium* exhibit a variety of immunomodulatory effects, such as dampening inflammation, enhancing NK cell activity and increasing sIgA secretion. As a result, *Lactobacillus* and *Bifidobacterium* are frequently used as probiotics to boost immunity and improve overall health in older people. In this study, we reported that high relative faecal abundances of *Lactobacillus* and *Bifidobacterium* are associated with reduced basal production of IL6 by monocytes, an increased frequency of IFNγ-expressing CD8 T cells and enhanced Th1 polarisation. Interestingly, supplementation of *Lactobacillus plantaraum* has been demonstrated to improve gut dysbiosis-associated phenotypical alterations of tolerogenic DCs, increasing their capacity for inducing Treg differentiation [531]. Supplementation of *Lactobacillus* and *Bifidobacterium* species has been shown to promote T helper cell expansion in older adults by reintroducing beneficial gut microbiota [532]. Further, *Lactobacillus* administration in adult mice

induces a shift in the Th1/Th2 balance toward Th1 immune responses, increasing the secretion of IL10 and IFNy [533].

SCFAs are the end-products of bacterial fermentation of non-digestible dietary fibres and key mediators of the microbiome-immune system axis [277]. Butyrate, in particular, has been shown to exert multiple immunomodulatory effects, including inducing the generation of IL10-producing Tregs [285], suppressing Th17 polarisation and enhancing Breg differentiation [284,286,287]. In this study, we observed strong positive associations between stool butyrate levels and the peripheral frequencies of naïve T cells and CM CD4 and CD8 T cells in older adults. High butyrate levels were also correlated with a reduced accumulation of terminally differentiated EMRA CD4 T cells, which exhibit mitochondrial dysfunction and impaired oxidative phosphorylation similar to that observed in senescent T cells [199,200]. On a similar note, an accumulation of senescent T cells was negatively associated with *Blautia*, which are SCFA-producing bacteria [534].

Butyrate exposure has been shown to enhance mitochondrial function and fatty acid oxidation in activated T cells, thereby favouring the survival of long-lived memory T cells over terminally differentiated T cells [535]. High faecal levels of acetate and propionate were also associated with lower IL6 expression densities on monocytes under basal conditions and increased circulating levels of anti-inflammatory IL10. Acetate and propionate display potent anti-inflammatory properties, dampening pro-inflammatory cytokine (IL6 and TNFα) production and upregulating anti-inflammatory (IL10) cytokine secretion *in vitro* [536].

Aged individuals also presented with lower faecal levels of the SBAs DCA, HDCA and UDCA compared to young subjects, the former of which was correlated with decreased basal IL6 production by monocytes and an increased frequency of IL6-expressing monocytes post stimulation. Although GDCA levels were unaltered with age, higher faecal levels in older adults were associated with an increased proportion of naïve CD4 T cells, fewer EMRA CD4 T cells and increased Breg generation. The loss of SBAs in old age was linked to the underrepresentation of *Bilophila*, *Blautia* and *Lachnospiraceae* in stool. *Lachnospiraceae* consist of *Clostridia* and *Blautia* species that express bile salt hydrolases, which convert host-derived primary bile acids into SBAs [537,538]. We observed a strong negative correlation between faecal *Lachnospiraceae* and the accumulation of Th17 cells in older adults. Further, *Clostridia* was associated with enhanced IL6 and TNFα responses by stimulated DCs. A lower abundance of *Bilophila*, *Blautia*, *Lachnospiraceae* and *Sutterella* in stool was also associated with the age-related decline in faecal acetate, butyrate, propionate, DCA, HDCA and UDCA levels.

Together, these findings shed light on the potential beneficial effects of key microbiota, including *Blautia, Clostridia*, *Lactobacillus* and *Bifidobacterium,* and their derivative metabolites on immune ageing, supporting existing evidence that probiotic supplementation could be used to reverse microbial dysbiosis and boost immunity in older adults [539-542]. Moreover, these data provide the rationale for further investigating the anti-immunesenescence properties of these novel microbiota taxa since they are not currently a component of probiotics.

Poor vaccine immunogenicity is often reported in older adults and is associated with shrinkage of the naïve lymphocyte pool, an accumulation of dysfunctional memory T

cells and B cells with limited repertoire diversity and impaired CD4 T helper cell functions, which together contribute towards low antibody titres upon vaccination [15,195,206,543,544]. Growing evidence demonstrates that the composition of the gut microbiome is an important determinant of immune responses and vaccine efficacy [545,546]. Indeed, several studies have linked enhanced vaccine responses with a high relative abundance of the Actinobacteria phylum and lower Bacteroidetes levels [547,548].

Here, we report a trend for increased relative abundances of *Bifidobacterium* and *Lactobacillus* in high influenza vaccine responding older adults compared to low responders. Consumption of prebiotics and probiotics containing *Bifidobacterium* and *Lactobacillus* species has been found to drastically enhance seroprotectivity and increase H1N1, H3N2 and B antigens in influenza vaccinated older adults [549]. Further, neutralising antibodies to SARS-CoV-2 tend to be higher in vaccinees that have a greater abundance of *Roseburia* species [546], which have been linked to elevated circulating levels of IL27 and improved T cell responses [550]. Contrary to our results, intestinal enrichment of *Bacteroides* was correlated with poor vaccine efficacy, though these studies investigated the impact of microbial composition on rotavirus and SARS-CoV-2 immunogenicity [546,551].

One mechanism by which microbiota modulate vaccine immunogenicity is through the production of microbial metabolites, including SCFAs and SBAs, which have been shown to support B cell metabolism and drive the generation of antibody-secreting B cells [288]. Although, faecal concentrations of microbial metabolites were comparable between low and high vaccine responders in this study, a reduction in SBA levels was previously found to contribute towards diminished vaccine responses [545,552]. These

contradicting findings highlight the need for larger sample sizes as well as *in vitro* and *in vivo* validation to understand the role that microbial metabolites play in vaccine immunogenicity.

4.3.1 Conclusion

In conclusion, our results identify novel bacterial species and their metabolites that could contribute towards immunesenescence and poor vaccine efficacy in older adults. Although large-scale studies are still imperative, our findings provide the building blocks for future identification of exact bacterial species linked to healthy immune outcomes. In the meantime, we propose the potential use of existing probiotics and other microbiome-targeted interventions to extend health span.

Chapter 5: Associations between dietary patterns and the immune system in older adults

This chapter contains text written by Jessica Conway and edited by Dr Niharika A Duggal from the following manuscript.

Conway J, Animesh A, Duggal NA. Integrated analysis revealing novel associations between dietary patterns and the immune system in older adults (In preparation).

5.1 Background

The immune system undergoes extensive remodelling with age, resulting in the loss of its functional capacity, termed immunesenescence, which contributes towards an increased risk of infection, chronic disease, autoimmunity and poor vaccine responses resulting in increased mortality in older adults [553]. None of these individual features listed above are sufficient to indicate the degree of immunesenescence. However, the trajectory of an individual's immune-ageing process can be quantified using the recently developed IMM-AGE score, which serves as a clinically meaningful biological clock that can also be used to predict all-cause mortality [400]. Nevertheless, not all individuals are impacted by ageing equally and environmental factors have been recognised as substantial drivers of interindividual variability of immune features during ageing.

A well-balanced diet is required to maintain immune system functionality and promote good health. The individual-level diet quality can be calculated on the basis of four key aspects of a high-quality diet (variety, adequacy, moderation and overall balance) using the Diet Quality Index (DQI) [395]. A nutritional model that reflects this is the MedDiet, inspired by some Mediterranean countries' traditional dietary patterns. This dietary pattern is characterized by the high consumption of fruits, vegetables, whole grains, legumes, nuts, fish and olive oil with low-to-moderate intake of meats, dairy products and processed foods [554]. High adherence to the MedDiet has been shown to protect against frailty and other chronic age-related diseases, such as CVD [381]. These pro-health and pro-longevity effects are attributed to the host's anti-inflammatory and immunomodulatory properties [555]. Furthermore, insufficient intake of key nutrients (e.g. zinc, vitamin B_{12} and vitamin D) can cause immune system

impairments and increase the host's vulnerability to viral infections and morbidity [556]. Thus, it is critical to identify food components and nutrients associated with the maintenance of immune health to codevelop interventions and recommendations that promote the development of healthier diets for older people.

In this chapter, we aimed to dissect the complex relationship between nutrition, diet and a range of innate and adaptive immune parameters.

5.2 Results

5.2.1 Participant demographics

Forty healthy young individuals (aged 18-37 years; 17 males) and 40 healthy old adults (aged 63-84 years; 18 males) were recruited into this study (Figure 5.1A). All participants were Caucasian and only 4% were smokers. Both cohorts displayed similar BMIs with 60% of volunteers falling within the normal BMI range (18.5 to 24.9 kg/m^2) (Table 4.1). FETA-derived nutrients, food groups, minerals and vitamins were also compared between healthy young and old participants (Table 4.2).

5.2.2 Links between dietary patterns and the ageing gut microbiome

Diet is a major determinant of gut microbiota composition and microbial metabolite production (i.e. short-chain fatty acids (SCFAs) and secondary bile acids (SBAs)) [253]. Here, a high MedDiet score (MDS) was negatively associated with the relative abundance of *Terrisporobacter* ($R = -0.4$, $p = 0.01$) in the aged faecal microbiome (Figure 5.1B). DQI is a composite indicator of an individual's diet and was evaluated via FFQ questionnaires. Surprisingly, a high-quality diet was correlated with lower relative faecal abundances of *Bilophila* ($R = -0.32$, $p = 0.05$) and *Lachnospiraceae* ($R = -0.47$, $p = 0.003$) as well as lower stool DCA ($R = -0.4$, $p = 0.01$) and UDCA ($R = -0.39$, $p = 0.01$) levels in aged participants (Figure 5.1B). Additionally, we observed a positive correlation between DQI and *Clostridiales* in older people ($R = 0.41$, $p = 0.009$) (Figure 5.1B). Regarding specific macronutrients, dietary fibre intake was negatively linked to serum LBP levels ($R = -0.33$, $p = 0.04$) and faecal *Lactobacillus* ($R = -0.39$, $p = 0.01$) (Figure 5.1B). Lastly, we observed a strong positive correlation between saturated fat intake and stool GDCA levels ($R = 0.31$, $p = 0.05$) in aged volunteers (Figure 5.1B).

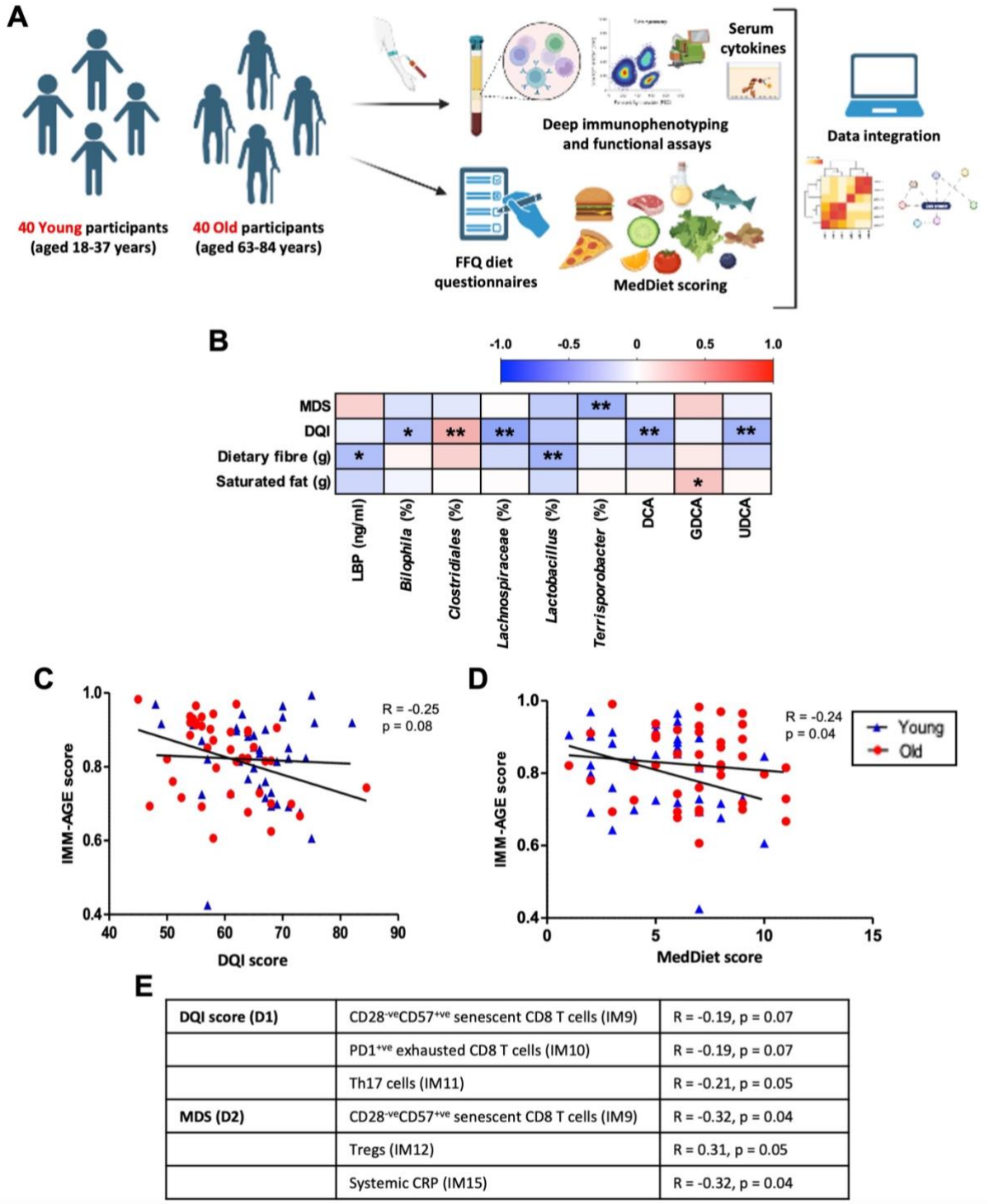

DQI score (D1)	$CD28^{-ve}CD57^{+ve}$ senescent CD8 T cells (IM9)	R = -0.19, p = 0.07
	$PD1^{+ve}$ exhausted CD8 T cells (IM10)	R = -0.19, p = 0.07
	Th17 cells (IM11)	R = -0.21, p = 0.05
MDS (D2)	$CD28^{-ve}CD57^{+ve}$ senescent CD8 T cells (IM9)	R = -0.32, p = 0.04
	Tregs (IM12)	R = 0.31, p = 0.05
	Systemic CRP (IM15)	R = -0.32, p = 0.04

Figure 5.1 Investigating Spearman-based correlations between dietary patterns and hallmarks of immunesenescence. (A) Study design. **(B)** Correlations (Spearman's) matrix depicting associations between dietary patterns and serum LBP levels, bacteria and secondary bile acids (DCA, GDCA and UDCA) in old adults (n = 40). Linear regression plots depicting associations between the IMM-AGE score and DQI **(C)** and the MedDiet Score **(D)** in healthy young (blue, n = 40) and old donors (red, n = 40). **(E)** Table showing associations between adherence to the MedDiet and a high DQI score and hallmarks of immunesenescence. Spearman correlations and p-values were determined using regression analysis.

	Young adults (n = 40)	Old adults (n = 40)	P-value
Age (years)	25.6 ± 0.9	73.1 ± 0.8	**<0.0001**
Male, n (%)	17 (43%)	18 (45%)	1
BMI (kg/m^2)	25.9 ± 1.1	24.7 ± 0.7	0.25
Smokers, n (%)	3 (8%)	0 (0%)	0.24

Table 4.1 Participant demographics. Values are expressed as mean ± standard error mean. Unpaired Student's T test, Mann Whitney U test and Fischer's exact test were used to determine p-values. Statistical significance was considered p ≤0.05, with significant p-values highlighted red.

	Young adults (n = 40)	Old adults (n = 40)	P-value
DQI	60.3 ± 1.9	65.4 ± 1.1	**0.003**
MedDiet	5.3 ± 0.4	6.8 ± 0.4	**0.004**
Food groups			
Carbohydrates (gm)	204.3 ± 8.5	186.5 ± 10.5	0.19
Protein (gm)	75.8 ± 4.6	73.1 ± 2.9	0.95
Total fat (gm)	69.7 ± 3.7	65.5 ± 4.3	0.46
Saturated fat (gm)	25.3 ± 1.3	25.3 ± 1.9	0.34
MUFA	25.5 ± 1.5	23.1 ± 1.6	0.28
PUFA	12.9 ± 0.9	11.4 ± 0.8	0.2
Cholesterol	241.3 ± 18.5	225.6 ± 12.6	0.58
Meat	91 ± 9.9	67.9 ± 7.1	0.13
Fish	29 ± 3.5	35.2 ± 2.9	0.18
Nuts	6.9 ± 1.4	11.8 ± 1.9	0.14
Vegetables	259 ± 17.5	287.1 ± 19.6	0.27
Fruit	190.4 ± 24	229.1 ± 25.8	0.14
Fibre (gm)	15.8 ± 1.1	17.8 ± 1	0.09
Minerals			

Calcium	848.6 ± 42.4	955.3 ± 45.3	**0.05**
Carotene	4038 ± 338.2	4178 ± 319.4	0.84
Chloride	3488 ± 191.5	3724 ± 251.2	0.45
Copper	1.1 ± 0.07	1.1 ± 0.06	0.91
Iron	9.8 ± 0.5	10.3 ± 0.5	0.42
Folate	255.3 ± 12.9	288.2 ± 15.4	0.11
Iodine	128.8 ± 8.4	149.5 ± 7.7	0.07
Potassium	3199 ± 154.9	3646 ± 148.1	0.04
Magnesium	297.7 ± 18.5	322.6 ± 13.8	0.09
Manganese	3.3 ± 0.2	3.9 ± 0.2	**0.03**
Sodium	2289 ± 103.7	2365 ± 140.7	0.66
Niacin	18.6 ± 1.1	19.8 ± 0.9	0.41
Phosphorus	1242 ± 53	1349 ± 52	0.15
Selenium	55.8 ± 3.9	58.4 ± 3	0.32
Nitrogen	11.8 ± 0.6	11.8 ± 0.5	0.96
Zinc	8.6 ± 0.5	8.4 ± 0.4	0.7
Vitamins			
Vitamin A	278.6 ± 23.2	362.7 ± 30.7	**0.02**
Vitamin B1 – thiamin	1.3 ± 0.1	1.4 ± 0.1	0.32
Vitamin B2 – riboflavin	1.5 ± 0.1	1.8 ± 0.1	**0.002**
Vitamin B6 – pyridoxine	1.9 ± 0.1	1.9 ± 0.1	1
Vitamin B12 – cobalamin	4.3 ± 0.4	5.5 ± 0.3	**0.02**
Vitamin C	118.6 ± 8.4	134.9 ± 10.8	0.26
Vitamin D	2.3 ± 0.3	2.2 ± 0.2	0.53
Vitamin E	11.7 ± 0.7	11 ± 0.7	0.42

Table 4.2 Daily average food and nutrient intake. Average daily consumption of foods and nutrients over the last 12 months. Values are expressed as mean ± standard error mean and p-values were calculated using Multiple Unpaired Student's T tests and Mann-Whitney U tests. P-values were adjusted using the Benjamini-Hochberg method and p ≤0.05 was considered significant. Abbreviations: MUFA, monounsaturated fatty acids; PUFA, polyunsaturated fatty acids.

5.2.3 Dietary patterns and features of immune ageing

Here, we observed a negative association between DQI scores and the immunological age (IMM-AGE score) of healthy aged donors (Figure 5.1C). Upon assessing the relationship between DQI score and different features of immunological ageing in older adults, we observed a negative correlation between the consumption of a poor-quality diet (low DQI score) and the systemic accumulation of pro-inflammatory $CD28^{-ve}CD57^{+ve}$ senescent CD8 T cells, exhausted $PD1^{+ve}$ CD8 T cells and Th17 cells (Figure 5.1E). A poor-quality diet was also positively associated with the secretion of anti-inflammatory cytokine IL10 by DCs (Figure 5.1E). Importantly, we found that a lower IMM-AGE score in older adults is correlated with a high MDS (Figure 5.1D). Additionally, a negative correlation was observed between the systemic accumulation of $CD28^{-ve}CD57^{+ve}$ senescent CD8 T cells, systemic CRP levels and MDSs (Figure 5.1E).

5.2.4 Dissecting an interrelationship between dietary components and immune ageing

Regarding DQI (DI1), the strongest associations seen were with high consumption of vegetables (DI9), dietary fibre (DI11) and fruit (DI10) (Figure 5.2A). DQI was also positively correlated with high fish intake (DI7). Regarding the MDS (DI2), the strongest associations found were with low meat consumption (DI6) and high consumption of dietary fibre (DI11), vegetables (DI9) and polyunsaturated fatty acids (PUFAs) (DI14) (Figure 5.2A). We also observed negative associations between the consumption of a diet rich in dietary fibre and PUFAs and the immunological age (IMM-AGE score) of aged hosts. Thus, it is unsurprising that consumption of a fibre-rich diet was linked with fewer circulating pro-inflammatory senescent and exhausted T cells and expansion of

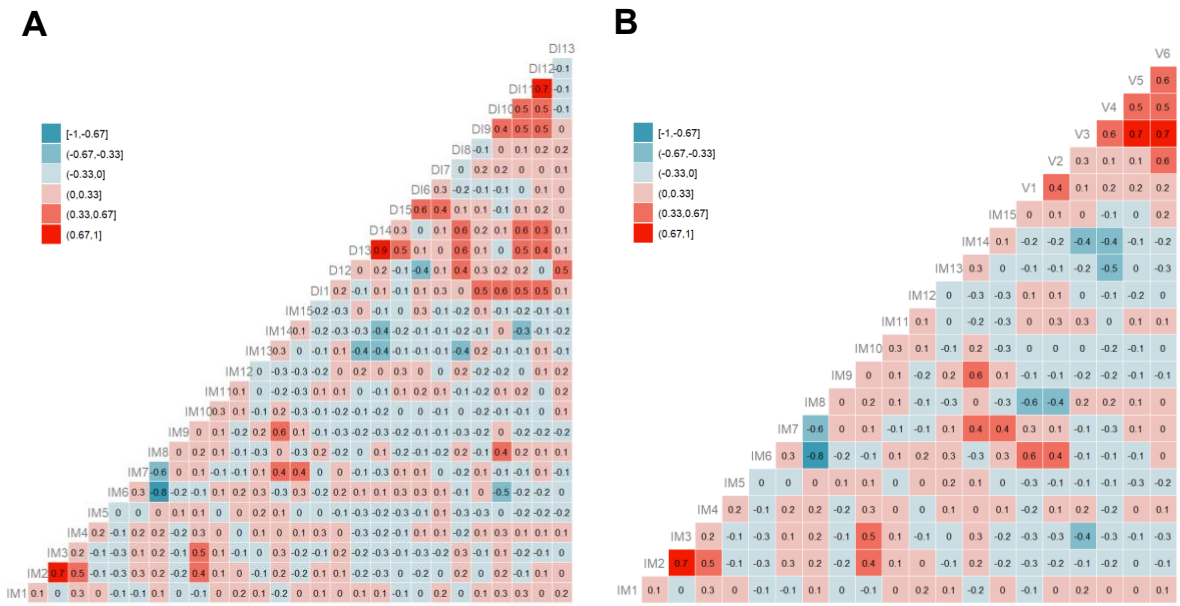

Figure 5.2 Associations between diet and hallmarks of innate and adaptive immune ageing. (A) Correlation matrix summarising associations between diet, specific food groups and innate and adaptive immune parameters in old (n = 40) participants. **(B)** Correlation matrix highlighting key associations between minerals, vitamins and innate and adaptive immune parameters in old (n = 40) participants. Red represents positive correlation coefficients, while blue denotes negative correlation coefficients. The Spearman's correlation coefficient range (-1 to 1) was divided into 6 classes as shown in the colour legend. IM1: TNFα secretion by monocytes under basal conditions, IM2: IL12 secretion by DCs upon stimulation, IM3: IL10 secretion by monocytes upon stimulation, IM4: IL6 secretion by DCs under basal conditions, IM5: IL6 secretion by DCs upon stimulation, IM6: Peripheral frequency of CM CD4 T cells, IM7: Peripheral frequency of CM CD8 T cells, IM8: Peripheral frequency of EMRA CD8 T cells, IM9: $CD28^{-ve}CD57^{+ve}$ senescent CD8 T cells, IM10: $PD1^{+ve}$ exhausted CD8 T cells, IM11: Th17 cells, IM12: Tregs, IM13: Bregs, IM14: IMM-AGE score, IM15: Systemic CRP levels, DI1: DQI, DI2: MDS, DI3: Monounsaturated fatty acids, DI4: PUFAs, DI5: Cholesterol, DI6: Meat, DI7: Fish, DI8: Nuts, DI9: Vegetable intake, DI10: Fruit, DI11: Dietary fibres, DI12: Carbohydrates, DI13: Alcohol intake, V1: Vitamin A, V2: Vitamin B_6, V3: Vitamin B_{12}, V4: Vitamin E, V5: Folate, V6: Zinc. Figures created by Dr Animesh Acharjee.

A

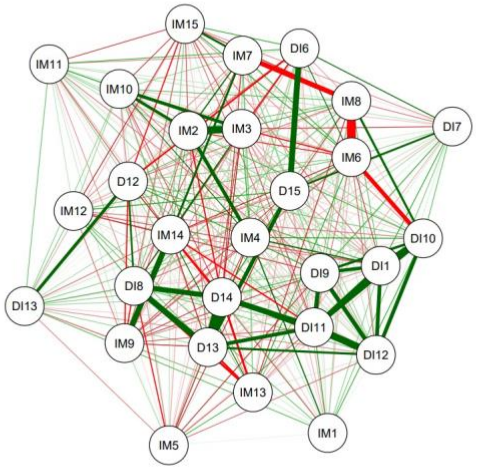

B

Dietary fibre (DI11)	IMM-AGE score (IM14)	R = -0.33, p = 0.03
	$CD28^{-ve}CD57^{+ve}$ senescent CD8 T cells (IM9)	R = -0.25, p = 0.05
PUFAs (DI4)	IMM-AGE score (IM14)	R = -0.39, p = 0.01
	$CD28^{-ve}CD57^{+ve}$ senescent CD8 T cells (IM9)	R = -0.25, p = 0.05
	$PD1^{+ve}$ exhausted CD8 T cells (IM10)	R = -0.22, p = 0.07
Fish intake (DI7)	$CD28^{-ve}CD57^{+ve}$ senescent CD8 T cells (IM9)	R = -0.29, p = 0.04
Nuts (DI8)	$IL10^{+ve}$ monocytes_LPS (IM3)	R = 0.29, p = 0.06
	$IL6^{+ve}$ DCs_LPS (IM5)	R = -0.31, p = 0.04
	$CD28^{-ve}CD57^{+ve}$ senescent CD8 T cells (IM9)	R = -0.31, p = 0.04
Cholesterol (DI5)	Central memory CD4 T cells (IM6)	R = 0.29, p = 0.06
	Th17 cells (IM11)	R = 0.32, p = 0.04
	Regulatory T cells (IM12)	R = 0.29, p = 0.05
Meat intake (DI6)	$IL10^{+ve}$ monocytes_LPS (IM3)	R = -0.31, p = 0.04
	Central memory CD8 T cells (IM6)	R = 0.3, p = 0.01
Alcohol intake (DI13)	Th17 cells (IM11)	R = 0.29, p = 0.07

Figure 5.3 Investigating Spearman-based correlations between dietary components and hallmarks of immunesenescence. (A) Network plot highlighting key associations between dietary patterns and consumption of dietary food groups and immunesenescence parameters in aged participants (n = 40) as nodes (circles). Red lines represent negative correlation coefficients, while green lines represent positive correlation coefficients. **(B)** Descriptive table showing Spearman's correlation efficient and p-values, which were determined via regression analysis, for each association shown in the network plot. IM1: TNFα secretion by monocytes under basal conditions, IM2: IL12 secretion by DCs upon stimulation, IM3: IL10 secretion by monocytes upon stimulation, IM4: IL6 secretion by DCs under basal conditions, IM5: IL6 secretion by DCs upon stimulation, IM6: Peripheral frequency of CM CD4 T cells, IM7: Peripheral frequency of CM CD8 T cells, IM8: Peripheral frequency of EMRA CD8 T cells, IM9: $CD28^{-ve}CD57^{+ve}$ senescent CD8 T cells, IM10: $PD1^{+ve}$ exhausted CD8 T cells, IM11: Th17 cells, IM12: Tregs, IM13: Bregs, IM14: IMM-AGE score, IM15: Systemic CRP levels, DI1: DQI, DI2: MDS, DI3: Monounsaturated fatty acids, DI4: PUFAs, DI5: Cholesterol, DI6: Meat, DI7: Fish, DI8: Nuts, DI9: Vegetable intake, DI10: Fruit, DI11: Dietary fibres, DI12: Carbohydrates, DI13: Alcohol intake. Figures created by Dr Animesh Acharjee.

A

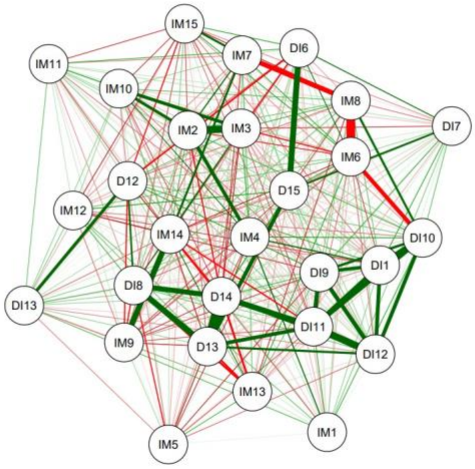

B

Dietary fibre (DI11)	IMM-AGE score (IM14)	R = -0.33, p = 0.03
	$CD28^{-ve}CD57^{+ve}$ senescent CD8 T cells (IM9)	R = -0.25, p = 0.05
PUFAs (DI4)	IMM-AGE score (IM14)	R = -0.39, p = 0.01
	$CD28^{-ve}CD57^{+ve}$ senescent CD8 T cells (IM9)	R = -0.25, p = 0.05
	$PD1^{+ve}$ exhausted CD8 T cells (IM10)	R = -0.22, p = 0.07
Fish intake (DI7)	$CD28^{-ve}CD57^{+ve}$ senescent CD8 T cells (IM9)	R = -0.29, p = 0.04
Nuts (DI8)	$IL10^{+ve}$ monocytes_LPS (IM3)	R = 0.29, p = 0.06
	$IL6^{+ve}$ DCs_LPS (IM5)	R = -0.31, p = 0.04
	$CD28^{-ve}CD57^{+ve}$ senescent CD8 T cells (IM9)	R = -0.31, p = 0.04
Cholesterol (DI5)	Central memory CD4 T cells (IM6)	R = 0.29, p = 0.06
	Th17 cells (IM11)	R = 0.32, p = 0.04
	Regulatory T cells (IM12)	R = 0.29, p = 0.05
Meat intake (DI6)	$IL10^{+ve}$ monocytes_LPS (IM3)	R = -0.31, p = 0.04
	Central memory CD8 T cells (IM6)	R = 0.3, p = 0.01
Alcohol intake (DI13)	Th17 cells (IM11)	R = 0.29, p = 0.07

Figure 5.4 Investigating Spearman-based correlations between dietary intake of vitamins/minerals and hallmarks of immunesenescence. (A) Network plot highlighting key associations between the intake of minerals/vitamins and immunesenescence parameters in aged participants (n = 40) as nodes (circles). Red lines represent negative correlation coefficients, while green lines represent positive correlation coefficients. **(B)** Descriptive table showing Spearman's correlation efficient and p-values, which were determined via regression analysis, for each association shown in the network plot. IM1: TNFα secretion by DCs under basal conditions, IM2: Naïve CD8 T cells, IM3: IL10 secretion by monocytes upon stimulation, IM4: IL6 secretion by DCs under basal conditions, IM5: IL6 secretion by DCs upon stimulation, IM6: Peripheral frequency of CM CD4 T cells, IM7: Peripheral frequency of CM CD8 T cells, IM8: Peripheral frequency of EMRA CD8 T cells, IM9: $CD28^{-ve}CD57^{+ve}$ senescent CD8 T cells, IM10: $PD1^{+ve}$ exhausted CD8 T cells, IM11: Th17 cells, IM12: Tregs, IM13: Bregs, IM14: IMM-AGE score, V1: Vitamin A, V2: Vitamin B_6, V3: Vitamin B_{12}, V4: Vitamin E, V5: Folate, V6: Zinc. Figures created by Dr Animesh Acharjee.

anti-inflammatory IL10-secreting monocytes (Figures 5.3A and 5.3B). Regarding specific food groups that are rich in the MedDiet, high intake of fish and nuts was associated with reduced basal secretion of pro-inflammatory cytokines by monocytes and DCs. Furthermore, we found that unhealthy dietary patterns, such as increased consumption of meat, cholesterol and alcohol, were correlated with increased Th17 polarisation, dampened basal secretion of IL6 by DCs and the accumulation of CM T cells (Figures 5.3A and 5.3B).

5.2.5 Dissecting an interrelationship between dietary vitamins/minerals and immune ageing

With regards to micronutrients, the consumption of a diet rich in vitamin A (retinol) was associated with fewer circulating terminally differentiated EMRA CD8 T cells, a higher frequency of CM CD8 T cells (Figures 5.4 and 5.4B) and increased secretion of anti-viral cytokine IFNγ by cytotoxic CD8 T cells (Figures 5.2B). Moreover, consumption of a diet rich in vitamin B_6 was linked with a reduced frequency of senescent CD8 T cells and an increased proportion of systemic naïve CD8 T cells, which together contribute towards a lower IMM-AGE score. Like vitamin A, older adults that consumed a diet rich in vitamin B_{12} also displayed fewer circulating terminally differentiated EMRA CD8 T cells and a higher frequency of CM CD8 T cells (Figures 5.4A and 5.4B). Interestingly, consumption of a vitamin E-rich diet was linked with fewer IL6-secreting DCs under basal conditions and a higher frequency of circulating Bregs (Figures 5.4A and 5.4B), highlighting the potential anti-inflammatory effects of vitamin E. Similar anti-inflammatory effects of folate were also identified (Figure 5.2B).

5.3 Discussion

Nutrition is critical for healthy ageing; thus, it is essential that we unravel the complex relationship between diet and immune ageing to identify nutritional components that strengthen immunity and promote healthy ageing (Figure 5.5). In this study, we observed for the first time that higher adherence to a MedDiet is associated with a lower immunological age driven by fewer systemic senescent T cells in healthy older adults. Adherence to a MedDiet is linked with high consumption of dietary fibres, which has been shown to attenuate pro-inflammatory cytokine production and promote IL10 secretion by DCs [557], which we also observed. Dietary fibre can be digested by gut bacteria, producing SCFAs, such as acetate, butyrate and propionate, that possess potent anti-inflammatory properties [320,385].

Overconsumption of saturated fats derived from red and processed meat, typical of a Western diet, can exert pro-inflammatory effects. In this study, we observed a positive correlation between dietary cholesterol intake and pro-inflammatory Th17 cells. This is unsurprising since transcriptional activity of RORγ, which controls the differentiation of CD4 T cells towards a Th17 phenotype, is governed by cholesterol synthesis [558]. In contrast, PUFAs found in high abundance in nuts, avocados, fish and olive oil possess anti-inflammatory properties [559]. In this study, we reported an association between the consumption of a diet rich in PUFA-containing fish and reduced accumulation of systemic senescent T cells in older adults. This is in line with the findings of another study that found that PUFAs ameliorate the induction of senescence in endothelial cells [560].

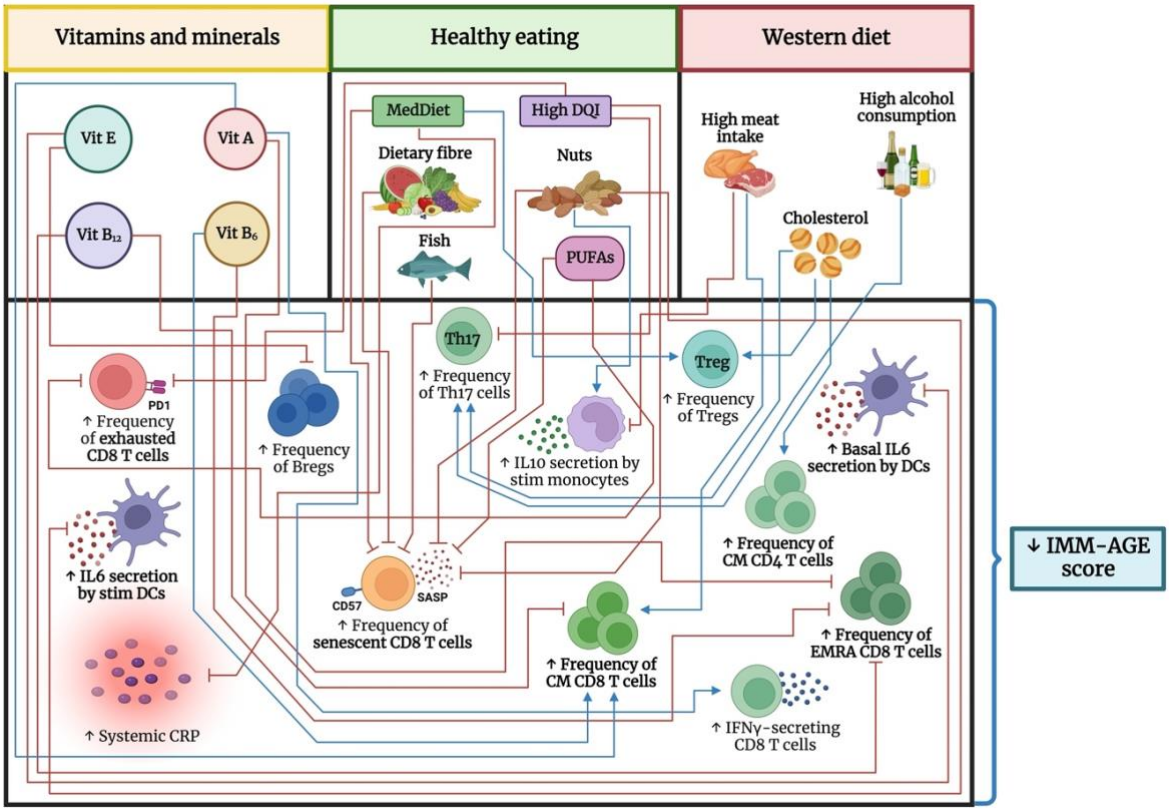

Figure 5.5 Key associations between dietary patterns, food groups, micronutrients and immunesenescence parameters in older adults. Blue lines denote positive correlations, while red lines indicate negative associations. In summary, increased consumption of food groups and macronutrients typically found in the Western diet, such as meat, alcohol and cholesterol, is linked with distributional shifts towards pro-inflammatory T cell subsets, contributing towards a more aged immune system in older adults. On the other hand, greater adherence to the MedDiet and consumption of a high-quality diet are correlated with a lower IMM-AGE score in older people due to the immune-protecting effects and anti-inflammatory properties of key food groups, namely dietary fibre, fish, nuts and PUFAs, that are enriched in the MedDiet. High intake of foods rich in vitamins and minerals can also have a beneficial effect on the immune system by suppressing the secretion of pro-inflammatory cytokines and preventing the accumulation of senescent and exhausted CD8 T cells.

Micronutrients, including magnesium, folate, iron, zinc, and vitamins B_6, B_{12}, C, D and E play a determinant role in the maintenance of host health and deficiencies have been associated with an increased incidence of bacterial and viral infections and autoimmunity in older people [561]. Vitamin B_6 acts as a co-factor for the production of thymic hormones, such as thymulin which stimulates T cell development [562]. Thus, it is unsurprising that we observed links between Vitamin B_6 consumption and a higher frequency of circulating naïve CD8 T cells, fewer senescent CD8 T cells and slower immune ageing. Vitamin E is an important fat-soluble antioxidant that is abundant in the MedDiet and has been shown to be efficacious in enhancing immune functions, especially in the aged population. In this study, we observed novel links between the consumption of a Vitamin E-rich diet and the expansion of immunoregulatory B cells.

5.3.1 Study limitations

Although this study provides significant insights into the links between diet and immunesenescence, a key limitation that must be acknowledged is that dietary data was self-reported, which might have introduced response bias. This can be avoided in future work by measuring nutritional biomarkers in the blood via LC-MS to assess nutritional status. However, blood sampling captures short-term nutrient intake (a few days to one month) and generally does not reflect absolute nutrient consumption [563]. Therefore, researchers should consider the use of diet-tracking apps that use image-based recognition and barcode scanners to record daily micro and macronutrient intake and estimate portion sizes. These apps tend to be older adult-friendly and their usage would minimise errors in memory, reduce possible response bias and improve accuracy in amount estimation [564].

5.3.2 Conclusion

In addition to genetic and environmental determinants of an individual's immune ageing trajectory, we provide evidence for nutrition as a key contributing factor to immune ageing, which is of utmost importance due to its modifiable nature [565]. This study provides compelling associate evidence between the adherence to the MedDiet and immune ageing in older adults. However, the effectiveness of a single approach in improving immune function is limited and this could be combined with nutritional supplements, such as vitamin B_6. Therefore, we propose a future interventional study evaluating the efficacy of adherence to the MedDiet alongside a multi-nutrient supplementation on immune ageing (IMM-AGE) in older adults. This would enable us to set new policy guidelines and start good education campaigns that promote healthy eating for lifelong immunity. Fortunately, the recently assembled Food4Years Ageing Network has taken the first step in this direction [566].

Chapter 6: General discussion

This chapter contains text written by Jessica Conway and edited by Dr Niharika A Duggal from the following publications.

Conway J, A Duggal N. Ageing of the gut microbiome: Potential influences on immune senescence and inflammageing. *Ageing Res Rev*. 2021; 68:101323.

Conway J, Rees NP, Duggal NA. Ageing of the Gut Microbiome and Its Potential Contribution Towards Immunesenescence and Inflammaging. In: Marotta, F. (eds) Gut Microbiota in Aging and Chronic Diseases. *Healthy Ageing and Longevity*. 2023; p.41-63.

Advances in modern medicine and experimental research have increased human longevity globally, driving an ever-expanding ageing population [1], a phenomenon described as the “silver tsunami”. However, advancing age is accompanied by an increased vulnerability to age-related pathologies, such as IBD, RA, Alzheimer’s disease and cancer, caused by the progressive decline in physiological function of organs and bodily systems [4]. Among these is the immune system which undergoes profound remodelling with age, hindering the host’s ability to mount robust immune responses to invading pathogens and vaccination [13].

In tandem with immunesenescence, ageing significantly impairs intestinal barrier integrity and alters the composition and metabolic profile of the gut microbiome, which has recently been recognised as a new hallmark of ageing (Figure 6.1) [4]. The gut microbiota not only modulates local intestinal homeostasis but also distantly influences various physiological processes, including the immune system, playing an integral role in health and disease [320]. Therefore, reversing age-related microbial dysbiosis and intestinal permeability in aged individuals could delay the onset of age-related diseases and promote healthy ageing. In support of this, animal studies have shown that recolonising the gut microbiome with health-associated bacteria extends lifespan and improves certain aspects of health [567,568].

This chapter will discuss the use of microbiome-based interventions as a novel strategy to combat immune ageing, focusing on gerobiotics, a new term that defines probiotic and postbiotic strains that delay the effects of ageing like immunesenescence [569]. Use of gerobiotics has the exciting potential for improving health span, and thus might also boost immunity and improve vaccine immunogenicity in older people.

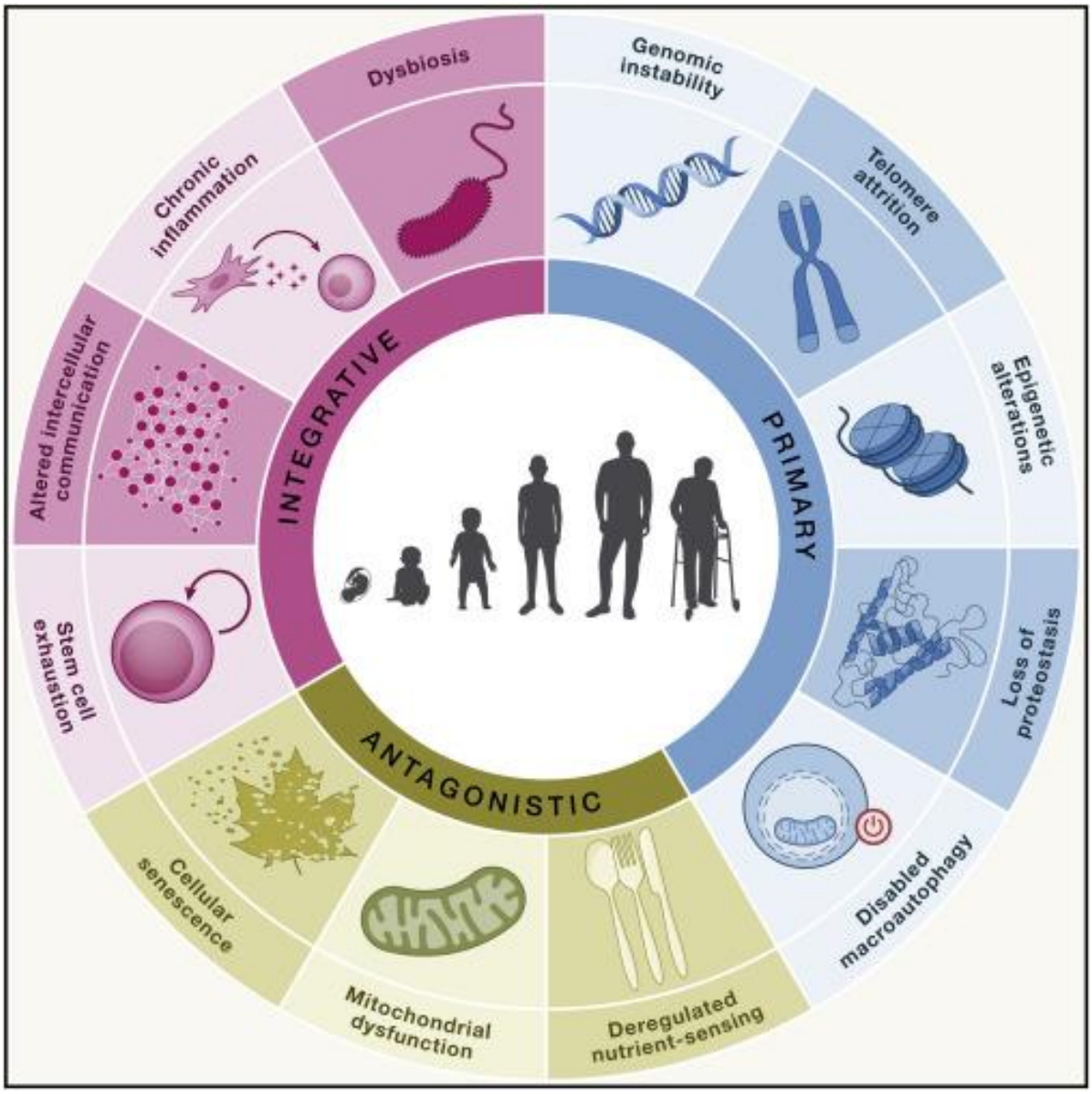

Figure 6.1 Hallmarks of ageing. A schematic drawing of the 12 hallmarks of ageing, including the recently recognised microbial dysbiosis, subdivided into those that are primary, antagonistic and integrative. Figure from [4].

6.1 Summary of main findings

Ageing is an inevitable natural process that impacts all individuals and its effects include intestinal barrier dysfunction, increased microbial translocation and altered gut microbiota composition. Concurrently with alterations in the immune system, **Chapter 3** demonstrated that healthy older adults exhibit increased intestinal membrane permeability and systemic microbial translocation possibly driven by the expansion of opportunistic bacteria (*Escherichia-Shigella*, *Peptostreptococcaceae* and *Paraprevotella*) and low bioavailability of microbiota-derived metabolites, namely propionate and GDCA (Figures 3.1 and 3.2). Enhanced microbial translocation was associated with the loss of RTEs, the accumulation of terminally differentiated and senescent T cells and possibly a compensatory expansion of anti-inflammatory Tregs in aged individuals, altogether contributing to accelerated immunological ageing (high IMM-AGE score) (Figures 3.3 and 3.4). Importantly, we confirmed a causal relationship between gut mucosal permeability and thymic ageing using an aged germ-free mouse model protected from intestinal barrier dysfunction (Figures 3.6-3.8). Moreover, we show that aged pro-inflammatory senescent T cells and Th17 cells have an enhanced capacity for gut homing, possibly contributing to age-related intestinal barrier damage upon tissue infiltration (Figure 3.9). These findings provide compelling evidence that age-related intestinal barrier failure drives systemic T cell immunesenescence and possibly gut homing of aged T cells which contribute towards the loss of intestinal barrier function in old age.

In **Chapter 4**, we confirmed that advancing age is accompanied by commensal depletion and pathobiont blooming (Figure 4.1), causing a shift in the metabolic profile of the gut microbiome (Figure 4.2). Most importantly, we identified several potential

gerobiotic taxa that were correlated with reduced basal cytokine (IL6, IL10 and TNF) production by monocytes and DCs; lower systemic levels of CRP; increased frequencies of CM CD4 T cells, IFN-producing CD8 T cells, Th1 and Th2 cells, IL10-secreting Tregs, naïve B cells and Bregs; and reduced accumulation of senescent CD4 and CD8 T cells, Th17 cells and memory B cells in older adults. These included *Bifidobacterium*, *Lactobacillus*, *Paraprevotella*, *Prevotella*, *Coprococcus*, *Lachnospiraceae*, *Collinsella*, *Terrisporobacter*, *Eggerthellaceae*, *Fournierella*, *Dialister*, *Bacteroidales*, *Gastranaerophilales*, *Blautia*, *Sutterella*, *Bilophila*, *Turicibacter*, *Eisenbergiella*, *Oscillibacter* and *Phascolarctobacterium* (Figures 4.3 and 4.4). These potential immune-enhancing effects were attributed to increased faecal levels of SCFAs (butyrate, acetate and propionate) and SBAs (DCA, GDCA) in aged individuals. Additionally in **Chapter 4**, we demonstrated that *Lactobacillus*, *Bifidobacterium*, Oscillibacter, *Bacteroides*, *Coprococcus*, *Anaerotruncas*, *Intestinibacter*, *Enterobacteriaceae*, *Oscillospira*, *Allistipes*, *Aldercreutzia*, *Flavonifractor*, *Negativibacillus* were all associated with good immunogenicity to influenza vaccination in older adults (Figure 4.6).

Finally in **Chapter 5**, we identified several strong correlations between diet and immune ageing, emphasising the potential for dietary interventions as an alternative strategy to tackle immunesenescence. For instance, increased consumption of foods and nutrients typically found in the Western diet, especially meat, alcohol and cholesterol, was linked with the peripheral expansion of Th17 cells and Tregs (Figure 5.3). However, high adherence to the MedDiet and consumption of a high-quality diet were associated with enhanced IL10 production by monocytes upon stimulation and a reduced senescent/exhausted CD8 T cell burden (Figure 5.1). These links were

attributed to the immunoprotective effects and anti-inflammatory properties of dietary fibre, fish, nuts and PUFAs, which led to slower immunological ageing (Figure 5.3). Additionally, a diet rich in Vit A, Vit B_6, Vit B_{12} and Vit E was correlated with decreased basal IL6 cytokine production by DCs and fewer Bregs and EMRA CD8 T cells (Figure 5.4).

6.2 Experimental limitations

Like all research studies, ours has a few limitations that should be noted. Firstly, our use of a strict inclusion criteria excluded older adults with any underlying comorbidities, immune-mediated diseases and gastrointestinal disorders. Our cohort of older adults, who were interested in biogerontology research and keen to partake in our study, were all extremely healthy, consumed a high-quality diet rich in dietary fibres and engaged in regular physical activity (only one individual was sedentary). Unfortunately, this might not be a true representation of the ageing population, which is malnourished, largely sedentary and ridden with multimorbidity [570-572]. Comorbidities, such as RA, metabolic syndrome, celiac diseases, malignancies, IBD and neurodegenerative disorders, are linked to altered gut microbial profiles [335,347,573,574]. This could impinge upon on the complex-dynamic crosstalk between the gut microbiome and immune system. This might also explain why we did not observe some key features of immune ageing that have been reported by earlier studies, which did not have such a strict inclusion criteria.

However, this strategy dissected the intrinsic effects of ageing from the influence of lifestyle factors and underlying conditions. Thus, we are confident that the novel interactions that we observed are features of biological ageing. However, in a current

ongoing study, we are addressing this by recruiting older individuals with underlying comorbidities to identify immune-microbiome signatures and interactions that differ in the ageing population with healthy vs unhealthy ageing trajectories. Another key limitation is that our results are based on a cohort of Caucasian participants, and we would like to validate our findings in a larger study (enabling us to dissect sex differences) conducted on older adults with more ethically and geographically diverse backgrounds.

Thirdly, the cross-sectional design of the current study enables us to assess the immune profile, microbial composition and dietary patterns in older adults at a single time point. However, faecal microbiota and dietary patterns have been found to vary within individuals over short time periods and fluctuations can impact immune function, necessitating longitudinal sampling to control for temporal variation in future studies. We plan to perform a longitudinal assessment of our cohort, which have been recently resampled two years after the original assessment, to help us identify signature deflections of microbiome-immune interactions as biomarkers of healthy ageing progression.

Like many studies, we employed faecal sampling for microbiota screening, which might have limited our scope of detection of locally enriched bacteria. Further, there is accumulating evidence that the faecal microbiome might not fully represent that of the intestines [575]. Therefore, precuring mucosal biopsies and swabs should be considered as an alternative approach for studying microbial signatures. However, mucosal sampling is extremely invasive, making it hard to obtain mucosal biopsies and swabs from healthy individuals. Microbial profiling was performed using 16S rRNA gene sequencing, which limited bacterial-identification at the phyla, family and genus

levels. Future work should employ shotgun metagenomic sequencing to assess age-related differences in species and strains. Another limitation of 16S rRNA gene sequencing is that it calculates relative microbial abundances rather than absolute abundances. One way around this is to use exogenous spike-in controls [576].

In our vaccine study, we evaluated immunogenicity by measuring influenza-virus specific antibody titres but did not perform *in vitro* functional assays. In current ongoing work, we are addressing this via opsonophagocytic killing assays, which utilise a PBMC/influenza virus coculture model to assess antibody-mediated phagocytosis of influenza virus by phagocytic cells. Additionally, we plan to use enzyme-linked immunosorbent spot (ELISpot) assays to measure the frequency of IgA-secreting B cells. Flow cytometry analysis will also be conducted to compare the circulating proportion of Tfh cells between low and high responding older adults.

6.3 Interventions that delay the onset of intestinal barrier dysfunction as an attractive approach to promote healthy immune ageing

Maintaining intestinal epithelium integrity is crucial for preserving organismal health throughout life. However, age-related intestinal barrier dysfunction is associated with microbial dysbiosis, metabolic defects, chronic immune activation, inflammageing and systemic health decline [68,577,578]. Compelling evidence from *Drosophila* and mouse studies have demonstrated that preserving intestinal barrier integrity successfully promotes longevity [579,580], leading researchers to propose the potential of restoring intestinal barrier function in aged individuals as an attractive strategy for promoting healthy immune ageing.

Prebiotics (indigestible fibre compounds, such as inulin and galacto-oligosaccharides) and probiotics (live strains of *Lactobacilli* and *Bifidobacterium*) confer various health-promoting benefits in animals and extend lifespan when consumed in sufficient amounts [580-583]. Evidence from clinical trials have shown that prebiotics and probiotics modify the gut flora and reduce intestinal permeability, thereby restoring microbial homeostasis [584,585]. Mechanistically, probiotic *Lactobacillus plantarum*, *Lactobacillus acidophilus* and *B*. *infantis* prevent IEC apoptosis and induce tight junction protein apical localization [438,586]. More importantly, probiotic cocktail administration can reverse microbial dysbiosis, increase SBA metabolism and stimulate tight junctions, thereby reducing gut leakage and intestinal inflammation in aged humans and mice [532,587].

Despite the promising beneficial effects of probiotics on intestinal health, very few studies have investigated the appropriate doses required for effective probiotic supplementation. Therefore, the use of prebiotics is an attractive alternative approach for the intestinal recolonization of postbiotic bacteria and maintenance of intestinal barrier integrity [370,588]. However, other several studies have implied that symbiotic consumption, synergistic combination of prebiotics and postbiotics, has a more protective effect on microbial diversity intestinal barrier function than postbiotics and prebiotics alone [589,590].

Faecal microbiota transplantation (FMT), involving the transfer of healthy young donor intestinal microorganisms into the gastrointestinal tract of recipients, has been reported to extend health span and lifespan in natural and accelerated ageing mouse models, possibly by reestablishing a healthy microbiome and restoring SCFA and SBA levels [567,591]. FMT-treated aged wild-type mice display a younger-like microbiota

signature (increased abundance of *Bifidobacterium* and *Ruminococcaceae*) and improved intestinal epithelial barrier function [591,592]. Interestingly, transfer of aged donor microbiota into young mice resulted in the emergence of hallmarks of ageing and the premature onset of age-related pathologies in receipts, which coincided with increased intestinal permeability [593].

Dietary interventions also have the potential to restore intestinal barrier integrity and promote greater microbial diversity in aged individuals. The MedDiet is a well-balanced diet that features high intake of fruits, vegetables, nuts, legumes, whole grains, fish and olive oil, and low consumption of meat, refined carbohydrates and sweets. Consumption of the MedDiet is highly effective in reducing the risk of metabolic syndromes [594], CVD and cancers [383,384], all of which are associated with intestinal barrier dysfunction [595-597]. High adherence to the MedDiet has been shown to increase microbial species richness and diversity, enhance SCFA production and improve epithelial barrier integrity [598,599], reducing frailty and improving overall health in older adults [381]. These microbiota-modifying effects are mainly mediated through the high intake of dietary fibers, which are essential for SCFA generation [385]. SCFAs, especially butyrate, enhance mucin secretion and facilitates tight junction assembly in the epithelium [600,601].

The use of novel therapeutics targets, such as metformin, rapamycin and resveratrol, have also been proposed as a potential strategy for repairing intestinal barrier integrity. Metformin and rapamycin are mammalian target of rapamycin (mTOR) inhibitors used to treat type 2 diabetes and cancers. Extensive research has revealed that both drugs delay the onset of age-related pathologies and extend lifespan in many animal models [602-605]. These anti-ageing effects are primarily mediated through improvements in

autophagy/mitophagy [605,606], enhanced mitochondrial function [604,607], protection against genomic instability [608], the prevention of cellular senescence and subsequent SASP inhibition [609,610]. Metformin and rapamycin also beneficially modulate the gut microbiome by promoting commensal colonisation, increasing SCFA production and dampening intestinal inflammation [611]. Furthermore, both drugs have been found to promote intestinal barrier integrity and inhibit microbial translocation by enhancing mucin production, upregulating tight junction proteins and modulating intestinal stem cell turnover [605,611,612].

Resveratrol is an antioxidant nutraceutical that promotes longevity in mice through the activation of sirtuins [613], thereby enhancing autophagy and halting cellular senescence progression [614,615]. There is also compelling evidence that resveratrol improves gut barrier integrity by inhibiting pathogen growth [616], increasing the abundance of commensals (*Bacteroides*, *Bifidobacterium* and *Lactobacillus*) [617], upregulating tight junction proteins and increasing butyrate levels [618,619]. Collectively, these findings support the argument for the use of interventions that restore a youthful microbiome and repair intestinal barrier damage in promoting healthy ageing in the elderly.

6.4 Designing a novel gerobiotic for boosting immune health and vaccine responses in older adults

The concept of gerobiotics has emerged as a novel strategy to increase the healthy life expectancy of humans. Gerobiotics include probiotic strains and postbiotics (microbial metabolites) that attenuate physiological features of ageing, thereby delaying the onset of age-related pathologies and extending longevity [569]. So far,

several probiotic strains have been demonstrated to target hallmarks of ageing in animal models. These include *Lactobacillus brevis* OW38 (reduces cellular senescence) [620], *L. plantarum* NDC 75017 (preserves mitochondrial function) [621], *Lacticaseibacillus paracasei* PS23 (positively modulates microbiota composition and reduce age-related gut permeability) and *L. plantarum* C29 (ameliorates inflammageing) [622,623]. Other prospective gerobiotics, such as *Lactobacillus casei* Shirota and *B. lactis* HN019, exert immune-enhancing effects, including improved NK cell tumoricidal activity, increased serum IL10 and IL12 levels [624], enhanced polymorphonuclear cell phagocytosis and lower incidence of infection [625,626], in older adults.

Although single-strain probiotics have high efficacy, multi-species supplementation may be more beneficial as a strategy for restoring microbial homeostasis and promoting immune health in older adults. Probiotic functionality is usually strain-specific, and *Lactobacillus* and *Bifidobacterium* have different enzymatic activities and molecular actions [627]. Therefore, developing a multi-species/multi-strain gerobiotic cocktail might provide wider coverage due to the synergistic and additive effects of combined usage [627]. This is supported by studies that have compared the effects of single-strain, multi-strain and multi-species probiotics, reporting higher efficacy in multi-species/multi-strain recipients [628,629].

Evidence from animal and human studies provide the rationale basis for gerobiotic therapy to restore microbiota composition, reduce intestinal barrier leakage, boost immunity and improve other ageing features. However, the road to developing prospective gerobiotics is long and begins with the screening of existing probiotic strains that exhibit immunomodulatory, anti-inflammatory, anti-allergy, anti-infection

and/or psychiatric activity [569] (Figure 6.2). This is followed by high-throughput screening of selected functional probiotics using *in vitro* cell models and/or invertebrate animal models (*Caenorhabditis elegans* and *Drosophila melanogaster*) to determine their mechanism of action and evaluate their ability to extend lifespan. Candidate strains should be further assessed in ageing and age-related disease animal models to determine their potential anti-ageing effects. Only then can candidate gerobiotics be confirmed in long-term human clinical studies by assessing changes in physiological, immunological and other blood-based biological markers [569].

6.5 Interventions for preventing and delaying immune ageing

Microbiome-based therapies have become an increasingly attractive target for anti-ageing therapies given their wide range of health benefits, including some beneficial effects on the immune system. Probiotics possess immunomodulatory properties and have been shown to induce anti-inflammatory cytokine production (IL10 and IL12) and enhance secretory IgA production [624,630]. Probiotic consumption can also lead to changes in T cell subset distribution including a decreased frequency of memory T cells, senescent CD8 T cells and γδT cells as well as an expansion of T helper cells and Tregs [631,632]. These immune-protecting effects have been attributed to increased butyrate production in the gut following probiotic intake [633]. Furthermore, daily probiotic consumption has been reported to improve vaccine responses and reduce susceptibility to respiratory infections in older people [634,635]. However, these health-promoting benefits of prebiotics and probiotics are short-lived with the gut microbiota returns to its pre-supplementation state within weeks of supplement discontinuation.

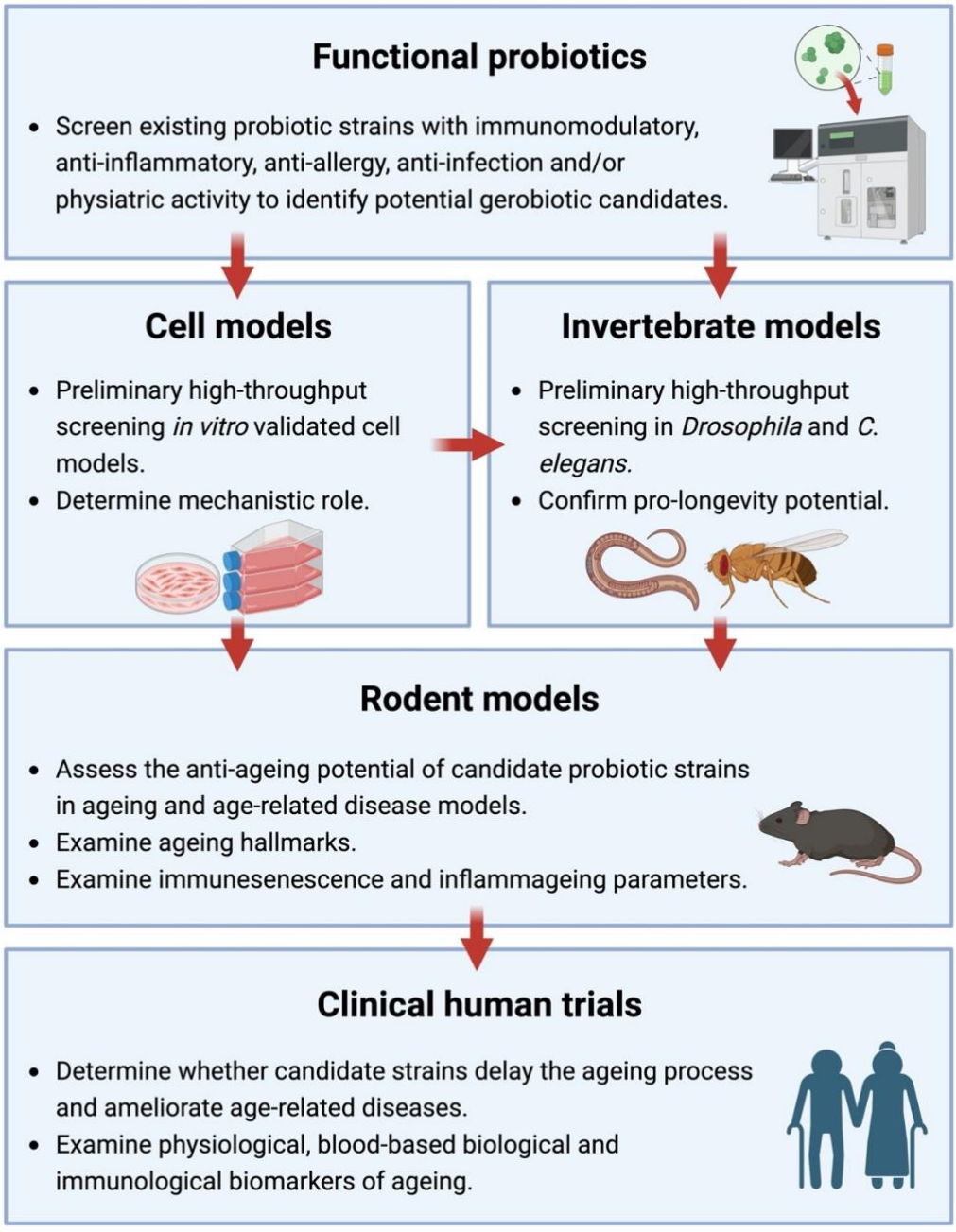

Figure 6.2 Strategies for developing potential gerobiotics with immune-enhancing properties. The first step is to form a functional probiotics bank for high-throughput screening in cell and invertebrate models to determine their mechanisms of action and ability to extend lifespan. Longevity-promoting strains are then evaluated in ageing and age-related disease rodent models for their ability to target hallmarks of ageing and prevent pathology onset. Lastly, these anti-ageing affects are validated in humans using long-term clinical studies that assess the efficacy and safety of prospective gerobiotics. Figure is adapted from [569].

Lifestyle changes also exert a beneficial effect on the intestinal microflora and improve gut barrier integrity, while restoring immune homeostasis and reducing inflammageing (Figure 1.6). Consumption of the MedDiet is associated with increased longevity and reduces the risk of frailty [381], cognitive impairment [382], CVD [383] and cancer in older adults [384]. High adherence to the MedDiet has also been associated with a lower Firmicutes/Bacteroidetes ratio, higher *Bifidobacterial* counts, a greater abundance of polysaccharide-degrading microbes and high faecal SCFA levels [385]. However, there is limited evidence that the MedDiet improves immunity mainly due to the short nature of these studies [388,389], indicating that dietary intervention success may require long-term adherence.

Caloric restriction is a dietary regime that reduces calorie intake to approximately 30% of ab libitum diet without incurring malnutrition. Caloric restriction is known to extend lifespan and delay the onset of age-related diseases in a variety of animal species including primates [636]. Studies in mice and rats demonstrated that short-term caloric restriction reduces the Firmicutes/Bacteroidetes ratio and increases *Lactobacillus* counts in the intestines, upregulating the expression of SCFA biosynthetic enzymes [637,638], Additionally, a 4-week caloric restriction diet was found to improve gut barrier integrity, thereby reducing both local and systemic inflammation in obese women [639]. Studies in caloric restricted aged mice have reported increased circulating naïve T cells, decreased senescent T cell frequency, enhanced T cell proliferation, improved TCR diversity and reduced serum levels of pro-inflammatory cytokines [640].

Regular physical activity is known to confer a wide range of health benefits including a longer life expectancy and a reduced risk of age-related disease [641,642]. Despite

these well-known effects, physical activity levels tend to decline with advancing age, and most older adults are largely sedentary. In fact, it is estimated that less than 10% of older adults in the UK meet the recommended guidelines of 150 minutes of aerobic exercise a week. Interestingly, maintenance of physical activity levels can increase the number of butyrate-producing bacteria, enhance intestinal membrane integrity and dampen intestinal inflammation in adult rodents, thereby improving their health status [643,644]. More recently, it was shown that high-fitness community-dwelling older adults have an increased abundance of *Bifidobacteriales* and *Clostridiales* species compared with low-fitness subjects [645]. Older adults that maintain high levels of physical activity throughout their adult life display fewer elements of immunesenescence and inflammageing, including an increased frequency of RTEs and naïve T cells, fewer memory T cells and reduced Th17 polarization [646].

In recent years, FMT has gained increasing attention due to its ability to restore normal microbiota composition and function in patients with intestinal dysbiosis caused by *C. difficile* infection and IBD [647,648]. Animal studies show that FMT administration not only re-establishes microbial communities, but also reduces intestinal permeability [649], enhances bile acid metabolism [650], increases IL10 production by leukocytes and decreases T cell responses by inhibiting antigen presentation [651]. Interestingly, a study in aged mice demonstrated that FMT corrects age-associated defects in GC reactions [390], suggesting FMT could also be used as an effective treatment for the restoration of immune responses, including vaccinations in older adults. However, FMT treatment has several limitations including donor microbiome variability, risk of transferring pathobionts and unknown long-term efficacy. Thus, the use of super

donors with high levels of butyrate-producing bacteria has been proposed as an alternative approach [652].

Another strategy that could be used to target age-related microbial dysbiosis and immune ageing is the generation of multi-strain bacterial cocktails. This novel therapy has been shown to restore intestinal homeostasis, increase SCFA production [532,633] and reduce intestinal permeability and inflammation. Interestingly, vitamin D supplementation and metformin have been linked with an increased abundance of beneficial commensals and enhanced intestinal barrier function as well as increased Treg polarisation [611,653,654].

6.6 Closing remarks

Global expansion of the ageing population has led to a growing need to identify novel interventions that reduce the burden of age-related diseases and infection by promoting healthy immune ageing. The gut microbiome has emerged as a central factor affecting human health via modulation of immune cell development and function. However, advancing age is accompanied by intestinal barrier dysfunction and microbial dysbiosis, paralleling the progressive decline in immune function. Although it is clear that gut microbiota shape the host's immune responses, only a handful of studies have examined the relationship between the ageing gut microbiome and immune ageing. In this thesis, we identified age-associated enhanced microbial translocation as a novel contributor towards thymic involution and T cell ageing. Furthermore, we identified novel bacterial species linked with immune ageing features and poor influenza vaccine immunogenicity in old age, which can be validated as microbiome-based intervention targets in future studies. Lastly, we explored the

potential for dietary patterns, such as the MedDiet and multi-vitamin supplementation, to promote healthy immune ageing in older people. These novel findings extend our understanding of the consequences of age-related changes in the microbial-immune-metabolic axis and provide evidence for designing future microbiome-targeted interventions that restore immune homeostasis in older people. Exploiting the restoration ability of these microbial targets provides new opportunities for the development of personalised treatments tailored to an individual's microbiota for optimal results for promoting healthy ageing. Further, our findings help bridge the widening gap between health span lifespan, which is recognised as a major priority by the UK government [3].

References

1. Organization WH. World health statistics 2022: monitoring health for the SDGs, sustainable development goals. Geneva 2022. Report No.: 9789240051140.
2. Statistics OfN. 2020-based Interim National Population Projections. Principal projection - UK population in age groups2022.
3. Committee SaTS. Ageing: Science, Technology and Healthy Living. House of Lords; 2021.
4. López-Otín C, Blasco MA, Partridge L, Serrano M, Kroemer G. Hallmarks of aging: An expanding universe. *Cell*. 2023;186(2):243-78.
5. Molony RD, Malawista A, Montgomery RR. Reduced dynamic range of antiviral innate immune responses in aging. *Exp Gerontol*. 2018;107:130-5.
6. Goronzy JJ, Weyand CM. Immune aging and autoimmunity. *Cell Mol Life Sci*. 2012;69(10):1615-23.
7. Fane M, Weeraratna AT. How the ageing microenvironment influences tumour progression. *Nat Rev Cancer*. 2020;20(2):89-106.
8. Prattichizzo F, De Nigris V, Spiga R, Mancuso E, La Sala L, Antonicelli R, et al. Inflammageing and metaflammation: The yin and yang of type 2 diabetes. *Ageing Res Rev*. 2018;41:1-17.
9. Mistriotis P, Andreadis ST. Vascular aging: Molecular mechanisms and potential treatments for vascular rejuvenation. *Ageing Res Rev*. 2017;37:94-116.
10. Chen Y, Liu BC, Glass K, Kirk MD. High incidence of hospitalisation due to infectious gastroenteritis in older people associated with poor self-rated health. *BMJ Open*. 2015;5(12):e010161.
11. Xia X, Jiang Q, McDermott J, Han JJ. Aging and Alzheimer's disease: Comparison and associations from molecular to system level. *Aging Cell*. 2018;17(5):e12802.
12. Gontijo Guerra S, Berbiche D, Vasiliadis HM. Measuring multimorbidity in older adults: comparing different data sources. *BMC Geriatr*. 2019;19(1):166.
13. Santoro A, Bientinesi E, Monti D. Immunosenescence and inflammaging in the aging process: age-related diseases or longevity? *Ageing Res Rev*. 2021;71:101422.
14. Frasca D, Romero M, Garcia D, Diaz A, Blomberg BB. Hyper-metabolic B cells in the spleens of old mice make antibodies with autoimmune specificities. *Immun Ageing*. 2021;18(1):9.
15. Frasca D, Blomberg BB. Aging induces B cell defects and decreased antibody responses to influenza infection and vaccination. *Immun Ageing*. 2020;17(1):37.
16. Palmer S, Albergante L, Blackburn CC, Newman TJ. Thymic involution and rising disease incidence with age. *Proc Natl Acad Sci U S A*. 2018;115(8):1883-8.
17. Yousefzadeh MJ, Flores RR, Zhu Y, Schmiechen ZC, Brooks RW, Trussoni CE, et al. An aged immune system drives senescence and ageing of solid organs. *Nature*. 2021;594(7861):100-5.
18. Desdin-Mico G, Soto-Heredero G, Aranda JF, Oller J, Carrasco E, Gabande-Rodriguez E, et al. T cells with dysfunctional mitochondria induce multimorbidity and premature senescence. *Science*. 2020;368(6497):1371-6.

19. Pang WW, Price EA, Sahoo D, Beerman I, Maloney WJ, Rossi DJ, et al. Human bone marrow hematopoietic stem cells are increased in frequency and myeloid-biased with age. *Proc Natl Acad Sci U S A*. 2011;108(50):20012-7.
20. Beerman I, Bhattacharya D, Zandi S, Sigvardsson M, Weissman IL, Bryder D, et al. Functionally distinct hematopoietic stem cells modulate hematopoietic lineage potential during aging by a mechanism of clonal expansion. *Proc Natl Acad Sci U S A*. 2010;107(12):5465-70.
21. Dykstra B, Olthof S, Schreuder J, Ritsema M, de Haan G. Clonal analysis reveals multiple functional defects of aged murine hematopoietic stem cells. *J Exp Med*. 2011;208(13):2691-703.
22. Rube CE, Fricke A, Widmann TA, Furst T, Madry H, Pfreundschuh M, et al. Accumulation of DNA damage in hematopoietic stem and progenitor cells during human aging. *PLoS One*. 2011;6(3):e17487.
23. Sun D, Luo M, Jeong M, Rodriguez B, Xia Z, Hannah R, et al. Epigenomic profiling of young and aged HSCs reveals concerted changes during aging that reinforce self-renewal. *Cell Stem Cell*. 2014;14(5):673-88.
24. Porto ML, Rodrigues BP, Menezes TN, Ceschim SL, Casarini DE, Gava AL, et al. Reactive oxygen species contribute to dysfunction of bone marrow hematopoietic stem cells in aged C57BL/6 J mice. *J Biomed Sci*. 2015;22:97.
25. Dong S, Wang Q, Kao YR, Diaz A, Tasset I, Kaushik S, et al. Chaperone-mediated autophagy sustains haematopoietic stem-cell function. *Nature*. 2021;591(7848):117-23.
26. Norddahl GL, Pronk CJ, Wahlestedt M, Sten G, Nygren JM, Ugale A, et al. Accumulating mitochondrial DNA mutations drive premature hematopoietic aging phenotypes distinct from physiological stem cell aging. *Cell Stem Cell*. 2011;8(5):499-510.
27. Flach J, Bakker ST, Mohrin M, Conroy PC, Pietras EM, Reynaud D, et al. Replication stress is a potent driver of functional decline in ageing haematopoietic stem cells. *Nature*. 2014;512(7513):198-202.
28. Florian MC, Dorr K, Niebel A, Daria D, Schrezenmeier H, Rojewski M, et al. Cdc42 activity regulates hematopoietic stem cell aging and rejuvenation. *Cell Stem Cell*. 2012;10(5):520-30.
29. Frisch BJ, Hoffman CM, Latchney SE, LaMere MW, Myers J, Ashton J, et al. Aged marrow macrophages expand platelet-biased hematopoietic stem cells via Interleukin1B. *JCI Insight*. 2019;5(10).
30. Leins H, Mulaw M, Eiwen K, Sakk V, Liang Y, Denkinger M, et al. Aged murine hematopoietic stem cells drive aging-associated immune remodeling. *Blood*. 2018;132(6):565-76.
31. Dugan B, Conway J, Duggal NA. Inflammaging as a target for healthy ageing. *Age Ageing*. 2023;52(2).
32. Morrisette-Thomas V, Cohen AA, Fulop T, Riesco E, Legault V, Li Q, et al. Inflamm-aging does not simply reflect increases in pro-inflammatory markers. *Mech Ageing Dev*. 2014;139:49-57.
33. Bartlett DB, Firth CM, Phillips AC, Moss P, Baylis D, Syddall H, et al. The age-related increase in low-grade systemic inflammation (Inflammaging) is not driven by cytomegalovirus infection. *Aging Cell*. 2012;11(5):912-5.

34. Fulop T, Larbi A, Dupuis G, Le Page A, Frost EH, Cohen AA, et al. Immunosenescence and Inflamm-Aging As Two Sides of the Same Coin: Friends or Foes? *Front Immunol*. 2017;8:1960.
35. Marcos-Perez D, Sanchez-Flores M, Maseda A, Lorenzo-Lopez L, Millan-Calenti JC, Gostner JM, et al. Frailty in Older Adults Is Associated With Plasma Concentrations of Inflammatory Mediators but Not With Lymphocyte Subpopulations. *Front Immunol*. 2018;9:1056.
36. Fielder E, Tweedy C, Wilson C, Oakley F, LeBeau FEN, Passos JF, et al. Anti-inflammatory treatment rescues memory deficits during aging in nfkb1(-/-) mice. *Aging Cell*. 2020;19(10):e13188.
37. Santoro A, Zhao J, Wu L, Carru C, Biagi E, Franceschi C. Microbiomes other than the gut: inflammaging and age-related diseases. *Semin Immunopathol*. 2020;42(5):589-605.
38. Zuhair M, Smit GSA, Wallis G, Jabbar F, Smith C, Devleesschauwer B, et al. Estimation of the worldwide seroprevalence of cytomegalovirus: A systematic review and meta-analysis. *Rev Med Virol*. 2019;29(3):e2034.
39. Simanek AM, Dowd JB, Pawelec G, Melzer D, Dutta A, Aiello AE. Seropositivity to cytomegalovirus, inflammation, all-cause and cardiovascular disease-related mortality in the United States. *PLoS One*. 2011;6(2):e16103.
40. Zhang W, Li H, Bream JH, Nilles TL, Leng SX, Margolick JB. Longitudinal association of cytokine-producing CMV-specific T cells with frailty in HIV-infected and -uninfected men who have sex with men. *Immun Ageing*. 2022;19(1):13.
41. Frasca D, Diaz A, Romero M, Landin AM, Blomberg BB. Cytomegalovirus (CMV) seropositivity decreases B cell responses to the influenza vaccine. *Vaccine*. 2015;33(12):1433-9.
42. Nicoli F, Clave E, Wanke K, von Braun A, Bondet V, Alanio C, et al. Primary immune responses are negatively impacted by persistent herpesvirus infections in older people: results from an observational study on healthy subjects and a vaccination trial on subjects aged more than 70 years old. *EBioMedicine*. 2022;76:103852.
43. Derhovanessian E, Theeten H, Hahnel K, Van Damme P, Cools N, Pawelec G. Cytomegalovirus-associated accumulation of late-differentiated CD4 T-cells correlates with poor humoral response to influenza vaccination. *Vaccine*. 2013;31(4):685-90.
44. van den Berg SPH, Wong A, Hendriks M, Jacobi RHJ, van Baarle D, van Beek J. Negative Effect of Age, but Not of Latent Cytomegalovirus Infection on the Antibody Response to a Novel Influenza Vaccine Strain in Healthy Adults. *Front Immunol*. 2018;9:82.
45. van den Berg SPH, Lanfermeijer J, Jacobi RHJ, Hendriks M, Vos M, van Schuijlenburg R, et al. Latent CMV Infection Is Associated With Lower Influenza Virus-Specific Memory T-Cell Frequencies, but Not With an Impaired T-Cell Response to Acute Influenza Virus Infection. *Front Immunol*. 2021;12:663664.
46. Hazeldine J, Lord JM. Innate immunesenescence: underlying mechanisms and clinical relevance. *Biogerontology*. 2015;16(2):187-201.
47. Austermann J, Roth J, Barczyk-Kahlert K. The Good and the Bad: Monocytes' and Macrophages' Diverse Functions in Inflammation. *Cells*. 2022;11(12).

48. Wong KL, Tai JJ, Wong WC, Han H, Sem X, Yeap WH, et al. Gene expression profiling reveals the defining features of the classical, intermediate, and nonclassical human monocyte subsets. *Blood*. 2011;118(5):e16-31.
49. Conway J, Certo M, Lord JM, Mauro C, Duggal NA. Understanding the role of host metabolites in the induction of immune senescence: Future strategies for keeping the ageing population healthy. *Br J Pharmacol*. 2022;179(9):1808-24.
50. Cros J, Cagnard N, Woollard K, Patey N, Zhang SY, Senechal B, et al. Human CD14dim monocytes patrol and sense nucleic acids and viruses via TLR7 and TLR8 receptors. *Immunity*. 2010;33(3):375-86.
51. Metcalf TU, Wilkinson PA, Cameron MJ, Ghneim K, Chiang C, Wertheimer AM, et al. Human Monocyte Subsets Are Transcriptionally and Functionally Altered in Aging in Response to Pattern Recognition Receptor Agonists. *J Immunol*. 2017;199(4):1405-17.
52. Qian F, Wang X, Zhang L, Chen S, Piecychna M, Allore H, et al. Age-associated elevation in TLR5 leads to increased inflammatory responses in the elderly. *Aging Cell*. 2012;11(1):104-10.
53. Nyugen J, Agrawal S, Gollapudi S, Gupta S. Impaired functions of peripheral blood monocyte subpopulations in aged humans. *J Clin Immunol*. 2010;30(6):806-13.
54. Seidler S, Zimmermann HW, Bartneck M, Trautwein C, Tacke F. Age-dependent alterations of monocyte subsets and monocyte-related chemokine pathways in healthy adults. *BMC Immunol*. 2010;11:30.
55. Hearps AC, Martin GE, Angelovich TA, Cheng WJ, Maisa A, Landay AL, et al. Aging is associated with chronic innate immune activation and dysregulation of monocyte phenotype and function. *Aging Cell*. 2012;11(5):867-75.
56. Ong SM, Hadadi E, Dang TM, Yeap WH, Tan CT, Ng TP, et al. The pro-inflammatory phenotype of the human non-classical monocyte subset is attributed to senescence. *Cell Death Dis*. 2018;9(3):266.
57. Merino A, Buendia P, Martin-Malo A, Aljama P, Ramirez R, Carracedo J. Senescent CD14+CD16+ monocytes exhibit proinflammatory and proatherosclerotic activity. *J Immunol*. 2011;186(3):1809-15.
58. Jackaman C, Radley-Crabb HG, Soffe Z, Shavlakadze T, Grounds MD, Nelson DJ. Targeting macrophages rescues age-related immune deficiencies in C57BL/6J geriatric mice. *Aging Cell*. 2013;12(3):345-57.
59. Ogawa T, Kitagawa M, Hirokawa K. Age-related changes of human bone marrow: a histometric estimation of proliferative cells, apoptotic cells, T cells, B cells and macrophages. *Mech Ageing Dev*. 2000;117(1-3):57-68.
60. Kirschner K, Chandra T, Kiselev V, Flores-Santa Cruz D, Macaulay IC, Park HJ, et al. Proliferation Drives Aging-Related Functional Decline in a Subpopulation of the Hematopoietic Stem Cell Compartment. *Cell Rep*. 2017;19(8):1503-11.
61. Puchta A, Naidoo A, Verschoor CP, Loukov D, Thevaranjan N, Mandur TS, et al. TNF Drives Monocyte Dysfunction with Age and Results in Impaired Anti-pneumococcal Immunity. *PLoS Pathog*. 2016;12(1):e1005368.
62. De Martinis M, Modesti M, Ginaldi L. Phenotypic and functional changes of circulating monocytes and polymorphonuclear leucocytes from elderly persons. *Immunol Cell Biol*. 2004;82(4):415-20.
63. McLachlan JA, Serkin CD, Morrey KM, Bakouche O. Antitumoral properties of aged human monocytes. *J Immunol*. 1995;154(2):832-43.

64. Albright JM, Dunn RC, Shults JA, Boe DM, Afshar M, Kovacs EJ. Advanced Age Alters Monocyte and Macrophage Responses. *Antioxid Redox Signal*. 2016;25(15):805-15.
65. Jacinto TA, Meireles GS, Dias AT, Aires R, Porto ML, Gava AL, et al. Increased ROS production and DNA damage in monocytes are biomarkers of aging and atherosclerosis. *Biol Res*. 2018;51(1):33.
66. Smallwood HS, Lopez-Ferrer D, Squier TC. Aging enhances the production of reactive oxygen species and bactericidal activity in peritoneal macrophages by upregulating classical activation pathways. *Biochemistry*. 2011;50(45):9911-22.
67. Hilmer SN, Cogger VC, Le Couteur DG. Basal activity of Kupffer cells increases with old age. *J Gerontol A Biol Sci Med Sci*. 2007;62(9):973-8.
68. Thevaranjan N, Puchta A, Schulz C, Naidoo A, Szamosi JC, Verschoor CP, et al. Age-Associated Microbial Dysbiosis Promotes Intestinal Permeability, Systemic Inflammation, and Macrophage Dysfunction. *Cell Host Microbe*. 2017;21(4):455-66 e4.
69. Aprahamian T, Takemura Y, Goukassian D, Walsh K. Ageing is associated with diminished apoptotic cell clearance in vivo. *Clin Exp Immunol*. 2008;152(3):448-55.
70. Arnardottir HH, Dalli J, Colas RA, Shinohara M, Serhan CN. Aging delays resolution of acute inflammation in mice: reprogramming the host response with novel nano-proresolving medicines. *J Immunol*. 2014;193(8):4235-44.
71. De Maeyer RPH, van de Merwe RC, Louie R, Bracken OV, Devine OP, Goldstein DR, et al. Blocking elevated p38 MAPK restores efferocytosis and inflammatory resolution in the elderly. *Nat Immunol*. 2020;21(6):615-25.
72. Herrero C, Marques L, Lloberas J, Celada A. IFN-gamma-dependent transcription of MHC class II IA is impaired in macrophages from aged mice. *J Clin Invest*. 2001;107(4):485-93.
73. Plowden J, Renshaw-Hoelscher M, Gangappa S, Engleman C, Katz JM, Sambhara S. Impaired antigen-induced CD8+ T cell clonal expansion in aging is due to defects in antigen presenting cell function. *Cell Immunol*. 2004;229(2):86-92.
74. Mengos AE, Gastineau DA, Gustafson MP. The CD14(+)HLA-DR(lo/neg) Monocyte: An Immunosuppressive Phenotype That Restrains Responses to Cancer Immunotherapy. *Front Immunol*. 2019;10:1147.
75. Strohacker K, Breslin WL, Carpenter KC, McFarlin BK. Aged mice have increased inflammatory monocyte concentration and altered expression of cell-surface functional receptors. *J Biosci*. 2012;37(1):55-62.
76. van Duin D, Allore HG, Mohanty S, Ginter S, Newman FK, Belshe RB, et al. Prevaccine determination of the expression of costimulatory B7 molecules in activated monocytes predicts influenza vaccine responses in young and older adults. *J Infect Dis*. 2007;195(11):1590-7.
77. van Duin D, Mohanty S, Thomas V, Ginter S, Montgomery RR, Fikrig E, et al. Age-associated defect in human TLR-1/2 function. *J Immunol*. 2007;178(2):970-5.
78. Renshaw M, Rockwell J, Engleman C, Gewirtz A, Katz J, Sambhara S. Cutting edge: impaired Toll-like receptor expression and function in aging. *J Immunol*. 2002;169(9):4697-701.

79. Boehmer ED, Goral J, Faunce DE, Kovacs EJ. Age-dependent decrease in Toll-like receptor 4-mediated proinflammatory cytokine production and mitogen-activated protein kinase expression. *J Leukoc Biol*. 2004;75(2):342-9.
80. Chelvarajan RL, Collins SM, Van Willigen JM, Bondada S. The unresponsiveness of aged mice to polysaccharide antigens is a result of a defect in macrophage function. *J Leukoc Biol*. 2005;77(4):503-12.
81. Kelly J, Ali Khan A, Yin J, Ferguson TA, Apte RS. Senescence regulates macrophage activation and angiogenic fate at sites of tissue injury in mice. *J Clin Invest*. 2007;117(11):3421-6.
82. Chen H, Ma F, Hu X, Jin T, Xiong C, Teng X. Elevated COX2 expression and PGE2 production by downregulation of RXRalpha in senescent macrophages. *Biochem Biophys Res Commun*. 2013;440(1):157-62.
83. Claycombe KJ, Wu D, Nikolova-Karakashian M, Palmer H, Beharka A, Paulson KE, et al. Ceramide mediates age-associated increase in macrophage cyclooxygenase-2 expression. *J Biol Chem*. 2002;277(34):30784-91.
84. Rathinam VA, Jiang Z, Waggoner SN, Sharma S, Cole LE, Waggoner L, et al. The AIM2 inflammasome is essential for host defense against cytosolic bacteria and DNA viruses. *Nat Immunol*. 2010;11(5):395-402.
85. Wang Q, Westra J, van der Geest KS, Moser J, Bijzet J, Kuiper T, et al. Reduced levels of cytosolic DNA sensor AIM2 are associated with impaired cytokine responses in healthy elderly. *Exp Gerontol*. 2016;78:39-46.
86. Karakaslar EO, Katiyar N, Hasham M, Youn A, Sharma S, Chung C-h, et al. Transcriptional activation of Jun and Fos members of the AP-1 complex is a conserved signature of immune aging that contributes to inflammaging. 2022.
87. Boehmer ED, Meehan MJ, Cutro BT, Kovacs EJ. Aging negatively skews macrophage TLR2- and TLR4-mediated pro-inflammatory responses without affecting the IL-2-stimulated pathway. *Mech Ageing Dev*. 2005;126(12):1305-13.
88. Fallah MP, Chelvarajan RL, Garvy BA, Bondada S. Role of phosphoinositide 3-kinase-Akt signaling pathway in the age-related cytokine dysregulation in splenic macrophages stimulated via TLR-2 or TLR-4 receptors. *Mech Ageing Dev*. 2011;132(6-7):274-86.
89. Patel AA, Ginhoux F, Yona S. Monocytes, macrophages, dendritic cells and neutrophils: an update on lifespan kinetics in health and disease. *Immunology*. 2021;163(3):250-61.
90. Hidalgo A, Chilvers ER, Summers C, Koenderman L. The Neutrophil Life Cycle. *Trends Immunol*. 2019;40(7):584-97.
91. Singhal A, Kumar S. Neutrophil and remnant clearance in immunity and inflammation. *Immunology*. 2022;165(1):22-43.
92. Wenisch C, Patruta S, Daxbock F, Krause R, Horl W. Effect of age on human neutrophil function. *J Leukoc Biol*. 2000;67(1):40-5.
93. Pillay J, Kamp VM, van Hoffen E, Visser T, Tak T, Lammers JW, et al. A subset of neutrophils in human systemic inflammation inhibits T cell responses through Mac-1. *J Clin Invest*. 2012;122(1):327-36.
94. Sauce D, Dong Y, Campillo-Gimenez L, Casulli S, Bayard C, Autran B, et al. Reduced Oxidative Burst by Primed Neutrophils in the Elderly Individuals Is Associated With Increased Levels of the CD16bright/CD62Ldim Immunosuppressive Subset. *J Gerontol A Biol Sci Med Sci*. 2017;72(2):163-72.

95. Sapey E, Greenwood H, Walton G, Mann E, Love A, Aaronson N, et al. Phosphoinositide 3-kinase inhibition restores neutrophil accuracy in the elderly: toward targeted treatments for immunosenescence. *Blood*. 2014;123(2):239-48.
96. Brubaker AL, Rendon JL, Ramirez L, Choudhry MA, Kovacs EJ. Reduced neutrophil chemotaxis and infiltration contributes to delayed resolution of cutaneous wound infection with advanced age. *J Immunol*. 2013;190(4):1746-57.
97. Barkaway A, Rolas L, Joulia R, Bodkin J, Lenn T, Owen-Woods C, et al. Age-related changes in the local milieu of inflamed tissues cause aberrant neutrophil trafficking and subsequent remote organ damage. *Immunity*. 2021;54(7):1494-510 e7.
98. Simell B, Vuorela A, Ekstrom N, Palmu A, Reunanen A, Meri S, et al. Aging reduces the functionality of anti-pneumococcal antibodies and the killing of Streptococcus pneumoniae by neutrophil phagocytosis. *Vaccine*. 2011;29(10):1929-34.
99. Butcher SK, Chahal H, Nayak L, Sinclair A, Henriquez NV, Sapey E, et al. Senescence in innate immune responses: reduced neutrophil phagocytic capacity and CD16 expression in elderly humans. *J Leukoc Biol*. 2001;70(6):881-6.
100. Emanuelli G, Lanzio M, Anfossi T, Romano S, Anfossi G, Calcamuggi G. Influence of age on polymorphonuclear leukocytes in vitro: phagocytic activity in healthy human subjects. *Gerontology*. 1986;32(6):308-16.
101. Ogawa K, Suzuki K, Okutsu M, Yamazaki K, Shinkai S. The association of elevated reactive oxygen species levels from neutrophils with low-grade inflammation in the elderly. *Immun Ageing*. 2008;5:13.
102. Kovalenko EI, Boyko AA, Semenkov VF, Lutsenko GV, Grechikhina MV, Kanevskiy LM, et al. ROS production, intracellular HSP70 levels and their relationship in human neutrophils: effects of age. *Oncotarget*. 2014;5(23):11800-12.
103. Braga PC, Sala MT, Dal Sasso M, Mancini L, Sandrini MC, Annoni G. Influence of age on oxidative bursts (chemiluminescence) of polymorphonuclear neutrophil leukocytes. *Gerontology*. 1998;44(4):192-7.
104. Fulop T, Larbi A, Douziech N, Fortin C, Guerard KP, Lesur O, et al. Signal transduction and functional changes in neutrophils with aging. *Aging Cell*. 2004;3(4):217-26.
105. Papayannopoulos V, Metzler KD, Hakkim A, Zychlinsky A. Neutrophil elastase and myeloperoxidase regulate the formation of neutrophil extracellular traps. *J Cell Biol*. 2010;191(3):677-91.
106. Tokuhiro T, Ishikawa A, Sato H, Takita S, Yoshikawa A, Anzai R, et al. Oxidized Phospholipids and Neutrophil Elastase Coordinately Play Critical Roles in NET Formation. *Front Cell Dev Biol*. 2021;9:718586.
107. Tseng CW, Kyme PA, Arruda A, Ramanujan VK, Tawackoli W, Liu GY. Innate immune dysfunctions in aged mice facilitate the systemic dissemination of methicillin-resistant S. aureus. *PLoS One*. 2012;7(7):e41454.
108. Hazeldine J, Harris P, Chapple IL, Grant M, Greenwood H, Livesey A, et al. Impaired neutrophil extracellular trap formation: a novel defect in the innate immune system of aged individuals. *Aging Cell*. 2014;13(4):690-8.

109. Sabbatini M, Bona E, Novello G, Migliario M, Reno F. Aging hampers neutrophil extracellular traps (NETs) efficacy. *Aging Clin Exp Res*. 2022;34(10):2345-53.
110. Fortin CF, Lesur O, Fulop T, Jr. Effects of aging on triggering receptor expressed on myeloid cells (TREM)-1-induced PMN functions. *FEBS Lett*. 2007;581(6):1173-8.
111. Guichard C, Pedruzzi E, Dewas C, Fay M, Pouzet C, Bens M, et al. Interleukin-8-induced priming of neutrophil oxidative burst requires sequential recruitment of NADPH oxidase components into lipid rafts. *J Biol Chem*. 2005;280(44):37021-32.
112. Lipschitz DA, Udupa KB, Boxer LA. The role of calcium in the age-related decline of neutrophil function. *Blood*. 1988;71(3):659-65.
113. Quatrini L, Della Chiesa M, Sivori S, Mingari MC, Pende D, Moretta L. Human NK cells, their receptors and function. *Eur J Immunol*. 2021;51(7):1566-79.
114. Wendt K, Wilk E, Buyny S, Buer J, Schmidt RE, Jacobs R. Gene and protein characteristics reflect functional diversity of CD56dim and CD56bright NK cells. *J Leukoc Biol*. 2006;80(6):1529-41.
115. Jacobs R, Hintzen G, Kemper A, Beul K, Kempf S, Behrens G, et al. CD56bright cells differ in their KIR repertoire and cytotoxic features from CD56dim NK cells. *Eur J Immunol*. 2001;31(10):3121-7.
116. Gounder SS, Abdullah BJJ, Radzuanb N, Zain F, Sait NBM, Chua C, et al. Effect of Aging on NK Cell Population and Their Proliferation at Ex Vivo Culture Condition. *Anal Cell Pathol (Amst)*. 2018;2018:7871814.
117. Hazeldine J, Lord JM. The impact of ageing on natural killer cell function and potential consequences for health in older adults. *Ageing Res Rev*. 2013;12(4):1069-78.
118. Chidrawar SM, Khan N, Chan YL, Nayak L, Moss PA. Ageing is associated with a decline in peripheral blood CD56bright NK cells. *Immun Ageing*. 2006;3:10.
119. Le Garff-Tavernier M, Beziat V, Decocq J, Siguret V, Gandjbakhch F, Pautas E, et al. Human NK cells display major phenotypic and functional changes over the life span. *Aging Cell*. 2010;9(4):527-35.
120. Lopez-Verges S, Milush JM, Pandey S, York VA, Arakawa-Hoyt J, Pircher H, et al. CD57 defines a functionally distinct population of mature NK cells in the human CD56dimCD16+ NK-cell subset. *Blood*. 2010;116(19):3865-74.
121. Pangrazzi L, Reidla J, Carmona Arana JA, Naismith E, Miggitsch C, Meryk A, et al. CD28 and CD57 define four populations with distinct phenotypic properties within human CD8(+) T cells. *Eur J Immunol*. 2020;50(3):363-79.
122. Brenchley JM, Karandikar NJ, Betts MR, Ambrozak DR, Hill BJ, Crotty LE, et al. Expression of CD57 defines replicative senescence and antigen-induced apoptotic death of CD8+ T cells. *Blood*. 2003;101(7):2711-20.
123. Bryceson YT, Ljunggren HG, Long EO. Minimal requirement for induction of natural cytotoxicity and intersection of activation signals by inhibitory receptors. *Blood*. 2009;114(13):2657-66.
124. Bryceson YT, March ME, Ljunggren HG, Long EO. Synergy among receptors on resting NK cells for the activation of natural cytotoxicity and cytokine secretion. *Blood*. 2006;107(1):159-66.
125. Almeida-Oliveira A, Smith-Carvalho M, Porto LC, Cardoso-Oliveira J, Ribeiro Ados S, Falcao RR, et al. Age-related changes in natural killer cell receptors from childhood through old age. *Hum Immunol*. 2011;72(4):319-29.

126. Hazeldine J, Hampson P, Lord JM. Reduced release and binding of perforin at the immunological synapse underlies the age-related decline in natural killer cell cytotoxicity. *Aging Cell*. 2012;11(5):751-9.
127. Lutz CT, Karapetyan A, Al-Attar A, Shelton BJ, Holt KJ, Tucker JH, et al. Human NK cells proliferate and die in vivo more rapidly than T cells in healthy young and elderly adults. *J Immunol*. 2011;186(8):4590-8.
128. Hayhoe RP, Henson SM, Akbar AN, Palmer DB. Variation of human natural killer cell phenotypes with age: identification of a unique KLRG1-negative subset. *Hum Immunol*. 2010;71(7):676-81.
129. Sagiv A, Biran A, Yon M, Simon J, Lowe SW, Krizhanovsky V. Granule exocytosis mediates immune surveillance of senescent cells. *Oncogene*. 2013;32(15):1971-7.
130. Ogata K, An E, Shioi Y, Nakamura K, Luo S, Yokose N, et al. Association between natural killer cell activity and infection in immunologically normal elderly people. *Clin Exp Immunol*. 2001;124(3):392-7.
131. Mysliwska J, Trzonkowski P, Szmit E, Brydak LB, Machala M, Mysliwski A. Immunomodulating effect of influenza vaccination in the elderly differing in health status. *Exp Gerontol*. 2004;39(10):1447-58.
132. Mariani E, Meneghetti A, Neri S, Ravaglia G, Forti P, Cattini L, et al. Chemokine production by natural killer cells from nonagenarians. *Eur J Immunol*. 2002;32(6):1524-9.
133. Mariani E, Pulsatelli L, Neri S, Dolzani P, Meneghetti A, Silvestri T, et al. RANTES and MIP-1alpha production by T lymphocytes, monocytes and NK cells from nonagenarian subjects. *Exp Gerontol*. 2002;37(2-3):219-26.
134. Krishnaraj R, Bhooma T. Cytokine sensitivity of human NK cells during immunosenescence. 2. IL2-induced interferon gamma secretion. *Immunol Lett*. 1996;50(1-2):59-63.
135. MacDonald KP, Munster DJ, Clark GJ, Dzionek A, Schmitz J, Hart DN. Characterization of human blood dendritic cell subsets. *Blood*. 2002;100(13):4512-20.
136. Ito T, Kanzler H, Duramad O, Cao W, Liu YJ. Specialization, kinetics, and repertoire of type 1 interferon responses by human plasmacytoid predendritic cells. *Blood*. 2006;107(6):2423-31.
137. Kadowaki N, Ho S, Antonenko S, Malefyt RW, Kastelein RA, Bazan F, et al. Subsets of human dendritic cell precursors express different toll-like receptors and respond to different microbial antigens. *J Exp Med*. 2001;194(6):863-9.
138. Nizzoli G, Krietsch J, Weick A, Steinfelder S, Facciotti F, Gruarin P, et al. Human CD1c+ dendritic cells secrete high levels of IL-12 and potently prime cytotoxic T-cell responses. *Blood*. 2013;122(6):932-42.
139. Sittig SP, Bakdash G, Weiden J, Skold AE, Tel J, Figdor CG, et al. A Comparative Study of the T Cell Stimulatory and Polarizing Capacity of Human Primary Blood Dendritic Cell Subsets. *Mediators Inflamm*. 2016;2016:3605643.
140. Jing Y, Shaheen E, Drake RR, Chen N, Gravenstein S, Deng Y. Aging is associated with a numerical and functional decline in plasmacytoid dendritic cells, whereas myeloid dendritic cells are relatively unaltered in human peripheral blood. *Hum Immunol*. 2009;70(10):777-84.

141. Perez-Cabezas B, Naranjo-Gomez M, Fernandez MA, Grifols JR, Pujol-Borrell R, Borras FE. Reduced numbers of plasmacytoid dendritic cells in aged blood donors. *Exp Gerontol*. 2007;42(10):1033-8.
142. Agrawal A, Agrawal S, Cao JN, Su H, Osann K, Gupta S. Altered innate immune functioning of dendritic cells in elderly humans: a role of phosphoinositide 3-kinase-signaling pathway. *J Immunol*. 2007;178(11):6912-22.
143. Hasegawa T, Feng Z, Yan Z, Ngo KH, Hosoi J, Demehri S. Reduction in Human Epidermal Langerhans Cells with Age Is Associated with Decline in CXCL14-Mediated Recruitment of CD14(+) Monocytes. *J Invest Dermatol*. 2020;140(7):1327-34.
144. Bhushan M, Cumberbatch M, Dearman RJ, Andrew SM, Kimber I, Griffiths CE. Tumour necrosis factor-alpha-induced migration of human Langerhans cells: the influence of ageing. *Br J Dermatol*. 2002;146(1):32-40.
145. Della Bella S, Bierti L, Presicce P, Arienti R, Valenti M, Saresella M, et al. Peripheral blood dendritic cells and monocytes are differently regulated in the elderly. *Clin Immunol*. 2007;122(2):220-8.
146. Garbe K, Bratke K, Wagner S, Virchow JC, Lommatzsch M. Plasmacytoid dendritic cells and their Toll-like receptor 9 expression selectively decrease with age. *Hum Immunol*. 2012;73(5):493-7.
147. Sridharan A, Esposo M, Kaushal K, Tay J, Osann K, Agrawal S, et al. Age-associated impaired plasmacytoid dendritic cell functions lead to decreased CD4 and CD8 T cell immunity. *Age (Dordr)*. 2011;33(3):363-76.
148. Chougnet CA, Thacker RI, Shehata HM, Hennies CM, Lehn MA, Lages CS, et al. Loss of Phagocytic and Antigen Cross-Presenting Capacity in Aging Dendritic Cells Is Associated with Mitochondrial Dysfunction. *J Immunol*. 2015;195(6):2624-32.
149. Prakash S, Agrawal S, Ma D, Gupta S, Peterson EM, Agrawal A. Dendritic cells from aged subjects display enhanced inflammatory responses to Chlamydophila pneumoniae. *Mediators Inflamm*. 2014;2014:436438.
150. Agrawal A, Tay J, Ton S, Agrawal S, Gupta S. Increased reactivity of dendritic cells from aged subjects to self-antigen, the human DNA. *J Immunol*. 2009;182(2):1138-45.
151. Zhao J, Zhao J, Legge K, Perlman S. Age-related increases in PGD(2) expression impair respiratory DC migration, resulting in diminished T cell responses upon respiratory virus infection in mice. *J Clin Invest*. 2011;121(12):4921-30.
152. Panda A, Qian F, Mohanty S, van Duin D, Newman FK, Zhang L, et al. Age-associated decrease in TLR function in primary human dendritic cells predicts influenza vaccine response. *J Immunol*. 2010;184(5):2518-27.
153. Kumar BV, Connors TJ, Farber DL. Human T Cell Development, Localization, and Function throughout Life. *Immunity*. 2018;48(2):202-13.
154. Liang Z, Dong X, Zhang Z, Zhang Q, Zhao Y. Age-related thymic involution: Mechanisms and functional impact. *Aging Cell*. 2022;21(8):e13671.
155. Van Vliet E, Jenkinson EJ, Kingston R, Owen JJ, Van Ewijk W. Stromal cell types in the developing thymus of the normal and nude mouse embryo. *Eur J Immunol*. 1985;15(7):675-81.

156. Aw D, Taylor-Brown F, Cooper K, Palmer DB. Phenotypical and morphological changes in the thymic microenvironment from ageing mice. *Biogerontology*. 2009;10(3):311-22.
157. Xing Y, Jameson SC, Hogquist KA. Thymoproteasome subunit-beta5T generates peptide-MHC complexes specialized for positive selection. *Proc Natl Acad Sci U S A*. 2013;110(17):6979-84.
158. Liu D, Kousa AI, O'Neill KE, Rouse P, Popis M, Farley AM, et al. Canonical Notch signaling controls the early thymic epithelial progenitor cell state and emergence of the medullary epithelial lineage in fetal thymus development. *Development*. 2020;147(12).
159. Alves NL, Richard-Le Goff O, Huntington ND, Sousa AP, Ribeiro VS, Bordack A, et al. Characterization of the thymic IL-7 niche in vivo. *Proc Natl Acad Sci U S A*. 2009;106(5):1512-7.
160. Lopes N, Boucherit N, Santamaria JC, Provin N, Charaix J, Ferrier P, et al. Thymocytes trigger self-antigen-controlling pathways in immature medullary thymic epithelial stages. *Elife*. 2022;11.
161. Malchow S, Leventhal DS, Lee V, Nishi S, Socci ND, Savage PA. Aire Enforces Immune Tolerance by Directing Autoreactive T Cells into the Regulatory T Cell Lineage. *Immunity*. 2016;44(5):1102-13.
162. Liston A, Lesage S, Wilson J, Peltonen L, Goodnow CC. Aire regulates negative selection of organ-specific T cells. *Nat Immunol*. 2003;4(4):350-4.
163. Palmer DB. The effect of age on thymic function. *Front Immunol*. 2013;4:316.
164. Aw D, Silva AB, Maddick M, von Zglinicki T, Palmer DB. Architectural changes in the thymus of aging mice. *Aging Cell*. 2008;7(2):158-67.
165. Yang H, Youm YH, Sun Y, Rim JS, Galban CJ, Vandanmagsar B, et al. Axin expression in thymic stromal cells contributes to an age-related increase in thymic adiposity and is associated with reduced thymopoiesis independently of ghrelin signaling. *J Leukoc Biol*. 2009;85(6):928-38.
166. Yang H, Youm YH, Dixit VD. Inhibition of thymic adipogenesis by caloric restriction is coupled with reduction in age-related thymic involution. *J Immunol*. 2009;183(5):3040-52.
167. Yue S, Zheng X, Zheng Y. Cell-type-specific role of lamin-B1 in thymus development and its inflammation-driven reduction in thymus aging. *Aging Cell*. 2019;18(4):e12952.
168. Ki S, Park D, Selden HJ, Seita J, Chung H, Kim J, et al. Global transcriptional profiling reveals distinct functions of thymic stromal subsets and age-related changes during thymic involution. *Cell Rep*. 2014;9(1):402-15.
169. Gray DH, Seach N, Ueno T, Milton MK, Liston A, Lew AM, et al. Developmental kinetics, turnover, and stimulatory capacity of thymic epithelial cells. *Blood*. 2006;108(12):3777-85.
170. Baran-Gale J, Morgan MD, Maio S, Dhalla F, Calvo-Asensio I, Deadman ME, et al. Ageing compromises mouse thymus function and remodels epithelial cell differentiation. *Elife*. 2020;9.
171. Aspinall R, Andrew D. Thymic atrophy in the mouse is a soluble problem of the thymic environment. *Vaccine*. 2000;18(16):1629-37.
172. Griffith AV, Fallahi M, Venables T, Petrie HT. Persistent degenerative changes in thymic organ function revealed by an inducible model of organ regrowth. *Aging Cell*. 2012;11(1):169-77.

173. Lepletier A, Hun ML, Hammett MV, Wong K, Naeem H, Hedger M, et al. Interplay between Follistatin, Activin A, and BMP4 Signaling Regulates Postnatal Thymic Epithelial Progenitor Cell Differentiation during Aging. *Cell Rep*. 2019;27(13):3887-901 e4.
174. Coder BD, Wang H, Ruan L, Su DM. Thymic involution perturbs negative selection leading to autoreactive T cells that induce chronic inflammation. *J Immunol*. 2015;194(12):5825-37.
175. Sempowski GD, Hale LP, Sundy JS, Massey JM, Koup RA, Douek DC, et al. Leukemia inhibitory factor, oncostatin M, IL-6, and stem cell factor mRNA expression in human thymus increases with age and is associated with thymic atrophy. *J Immunol*. 2000;164(4):2180-7.
176. Dixit VD, Yang H, Sun Y, Weeraratna AT, Youm YH, Smith RG, et al. Ghrelin promotes thymopoiesis during aging. *J Clin Invest*. 2007;117(10):2778-90.
177. Min H, Montecino-Rodriguez E, Dorshkind K. Reduction in the developmental potential of intrathymic T cell progenitors with age. *J Immunol*. 2004;173(1):245-50.
178. Thoman ML. The pattern of T lymphocyte differentiation is altered during thymic involution. *Mech Ageing Dev*. 1995;82(2-3):155-70.
179. Aw D, Silva AB, Palmer DB. The effect of age on the phenotype and function of developing thymocytes. *J Comp Pathol*. 2010;142 Suppl 1:S45-59.
180. Aw D, Silva AB, Palmer DB. Is thymocyte development functional in the aged? *Aging (Albany NY)*. 2009;1(2):146-53.
181. Lau LL, Spain LM. Altered aging-related thymic involution in T cell receptor transgenic, MHC-deficient, and CD4-deficient mice. *Mech Ageing Dev*. 2000;114(2):101-21.
182. Hale JS, Boursalian TE, Turk GL, Fink PJ. Thymic output in aged mice. *Proc Natl Acad Sci U S A*. 2006;103(22):8447-52.
183. Mitchell WA, Lang PO, Aspinall R. Tracing thymic output in older individuals. *Clin Exp Immunol*. 2010;161(3):497-503.
184. Haines CJ, Giffon TD, Lu LS, Lu X, Tessier-Lavigne M, Ross DT, et al. Human CD4+ T cell recent thymic emigrants are identified by protein tyrosine kinase 7 and have reduced immune function. *J Exp Med*. 2009;206(2):275-85.
185. Egorov ES, Kasatskaya SA, Zubov VN, Izraelson M, Nakonechnaya TO, Staroverov DB, et al. The Changing Landscape of Naive T Cell Receptor Repertoire With Human Aging. *Front Immunol*. 2018;9:1618.
186. Saule P, Trauet J, Dutriez V, Lekeux V, Dessaint JP, Labalette M. Accumulation of memory T cells from childhood to old age: central and effector memory cells in CD4(+) versus effector memory and terminally differentiated memory cells in CD8(+) compartment. *Mech Ageing Dev*. 2006;127(3):274-81.
187. Herndler-Brandstetter D, Landgraf K, Tzankov A, Jenewein B, Brunauer R, Laschober GT, et al. The impact of aging on memory T cell phenotype and function in the human bone marrow. *J Leukoc Biol*. 2012;91(2):197-205.
188. Mousset CM, Hobo W, Woestenenk R, Preijers F, Dolstra H, van der Waart AB. Comprehensive Phenotyping of T Cells Using Flow Cytometry. *Cytometry A*. 2019;95(6):647-54.
189. Gehad A, Teague JE, Matos TR, Huang V, Yang C, Watanabe R, et al. A primary role for human central memory cells in tissue immunosurveillance. *Blood Adv*. 2018;2(3):292-8.

190. Sallusto F, Lenig D, Forster R, Lipp M, Lanzavecchia A. Two subsets of memory T lymphocytes with distinct homing potentials and effector functions. *Nature*. 1999;401(6754):708-12.
191. Li M, Yao D, Zeng X, Kasakovski D, Zhang Y, Chen S, et al. Age related human T cell subset evolution and senescence. *Immun Ageing*. 2019;16:24.
192. Quinn KM, Fox A, Harland KL, Russ BE, Li J, Nguyen THO, et al. Age-Related Decline in Primary CD8(+) T Cell Responses Is Associated with the Development of Senescence in Virtual Memory CD8(+) T Cells. *Cell Rep*. 2018;23(12):3512-24.
193. Callender LA, Carroll EC, Garrod-Ketchley C, Schroth J, Bystrom J, Berryman V, et al. Altered Nutrient Uptake Causes Mitochondrial Dysfunction in Senescent CD8(+) EMRA T Cells During Type 2 Diabetes. *Front Aging*. 2021;2:681428.
194. Callender LA, Carroll EC, Beal RWJ, Chambers ES, Nourshargh S, Akbar AN, et al. Human CD8(+) EMRA T cells display a senescence-associated secretory phenotype regulated by p38 MAPK. *Aging Cell*. 2018;17(1).
195. Palacios-Pedrero MÁ, Jansen JM, Blume C, Stanislawski N, Jonczyk R, Molle A, et al. Signs of immunosenescence correlate with poor outcome of mRNA COVID-19 vaccination in older adults. *Nature Aging*. 2022;2(10):896-905.
196. Wagar LE, Gentleman B, Pircher H, McElhaney JE, Watts TH. Influenza-specific T cells from older people are enriched in the late effector subset and their presence inversely correlates with vaccine response. *PLoS One*. 2011;6(8):e23698.
197. Mueller SN, Ahmed R. High antigen levels are the cause of T cell exhaustion during chronic viral infection. *Proc Natl Acad Sci U S A*. 2009;106(21):8623-8.
198. Vardhana SA, Hwee MA, Berisa M, Wells DK, Yost KE, King B, et al. Impaired mitochondrial oxidative phosphorylation limits the self-renewal of T cells exposed to persistent antigen. *Nat Immunol*. 2020;21(9):1022-33.
199. Scharping NE, Rivadeneira DB, Menk AV, Vignali PDA, Ford BR, Rittenhouse NL, et al. Mitochondrial stress induced by continuous stimulation under hypoxia rapidly drives T cell exhaustion. *Nat Immunol*. 2021;22(2):205-15.
200. Callender LA, Carroll EC, Bober EA, Akbar AN, Solito E, Henson SM. Mitochondrial mass governs the extent of human T cell senescence. *Aging Cell*. 2020;19(2):e13067.
201. Wherry EJ, Ha SJ, Kaech SM, Haining WN, Sarkar S, Kalia V, et al. Molecular signature of CD8+ T cell exhaustion during chronic viral infection. *Immunity*. 2007;27(4):670-84.
202. Blackburn SD, Shin H, Haining WN, Zou T, Workman CJ, Polley A, et al. Coregulation of CD8+ T cell exhaustion by multiple inhibitory receptors during chronic viral infection. *Nat Immunol*. 2009;10(1):29-37.
203. Elyahu Y, Hekselman I, Eizenberg-Magar I, Berner O, Strominger I, Schiller M, et al. Aging promotes reorganization of the CD4 T cell landscape toward extreme regulatory and effector phenotypes. *Sci Adv*. 2019;5(8):eaaw8330.
204. Lee KA, Shin KS, Kim GY, Song YC, Bae EA, Kim IK, et al. Characterization of age-associated exhausted CD8(+) T cells defined by increased expression of Tim-3 and PD-1. *Aging Cell*. 2016;15(2):291-300.
205. Mogilenko DA, Shpynov O, Andhey PS, Arthur L, Swain A, Esaulova E, et al. Comprehensive Profiling of an Aging Immune System Reveals Clonal GZMK(+)

CD8(+) T Cells as Conserved Hallmark of Inflammaging. *Immunity*. 2021;54(1):99-115 e12.
206. Eaton SM, Burns EM, Kusser K, Randall TD, Haynes L. Age-related defects in CD4 T cell cognate helper function lead to reductions in humoral responses. *J Exp Med*. 2004;200(12):1613-22.
207. Yu M, Li G, Lee WW, Yuan M, Cui D, Weyand CM, et al. Signal inhibition by the dual-specific phosphatase 4 impairs T cell-dependent B-cell responses with age. *Proc Natl Acad Sci U S A*. 2012;109(15):E879-88.
208. Uciechowski P, Kahmann L, Plumakers B, Malavolta M, Mocchegiani E, Dedoussis G, et al. TH1 and TH2 cell polarization increases with aging and is modulated by zinc supplementation. *Exp Gerontol*. 2008;43(5):493-8.
209. Sakata-Kaneko S, Wakatsuki Y, Matsunaga Y, Usui T, Kita T. Altered Th1/Th2 commitment in human CD4+ T cells with ageing. *Clin Exp Immunol*. 2000;120(2):267-73.
210. van der Geest KSM, Kroesen BJ, Horst G, Abdulahad WH, Brouwer E, Boots AMH. Impact of Aging on the Frequency, Phenotype, and Function of CD161-Expressing T Cells. *Front Immunol*. 2018;9:752.
211. Mansfield AS, Nevala WK, Dronca RS, Leontovich AA, Shuster L, Markovic SN. Normal ageing is associated with an increase in Th2 cells, MCP-1 (CCL1) and RANTES (CCL5), with differences in sCD40L and PDGF-AA between sexes. *Clin Exp Immunol*. 2012;170(2):186-93.
212. Lim MA, Lee J, Park JS, Jhun JY, Moon YM, Cho ML, et al. Increased Th17 differentiation in aged mice is significantly associated with high IL-1beta level and low IL-2 expression. *Exp Gerontol*. 2014;49:55-62.
213. Schmitt V, Rink L, Uciechowski P. The Th17/Treg balance is disturbed during aging. *Exp Gerontol*. 2013;48(12):1379-86.
214. Nishioka T, Shimizu J, Iida R, Yamazaki S, Sakaguchi S. CD4+CD25+Foxp3+ T cells and CD4+CD25-Foxp3+ T cells in aged mice. *J Immunol*. 2006;176(11):6586-93.
215. Garg SK, Delaney C, Toubai T, Ghosh A, Reddy P, Banerjee R, et al. Aging is associated with increased regulatory T-cell function. *Aging Cell*. 2014;13(3):441-8.
216. Herati RS, Reuter MA, Dolfi DV, Mansfield KD, Aung H, Badwan OZ, et al. Circulating CXCR5+PD-1+ response predicts influenza vaccine antibody responses in young adults but not elderly adults. *J Immunol*. 2014;193(7):3528-37.
217. Sage PT, Tan CL, Freeman GJ, Haigis M, Sharpe AH. Defective TFH Cell Function and Increased TFR Cells Contribute to Defective Antibody Production in Aging. *Cell Rep*. 2015;12(2):163-71.
218. Lefebvre JS, Masters AR, Hopkins JW, Haynes L. Age-related impairment of humoral response to influenza is associated with changes in antigen specific T follicular helper cell responses. *Sci Rep*. 2016;6:25051.
219. Lumeng CN, Liu J, Geletka L, Delaney C, Delproposto J, Desai A, et al. Aging is associated with an increase in T cells and inflammatory macrophages in visceral adipose tissue. *J Immunol*. 2011;187(12):6208-16.
220. Nurieva RI, Chung Y, Martinez GJ, Yang XO, Tanaka S, Matskevitch TD, et al. Bcl6 mediates the development of T follicular helper cells. *Science*. 2009;325(5943):1001-5.

221. Pallikkuth S, de Armas LR, Rinaldi S, George VK, Pan L, Arheart KL, et al. Dysfunctional peripheral T follicular helper cells dominate in people with impaired influenza vaccine responses: Results from the FLORAH study. *PLoS Biol*. 2019;17(5):e3000257.
222. Almanan M, Raynor J, Ogunsulire I, Malyshkina A, Mukherjee S, Hummel SA, et al. IL-10-producing Tfh cells accumulate with age and link inflammation with age-related immune suppression. *Sci Adv*. 2020;6(31):eabb0806.
223. Li G, Yu M, Lee WW, Tsang M, Krishnan E, Weyand CM, et al. Decline in miR-181a expression with age impairs T cell receptor sensitivity by increasing DUSP6 activity. *Nat Med*. 2012;18(10):1518-24.
224. Griffith JF, Yeung DK, Ma HT, Leung JC, Kwok TC, Leung PC. Bone marrow fat content in the elderly: a reversal of sex difference seen in younger subjects. *J Magn Reson Imaging*. 2012;36(1):225-30.
225. Bilwani FA, Knight KL. Adipocyte-derived soluble factor(s) inhibits early stages of B lymphopoiesis. *J Immunol*. 2012;189(9):4379-86.
226. Tuljapurkar SR, McGuire TR, Brusnahan SK, Jackson JD, Garvin KL, Kessinger MA, et al. Changes in human bone marrow fat content associated with changes in hematopoietic stem cell numbers and cytokine levels with aging. *J Anat*. 2011;219(5):574-81.
227. Guerrettaz LM, Johnson SA, Cambier JC. Acquired hematopoietic stem cell defects determine B-cell repertoire changes associated with aging. *Proc Natl Acad Sci U S A*. 2008;105(33):11898-902.
228. Stephan RP, Reilly CR, Witte PL. Impaired Ability of Bone Marrow Stromal Cells to Support B-Lymphopoiesis With Age. *Blood*. 1998;91(1):75-88.
229. Helbling PM, Pineiro-Yanez E, Gerosa R, Boettcher S, Al-Shahrour F, Manz MG, et al. Global Transcriptomic Profiling of the Bone Marrow Stromal Microenvironment during Postnatal Development, Aging, and Inflammation. *Cell Rep*. 2019;29(10):3313-30 e4.
230. Labrie JE, 3rd, Sah AP, Allman DM, Cancro MP, Gerstein RM. Bone marrow microenvironmental changes underlie reduced RAG-mediated recombination and B cell generation in aged mice. *J Exp Med*. 2004;200(4):411-23.
231. Alter-Wolf S, Blomberg BB, Riley RL. Deviation of the B cell pathway in senescent mice is associated with reduced surrogate light chain expression and altered immature B cell generation, phenotype, and light chain expression. *J Immunol*. 2009;182(1):138-47.
232. Colonna-Romano G, Aquino A, Bulati M, Di Lorenzo G, Listi F, Vitello S, et al. Memory B cell subpopulations in the aged. *Rejuvenation Res*. 2006;9(1):149-52.
233. Tabibian-Keissar H, Hazanov L, Schiby G, Rosenthal N, Rakovsky A, Michaeli M, et al. Aging affects B-cell antigen receptor repertoire diversity in primary and secondary lymphoid tissues. *Eur J Immunol*. 2016;46(2):480-92.
234. Frasca D, Diaz A, Romero M, Landin AM, Blomberg BB. High TNF-alpha levels in resting B cells negatively correlate with their response. *Exp Gerontol*. 2014;54:116-22.
235. Le Gallou S, Zhou Z, Thai LH, Fritzen R, de Los Aires AV, Megret J, et al. A splenic IgM memory subset with antibacterial specificities is sustained from persistent mucosal responses. *J Exp Med*. 2018;215(8):2035-53.

236. Xu Z, Zan H, Pone EJ, Mai T, Casali P. Immunoglobulin class-switch DNA recombination: induction, targeting and beyond. *Nat Rev Immunol*. 2012;12(7):517-31.
237. Frasca D, Landin AM, Lechner SC, Ryan JG, Schwartz R, Riley RL, et al. Aging down-regulates the transcription factor E2A, activation-induced cytidine deaminase, and Ig class switch in human B cells. *J Immunol*. 2008;180(8):5283-90.
238. Shi Y, Yamazaki T, Okubo Y, Uehara Y, Sugane K, Agematsu K. Regulation of aged humoral immune defense against pneumococcal bacteria by IgM memory B cell. *J Immunol*. 2005;175(5):3262-7.
239. Martin V, Wu YC, Kipling D, Dunn-Walters DK. Age-related aspects of human IgM(+) B cell heterogeneity. *Ann N Y Acad Sci*. 2015;1362(1):153-63.
240. Frasca D, Van der Put E, Riley RL, Blomberg BB. Reduced Ig class switch in aged mice correlates with decreased E47 and activation-induced cytidine deaminase. *J Immunol*. 2004;172(4):2155-62.
241. Frasca D, Diaz A, Romero M, Blomberg BB. Human peripheral late/exhausted memory B cells express a senescent-associated secretory phenotype and preferentially utilize metabolic signaling pathways. *Exp Gerontol*. 2017;87(Pt A):113-20.
242. Duggal NA, Upton J, Phillips AC, Sapey E, Lord JM. An age-related numerical and functional deficit in CD19(+) CD24(hi) CD38(hi) B cells is associated with an increase in systemic autoimmunity. *Aging Cell*. 2013;12(5):873-81.
243. Hao Y, O'Neill P, Naradikian MS, Scholz JL, Cancro MP. A B-cell subset uniquely responsive to innate stimuli accumulates in aged mice. *Blood*. 2011;118(5):1294-304.
244. Rubtsov AV, Rubtsova K, Fischer A, Meehan RT, Gillis JZ, Kappler JW, et al. Toll-like receptor 7 (TLR7)-driven accumulation of a novel CD11c(+) B-cell population is important for the development of autoimmunity. *Blood*. 2011;118(5):1305-15.
245. Frasca D, Diaz A, Romero M, Blomberg BB. The generation of memory B cells is maintained, but the antibody response is not, in the elderly after repeated influenza immunizations. *Vaccine*. 2016;34(25):2834-40.
246. Goenka R, Scholz JL, Naradikian MS, Cancro MP. Memory B cells form in aged mice despite impaired affinity maturation and germinal center kinetics. *Exp Gerontol*. 2014;54:109-15.
247. Martinez-Guryn K, Hubert N, Frazier K, Urlass S, Musch MW, Ojeda P, et al. Small Intestine Microbiota Regulate Host Digestive and Absorptive Adaptive Responses to Dietary Lipids. *Cell Host Microbe*. 2018;23(4):458-69 e5.
248. Mardinoglu A, Shoaie S, Bergentall M, Ghaffari P, Zhang C, Larsson E, et al. The gut microbiota modulates host amino acid and glutathione metabolism in mice. *Mol Syst Biol*. 2015;11(10):834.
249. Soto-Martin EC, Warnke I, Farquharson FM, Christodoulou M, Horgan G, Derrien M, et al. Vitamin Biosynthesis by Human Gut Butyrate-Producing Bacteria and Cross-Feeding in Synthetic Microbial Communities. *mBio*. 2020;11(4).
250. Martens EC, Lowe EC, Chiang H, Pudlo NA, Wu M, McNulty NP, et al. Recognition and degradation of plant cell wall polysaccharides by two human gut symbionts. *PLoS Biol*. 2011;9(12):e1001221.

251. Erny D, Hrabe de Angelis AL, Jaitin D, Wieghofer P, Staszewski O, David E, et al. Host microbiota constantly control maturation and function of microglia in the CNS. *Nat Neurosci*. 2015;18(7):965-77.
252. Wesemann DR, Portuguese AJ, Meyers RM, Gallagher MP, Cluff-Jones K, Magee JM, et al. Microbial colonization influences early B-lineage development in the gut lamina propria. *Nature*. 2013;501(7465):112-5.
253. Claesson MJ, Jeffery IB, Conde S, Power SE, O'Connor EM, Cusack S, et al. Gut microbiota composition correlates with diet and health in the elderly. *Nature*. 2012;488(7410):178-84.
254. Huang WC, Chen YH, Chuang HL, Chiu CC, Huang CC. Investigation of the Effects of Microbiota on Exercise Physiological Adaption, Performance, and Energy Utilization Using a Gnotobiotic Animal Model. *Front Microbiol*. 2019;10:1906.
255. Lee SH, Yun Y, Kim SJ, Lee EJ, Chang Y, Ryu S, et al. Association between Cigarette Smoking Status and Composition of Gut Microbiota: Population-Based Cross-Sectional Study. *J Clin Med*. 2018;7(9).
256. Smith RP, Easson C, Lyle SM, Kapoor R, Donnelly CP, Davidson EJ, et al. Gut microbiome diversity is associated with sleep physiology in humans. *PLoS One*. 2019;14(10):e0222394.
257. Barandouzi ZA, Starkweather AR, Henderson WA, Gyamfi A, Cong XS. Altered Composition of Gut Microbiota in Depression: A Systematic Review. *Front Psychiatry*. 2020;11:541.
258. Sun L, Zhang X, Zhang Y, Zheng K, Xiang Q, Chen N, et al. Antibiotic-Induced Disruption of Gut Microbiota Alters Local Metabolomes and Immune Responses. *Front Cell Infect Microbiol*. 2019;9:99.
259. Qin J, Li R, Raes J, Arumugam M, Burgdorf KS, Manichanh C, et al. A human gut microbial gene catalogue established by metagenomic sequencing. *Nature*. 2010;464(7285):59-65.
260. Hergott CB, Roche AM, Tamashiro E, Clarke TB, Bailey AG, Laughlin A, et al. Peptidoglycan from the gut microbiota governs the lifespan of circulating phagocytes at homeostasis. *Blood*. 2016;127(20):2460-71.
261. Weaver LK, Minichino D, Biswas C, Chu N, Lee JJ, Bittinger K, et al. Microbiota-dependent signals are required to sustain TLR-mediated immune responses. *JCI Insight*. 2019;4(1).
262. Haverson K, Rehakova Z, Sinkora J, Sver L, Bailey M. Immune development in jejunal mucosa after colonization with selected commensal gut bacteria: a study in germ-free pigs. *Vet Immunol Immunopathol*. 2007;119(3-4):243-53.
263. Hapfelmeier S, Lawson MA, Slack E, Kirundi JK, Stoel M, Heikenwalder M, et al. Reversible microbial colonization of germ-free mice reveals the dynamics of IgA immune responses. *Science*. 2010;328(5986):1705-9.
264. Hrdy J, Alard J, Couturier-Maillard A, Boulard O, Boutillier D, Delacre M, et al. Lactobacillus reuteri 5454 and Bifidobacterium animalis ssp. lactis 5764 improve colitis while differentially impacting dendritic cells maturation and antimicrobial responses. *Sci Rep*. 2020;10(1):5345.
265. Gill HS, Rutherfurd KJ, Cross ML. Dietary probiotic supplementation enhances natural killer cell activity in the elderly: an investigation of age-related immunological changes. *J Clin Immunol*. 2001;21(4):264-71.

266. Maneerat S, Lehtinen MJ, Childs CE, Forssten SD, Alhoniemi E, Tiphaine M, et al. Consumption of Bifidobacterium lactis Bi-07 by healthy elderly adults enhances phagocytic activity of monocytes and granulocytes. *J Nutr Sci*. 2013;2:e44.
267. Goto Y, Panea C, Nakato G, Cebula A, Lee C, Diez MG, et al. Segmented filamentous bacteria antigens presented by intestinal dendritic cells drive mucosal Th17 cell differentiation. *Immunity*. 2014;40(4):594-607.
268. Ramakrishna C, Kujawski M, Chu H, Li L, Mazmanian SK, Cantin EM. Bacteroides fragilis polysaccharide A induces IL-10 secreting B and T cells that prevent viral encephalitis. *Nat Commun*. 2019;10(1):2153.
269. Round JL, Mazmanian SK. Inducible Foxp3+ regulatory T-cell development by a commensal bacterium of the intestinal microbiota. *Proc Natl Acad Sci U S A*. 2010;107(27):12204-9.
270. Smits HH, van Beelen AJ, Hessle C, Westland R, de Jong E, Soeteman E, et al. Commensal Gram-negative bacteria prime human dendritic cells for enhanced IL-23 and IL-27 expression and enhanced Th1 development. *Eur J Immunol*. 2004;34(5):1371-80.
271. Lecuyer E, Rakotobe S, Lengline-Garnier H, Lebreton C, Picard M, Juste C, et al. Segmented filamentous bacterium uses secondary and tertiary lymphoid tissues to induce gut IgA and specific T helper 17 cell responses. *Immunity*. 2014;40(4):608-20.
272. Conway J, Rees NP, Duggal NA. Ageing of the Gut Microbiome and Its Potential Contribution Towards Immunesenescence and Inflammaging. Gut Microbiota in Aging and Chronic Diseases. Healthy Ageing and Longevity2023. p. 41-63.
273. Boullier S, Tanguy M, Kadaoui KA, Caubet C, Sansonetti P, Corthesy B, et al. Secretory IgA-mediated neutralization of Shigella flexneri prevents intestinal tissue destruction by down-regulating inflammatory circuits. *J Immunol*. 2009;183(9):5879-85.
274. Chu H, Mazmanian SK. Innate immune recognition of the microbiota promotes host-microbial symbiosis. *Nat Immunol*. 2013;14(7):668-75.
275. Wlodarska M, Thaiss CA, Nowarski R, Henao-Mejia J, Zhang JP, Brown EM, et al. NLRP6 inflammasome orchestrates the colonic host-microbial interface by regulating goblet cell mucus secretion. *Cell*. 2014;156(5):1045-59.
276. Birchenough GM, Nystrom EE, Johansson ME, Hansson GC. A sentinel goblet cell guards the colonic crypt by triggering Nlrp6-dependent Muc2 secretion. *Science*. 2016;352(6293):1535-42.
277. Kim CH. Immune regulation by microbiome metabolites. *Immunology*. 2018;154(2):220-9.
278. Parada Venegas D, De la Fuente MK, Landskron G, Gonzalez MJ, Quera R, Dijkstra G, et al. Short Chain Fatty Acids (SCFAs)-Mediated Gut Epithelial and Immune Regulation and Its Relevance for Inflammatory Bowel Diseases. *Front Immunol*. 2019;10:277.
279. Schulthess J, Pandey S, Capitani M, Rue-Albrecht KC, Arnold I, Franchini F, et al. The Short Chain Fatty Acid Butyrate Imprints an Antimicrobial Program in Macrophages. *Immunity*. 2019;50(2):432-45 e7.
280. Huang C, Du W, Ni Y, Lan G, Shi G. The effect of short-chain fatty acids on M2 macrophages polarization in vitro and in vivo. *Clin Exp Immunol*. 2022;207(1):53-64.

281. Vinolo MA, Ferguson GJ, Kulkarni S, Damoulakis G, Anderson K, Bohlooly YM, et al. SCFAs induce mouse neutrophil chemotaxis through the GPR43 receptor. *PLoS One*. 2011;6(6):e21205.
282. Sina C, Gavrilova O, Forster M, Till A, Derer S, Hildebrand F, et al. G protein-coupled receptor 43 is essential for neutrophil recruitment during intestinal inflammation. *J Immunol*. 2009;183(11):7514-22.
283. Nastasi C, Fredholm S, Willerslev-Olsen A, Hansen M, Bonefeld CM, Geisler C, et al. Butyrate and propionate inhibit antigen-specific CD8(+) T cell activation by suppressing IL-12 production by antigen-presenting cells. *Sci Rep*. 2017;7(1):14516.
284. Zhang M, Zhou Q, Dorfman RG, Huang X, Fan T, Zhang H, et al. Butyrate inhibits interleukin-17 and generates Tregs to ameliorate colorectal colitis in rats. *BMC Gastroenterol*. 2016;16(1):84.
285. Furusawa Y, Obata Y, Fukuda S, Endo TA, Nakato G, Takahashi D, et al. Commensal microbe-derived butyrate induces the differentiation of colonic regulatory T cells. *Nature*. 2013;504(7480):446-50.
286. Park J, Kim M, Kang SG, Jannasch AH, Cooper B, Patterson J, et al. Short-chain fatty acids induce both effector and regulatory T cells by suppression of histone deacetylases and regulation of the mTOR-S6K pathway. *Mucosal Immunol*. 2015;8(1):80-93.
287. Rosser EC, Piper CJM, Matei DE, Blair PA, Rendeiro AF, Orford M, et al. Microbiota-Derived Metabolites Suppress Arthritis by Amplifying Aryl-Hydrocarbon Receptor Activation in Regulatory B Cells. *Cell Metab*. 2020;31(4):837-51 e10.
288. Kim M, Qie Y, Park J, Kim CH. Gut Microbial Metabolites Fuel Host Antibody Responses. *Cell Host Microbe*. 2016;20(2):202-14.
289. Feng Y, Wang Y, Wang P, Huang Y, Wang F. Short-Chain Fatty Acids Manifest Stimulative and Protective Effects on Intestinal Barrier Function Through the Inhibition of NLRP3 Inflammasome and Autophagy. *Cell Physiol Biochem*. 2018;49(1):190-205.
290. Guzior DV, Quinn RA. Review: microbial transformations of human bile acids. *Microbiome*. 2021;9(1):140.
291. Chen ML, Takeda K, Sundrud MS. Emerging roles of bile acids in mucosal immunity and inflammation. *Mucosal Immunol*. 2019;12(4):851-61.
292. Vavassori P, Mencarelli A, Renga B, Distrutti E, Fiorucci S. The bile acid receptor FXR is a modulator of intestinal innate immunity. *J Immunol*. 2009;183(10):6251-61.
293. Gadaleta RM, van Erpecum KJ, Oldenburg B, Willemsen EC, Renooij W, Murzilli S, et al. Farnesoid X receptor activation inhibits inflammation and preserves the intestinal barrier in inflammatory bowel disease. *Gut*. 2011;60(4):463-72.
294. Sinha SR, Haileselassie Y, Nguyen LP, Tropini C, Wang M, Becker LS, et al. Dysbiosis-Induced Secondary Bile Acid Deficiency Promotes Intestinal Inflammation. *Cell Host Microbe*. 2020;27(4):659-70 e5.
295. Guo C, Xie S, Chi Z, Zhang J, Liu Y, Zhang L, et al. Bile Acids Control Inflammation and Metabolic Disorder through Inhibition of NLRP3 Inflammasome. *Immunity*. 2016;45(4):802-16.

296. Lajczak-McGinley NK, Porru E, Fallon CM, Smyth J, Curley C, McCarron PA, et al. The secondary bile acids, ursodeoxycholic acid and lithocholic acid, protect against intestinal inflammation by inhibition of epithelial apoptosis. *Physiol Rep*. 2020;8(12):e14456.
297. Golden JM, Escobar OH, Nguyen MVL, Mallicote MU, Kavarian P, Frey MR, et al. Ursodeoxycholic acid protects against intestinal barrier breakdown by promoting enterocyte migration via EGFR- and COX-2-dependent mechanisms. *Am J Physiol Gastrointest Liver Physiol*. 2018;315(2):G259-G71.
298. Wammers M, Schupp AK, Bode JG, Ehlting C, Wolf S, Deenen R, et al. Reprogramming of pro-inflammatory human macrophages to an anti-inflammatory phenotype by bile acids. *Sci Rep*. 2018;8(1):255.
299. Wang L, Gong Z, Zhang X, Zhu F, Liu Y, Jin C, et al. Gut microbial bile acid metabolite skews macrophage polarization and contributes to high-fat diet-induced colonic inflammation. *Gut Microbes*. 2020;12(1):1-20.
300. Ichikawa R, Takayama T, Yoneno K, Kamada N, Kitazume MT, Higuchi H, et al. Bile acids induce monocyte differentiation toward interleukin-12 hypo-producing dendritic cells via a TGR5-dependent pathway. *Immunology*. 2012;136(2):153-62.
301. Hu J, Wang C, Huang X, Yi S, Pan S, Zhang Y, et al. Gut microbiota-mediated secondary bile acids regulate dendritic cells to attenuate autoimmune uveitis through TGR5 signaling. *Cell Rep*. 2021;36(12):109726.
302. Campbell C, McKenney PT, Konstantinovsky D, Isaeva OI, Schizas M, Verter J, et al. Bacterial metabolism of bile acids promotes generation of peripheral regulatory T cells. *Nature*. 2020;581(7809):475-9.
303. Carriche GM, Almeida L, Stuve P, Velasquez L, Dhillon-LaBrooy A, Roy U, et al. Regulating T-cell differentiation through the polyamine spermidine. *J Allergy Clin Immunol*. 2021;147(1):335-48 e11.
304. Zhang H, Alsaleh G, Feltham J, Sun Y, Napolitano G, Riffelmacher T, et al. Polyamines Control eIF5A Hypusination, TFEB Translation, and Autophagy to Reverse B Cell Senescence. *Mol Cell*. 2019;76(1):110-25 e9.
305. Ye J, Qiu J, Bostick JW, Ueda A, Schjerven H, Li S, et al. The Aryl Hydrocarbon Receptor Preferentially Marks and Promotes Gut Regulatory T Cells. *Cell Rep*. 2017;21(8):2277-90.
306. Wu K, Yuan Y, Yu H, Dai X, Wang S, Sun Z, et al. The gut microbial metabolite trimethylamine N-oxide aggravates GVHD by inducing M1 macrophage polarization in mice. *Blood*. 2020;136(4):501-15.
307. Krishnan S, Ding Y, Saeidi N, Choi M, Sridharan GV, Sherr DH, et al. Gut Microbiota-Derived Tryptophan Metabolites Modulate Inflammatory Response in Hepatocytes and Macrophages. *Cell Rep*. 2019;28(12):3285.
308. Macia L, Nanan R, Hosseini-Beheshti E, Grau GE. Host- and Microbiota-Derived Extracellular Vesicles, Immune Function, and Disease Development. *Int J Mol Sci*. 2019;21(1).
309. Schetters STT, Jong WSP, Horrevorts SK, Kruijssen LJW, Engels S, Stolk D, et al. Outer membrane vesicles engineered to express membrane-bound antigen program dendritic cells for cross-presentation to CD8(+) T cells. *Acta Biomater*. 2019;91:248-57.
310. Kang CS, Ban M, Choi EJ, Moon HG, Jeon JS, Kim DK, et al. Extracellular vesicles derived from gut microbiota, especially Akkermansia muciniphila,

protect the progression of dextran sulfate sodium-induced colitis. *PLoS One*. 2013;8(10):e76520.
311. Shen Y, Giardino Torchia ML, Lawson GW, Karp CL, Ashwell JD, Mazmanian SK. Outer membrane vesicles of a human commensal mediate immune regulation and disease protection. *Cell Host Microbe*. 2012;12(4):509-20.
312. Cecil JD, O'Brien-Simpson NM, Lenzo JC, Holden JA, Singleton W, Perez-Gonzalez A, et al. Outer Membrane Vesicles Prime and Activate Macrophage Inflammasomes and Cytokine Secretion In Vitro and In Vivo. *Front Immunol*. 2017;8:1017.
313. Anfossi S, Calin GA. Gut microbiota: a new player in regulating immune- and chemo-therapy efficacy. *Cancer Drug Resist*. 2020;3(3):356-70.
314. Biagi E, Franceschi C, Rampelli S, Severgnini M, Ostan R, Turroni S, et al. Gut Microbiota and Extreme Longevity. *Curr Biol*. 2016;26(11):1480-5.
315. Salazar N, Arboleya S, Fernandez-Navarro T, de Los Reyes-Gavilan CG, Gonzalez S, Gueimonde M. Age-Associated Changes in Gut Microbiota and Dietary Components Related with the Immune System in Adulthood and Old Age: A Cross-Sectional Study. *Nutrients*. 2019;11(8).
316. Santoro A, Ostan R, Candela M, Biagi E, Brigidi P, Capri M, et al. Gut microbiota changes in the extreme decades of human life: a focus on centenarians. *Cell Mol Life Sci*. 2018;75(1):129-48.
317. Tavella T, Rampelli S, Guidarelli G, Bazzocchi A, Gasperini C, Pujos-Guillot E, et al. Elevated gut microbiome abundance of Christensenellaceae, Porphyromonadaceae and Rikenellaceae is associated with reduced visceral adipose tissue and healthier metabolic profile in Italian elderly. *Gut Microbes*. 2021;13(1):1-19.
318. Claesson MJ, Cusack S, O'Sullivan O, Greene-Diniz R, de Weerd H, Flannery E, et al. Composition, variability, and temporal stability of the intestinal microbiota of the elderly. *Proc Natl Acad Sci U S A*. 2011;108 Suppl 1(Suppl 1):4586-91.
319. Rampelli S, Candela M, Turroni S, Biagi E, Collino S, Franceschi C, et al. Functional metagenomic profiling of intestinal microbiome in extreme ageing. *Aging (Albany NY)*. 2013;5(12):902-12.
320. Conway J, N AD. Ageing of the gut microbiome: Potential influences on immune senescence and inflammageing. *Ageing Res Rev*. 2021;68:101323.
321. Blacher E, Levy M, Tatirovsky E, Elinav E. Microbiome-Modulated Metabolites at the Interface of Host Immunity. *J Immunol*. 2017;198(2):572-80.
322. Langsetmo L, Johnson A, Demmer RT, Fino N, Orwoll ES, Ensrud KE, et al. The Association between Objectively Measured Physical Activity and the Gut Microbiome among Older Community Dwelling Men. *J Nutr Health Aging*. 2019;23(6):538-46.
323. Mitchell EL, Davis AT, Brass K, Dendinger M, Barner R, Gharaibeh R, et al. Reduced Intestinal Motility, Mucosal Barrier Function, and Inflammation in Aged Monkeys. *J Nutr Health Aging*. 2017;21(4):354-61.
324. Dethlefsen L, Relman DA. Incomplete recovery and individualized responses of the human distal gut microbiota to repeated antibiotic perturbation. *Proc Natl Acad Sci U S A*. 2011;108 Suppl 1(Suppl 1):4554-61.
325. Grayson MH, Camarda LE, Hussain SA, Zemple SJ, Hayward M, Lam V, et al. Intestinal Microbiota Disruption Reduces Regulatory T Cells and Increases

Respiratory Viral Infection Mortality Through Increased IFNgamma Production. *Front Immunol*. 2018;9:1587.
326. Groves HT, Cuthbertson L, James P, Moffatt MF, Cox MJ, Tregoning JS. Respiratory Disease following Viral Lung Infection Alters the Murine Gut Microbiota. *Front Immunol*. 2018;9:182.
327. Ticinesi A, Nouvenne A, Cerundolo N, Catania P, Prati B, Tana C, et al. Gut Microbiota, Muscle Mass and Function in Aging: A Focus on Physical Frailty and Sarcopenia. *Nutrients*. 2019;11(7).
328. Buford TW, Carter CS, VanDerPol WJ, Chen D, Lefkowitz EJ, Eipers P, et al. Composition and richness of the serum microbiome differ by age and link to systemic inflammation. *Geroscience*. 2018;40(3):257-68.
329. Picca A, Fanelli F, Calvani R, Mule G, Pesce V, Sisto A, et al. Gut Dysbiosis and Muscle Aging: Searching for Novel Targets against Sarcopenia. *Mediators Inflamm*. 2018;2018:7026198.
330. Jackson MA, Jeffery IB, Beaumont M, Bell JT, Clark AG, Ley RE, et al. Signatures of early frailty in the gut microbiota. *Genome Med*. 2016;8(1):8.
331. Lahiri S, Kim H, Garcia-Perez I, Reza MM, Martin KA, Kundu P, et al. The gut microbiota influences skeletal muscle mass and function in mice. *Sci Transl Med*. 2019;11(502).
332. Walsh ME, Bhattacharya A, Sataranatarajan K, Qaisar R, Sloane L, Rahman MM, et al. The histone deacetylase inhibitor butyrate improves metabolism and reduces muscle atrophy during aging. *Aging Cell*. 2015;14(6):957-70.
333. Everhov AH, Halfvarson J, Myrelid P, Sachs MC, Nordenvall C, Soderling J, et al. Incidence and Treatment of Patients Diagnosed With Inflammatory Bowel Diseases at 60 Years or Older in Sweden. *Gastroenterology*. 2018;154(3):518-28 e15.
334. Gevers D, Kugathasan S, Denson LA, Vazquez-Baeza Y, Van Treuren W, Ren B, et al. The treatment-naive microbiome in new-onset Crohn's disease. *Cell Host Microbe*. 2014;15(3):382-92.
335. Zhang X, Zhang D, Jia H, Feng Q, Wang D, Liang D, et al. The oral and gut microbiomes are perturbed in rheumatoid arthritis and partly normalized after treatment. *Nat Med*. 2015;21(8):895-905.
336. Wu HJ, Ivanov, II, Darce J, Hattori K, Shima T, Umesaki Y, et al. Gut-residing segmented filamentous bacteria drive autoimmune arthritis via T helper 17 cells. *Immunity*. 2010;32(6):815-27.
337. Teng F, Klinger CN, Felix KM, Bradley CP, Wu E, Tran NL, et al. Gut Microbiota Drive Autoimmune Arthritis by Promoting Differentiation and Migration of Peyer's Patch T Follicular Helper Cells. *Immunity*. 2016;44(4):875-88.
338. Maffei VJ, Kim S, Blanchard Et, Luo M, Jazwinski SM, Taylor CM, et al. Biological Aging and the Human Gut Microbiota. *J Gerontol A Biol Sci Med Sci*. 2017;72(11):1474-82.
339. Odamaki T, Kato K, Sugahara H, Hashikura N, Takahashi S, Xiao JZ, et al. Age-related changes in gut microbiota composition from newborn to centenarian: a cross-sectional study. *BMC Microbiol*. 2016;16:90.
340. Donato AJ, Magerko KA, Lawson BR, Durrant JR, Lesniewski LA, Seals DR. SIRT-1 and vascular endothelial dysfunction with ageing in mice and humans. *J Physiol*. 2011;589(Pt 18):4545-54.

341. Brunt VE, Gioscia-Ryan RA, Richey JJ, Zigler MC, Cuevas LM, Gonzalez A, et al. Suppression of the gut microbiome ameliorates age-related arterial dysfunction and oxidative stress in mice. *J Physiol*. 2019;597(9):2361-78.
342. Karlsson FH, Fak F, Nookaew I, Tremaroli V, Fagerberg B, Petranovic D, et al. Symptomatic atherosclerosis is associated with an altered gut metagenome. *Nat Commun*. 2012;3:1245.
343. Wang Z, Klipfell E, Bennett BJ, Koeth R, Levison BS, Dugar B, et al. Gut flora metabolism of phosphatidylcholine promotes cardiovascular disease. *Nature*. 2011;472(7341):57-63.
344. Minter MR, Zhang C, Leone V, Ringus DL, Zhang X, Oyler-Castrillo P, et al. Antibiotic-induced perturbations in gut microbial diversity influences neuro-inflammation and amyloidosis in a murine model of Alzheimer's disease. *Sci Rep*. 2016;6:30028.
345. Harach T, Marungruang N, Duthilleul N, Cheatham V, Mc Coy KD, Frisoni G, et al. Reduction of Abeta amyloid pathology in APPPS1 transgenic mice in the absence of gut microbiota. *Sci Rep*. 2017;7:41802.
346. Zhan X, Stamova B, Jin LW, DeCarli C, Phinney B, Sharp FR. Gram-negative bacterial molecules associate with Alzheimer disease pathology. *Neurology*. 2016;87(22):2324-32.
347. Vogt NM, Kerby RL, Dill-McFarland KA, Harding SJ, Merluzzi AP, Johnson SC, et al. Gut microbiome alterations in Alzheimer's disease. *Sci Rep*. 2017;7(1):13537.
348. Cattaneo A, Cattane N, Galluzzi S, Provasi S, Lopizzo N, Festari C, et al. Association of brain amyloidosis with pro-inflammatory gut bacterial taxa and peripheral inflammation markers in cognitively impaired elderly. *Neurobiol Aging*. 2017;49:60-8.
349. Kong F, Deng F, Li Y, Zhao J. Identification of gut microbiome signatures associated with longevity provides a promising modulation target for healthy aging. *Gut Microbes*. 2019;10(2):210-5.
350. Kim BS, Choi CW, Shin H, Jin SP, Bae JS, Han M, et al. Comparison of the Gut Microbiota of Centenarians in Longevity Villages of South Korea with Those of Other Age Groups. *J Microbiol Biotechnol*. 2019;29(3):429-40.
351. Chelakkot C, Ghim J, Ryu SH. Mechanisms regulating intestinal barrier integrity and its pathological implications. *Exp Mol Med*. 2018;50(8):1-9.
352. Miao W, Wu X, Wang K, Wang W, Wang Y, Li Z, et al. Sodium Butyrate Promotes Reassembly of Tight Junctions in Caco-2 Monolayers Involving Inhibition of MLCK/MLC2 Pathway and Phosphorylation of PKCbeta2. *Int J Mol Sci*. 2016;17(10).
353. Liang L, Liu L, Zhou W, Yang C, Mai G, Li H, et al. Gut microbiota-derived butyrate regulates gut mucus barrier repair by activating the macrophage/WNT/ERK signaling pathway. *Clin Sci (Lond)*. 2022;136(4):291-307.
354. Yue X, Wen S, Long-Kun D, Man Y, Chang S, Min Z, et al. Three important short-chain fatty acids (SCFAs) attenuate the inflammatory response induced by 5-FU and maintain the integrity of intestinal mucosal tight junction. *BMC Immunol*. 2022;23(1):19.

355. Pearce SC, Weber GJ, van Sambeek DM, Soares JW, Racicot K, Breault DT. Intestinal enteroids recapitulate the effects of short-chain fatty acids on the intestinal epithelium. *PLoS One*. 2020;15(4):e0230231.
356. Ma X, Fan PX, Li LS, Qiao SY, Zhang GL, Li DF. Butyrate promotes the recovering of intestinal wound healing through its positive effect on the tight junctions. *J Anim Sci*. 2012;90 Suppl 4:266-8.
357. Wu W, Sun M, Chen F, Cao AT, Liu H, Zhao Y, et al. Microbiota metabolite short-chain fatty acid acetate promotes intestinal IgA response to microbiota which is mediated by GPR43. *Mucosal Immunol*. 2017;10(4):946-56.
358. Zhao Y, Chen F, Wu W, Sun M, Bilotta AJ, Yao S, et al. GPR43 mediates microbiota metabolite SCFA regulation of antimicrobial peptide expression in intestinal epithelial cells via activation of mTOR and STAT3. *Mucosal Immunol*. 2018;11(3):752-62.
359. Mantis NJ, Rol N, Corthesy B. Secretory IgA's complex roles in immunity and mucosal homeostasis in the gut. *Mucosal Immunol*. 2011;4(6):603-11.
360. Elderman M, Sovran B, Hugenholtz F, Graversen K, Huijskes M, Houtsma E, et al. The effect of age on the intestinal mucus thickness, microbiota composition and immunity in relation to sex in mice. *PLoS One*. 2017;12(9):e0184274.
361. Tran L, Greenwood-Van Meerveld B. Age-associated remodeling of the intestinal epithelial barrier. *J Gerontol A Biol Sci Med Sci*. 2013;68(9):1045-56.
362. Wilson QN, Wells M, Davis AT, Sherrill C, Tsilimigras MCB, Jones RB, et al. Greater Microbial Translocation and Vulnerability to Metabolic Disease in Healthy Aged Female Monkeys. *Sci Rep*. 2018;8(1):11373.
363. Luchetti MM, Ciccia F, Avellini C, Benfaremo D, Rizzo A, Spadoni T, et al. Gut epithelial impairment, microbial translocation and immune system activation in inflammatory bowel disease-associated spondyloarthritis. *Rheumatology (Oxford)*. 2021;60(1):92-102.
364. Chang J, Leong RW, Wasinger VC, Ip M, Yang M, Phan TG. Impaired Intestinal Permeability Contributes to Ongoing Bowel Symptoms in Patients With Inflammatory Bowel Disease and Mucosal Healing. *Gastroenterology*. 2017;153(3):723-31 e1.
365. Audo R, Sanchez P, Rivière B, Mielle J, Tan J, Lukas C, et al. Rheumatoid arthritis is associated with increased gut permeability and bacterial translocation that are reversed by inflammation control. *Rheumatology*. 2022.
366. Brenchley JM, Price DA, Schacker TW, Asher TE, Silvestri G, Rao S, et al. Microbial translocation is a cause of systemic immune activation in chronic HIV infection. *Nat Med*. 2006;12(12):1365-71.
367. Klatt NR, Harris LD, Vinton CL, Sung H, Briant JA, Tabb B, et al. Compromised gastrointestinal integrity in pigtail macaques is associated with increased microbial translocation, immune activation, and IL-17 production in the absence of SIV infection. *Mucosal Immunol*. 2010;3(4):387-98.
368. Younas M, Psomas C, Reynes C, Cezar R, Kundura L, Portales P, et al. Microbial Translocation Is Linked to a Specific Immune Activation Profile in HIV-1-Infected Adults With Suppressed Viremia. *Front Immunol*. 2019;10:2185.
369. Conlon MA, Bird AR. The impact of diet and lifestyle on gut microbiota and human health. *Nutrients*. 2014;7(1):17-44.
370. Costabile A, Klinder A, Fava F, Napolitano A, Fogliano V, Leonard C, et al. Whole-grain wheat breakfast cereal has a prebiotic effect on the human gut

microbiota: a double-blind, placebo-controlled, crossover study. *Br J Nutr*. 2008;99(1):110-20.
371. David LA, Maurice CF, Carmody RN, Gootenberg DB, Button JE, Wolfe BE, et al. Diet rapidly and reproducibly alters the human gut microbiome. *Nature*. 2014;505(7484):559-63.
372. Wu GD, Chen J, Hoffmann C, Bittinger K, Chen YY, Keilbaugh SA, et al. Linking long-term dietary patterns with gut microbial enterotypes. *Science*. 2011;334(6052):105-8.
373. Lecomte V, Kaakoush NO, Maloney CA, Raipuria M, Huinao KD, Mitchell HM, et al. Changes in gut microbiota in rats fed a high fat diet correlate with obesity-associated metabolic parameters. *PLoS One*. 2015;10(5):e0126931.
374. Caesar R, Tremaroli V, Kovatcheva-Datchary P, Cani PD, Backhed F. Crosstalk between Gut Microbiota and Dietary Lipids Aggravates WAT Inflammation through TLR Signaling. *Cell Metab*. 2015;22(4):658-68.
375. Chassaing B, Koren O, Goodrich JK, Poole AC, Srinivasan S, Ley RE, et al. Dietary emulsifiers impact the mouse gut microbiota promoting colitis and metabolic syndrome. *Nature*. 2015;519(7541):92-6.
376. Suez J, Korem T, Zeevi D, Zilberman-Schapira G, Thaiss CA, Maza O, et al. Artificial sweeteners induce glucose intolerance by altering the gut microbiota. *Nature*. 2014;514(7521):181-6.
377. Dorrington N, Fallaize R, Hobbs DA, Weech M, Lovegrove JA. A Review of Nutritional Requirements of Adults Aged >/=65 Years in the UK. *J Nutr*. 2020;150(9):2245-56.
378. Drewnowski A, Shultz JM. Impact of aging on eating behaviors, food choices, nutrition, and health status. *J Nutr Health Aging*. 2001;5(2):75-9.
379. Leslie W, Hankey C. Aging, Nutritional Status and Health. *Healthcare (Basel)*. 2015;3(3):648-58.
380. Favaro-Moreira NC, Krausch-Hofmann S, Matthys C, Vereecken C, Vanhauwaert E, Declercq A, et al. Risk Factors for Malnutrition in Older Adults: A Systematic Review of the Literature Based on Longitudinal Data. *Adv Nutr*. 2016;7(3):507-22.
381. Ghosh TS, Rampelli S, Jeffery IB, Santoro A, Neto M, Capri M, et al. Mediterranean diet intervention alters the gut microbiome in older people reducing frailty and improving health status: the NU-AGE 1-year dietary intervention across five European countries. *Gut*. 2020;69(7):1218-28.
382. Valls-Pedret C, Sala-Vila A, Serra-Mir M, Corella D, de la Torre R, Martinez-Gonzalez MA, et al. Mediterranean Diet and Age-Related Cognitive Decline: A Randomized Clinical Trial. *JAMA Intern Med*. 2015;175(7):1094-103.
383. Estruch R, Ros E, Salas-Salvado J, Covas MI, Corella D, Aros F, et al. Primary Prevention of Cardiovascular Disease with a Mediterranean Diet Supplemented with Extra-Virgin Olive Oil or Nuts. *N Engl J Med*. 2018;378(25):e34.
384. Toledo E, Salas-Salvado J, Donat-Vargas C, Buil-Cosiales P, Estruch R, Ros E, et al. Mediterranean Diet and Invasive Breast Cancer Risk Among Women at High Cardiovascular Risk in the PREDIMED Trial: A Randomized Clinical Trial. *JAMA Intern Med*. 2015;175(11):1752-60.
385. Garcia-Mantrana I, Selma-Royo M, Alcantara C, Collado MC. Shifts on Gut Microbiota Associated to Mediterranean Diet Adherence and Specific Dietary Intakes on General Adult Population. *Front Microbiol*. 2018;9:890.

386. Camargo A, Delgado-Lista J, Garcia-Rios A, Cruz-Teno C, Yubero-Serrano EM, Perez-Martinez P, et al. Expression of proinflammatory, proatherogenic genes is reduced by the Mediterranean diet in elderly people. *Br J Nutr*. 2012;108(3):500-8.
387. Mena MP, Sacanella E, Vazquez-Agell M, Morales M, Fito M, Escoda R, et al. Inhibition of circulating immune cell activation: a molecular antiinflammatory effect of the Mediterranean diet. *Am J Clin Nutr*. 2009;89(1):248-56.
388. Clements SJ, Maijo M, Ivory K, Nicoletti C, Carding SR. Age-Associated Decline in Dendritic Cell Function and the Impact of Mediterranean Diet Intervention in Elderly Subjects. *Front Nutr*. 2017;4:65.
389. Maijo M, Ivory K, Clements SJ, Dainty JR, Jennings A, Gillings R, et al. One-Year Consumption of a Mediterranean-Like Dietary Pattern With Vitamin D3 Supplements Induced Small Scale but Extensive Changes of Immune Cell Phenotype, Co-receptor Expression and Innate Immune Responses in Healthy Elderly Subjects: Results From the United Kingdom Arm of the NU-AGE Trial. *Front Physiol*. 2018;9:997.
390. Stebegg M, Silva-Cayetano A, Innocentin S, Jenkins TP, Cantacessi C, Gilbert C, et al. Heterochronic faecal transplantation boosts gut germinal centres in aged mice. *Nat Commun*. 2019;10(1):2443.
391. Ware J, Jr., Kosinski M, Keller SD. A 12-Item Short-Form Health Survey: construction of scales and preliminary tests of reliability and validity. *Med Care*. 1996;34(3):220-33.
392. Buysse DJ, Reynolds CF, 3rd, Monk TH, Berman SR, Kupfer DJ. The Pittsburgh Sleep Quality Index: a new instrument for psychiatric practice and research. *Psychiatry Res*. 1989;28(2):193-213.
393. Zigmond AS, Snaith RP. The hospital anxiety and depression scale. *Acta Psychiatr Scand*. 1983;67(6):361-70.
394. Mulligan AA, Luben RN, Bhaniani A, Parry-Smith DJ, O'Connor L, Khawaja AP, et al. A new tool for converting food frequency questionnaire data into nutrient and food group values: FETA research methods and availability. *BMJ Open*. 2014;4(3):e004503.
395. Kim S, Haines PS, Siega-Riz AM, Popkin BM. The Diet Quality Index-International (DQI-I) provides an effective tool for cross-national comparison of diet quality as illustrated by China and the United States. *J Nutr*. 2003;133(11):3476-84.
396. Martinez-Gonzalez MA, Garcia-Arellano A, Toledo E, Salas-Salvado J, Buil-Cosiales P, Corella D, et al. A 14-item Mediterranean diet assessment tool and obesity indexes among high-risk subjects: the PREDIMED trial. *PLoS One*. 2012;7(8):e43134.
397. Duggal NA, Upton J, Phillips AC, Hampson P, Lord JM. Depressive symptoms post hip fracture in older adults are associated with phenotypic and functional alterations in T cells. *Immun Ageing*. 2014;11(1):25.
398. Pelchen-Matthews A, Parsons IJ, Marsh M. Phorbol ester-induced downregulation of CD4 is a multistep process involving dissociation from p56lck, increased association with clathrin-coated pits, and altered endosomal sorting. *J Exp Med*. 1993;178(4):1209-22.

399. Foster MA, Bentley C, Hazeldine J, Acharjee A, Nahman O, Shen-Orr SS, et al. Investigating the potential of a prematurely aged immune phenotype in severely injured patients as predictor of risk of sepsis. *Immun Ageing*. 2022;19(1):60.
400. Alpert A, Pickman Y, Leipold M, Rosenberg-Hasson Y, Ji X, Gaujoux R, et al. A clinically meaningful metric of immune age derived from high-dimensional longitudinal monitoring. *Nat Med*. 2019;25(3):487-95.
401. Yu G, He QY. ReactomePA: an R/Bioconductor package for reactome pathway analysis and visualization. *Mol Biosyst*. 2016;12(2):477-9.
402. Carlson M. org.Hs.eg.db: Genome wide annotation for Human, primarily based on mapping using Entrez Gene identifiers. 3.17 ed2019.
403. Shaw AG, Sim K, Powell E, Cornwell E, Cramer T, McClure ZE, et al. Latitude in sample handling and storage for infant faecal microbiota studies: the elephant in the room? *Microbiome*. 2016;4(1):40.
404. NanoString. Custom Solutions Overview [Available from: https://nanostring.com/products/ncounter-assays-panels/ncounter-custom-solutions/custom-solutions-overview/.
405. Hoyt JM, Wilson SK, Kasa M, Rise JS, Topalidou I, Ailion M. The SEK-1 p38 MAP Kinase Pathway Modulates Gq Signaling in Caenorhabditis elegans. *G3 (Bethesda)*. 2017;7(9):2979-89.
406. Schloss PD, Westcott SL, Ryabin T, Hall JR, Hartmann M, Hollister EB, et al. Introducing mothur: open-source, platform-independent, community-supported software for describing and comparing microbial communities. *Appl Environ Microbiol*. 2009;75(23):7537-41.
407. Hiltemann S, Batut B, Clements D. 16S Microbial Analysis with mothur (extended) (Galaxy Training Materials) [Available from: https://training.galaxyproject.org/training-material/topics/metagenomics/tutorials/mothur-miseq-sop/tutorial.html
408. Glockner FO, Yilmaz P, Quast C, Gerken J, Beccati A, Ciuprina A, et al. 25 years of serving the community with ribosomal RNA gene reference databases and tools. *J Biotechnol*. 2017;261:169-76.
409. Organization WH. Manual for the laboratory diagnosis and virological surveillance of influenza: World Health Organization; 2011.
410. Lin YP, Gregory V, Collins P, Kloess J, Wharton S, Cattle N, et al. Neuraminidase receptor binding variants of human influenza A(H3N2) viruses resulting from substitution of aspartic acid 151 in the catalytic site: a role in virus attachment? *J Virol*. 2010;84(13):6769-81.
411. Coudeville L, Bailleux F, Riche B, Megas F, Andre P, Ecochard R. Relationship between haemagglutination-inhibiting antibody titres and clinical protection against influenza: development and application of a bayesian random-effects model. *BMC Med Res Methodol*. 2010;10:18.
412. Schneider CA, Rasband WS, Eliceiri KW. NIH Image to ImageJ: 25 years of image analysis. *Nat Methods*. 2012;9(7):671-5.
413. Ye J, Coulouris G, Zaretskaya I, Cutcutache I, Rozen S, Madden TL. Primer-BLAST: a tool to design target-specific primers for polymerase chain reaction. *BMC Bioinformatics*. 2012;13:134.
414. Bosch S, Acharjee A, Quraishi MN, Bijnsdorp IV, Rojas P, Bakkali A, et al. Integration of stool microbiota, proteome and amino acid profiles to discriminate

patients with adenomas and colorectal cancer. *Gut Microbes*. 2022;14(1):2139979.
415. Paray BA, Albeshr MF, Jan AT, Rather IA. Leaky Gut and Autoimmunity: An Intricate Balance in Individuals Health and the Diseased State. *Int J Mol Sci*. 2020;21(24).
416. Salazar AM, Aparicio R, Clark RI, Rera M, Walker DW. Intestinal barrier dysfunction: an evolutionarily conserved hallmark of aging. *Dis Model Mech*. 2023;16(4).
417. Rera M, Azizi MJ, Walker DW. Organ-specific mediation of lifespan extension: more than a gut feeling? *Ageing Res Rev*. 2013;12(1):436-44.
418. Stehle JR, Jr., Leng X, Kitzman DW, Nicklas BJ, Kritchevsky SB, High KP. Lipopolysaccharide-binding protein, a surrogate marker of microbial translocation, is associated with physical function in healthy older adults. *J Gerontol A Biol Sci Med Sci*. 2012;67(11):1212-8.
419. Groschwitz KR, Hogan SP. Intestinal barrier function: molecular regulation and disease pathogenesis. *J Allergy Clin Immunol*. 2009;124(1):3-20; quiz 1-2.
420. Kelesidis T, Kendall MA, Yang OO, Hodis HN, Currier JS. Biomarkers of microbial translocation and macrophage activation: association with progression of subclinical atherosclerosis in HIV-1 infection. *J Infect Dis*. 2012;206(10):1558-67.
421. Mishra SP, Wang B, Wang S, Nagpal R, Miller B, Jain S, et al. Microbiota induces aging-related leaky gut and inflammation by dampening mucin barriers and butyrate-FFAR2/3 signaling. *bioRxiv*. 2021:456856.
422. Herndler-Brandstetter D, Landgraf K, Jenewein B, Tzankov A, Brunauer R, Brunner S, et al. Human bone marrow hosts polyfunctional memory CD4+ and CD8+ T cells with close contact to IL-15-producing cells. *J Immunol*. 2011;186(12):6965-71.
423. Zizzo G, De Santis M, Bosello SL, Fedele AL, Peluso G, Gremese E, et al. Synovial fluid-derived T helper 17 cells correlate with inflammatory activity in arthritis, irrespectively of diagnosis. *Clin Immunol*. 2011;138(1):107-16.
424. Wei X, Zhang J, Gu Q, Huang M, Zhang W, Guo J, et al. Reciprocal Expression of IL-35 and IL-10 Defines Two Distinct Effector Treg Subsets that Are Required for Maintenance of Immune Tolerance. *Cell Rep*. 2017;21(7):1853-69.
425. Lord JM, Veenith T, Sullivan J, Sharma-Oates A, Richter AG, Greening NJ, et al. Accelarated immune ageing is associated with COVID-19 disease severity. *Immun Ageing*. 2024;21(1):6.
426. Zheng R, Zhang Y, Zhang K, Yuan Y, Jia S, Liu J. The Complement System, Aging, and Aging-Related Diseases. *Int J Mol Sci*. 2022;23(15).
427. Ueda K, Arakawa H, Nakamura Y. Dual-specificity phosphatase 5 (DUSP5) as a direct transcriptional target of tumor suppressor p53. *Oncogene*. 2003;22(36):5586-91.
428. Brinkhof B, Zhang B, Cui Z, Yea H, Wang H. ALCAM (CD166) as a gene expression marker for human mesenchymal stromal cell characterisation. *Gene X*. 2020;5:100031.
429. Korsmeyer SJ, Wei MC, Saito M, Weiler S, Oh KJ, Schlesinger PH. Pro-apoptotic cascade activates BID, which oligomerizes BAK or BAX into pores that result in the release of cytochrome c. *Cell Death Differ*. 2000;7(12):1166-73.

430. Lagresle-Peyrou C, Millili M, Luce S, Boned A, Sadek H, Rouiller J, et al. The BLNK adaptor protein has a nonredundant role in human B-cell differentiation. *J Allergy Clin Immunol*. 2014;134(1):145-54.
431. Guo X, Hu W, Gao Z, Fan Y, Wu Q, Li W. Identification of PLOD3 and LRRN3 as potential biomarkers for Parkinson's disease based on integrative analysis. *NPJ Parkinsons Dis*. 2023;9(1):82.
432. Neo SY, Yang Y, Record J, Ma R, Chen X, Chen Z, et al. CD73 immune checkpoint defines regulatory NK cells within the tumor microenvironment. *J Clin Invest*. 2020;130(3):1185-98.
433. Chen S, Fan J, Zhang M, Qin L, Dominguez D, Long A, et al. CD73 expression on effector T cells sustained by TGF-beta facilitates tumor resistance to anti-4-1BB/CD137 therapy. *Nat Commun*. 2019;10(1):150.
434. de Mattos Barbosa MG, Lefferts AR, Huynh D, Liu H, Zhang Y, Fu B, et al. TNFRSF13B genotypes control immune-mediated pathology by regulating the functions of innate B cells. *JCI Insight*. 2021;6(17).
435. Feng Z, Zhang Y, He M, Han Y, Cai C, Liu S, et al. AMICA1 is a diagnostic and prognostic biomarker and induces immune cells infiltration by activating cGAS-STING signaling in lung adenocarcinoma. *Cancer Cell Int*. 2022;22(1):111.
436. Lee IH, Kawai Y, Fergusson MM, Rovira, II, Bishop AJ, Motoyama N, et al. Atg7 modulates p53 activity to regulate cell cycle and survival during metabolic stress. *Science*. 2012;336(6078):225-8.
437. Zhao J, Zhang L, Lu A, Han Y, Colangelo D, Bukata C, et al. ATM is a key driver of NF-kappaB-dependent DNA-damage-induced senescence, stem cell dysfunction and aging. *Aging (Albany NY)*. 2020;12(6):4688-710.
438. Menning A, Hopken UE, Siegmund K, Lipp M, Hamann A, Huehn J. Distinctive role of CCR7 in migration and functional activity of naive- and effector/memory-like Treg subsets. *Eur J Immunol*. 2007;37(6):1575-83.
439. Parish ST, Wu JE, Effros RB. Sustained CD28 expression delays multiple features of replicative senescence in human CD8 T lymphocytes. *J Clin Immunol*. 2010;30(6):798-805.
440. Zhu LL, Zhao XQ, Jiang C, You Y, Chen XP, Jiang YY, et al. C-type lectin receptors Dectin-3 and Dectin-2 form a heterodimeric pattern-recognition receptor for host defense against fungal infection. *Immunity*. 2013;39(2):324-34.
441. Shao S, Ju M, Lei J, Lu X, Li H, Wang D, et al. Egr-1 inhibits colon cancer cell proliferation, migration and invasion via regulating CDKL1 at the transcriptional level. *Oncol Rep*. 2021;46(2).
442. Hop HT, Arayan LT, Huy TXN, Reyes AWB, Vu SH, Min W, et al. The Key Role of c-Fos for Immune Regulation and Bacterial Dissemination in Brucella Infected Macrophage. *Front Cell Infect Microbiol*. 2018;8:287.
443. Irving J, Feng J, Wistrom C, Pikaart M, Villeponteau B. An altered repertoire of fos/jun (AP-1) at the onset of replicative senescence. *Exp Cell Res*. 1992;202(1):161-6.
444. Barnes BJ, Moore PA, Pitha PM. Virus-specific activation of a novel interferon regulatory factor, IRF-5, results in the induction of distinct interferon alpha genes. *J Biol Chem*. 2001;276(26):23382-90.

445. Cheng XT, Xie YX, Zhou B, Huang N, Farfel-Becker T, Sheng ZH. Characterization of LAMP1-labeled nondegradative lysosomal and endocytic compartments in neurons. *J Cell Biol*. 2018;217(9):3127-39.
446. Jamilloux Y, Lefeuvre L, Magnotti F, Martin A, Benezech S, Allatif O, et al. Familial Mediterranean fever mutations are hypermorphic mutations that specifically decrease the activation threshold of the Pyrin inflammasome. *Rheumatology (Oxford)*. 2018;57(1):100-11.
447. Schaeuble K, Cannelle H, Favre S, Huang HY, Oberle SG, Speiser DE, et al. Attenuation of chronic antiviral T-cell responses through constitutive COX2-dependent prostanoid synthesis by lymph node fibroblasts. *PLoS Biol*. 2019;17(7):e3000072.
448. Sabroe I, Jones EC, Usher LR, Whyte MK, Dower SK. Toll-like receptor (TLR)2 and TLR4 in human peripheral blood granulocytes: a critical role for monocytes in leukocyte lipopolysaccharide responses. *J Immunol*. 2002;168(9):4701-10.
449. Moen SH, Ehrnstrom B, Kojen JF, Yurchenko M, Beckwith KS, Afset JE, et al. Human Toll-like Receptor 8 (TLR8) Is an Important Sensor of Pyogenic Bacteria, and Is Attenuated by Cell Surface TLR Signaling. *Front Immunol*. 2019;10:1209.
450. Chipuk JE, Fisher JC, Dillon CP, Kriwacki RW, Kuwana T, Green DR. Mechanism of apoptosis induction by inhibition of the anti-apoptotic BCL-2 proteins. *Proc Natl Acad Sci U S A*. 2008;105(51):20327-32.
451. McComb S, Chan PK, Guinot A, Hartmannsdottir H, Jenni S, Dobay MP, et al. Efficient apoptosis requires feedback amplification of upstream apoptotic signals by effector caspase-3 or -7. *Sci Adv*. 2019;5(7):eaau9433.
452. Takheaw N, Earwong P, Laopajon W, Pata S, Kasinrerk W. Interaction of CD99 and its ligand upregulates IL-6 and TNF-alpha upon T cell activation. *PLoS One*. 2019;14(5):e0217393.
453. Pasello M, Manara MC, Scotlandi K. CD99 at the crossroads of physiology and pathology. *J Cell Commun Signal*. 2018;12(1):55-68.
454. Ito T, Young MJ, Li R, Jain S, Wernitznig A, Krill-Burger JM, et al. Paralog knockout profiling identifies DUSP4 and DUSP6 as a digenic dependence in MAPK pathway-driven cancers. *Nat Genet*. 2021;53(12):1664-72.
455. Bignon A, Regent A, Klipfel L, Desnoyer A, de la Grange P, Martinez V, et al. DUSP4-mediated accelerated T-cell senescence in idiopathic CD4 lymphopenia. *Blood*. 2015;125(16):2507-18.
456. Dong C, Juedes AE, Temann UA, Shresta S, Allison JP, Ruddle NH, et al. ICOS co-stimulatory receptor is essential for T-cell activation and function. *Nature*. 2001;409(6816):97-101.
457. Henson SM, Franzese O, Macaulay R, Libri V, Azevedo RI, Kiani-Alikhan S, et al. KLRG1 signaling induces defective Akt (ser473) phosphorylation and proliferative dysfunction of highly differentiated CD8+ T cells. *Blood*. 2009;113(26):6619-28.
458. Dietmann AS, Kruse N, Stork L, Gloth M, Bruck W, Metz I. Neurofilament light chains in serum as biomarkers of axonal damage in early MS lesions: a histological-serological correlative study. *J Neurol*. 2023;270(3):1416-29.
459. Hall JA, Pokrovskii M, Kroehling L, Kim BR, Kim SY, Wu L, et al. Transcription factor RORalpha enforces stability of the Th17 cell effector program by binding to a Rorc cis-regulatory element. *Immunity*. 2022;55(11):2027-43 e9.

460. Li Y, Deng W, Wu J, He Q, Yang G, Luo X, et al. TXNIP Exacerbates the Senescence and Aging-Related Dysfunction of beta Cells by Inducing Cell Cycle Arrest Through p38-p16/p21-CDK-Rb Pathway. *Antioxid Redox Signal*. 2023;38(7-9):480-95.
461. Wang YP, Zhou LS, Zhao YZ, Wang SW, Chen LL, Liu LX, et al. Regulation of G6PD acetylation by SIRT2 and KAT9 modulates NADPH homeostasis and cell survival during oxidative stress. *EMBO J*. 2014;33(12):1304-20.
462. Li Y, Goronzy JJ, Weyand CM. DNA damage, metabolism and aging in pro-inflammatory T cells: Rheumatoid arthritis as a model system. *Exp Gerontol*. 2018;105:118-27.
463. Huang YH, Zhu C, Kondo Y, Anderson AC, Gandhi A, Russell A, et al. CEACAM1 regulates TIM-3-mediated tolerance and exhaustion. *Nature*. 2015;517(7534):386-90.
464. Marturano J, Longhi R, Casorati G, Protti MP. MAGE-A3(161-175) contains an HLA-DRbeta4 restricted natural epitope poorly formed through indirect presentation by dendritic cells. *Cancer Immunol Immunother*. 2008;57(2):207-15.
465. Parham C, Chirica M, Timans J, Vaisberg E, Travis M, Cheung J, et al. A receptor for the heterodimeric cytokine IL-23 is composed of IL-12Rbeta1 and a novel cytokine receptor subunit, IL-23R. *J Immunol*. 2002;168(11):5699-708.
466. Brown DP, Jones DC, Anderson KJ, Lapaque N, Buerki RA, Trowsdale J, et al. The inhibitory receptor LILRB4 (ILT3) modulates antigen presenting cell phenotype and, along with LILRB2 (ILT4), is upregulated in response to Salmonella infection. *BMC Immunol*. 2009;10:56.
467. Fritsch M, Gunther SD, Schwarzer R, Albert MC, Schorn F, Werthenbach JP, et al. Caspase-8 is the molecular switch for apoptosis, necroptosis and pyroptosis. *Nature*. 2019;575(7784):683-7.
468. Das N, Dewan V, Grace PM, Gunn RJ, Tamura R, Tzarum N, et al. HMGB1 Activates Proinflammatory Signaling via TLR5 Leading to Allodynia. *Cell Rep*. 2016;17(4):1128-40.
469. Wu C, Sakorafas P, Miller R, McCarthy D, Scesney S, Dixon R, et al. IL-18 receptor beta-induced changes in the presentation of IL-18 binding sites affect ligand binding and signal transduction. *J Immunol*. 2003;170(11):5571-7.
470. Chiang HY, Chu PH, Lee TH. MFG-E8 mediates arterial aging by promoting the proinflammatory phenotype of vascular smooth muscle cells. *J Biomed Sci*. 2019;26(1):61.
471. Corcoran L, Emslie D, Kratina T, Shi W, Hirsch S, Taubenheim N, et al. Oct2 and Obf1 as Facilitators of B:T Cell Collaboration during a Humoral Immune Response. *Front Immunol*. 2014;5:108.
472. Tewari R, Shayahati B, Fan Y, Akimzhanov AM. T cell receptor-dependent S-acylation of ZAP-70 controls activation of T cells. *J Biol Chem*. 2021;296:100311.
473. Voetmann LM, Rolin B, Kirk RK, Pyke C, Hansen AK. The intestinal permeability marker FITC-dextran 4kDa should be dosed according to lean body mass in obese mice. *Nutr Diabetes*. 2023;13(1):1.
474. Nitta T, Takayanagi H. Non-Epithelial Thymic Stromal Cells: Unsung Heroes in Thymus Organogenesis and T Cell Development. *Front Immunol*. 2020;11:620894.

475. Gui J, Zhu X, Dohkan J, Cheng L, Barnes PF, Su DM. The aged thymus shows normal recruitment of lymphohematopoietic progenitors but has defects in thymic epithelial cells. *Int Immunol*. 2007;19(10):1201-11.
476. Flores KG, Li J, Sempowski GD, Haynes BF, Hale LP. Analysis of the human thymic perivascular space during aging. *J Clin Invest*. 1999;104(8):1031-9.
477. Freund A, Laberge RM, Demaria M, Campisi J. Lamin B1 loss is a senescence-associated biomarker. *Mol Biol Cell*. 2012;23(11):2066-75.
478. Habtezion A, Nguyen LP, Hadeiba H, Butcher EC. Leukocyte Trafficking to the Small Intestine and Colon. *Gastroenterology*. 2016;150(2):340-54.
479. Stefanich EG, Danilenko DM, Wang H, O'Byrne S, Erickson R, Gelzleichter T, et al. A humanized monoclonal antibody targeting the beta7 integrin selectively blocks intestinal homing of T lymphocytes. *Br J Pharmacol*. 2011;162(8):1855-70.
480. Schmutz C, Cartwright A, Williams H, Haworth O, Williams JH, Filer A, et al. Monocytes/macrophages express chemokine receptor CCR9 in rheumatoid arthritis and CCL25 stimulates their differentiation. *Arthritis Res Ther*. 2010;12(4):R161.
481. Wendland M, Czeloth N, Mach N, Malissen B, Kremmer E, Pabst O, et al. CCR9 is a homing receptor for plasmacytoid dendritic cells to the small intestine. *Proc Natl Acad Sci U S A*. 2007;104(15):6347-52.
482. Walker EM, Slisarenko N, Gerrets GL, Kissinger PJ, Didier ES, Kuroda MJ, et al. Inflammaging phenotype in rhesus macaques is associated with a decline in epithelial barrier-protective functions and increased pro-inflammatory function in CD161-expressing cells. *Geroscience*. 2019;41(6):739-57.
483. Gulhane M, Murray L, Lourie R, Tong H, Sheng YH, Wang R, et al. High Fat Diets Induce Colonic Epithelial Cell Stress and Inflammation that is Reversed by IL-22. *Sci Rep*. 2016;6:28990.
484. Hung TV, Suzuki T. Dietary Fermentable Fiber Reduces Intestinal Barrier Defects and Inflammation in Colitic Mice. *J Nutr*. 2016;146(10):1970-9.
485. Yan H, Ajuwon KM. Butyrate modifies intestinal barrier function in IPEC-J2 cells through a selective upregulation of tight junction proteins and activation of the Akt signaling pathway. *PLoS One*. 2017;12(6):e0179586.
486. Lo Conte M, Antonini Cencicchio M, Ulaszewska M, Nobili A, Cosorich I, Ferrarese R, et al. A diet enriched in omega-3 PUFA and inulin prevents type 1 diabetes by restoring gut barrier integrity and immune homeostasis in NOD mice. *Front Immunol*. 2022;13:1089987.
487. Cruz-Adalia A, Ramirez-Santiago G, Osuna-Perez J, Torres-Torresano M, Zorita V, Martinez-Riano A, et al. Conventional CD4(+) T cells present bacterial antigens to induce cytotoxic and memory CD8(+) T cell responses. *Nat Commun*. 2017;8(1):1591.
488. Kumar R, Sharma A, Gupta M, Padwad Y, Sharma R. Cell-Free Culture Supernatant of Probiotic Lactobacillus fermentum Protects Against H(2)O(2)-Induced Premature Senescence by Suppressing ROS-Akt-mTOR Axis in Murine Preadipocytes. *Probiotics Antimicrob Proteins*. 2020;12(2):563-76.
489. Gervason S, Napoli M, Dreux-Zhiga A, Lazzarelli C, Garcier S, Briand A, et al. Attenuation of negative effects of senescence in human skin using an extract from Sphingomonas hydrophobicum: development of new skin care solution. *Int J Cosmet Sci*. 2019;41(4):391-7.

490. Pieren DKJ, Smits NAM, van de Garde MDB, Guichelaar T. Response kinetics reveal novel features of ageing in murine T cells. *Sci Rep*. 2019;9(1):5587.
491. Liu X, Mo W, Ye J, Li L, Zhang Y, Hsueh EC, et al. Regulatory T cells trigger effector T cell DNA damage and senescence caused by metabolic competition. *Nature Communications*. 2018;9(1).
492. Tzika AA, Constantinou C, Bandyopadhaya A, Psychogios N, Lee S, Mindrinos M, et al. A small volatile bacterial molecule triggers mitochondrial dysfunction in murine skeletal muscle. *PLoS One*. 2013;8(9):e74528.
493. Yager EJ, Ahmed M, Lanzer K, Randall TD, Woodland DL, Blackman MA. Age-associated decline in T cell repertoire diversity leads to holes in the repertoire and impaired immunity to influenza virus. *J Exp Med*. 2008;205(3):711-23.
494. Czamara K, Stojak M, Pacia MZ, Zieba A, Baranska M, Chlopicki S, et al. Lipid Droplets Formation Represents an Integral Component of Endothelial Inflammation Induced by LPS. *Cells*. 2021;10(6).
495. Kim CO, Huh AJ, Han SH, Kim JM. Analysis of cellular senescence induced by lipopolysaccharide in pulmonary alveolar epithelial cells. *Arch Gerontol Geriatr*. 2012;54(2):e35-41.
496. Budamagunta V, Manohar-Sindhu S, Yang Y, He Y, Traktuev DO, Foster TC, et al. Senescence-associated hyper-activation to inflammatory stimuli in vitro. *Aging (Albany NY)*. 2021;13(15):19088-107.
497. Majumdar S, Adiga V, Raghavan A, Rananaware SR, Nandi D. Comparative analysis of thymic subpopulations during different modes of atrophy identifies the reactive oxygen species scavenger, N-acetyl cysteine, to increase the survival of thymocytes during infection-induced and lipopolysaccharide-induced thymic atrophy. *Immunology*. 2019;157(1):21-36.
498. Tsuji T, Asano Y, Handa T, Honma Y, Ichinose Y, Yokochi T. Induction of apoptosis in lymphoid tissues of mice after intramuscular injection of enterotoxigenic Escherichia coli enterotoxin. *Immunobiology*. 2000;201(3-4):377-90.
499. Zhang YH, Takahashi K, Jiang GZ, Kawai M, Fukada M, Yokochi T. In vivo induction of apoptosis (programmed cell death) in mouse thymus by administration of lipopolysaccharide. *Infect Immun*. 1993;61(12):5044-8.
500. Soderholm AT, Pedicord VA. Intestinal epithelial cells: at the interface of the microbiota and mucosal immunity. *Immunology*. 2019;158(4):267-80.
501. Fu H, Jangani M, Parmar A, Wang G, Coe D, Spear S, et al. A Subset of CCL25-Induced Gut-Homing T Cells Affects Intestinal Immunity to Infection and Cancer. *Front Immunol*. 2019;10:271.
502. Le N, Mazahery C, Nguyen K, Levine AD. Regulation of Intestinal Epithelial Barrier and Immune Function by Activated T Cells. *Cell Mol Gastroenterol Hepatol*. 2021;11(1):55-76.
503. Nizzoli G, Burrello C, Cribiu FM, Lovati G, Ercoli G, Botti F, et al. Pathogenicity of In Vivo Generated Intestinal Th17 Lymphocytes is IFNgamma Dependent. *J Crohns Colitis*. 2018;12(8):981-92.
504. Acosta JC, Banito A, Wuestefeld T, Georgilis A, Janich P, Morton JP, et al. A complex secretory program orchestrated by the inflammasome controls paracrine senescence. *Nat Cell Biol*. 2013;15(8):978-90.

505. Laberge RM, Awad P, Campisi J, Desprez PY. Epithelial-mesenchymal transition induced by senescent fibroblasts. *Cancer Microenviron*. 2012;5(1):39-44.
506. Nighot P, Al-Sadi R, Rawat M, Guo S, Watterson DM, Ma T. Matrix metalloproteinase 9-induced increase in intestinal epithelial tight junction permeability contributes to the severity of experimental DSS colitis. *Am J Physiol Gastrointest Liver Physiol*. 2015;309(12):G988-97.
507. Xiao Y, Lian H, Zhong XS, Krishnachaitanya SS, Cong Y, Dashwood RH, et al. Matrix metalloproteinase 7 contributes to intestinal barrier dysfunction by degrading tight junction protein Claudin-7. *Front Immunol*. 2022;13:1020902.
508. Saccon TD, Nagpal R, Yadav H, Cavalcante MB, Nunes ADC, Schneider A, et al. Senolytic Combination of Dasatinib and Quercetin Alleviates Intestinal Senescence and Inflammation and Modulates the Gut Microbiome in Aged Mice. *J Gerontol A Biol Sci Med Sci*. 2021;76(11):1895-905.
509. Monaghan TM, Duggal NA, Rosati E, Griffin R, Hughes J, Roach B, et al. A Multi-Factorial Observational Study on Sequential Fecal Microbiota Transplant in Patients with Medically Refractory Clostridioides difficile Infection. *Cells*. 2021;10(11).
510. Gori A, Rizzardini G, Van't Land B, Amor KB, van Schaik J, Torti C, et al. Specific prebiotics modulate gut microbiota and immune activation in HAART-naive HIV-infected adults: results of the "COPA" pilot randomized trial. *Mucosal Immunol*. 2011;4(5):554-63.
511. Mittelbrunn M, Kroemer G. Hallmarks of T cell aging. *Nat Immunol*. 2021;22(6):687-98.
512. Balakrishnan B, Luckey D, Taneja V. Autoimmunity-Associated Gut Commensals Modulate Gut Permeability and Immunity in Humanized Mice. *Mil Med*. 2019;184(Suppl 1):529-36.
513. Chen H, Ou R, Tang N, Su W, Yang R, Yu X, et al. Alternation of the gut microbiota in irritable bowel syndrome: an integrated analysis based on multicenter amplicon sequencing data. *J Transl Med*. 2023;21(1):117.
514. Que Y, Cao M, He J, Zhang Q, Chen Q, Yan C, et al. Gut Bacterial Characteristics of Patients With Type 2 Diabetes Mellitus and the Application Potential. *Front Immunol*. 2021;12:722206.
515. Sato Y, Atarashi K, Plichta DR, Arai Y, Sasajima S, Kearney SM, et al. Novel bile acid biosynthetic pathways are enriched in the microbiome of centenarians. *Nature*. 2021;599(7885):458-64.
516. Lee G, Lee H, Hong J, Lee SH, Jung BH. Quantitative profiling of bile acids in rat bile using ultrahigh-performance liquid chromatography-orbitrap mass spectrometry: Alteration of the bile acid composition with aging. *J Chromatogr B Analyt Technol Biomed Life Sci*. 2016;1031:37-49.
517. Saleri R, Borghetti P, Ravanetti F, Cavalli V, Ferrari L, De Angelis E, et al. Effects of different short-chain fatty acids (SCFA) on gene expression of proteins involved in barrier function in IPEC-J2. *Porcine Health Manag*. 2022;8(1):21.
518. Bilotta AJ, Ma C, Yang W, Yu Y, Yu Y, Zhao X, et al. Propionate Enhances Cell Speed and Persistence to Promote Intestinal Epithelial Turnover and Repair. *Cell Mol Gastroenterol Hepatol*. 2021;11(4):1023-44.

519. van der Lugt B, Vos MCP, Grootte Bromhaar M, Ijssennagger N, Vrieling F, Meijerink J, et al. The effects of sulfated secondary bile acids on intestinal barrier function and immune response in an inflammatory in vitro human intestinal model. *Heliyon*. 2022;8(2):e08883.
520. Giannos P, Prokopidis K, Isanejad M, Wright HL. Markers of immune dysregulation in response to the ageing gut: insights from aged murine gut microbiota transplants. *BMC Gastroenterol*. 2022;22(1):533.
521. Fransen F, van Beek AA, Borghuis T, Aidy SE, Hugenholtz F, van der Gaast-de Jongh C, et al. Aged Gut Microbiota Contributes to Systemical Inflammaging after Transfer to Germ-Free Mice. *Front Immunol*. 2017;8:1385.
522. Pallikkuth S, Mendez R, Russell K, Sirupangi T, Kvistad D, Pahwa R, et al. Age Associated Microbiome and Microbial Metabolites Modulation and Its Association With Systemic Inflammation in a Rhesus Macaque Model. *Front Immunol*. 2021;12:748397.
523. Finotello F, Mastrorilli E, Di Camillo B. Measuring the diversity of the human microbiota with targeted next-generation sequencing. *Brief Bioinform*. 2018;19(4):679-92.
524. Willis AD. Rarefaction, Alpha Diversity, and Statistics. *Front Microbiol*. 2019;10:2407.
525. Biagi E, Nylund L, Candela M, Ostan R, Bucci L, Pini E, et al. Through ageing, and beyond: gut microbiota and inflammatory status in seniors and centenarians. *PLoS One*. 2010;5(5):e10667.
526. Vaiserman A, Romanenko M, Piven L, Moseiko V, Lushchak O, Kryzhanovska N, et al. Differences in the gut Firmicutes to Bacteroidetes ratio across age groups in healthy Ukrainian population. *BMC Microbiol*. 2020;20(1):221.
527. Leite G, Pimentel M, Barlow GM, Chang C, Hosseini A, Wang J, et al. Age and the aging process significantly alter the small bowel microbiome. *Cell Rep*. 2021;36(13):109765.
528. Guinan J, Wang S, Hazbun TR, Yadav H, Thangamani S. Antibiotic-induced decreases in the levels of microbial-derived short-chain fatty acids correlate with increased gastrointestinal colonization of Candida albicans. *Sci Rep*. 2019;9(1):8872.
529. Inagaki T, Moschetta A, Lee Y-K, Peng L, Zhao G, Downes M, et al. Regulation of antibacterial defense in the small intestine by the nuclear bile acid receptor. *Proceedings of the National Academy of Sciences*. 2006;103(10):3920-5.
530. Luu M, Pautz S, Kohl V, Singh R, Romero R, Lucas S, et al. The short-chain fatty acid pentanoate suppresses autoimmunity by modulating the metabolic-epigenetic crosstalk in lymphocytes. *Nat Commun*. 2019;10(1):760.
531. Bashir H, Singh S, Singh RP, Agrewala JN, Kumar R. Age-mediated gut microbiota dysbiosis promotes the loss of dendritic cells tolerance. *Aging Cell*. 2023;22(6):e13838.
532. Ahmadi S, Wang S, Nagpal R, Wang B, Jain S, Razazan A, et al. A human-origin probiotic cocktail ameliorates aging-related leaky gut and inflammation via modulating the microbiota/taurine/tight junction axis. *JCI Insight*. 2020;5(9).
533. Velez EM, Maldonado Galdeano C, Carmuega E, Weill R, Bibas Bonet ME, Perdigon G. Probiotic fermented milk consumption modulates the allergic process induced by ovoalbumin in mice. *Br J Nutr*. 2015;114(4):566-76.

534. Liu X, Mao B, Gu J, Wu J, Cui S, Wang G, et al. Blautia-a new functional genus with potential probiotic properties? *Gut Microbes*. 2021;13(1):1-21.
535. Bachem A, Makhlouf C, Binger KJ, de Souza DP, Tull D, Hochheiser K, et al. Microbiota-Derived Short-Chain Fatty Acids Promote the Memory Potential of Antigen-Activated CD8(+) T Cells. *Immunity*. 2019;51(2):285-97 e5.
536. Ciarlo E, Heinonen T, Herderschee J, Fenwick C, Mombelli M, Le Roy D, et al. Impact of the microbial derived short chain fatty acid propionate on host susceptibility to bacterial and fungal infections in vivo. *Sci Rep*. 2016;6:37944.
537. Vital M, Rud T, Rath S, Pieper DH, Schluter D. Diversity of Bacteria Exhibiting Bile Acid-inducible 7alpha-dehydroxylation Genes in the Human Gut. *Comput Struct Biotechnol J*. 2019;17:1016-9.
538. Heinken A, Ravcheev DA, Baldini F, Heirendt L, Fleming RMT, Thiele I. Systematic assessment of secondary bile acid metabolism in gut microbes reveals distinct metabolic capabilities in inflammatory bowel disease. *Microbiome*. 2019;7(1):75.
539. Costabile A, Bergillos-Meca T, Rasinkangas P, Korpela K, de Vos WM, Gibson GR. Effects of Soluble Corn Fiber Alone or in Synbiotic Combination with Lactobacillus rhamnosus GG and the Pilus-Deficient Derivative GG-PB12 on Fecal Microbiota, Metabolism, and Markers of Immune Function: A Randomized, Double-Blind, Placebo-Controlled, Crossover Study in Healthy Elderly (Saimes Study). *Front Immunol*. 2017;8:1443.
540. Miyazawa K, Kawase M, Kubota A, Yoda K, Harata G, Hosoda M, et al. Heat-killed Lactobacillus gasseri can enhance immunity in the elderly in a double-blind, placebo-controlled clinical study. *Beneficial Microbes*. 2015;6(4):441-9.
541. Makino S, Ikegami S, Kume A, Horiuchi H, Sasaki H, Orii N. Reducing the risk of infection in the elderly by dietary intake of yoghurt fermented with Lactobacillus delbrueckii ssp. bulgaricus OLL1073R-1. *Br J Nutr*. 2010;104(7):998-1006.
542. Lee A, Lee YJ, Yoo HJ, Kim M, Chang Y, Lee DS, et al. Consumption of Dairy Yogurt Containing Lactobacillus paracasei ssp. paracasei, Bifidobacterium animalis ssp. lactis and Heat-Treated Lactobacillus plantarum Improves Immune Function Including Natural Killer Cell Activity. *Nutrients*. 2017;9(6).
543. Cicin-Sain L, Smyk-Pearson S, Currier N, Byrd L, Koudelka C, Robinson T, et al. Loss of naive T cells and repertoire constriction predict poor response to vaccination in old primates. *J Immunol*. 2010;184(12):6739-45.
544. Wagner A, Garner-Spitzer E, Jasinska J, Kollaritsch H, Stiasny K, Kundi M, et al. Age-related differences in humoral and cellular immune responses after primary immunisation: indications for stratified vaccination schedules. *Sci Rep*. 2018;8(1):9825.
545. Hagan T, Cortese M, Rouphael N, Boudreau C, Linde C, Maddur MS, et al. Antibiotics-Driven Gut Microbiome Perturbation Alters Immunity to Vaccines in Humans. *Cell*. 2019;178(6):1313-28 e13.
546. Ng SC, Peng Y, Zhang L, Mok CK, Zhao S, Li A, et al. Gut microbiota composition is associated with SARS-CoV-2 vaccine immunogenicity and adverse events. *Gut*. 2022;71(6):1106-16.
547. Eloe-Fadrosh EA, McArthur MA, Seekatz AM, Drabek EF, Rasko DA, Sztein MB, et al. Impact of oral typhoid vaccination on the human gut microbiota and

correlations with s. Typhi-specific immunological responses. *PLoS One*. 2013;8(4):e62026.
548. Huda MN, Lewis Z, Kalanetra KM, Rashid M, Ahmad SM, Raqib R, et al. Stool microbiota and vaccine responses of infants. *Pediatrics*. 2014;134(2):e362-72.
549. Akatsu H, Nagafuchi S, Kurihara R, Okuda K, Kanesaka T, Ogawa N, et al. Enhanced vaccination effect against influenza by prebiotics in elderly patients receiving enteral nutrition. *Geriatr Gerontol Int*. 2016;16(2):205-13.
550. Borgognone A, Elizalde-Torrent A, Casadella M, Romero L, Escriba T, Parera M, et al. Vaccination with an HIV T-cell immunogen induces alterations in the mouse gut microbiota. *NPJ Biofilms Microbiomes*. 2022;8(1):104.
551. Harris VC, Haak BW, Handley SA, Jiang B, Velasquez DE, Hykes BL, Jr., et al. Effect of Antibiotic-Mediated Microbiome Modulation on Rotavirus Vaccine Immunogenicity: A Human, Randomized-Control Proof-of-Concept Trial. *Cell Host Microbe*. 2018;24(2):197-207 e4.
552. Alexander JL, Mullish BH, Danckert NP, Liu Z, Olbei ML, Saifuddin A, et al. The gut microbiota and metabolome are associated with diminished COVID-19 vaccine-induced antibody responses in immunosuppressed inflammatory bowel disease patients. *EBioMedicine*. 2023;88:104430.
553. Duggal NA. Reversing the immune ageing clock: lifestyle modifications and pharmacological interventions. *Biogerontology*. 2018;19(6):481-96.
554. Trichopoulou A, Martinez-Gonzalez MA, Tong TY, Forouhi NG, Khandelwal S, Prabhakaran D, et al. Definitions and potential health benefits of the Mediterranean diet: views from experts around the world. *BMC Med*. 2014;12:112.
555. Lopez-Garcia E, Schulze MB, Fung TT, Meigs JB, Rifai N, Manson JE, et al. Major dietary patterns are related to plasma concentrations of markers of inflammation and endothelial dysfunction. *Am J Clin Nutr*. 2004;80(4):1029-35.
556. Chen KW, Chen CW, Yuan KC, Wang IT, Hung FM, Wang AY, et al. Prevalence of Vitamin D Deficiency and Associated Factors in Critically Ill Patients: A Multicenter Observational Study. *Front Nutr*. 2021;8:768804.
557. Bermudez-Brito M, Sahasrabudhe NM, Rosch C, Schols HA, Faas MM, de Vos P. The impact of dietary fibers on dendritic cell responses in vitro is dependent on the differential effects of the fibers on intestinal epithelial cells. *Mol Nutr Food Res*. 2015;59(4):698-710.
558. Hu X, Wang Y, Hao LY, Liu X, Lesch CA, Sanchez BM, et al. Sterol metabolism controls T(H)17 differentiation by generating endogenous RORgamma agonists. *Nat Chem Biol*. 2015;11(2):141-7.
559. Honda KL, Lamon-Fava S, Matthan NR, Wu D, Lichtenstein AH. Docosahexaenoic acid differentially affects TNFalpha and IL-6 expression in LPS-stimulated RAW 264.7 murine macrophages. *Prostaglandins Leukot Essent Fatty Acids*. 2015;97:27-34.
560. Yamagata K, Suzuki S, Tagami M. Docosahexaenoic acid prevented tumor necrosis factor alpha-induced endothelial dysfunction and senescence. *Prostaglandins Leukot Essent Fatty Acids*. 2016;104:11-8.
561. Hamer DH, Sempertegui F, Estrella B, Tucker KL, Rodriguez A, Egas J, et al. Micronutrient deficiencies are associated with impaired immune response and higher burden of respiratory infections in elderly Ecuadorians. *J Nutr*. 2009;139(1):113-9.

562. Savino W, Dardenne M. Nutritional imbalances and infections affect the thymus: consequences on T-cell-mediated immune responses. *Proc Nutr Soc*. 2010;69(4):636-43.
563. Berger MM, Talwar D, Shenkin A. Pitfalls in the interpretation of blood tests used to assess and monitor micronutrient nutrition status. *Nutr Clin Pract*. 2023;38(1):56-69.
564. Eicher-Miller HA, Prapkree L, Palacios C. Expanding the Capabilities of Nutrition Research and Health Promotion Through Mobile-Based Applications. *Adv Nutr*. 2021;12(3):1032-41.
565. Kiefte-de Jong JC, Mathers JC, Franco OH. Nutrition and healthy ageing: the key ingredients. *Proc Nutr Soc*. 2014;73(2):249-59.
566. Clegg ME, Methven L, Lanham-New SA, Green MA, Duggal NA, Hetherington MM. The Food4Years Ageing Network: Improving foods and diets as a strategy for supporting quality of life, independence and healthspan in older adults. *Nutr Bull*. 2023;48(1):124-33.
567. Barcena C, Valdes-Mas R, Mayoral P, Garabaya C, Durand S, Rodriguez F, et al. Healthspan and lifespan extension by fecal microbiota transplantation into progeroid mice. *Nat Med*. 2019;25(8):1234-42.
568. Kumar A, Joishy T, Das S, Kalita MC, Mukherjee AK, Khan MR. A Potential Probiotic Lactobacillus plantarum JBC5 Improves Longevity and Healthy Aging by Modulating Antioxidative, Innate Immunity and Serotonin-Signaling Pathways in Caenorhabditis elegans. *Antioxidants (Basel)*. 2022;11(2).
569. Tsai YC, Cheng LH, Liu YW, Jeng OJ, Lee YK. Gerobiotics: probiotics targeting fundamental aging processes. *Biosci Microbiota Food Health*. 2021;40(1):1-11.
570. Shakersain B, Santoni G, Faxen-Irving G, Rizzuto D, Fratiglioni L, Xu W. Nutritional status and survival among old adults: an 11-year population-based longitudinal study. *Eur J Clin Nutr*. 2016;70(3):320-5.
571. Gomes M, Figueiredo D, Teixeira L, Poveda V, Paul C, Santos-Silva A, et al. Physical inactivity among older adults across Europe based on the SHARE database. *Age Ageing*. 2017;46(1):71-7.
572. Chowdhury SR, Chandra Das D, Sunna TC, Beyene J, Hossain A. Global and regional prevalence of multimorbidity in the adult population in community settings: a systematic review and meta-analysis. *EClinicalMedicine*. 2023;57:101860.
573. Ghosh TS, Das M, Jeffery IB, O'Toole PW. Adjusting for age improves identification of gut microbiome alterations in multiple diseases. *Elife*. 2020;9.
574. Bodkhe R, Shetty SA, Dhotre DP, Verma AK, Bhatia K, Mishra A, et al. Comparison of Small Gut and Whole Gut Microbiota of First-Degree Relatives With Adult Celiac Disease Patients and Controls. *Front Microbiol*. 2019;10:164.
575. Vaga S, Lee S, Ji B, Andreasson A, Talley NJ, Agreus L, et al. Compositional and functional differences of the mucosal microbiota along the intestine of healthy individuals. *Sci Rep*. 2020;10(1):14977.
576. Zaramela LS, Tjuanta M, Moyne O, Neal M, Zengler K. synDNA-a Synthetic DNA Spike-in Method for Absolute Quantification of Shotgun Metagenomic Sequencing. *mSystems*. 2022;7(6):e0044722.
577. Rera M, Clark RI, Walker DW. Intestinal barrier dysfunction links metabolic and inflammatory markers of aging to death in Drosophila. *Proc Natl Acad Sci U S A*. 2012;109(52):21528-33.

578. Hunt PW, Sinclair E, Rodriguez B, Shive C, Clagett B, Funderburg N, et al. Gut epithelial barrier dysfunction and innate immune activation predict mortality in treated HIV infection. *J Infect Dis*. 2014;210(8):1228-38.
579. Akagi K, Wilson KA, Katewa SD, Ortega M, Simons J, Hilsabeck TA, et al. Dietary restriction improves intestinal cellular fitness to enhance gut barrier function and lifespan in D. melanogaster. *PLoS Genet*. 2018;14(11):e1007777.
580. Matsumoto M, Kurihara S, Kibe R, Ashida H, Benno Y. Longevity in mice is promoted by probiotic-induced suppression of colonic senescence dependent on upregulation of gut bacterial polyamine production. *PLoS One*. 2011;6(8):e23652.
581. Fang X, Yue M, Wei J, Wang Y, Hong D, Wang B, et al. Evaluation of the Anti-Aging Effects of a Probiotic Combination Isolated From Centenarians in a SAMP8 Mouse Model. *Front Immunol*. 2021;12:792746.
582. Lin SW, Tsai YS, Chen YL, Wang MF, Chen CC, Lin WH, et al. Lactobacillus plantarum GKM3 Promotes Longevity, Memory Retention, and Reduces Brain Oxidation Stress in SAMP8 Mice. *Nutrients*. 2021;13(8).
583. Li T, Yang S, Liu X, Li Y, Gu Z, Jiang Z. Dietary neoagarotetraose extends lifespan and impedes brain aging in mice via regulation of microbiota-gut-brain axis. *J Adv Res*. 2023.
584. Wilms E, Jonkers D, Savelkoul HFJ, Elizalde M, Tischmann L, de Vos P, et al. The Impact of Pectin Supplementation on Intestinal Barrier Function in Healthy Young Adults and Healthy Elderly. *Nutrients*. 2019;11(7).
585. Cheng W, Lu J, Lin W, Wei X, Li H, Zhao X, et al. Effects of a galacto-oligosaccharide-rich diet on fecal microbiota and metabolite profiles in mice. *Food Funct*. 2018;9(3):1612-20.
586. Karczewski J, Troost FJ, Konings I, Dekker J, Kleerebezem M, Brummer RJ, et al. Regulation of human epithelial tight junction proteins by Lactobacillus plantarum in vivo and protective effects on the epithelial barrier. *Am J Physiol Gastrointest Liver Physiol*. 2010;298(6):G851-9.
587. Mennigen R, Nolte K, Rijcken E, Utech M, Loeffler B, Senninger N, et al. Probiotic mixture VSL#3 protects the epithelial barrier by maintaining tight junction protein expression and preventing apoptosis in a murine model of colitis. *Am J Physiol Gastrointest Liver Physiol*. 2009;296(5):G1140-9.
588. Tian S, Wang J, Gao R, Wang J, Zhu W. Galacto-oligosaccharides directly attenuate lipopolysaccharides-induced inflammatory response, oxidative stress and barrier impairment in intestinal epithelium. *Journal of Functional Foods*. 2022;91.
589. Hong L, Lee SM, Kim WS, Choi YJ, Oh SH, Li YL, et al. Synbiotics Containing Nanoprebiotics: A Novel Therapeutic Strategy to Restore Gut Dysbiosis. *Front Microbiol*. 2021;12:715241.
590. Xue Z, Yu J, Zhao M, Kang W, Ma Z. Effects of synbiotics on intestinal mucosal barrier in rat model. *Clinical Nutrition Experimental*. 2017;13:12-21.
591. Ma J, Liu Z, Gao X, Bao Y, Hong Y, He X, et al. Gut microbiota remodeling improves natural aging-related disorders through Akkermansia muciniphila and its derived acetic acid. *Pharmacol Res*. 2023;189:106687.
592. Xu L, Zhang Q, Dou X, Wang Y, Wang J, Zhou Y, et al. Fecal microbiota transplantation from young donor mice improves ovarian function in aged mice. *J Genet Genomics*. 2022;49(11):1042-52.

593. Parker A, Romano S, Ansorge R, Aboelnour A, Le Gall G, Savva GM, et al. Fecal microbiota transfer between young and aged mice reverses hallmarks of the aging gut, eye, and brain. *Microbiome*. 2022;10(1):68.
594. Sotos-Prieto M, Ortola R, Ruiz-Canela M, Garcia-Esquinas E, Martinez-Gomez D, Lopez-Garcia E, et al. Association between the Mediterranean lifestyle, metabolic syndrome and mortality: a whole-country cohort in Spain. *Cardiovasc Diabetol*. 2021;20(1):5.
595. Cani PD, Amar J, Iglesias MA, Poggi M, Knauf C, Bastelica D, et al. Metabolic endotoxemia initiates obesity and insulin resistance. *Diabetes*. 2007;56(7):1761-72.
596. Zhou X, Li J, Guo J, Geng B, Ji W, Zhao Q, et al. Gut-dependent microbial translocation induces inflammation and cardiovascular events after ST-elevation myocardial infarction. *Microbiome*. 2018;6(1):66.
597. de Waal GM, de Villiers WJS, Forgan T, Roberts T, Pretorius E. Colorectal cancer is associated with increased circulating lipopolysaccharide, inflammation and hypercoagulability. *Sci Rep*. 2020;10(1):8777.
598. McLeod A, Bernabe B, Schiffer L, Fitzgibbon M, Tussing-Humphreys L. Effect of a Mediterranean Diet Intervention with and Without Weight Loss on the Gut Microbiota in Obese, Older Adults. *Current Developments in Nutrition*. 2020;4.
599. Seethaler B, Lehnert K, Yahiaoui-Doktor M, Basrai M, Vetter W, Kiechle M, et al. Omega-3 polyunsaturated fatty acids improve intestinal barrier integrity-albeit to a lesser degree than short-chain fatty acids: an exploratory analysis of the randomized controlled LIBRE trial. *Eur J Nutr*. 2023;62(7):2779-91.
600. Jung TH, Han KS, Park JH, Hwang HJ. Butyrate modulates mucin secretion and bacterial adherence in LoVo cells via MAPK signaling. *PLoS One*. 2022;17(7):e0269872.
601. Peng L, Li ZR, Green RS, Holzman IR, Lin J. Butyrate enhances the intestinal barrier by facilitating tight junction assembly via activation of AMP-activated protein kinase in Caco-2 cell monolayers. *J Nutr*. 2009;139(9):1619-25.
602. Martin-Montalvo A, Mercken EM, Mitchell SJ, Palacios HH, Mote PL, Scheibye-Knudsen M, et al. Metformin improves healthspan and lifespan in mice. *Nat Commun*. 2013;4:2192.
603. Bitto A, Ito TK, Pineda VV, LeTexier NJ, Huang HZ, Sutlief E, et al. Transient rapamycin treatment can increase lifespan and healthspan in middle-aged mice. *Elife*. 2016;5.
604. De Haes W, Frooninckx L, Van Assche R, Smolders A, Depuydt G, Billen J, et al. Metformin promotes lifespan through mitohormesis via the peroxiredoxin PRDX-2. *Proc Natl Acad Sci U S A*. 2014;111(24):E2501-9.
605. Juricic P, Lu YX, Leech T, Drews LF, Paulitz J, Lu J, et al. Long-lasting geroprotection from brief rapamycin treatment in early adulthood by persistently increased intestinal autophagy. *Nat Aging*. 2022;2(9):824-36.
606. Chen J, Ou Y, Li Y, Hu S, Shao LW, Liu Y. Metformin extends C. elegans lifespan through lysosomal pathway. *Elife*. 2017;6.
607. Bielas J, Herbst A, Widjaja K, Hui J, Aiken JM, McKenzie D, et al. Long term rapamycin treatment improves mitochondrial DNA quality in aging mice. *Exp Gerontol*. 2018;106:125-31.
608. Lee YS, Doonan BB, Wu JM, Hsieh TC. Combined metformin and resveratrol confers protection against UVC-induced DNA damage in A549 lung cancer cells

via modulation of cell cycle checkpoints and DNA repair. *Oncol Rep*. 2016;35(6):3735-41.
609. Moiseeva O, Deschenes-Simard X, St-Germain E, Igelmann S, Huot G, Cadar AE, et al. Metformin inhibits the senescence-associated secretory phenotype by interfering with IKK/NF-kappaB activation. *Aging Cell*. 2013;12(3):489-98.
610. Wang R, Yu Z, Sunchu B, Shoaf J, Dang I, Zhao S, et al. Rapamycin inhibits the secretory phenotype of senescent cells by a Nrf2-independent mechanism. *Aging Cell*. 2017;16(3):564-74.
611. Ahmadi S, Razazan A, Nagpal R, Jain S, Wang B, Mishra SP, et al. Metformin Reduces Aging-Related Leaky Gut and Improves Cognitive Function by Beneficially Modulating Gut Microbiome/Goblet Cell/Mucin Axis. *J Gerontol A Biol Sci Med Sci*. 2020;75(7):e9-e21.
612. Jang H, Kim S, Kim H, Oh SH, Kwak SY, Joo HW, et al. Metformin Protects the Intestinal Barrier by Activating Goblet Cell Maturation and Epithelial Proliferation in Radiation-Induced Enteropathy. *Int J Mol Sci*. 2022;23(11).
613. Baur JA, Pearson KJ, Price NL, Jamieson HA, Lerin C, Kalra A, et al. Resveratrol improves health and survival of mice on a high-calorie diet. *Nature*. 2006;444(7117):337-42.
614. Morselli E, Maiuri MC, Markaki M, Megalou E, Pasparaki A, Palikaras K, et al. Caloric restriction and resveratrol promote longevity through the Sirtuin-1-dependent induction of autophagy. *Cell Death Dis*. 2010;1(1):e10.
615. He S, Zhou M, Zheng H, Wang Y, Wu S, Gao Y, et al. Resveratrol inhibits the progression of premature senescence partially by regulating v-rel avian reticuloendotheliosis viral oncogene homolog A (RELA) and sirtuin 1 (SIRT1). *Ren Fail*. 2022;44(1):171-83.
616. Hwang D, Lim YH. Resveratrol antibacterial activity against Escherichia coli is mediated by Z-ring formation inhibition via suppression of FtsZ expression. *Sci Rep*. 2015;5:10029.
617. Chen ML, Yi L, Zhang Y, Zhou X, Ran L, Yang J, et al. Resveratrol Attenuates Trimethylamine-N-Oxide (TMAO)-Induced Atherosclerosis by Regulating TMAO Synthesis and Bile Acid Metabolism via Remodeling of the Gut Microbiota. *mBio*. 2016;7(2):e02210-15.
618. Song X, Liu L, Peng S, Liu T, Chen Y, Jia R, et al. Resveratrol regulates intestinal barrier function in cyclophosphamide-induced immunosuppressed mice. *J Sci Food Agric*. 2022;102(3):1205-15.
619. Qiu Y, Yang J, Wang L, Yang X, Gao K, Zhu C, et al. Dietary resveratrol attenuation of intestinal inflammation and oxidative damage is linked to the alteration of gut microbiota and butyrate in piglets challenged with deoxynivalenol. *J Anim Sci Biotechnol*. 2021;12(1):71.
620. Jeong JJ, Kim KA, Hwang YJ, Han MJ, Kim DH. Anti-inflammaging effects of Lactobacillus brevis OW38 in aged mice. *Benef Microbes*. 2016;7(5):707-18.
621. Woo JY, Gu W, Kim KA, Jang SE, Han MJ, Kim DH. Lactobacillus pentosus var. plantarum C29 ameliorates memory impairment and inflammaging in a D-galactose-induced accelerated aging mouse model. *Anaerobe*. 2014;27:22-6.
622. Peng X, Meng J, Chi T, Liu P, Man C, Liu S, et al. Lactobacillus plantarum NDC 75017 alleviates the learning and memory ability in aging rats by reducing mitochondrial dysfunction. *Exp Ther Med*. 2014;8(6):1841-6.

623. Chen LH, Wang MF, Chang CC, Huang SY, Pan CH, Yeh YT, et al. Lacticaseibacillus paracasei PS23 Effectively Modulates Gut Microbiota Composition and Improves Gastrointestinal Function in Aged SAMP8 Mice. *Nutrients*. 2021;13(4).
624. Dong H, Rowland I, Thomas LV, Yaqoob P. Immunomodulatory effects of a probiotic drink containing Lactobacillus casei Shirota in healthy older volunteers. *Eur J Nutr*. 2013;52(8):1853-63.
625. Nagata S, Asahara T, Wang C, Suyama Y, Chonan O, Takano K, et al. The Effectiveness of Lactobacillus Beverages in Controlling Infections among the Residents of an Aged Care Facility: A Randomized Placebo-Controlled Double-Blind Trial. *Ann Nutr Metab*. 2016;68(1):51-9.
626. Miller LE, Lehtoranta L, Lehtinen MJ. The Effect of Bifidobacterium animalis ssp. lactis HN019 on Cellular Immune Function in Healthy Elderly Subjects: Systematic Review and Meta-Analysis. *Nutrients*. 2017;9(3).
627. Puvanasundram P, Chong CM, Sabri S, Yusoff MS, Karim M. Multi-strain probiotics: Functions, effectiveness and formulations for aquaculture applications. *Aquaculture Reports*. 2021;21.
628. Timmerman HM, Koning CJ, Mulder L, Rombouts FM, Beynen AC. Monostrain, multistrain and multispecies probiotics--A comparison of functionality and efficacy. *Int J Food Microbiol*. 2004;96(3):219-33.
629. Timmerman HM, Niers LE, Ridwan BU, Koning CJ, Mulder L, Akkermans LM, et al. Design of a multispecies probiotic mixture to prevent infectious complications in critically ill patients. *Clin Nutr*. 2007;26(4):450-9.
630. Lefevre M, Racedo SM, Ripert G, Housez B, Cazaubiel M, Maudet C, et al. Probiotic strain Bacillus subtilis CU1 stimulates immune system of elderly during common infectious disease period: a randomized, double-blind placebo-controlled study. *Immun Ageing*. 2015;12:24.
631. Mane J, Pedrosa E, Loren V, Gassull MA, Espadaler J, Cune J, et al. A mixture of Lactobacillus plantarum CECT 7315 and CECT 7316 enhances systemic immunity in elderly subjects. A dose-response, double-blind, placebo-controlled, randomized pilot trial. *Nutr Hosp*. 2011;26(1):228-35.
632. Finamore A, Roselli M, Donini L, Brasili DE, Rami R, Carnevali P, et al. Supplementation with Bifidobacterium longum Bar33 and Lactobacillus helveticus Bar13 mixture improves immunity in elderly humans (over 75 years) and aged mice. *Nutrition*. 2019;63-64:184-92.
633. Nagpal R, Wang S, Ahmadi S, Hayes J, Gagliano J, Subashchandrabose S, et al. Human-origin probiotic cocktail increases short-chain fatty acid production via modulation of mice and human gut microbiome. *Sci Rep*. 2018;8(1):12649.
634. Eguchi K, Fujitani N, Nakagawa H, Miyazaki T. Prevention of respiratory syncytial virus infection with probiotic lactic acid bacterium Lactobacillus gasseri SBT2055. *Sci Rep*. 2019;9(1):4812.
635. Boge T, Remigy M, Vaudaine S, Tanguy J, Bourdet-Sicard R, van der Werf S. A probiotic fermented dairy drink improves antibody response to influenza vaccination in the elderly in two randomised controlled trials. *Vaccine*. 2009;27(41):5677-84.
636. Mattison JA, Colman RJ, Beasley TM, Allison DB, Kemnitz JW, Roth GS, et al. Caloric restriction improves health and survival of rhesus monkeys. *Nat Commun*. 2017;8:14063.

637. Fabbiano S, Suarez-Zamorano N, Chevalier C, Lazarevic V, Kieser S, Rigo D, et al. Functional Gut Microbiota Remodeling Contributes to the Caloric Restriction-Induced Metabolic Improvements. *Cell Metab*. 2018;28(6):907-21 e7.
638. Tanca A, Abbondio M, Palomba A, Fraumene C, Marongiu F, Serra M, et al. Caloric restriction promotes functional changes involving short-chain fatty acid biosynthesis in the rat gut microbiota. *Sci Rep*. 2018;8(1):14778.
639. Ott B, Skurk T, Hastreiter L, Lagkouvardos I, Fischer S, Buttner J, et al. Effect of caloric restriction on gut permeability, inflammation markers, and fecal microbiota in obese women. *Sci Rep*. 2017;7(1):11955.
640. Messaoudi I, Warner J, Fischer M, Park B, Hill B, Mattison J, et al. Delay of T cell senescence by caloric restriction in aged long-lived nonhuman primates. *Proc Natl Acad Sci U S A*. 2006;103(51):19448-53.
641. Chudasama YV, Khunti KK, Zaccardi F, Rowlands AV, Yates T, Gillies CL, et al. Physical activity, multimorbidity, and life expectancy: a UK Biobank longitudinal study. *BMC Med*. 2019;17(1):108.
642. Cabanas-Sanchez V, Guallar-Castillon P, Higueras-Fresnillo S, Garcia-Esquinas E, Rodriguez-Artalejo F, Martinez-Gomez D. Physical Activity, Sitting Time, and Mortality From Inflammatory Diseases in Older Adults. *Front Physiol*. 2018;9:898.
643. Matsumoto M, Inoue R, Tsukahara T, Ushida K, Chiji H, Matsubara N, et al. Voluntary running exercise alters microbiota composition and increases n-butyrate concentration in the rat cecum. *Biosci Biotechnol Biochem*. 2008;72(2):572-6.
644. Campbell SC, Wisniewski PJ, Noji M, McGuinness LR, Haggblom MM, Lightfoot SA, et al. The Effect of Diet and Exercise on Intestinal Integrity and Microbial Diversity in Mice. *PLoS One*. 2016;11(3):e0150502.
645. Castro-Mejia JL, Khakimov B, Krych L, Bulow J, Bechshoft RL, Hojfeldt G, et al. Physical fitness in community-dwelling older adults is linked to dietary intake, gut microbiota, and metabolomic signatures. *Aging Cell*. 2020;19(3):e13105.
646. Duggal NA, Pollock RD, Lazarus NR, Harridge S, Lord JM. Major features of immunesenescence, including reduced thymic output, are ameliorated by high levels of physical activity in adulthood. *Aging Cell*. 2018;17(2).
647. Sokol H, Landman C, Seksik P, Berard L, Montil M, Nion-Larmurier I, et al. Fecal microbiota transplantation to maintain remission in Crohn's disease: a pilot randomized controlled study. *Microbiome*. 2020;8(1):12.
648. van Nood E, Vrieze A, Nieuwdorp M, Fuentes S, Zoetendal EG, de Vos WM, et al. Duodenal infusion of donor feces for recurrent Clostridium difficile. *N Engl J Med*. 2013;368(5):407-15.
649. Li M, Liang P, Li Z, Wang Y, Zhang G, Gao H, et al. Fecal microbiota transplantation and bacterial consortium transplantation have comparable effects on the re-establishment of mucosal barrier function in mice with intestinal dysbiosis. *Front Microbiol*. 2015;6:692.
650. Weingarden AR, Chen C, Bobr A, Yao D, Lu Y, Nelson VM, et al. Microbiota transplantation restores normal fecal bile acid composition in recurrent Clostridium difficile infection. *Am J Physiol Gastrointest Liver Physiol*. 2014;306(4):G310-9.

651. Burrello C, Garavaglia F, Cribiu FM, Ercoli G, Lopez G, Troisi J, et al. Therapeutic faecal microbiota transplantation controls intestinal inflammation through IL10 secretion by immune cells. *Nat Commun*. 2018;9(1):5184.
652. Wilson BC, Vatanen T, Cutfield WS, O'Sullivan JM. The Super-Donor Phenomenon in Fecal Microbiota Transplantation. *Front Cell Infect Microbiol*. 2019;9:2.
653. Cantorna MT, Lin YD, Arora J, Bora S, Tian Y, Nichols RG, et al. Vitamin D Regulates the Microbiota to Control the Numbers of RORgammat/FoxP3+ Regulatory T Cells in the Colon. *Front Immunol*. 2019;10:1772.
654. Pryor R, Norvaisas P, Marinos G, Best L, Thingholm LB, Quintaneiro LM, et al. Host-Microbe-Drug-Nutrient Screen Identifies Bacterial Effectors of Metformin Therapy. *Cell*. 2019;178(6):1299-312 e29.

Appendix 1: Questionnaires

1) General health questionnaire pack

The University of Birmingham

UNIVERSITY OF BIRMINGHAM

Gut microbiome dysbiosis and Immune ageing

Questionnaire Pack

Participant NAME _____

Participant NUMBER _____

Date ……..

General Information

Date of Birth ..... Height ..... Weight .....

Sex: Male Female

Age .....

Ethnicity: Asian Black White Other
If other, please state .....

Biological Impedance analysis

Total body fat (%) …….Total body fat (kg)……..

Total body lean mass (%)…….Total body lean (kg)……..

Health Behaviour

Please circle the appropriate answer

Over the last year, how many cigarettes, on average, did you smoke per day?	None	1-5	6-10	11-20	21+	40+
Over the last year, on average, how often have you taken an alcoholic drink?	Never	Special Occasions only	1-2 per month	1-2 per week	Almost daily	2 per day or more

For the following question, please base your answers on the following:
1 unit = ½ pint of beer, 1 small glass of wine, 1 measure of spirit
Remember that home poured measures are likely to be larger
1 bottle of wine = 6 glasses, 1 average bottle of spirits = 27 measures

Over the last year, on average, how many units did you drink per week?	None	1-5	6-10	11-20	20-40	41+

Over the last year, how many hours per week on average, have you spent participating in activities which are:

Mildly energetic e.g. walking?	0	1-2	3-5	6-8	9-10	11+
Moderately energetic e.g. leisurely swimming, golf	0	1-2	3-5	6-8	9-10	11+
Vigorously energetic e.g. running, squash	0	1-2	3-5	6-8	9-10	11+

Over the last year, how many hours per week on average, have you spent participating in activities which are:

Hours of TV or video watched per day	None	<1 hr /day	1-2 hr /day	2-3 hr/day	3-4 hr/day	>4hr/ day
On a weekday before 6 pm						
On a weekday after 6 pm						
On a weekend before 6 pm						
On a weekdend after 6 pm						

Stairs climbing at home

Number of times you climbed up a flight of stairs (approx. 10 steps) each day at home	None	1-5 times	6 -10 times	11-15 times	16-20 times	>20 times
On a weekday						
On a weekend						

This survey asks for your views about your health. This information will help keep track of how you feel and how well you are able to do your usual activities. ***Thank you for completing this survey!***

For each of the following questions, please mark an ☒ in the one box that best describes your answer.

1. In general, would you say your health is:

Excellent	Very good	Good	Fair	Poor
☐1	☐2	☐3	☐4	☐5

2. The following questions are about activities you might do during a typical day. Does <u>your health now limit you</u> in these activities? If so, how much?

	Yes, limited a lot	Yes, limited a little	No, not limited at all
a. <u>Moderate activities</u>, such as moving a table, pushing a vacuum cleaner, bowling, or playing golf	☐1	☐2	☐3
b. Climbing <u>several</u> flights of stairs	☐1	☐2	☐3

3. **During the past 4 weeks, how much of the time have you had any of the following problems with your work or other regular daily activities as a result of your physical health?**

	All of the time	Most of the time	Some of the time	A little of the time	None of the time
a. Accomplished less than you would like	☐1	☐2	☐3	☐4	☐5
b. Were limited in the kind of work or other activities	☐1	☐2	☐3	☐4	☐5

4. **During the past 4 weeks, how much of the time have you had any of the following problems with your work or other regular daily activities as a result of any emotional problems (such as feeling depressed or anxious)?**

	All of the time	Most of the time	Some of the time	A little of the time	None of the time
a. Accomplished less than you would like	☐1	☐2	☐3	☐4	☐5
b. Did work or other activities less carefully than usual	☐1	☐2	☐3	☐4	☐5

5. **During the past 4 weeks, how much did pain interfere with your normal work (including both work outside the home and housework)?**

Not at all	A little bit	Moderately	Quite a bit	Extremely
☐1	☐2	☐3	☐4	☐5

6. **These questions are about how you feel and how things have been with you during the past 4 weeks. For each question, please give the one answer that comes closest to the way you have been feeling. How much of the time during the past 4 weeks...**

	All of the time	Most of the time	Some of the time	A little of the time	None of the time
a. Have you felt calm and peaceful?	☐1	☐2	☐3	☐4	☐5
b. Did you have a lot of energy?	☐1	☐2	☐3	☐4	☐5
c. Have you felt downhearted and depressed?	☐1	☐2	☐3	☐4	☐5

7. **During the past 4 weeks, how much of the time has your physical health or emotional problems interfered with your social activities (like visiting friends, relatives, etc.)?**

All of the time	Most of the time	Some of the time	A little of the time	None of the time
☐1	☐2	☐3	☐4	☐5

PITTSBURGH SLEEP QUALITY INDEX

INSTRUCTIONS:
The following questions relate to your usual sleep habits during the past month only. Your answers should indicate the most accurate reply for the majority of days and nights in the past month. Please answer all questions.

1. During the past month, what time have you usually gone to bed at night?

   BED TIME _____

2. During the past month, how long (in minutes) has it usually taken you to fall asleep each night?

   NUMBER OF MINUTES _____

3. During the past month, what time have you usually gotten up in the morning?

   GETTING UP TIME _____

4. During the past month, how many hours of actual sleep did you get at night? (This may be different than the number of hours you spent in bed.)

   HOURS OF SLEEP PER NIGHT _____

For each of the remaining questions, check the one best response. Please answer all questions.

5. During the past month, how often have you had trouble sleeping because you . . .

a) Cannot get to sleep within 30 minutes

Not during the past month_____	Less than once a week_____	Once or twice a week_____	Three or more times a week_____

b) Wake up in the middle of the night or early morning

Not during the past month_____	Less than once a week_____	Once or twice a week_____	Three or more times a week_____

c) Have to get up to use the bathroom

Not during the past month_____	Less than once a week_____	Once or twice a week_____	Three or more times a week_____

d) Cannot breathe comfortably

Not during the past month_____ Less than once a week_____ Once or twice a week_____ Three or more times a week_____

e) Cough or snore loudly

Not during the past month_____ Less than once a week_____ Once or twice a week_____ Three or more times a week_____

f) Feel too cold

Not during the past month_____ Less than once a week_____ Once or twice a week_____ Three or more times a week_____

g) Feel too hot

Not during the past month_____ Less than once a week_____ Once or twice a week_____ Three or more times a week_____

h) Had bad dreams

Not during the past month_____ Less than once a week_____ Once or twice a week_____ Three or more times a week_____

i) Have pain

Not during the past month_____ Less than once a week_____ Once or twice a week_____ Three or more times a week_____

j) Other reason(s), please describe_____

_____

How often during the past month have you had trouble sleeping because of this?

Not during the past month_____ Less than once a week_____ Once or twice a week_____ Three or more times a week_____

6. During the past month, how would you rate your sleep quality overall?

Very good _____

Fairly good _____

Fairly bad _____

Very bad _____

7. During the past month, how often have you taken medicine to help you sleep (prescribed or "over the counter")?

Not during the past month_____ Less than once a week_____ Once or twice a week_____ Three or more times a week_____

8. During the past month, how often have you had trouble staying awake while driving, eating meals, or engaging in social activity?

Not during the past month_____ Less than once a week_____ Once or twice a week_____ Three or more times a week_____

9. During the past month, how much of a problem has it been for you to keep up enough enthusiasm to get things done?

No problem at all _____

Only a very slight problem _____

Somewhat of a problem _____

A very big problem _____

10. Do you have a bed partner or room mate?

No bed partner or room mate _____

Partner/room mate in other room _____

Partner in same room, but not same bed _____

Partner in same bed _____

If you have a room mate or bed partner, ask him/her how often in the past month you have had . . .

a) Loud snoring

Not during the past month_____ Less than once a week_____ Once or twice a week_____ Three or more times a week_____

b) Long pauses between breaths while asleep

Not during the past month_____ Less than once a week_____ Once or twice a week_____ Three or more times a week_____

c) Legs twitching or jerking while you sleep

Not during the past month_____ Less than once a week_____ Once or twice a week_____ Three or more times a week_____

Hospital Anxiety and Depression Scale (HADS)

Choose one response for each of the questions below.

A.	I feel tense or "wound up"…..		
	Most of the time	☐	3
	A lot of the time	☐	2
	From time to time, occasionally	☐	1
	Not at all	☐	0
D	I still enjoy the things I used to enjoy…..		
	Definitely as much	☐	0
	Not quite so much	☐	1
	Only a little	☐	2
	Hardly at all	☐	3
A	I get frightened feeling as if something awful is about to happen…..		
	Very definitely and quite badly	☐	3
	Yes, but not too badly	☐	2
	A little, but it doesn't worry me	☐	1
	Not at all	☐	0
D	I can laugh and see the funny side of things…..		
	As much as I always could	☐	0
	Not quite so much now	☐	1
	Definitely not so much now	☐	2
	Not at all	☐	3
A	Worrying thoughts go through my mind….		
	A great deal of the time	☐	3
	A lot of the time	☐	2
	From time to time but not too often	☐	1
	Only occasionally	☐	0
D	I feel cheerful….		
	Not at all	☐	3
	Not often	☐	2
	Sometimes	☐	1
	Most of the time	☐	0

A I can sit at ease and feel relaxed.....

Definitely		0
Usually		1
Not often		2
Not at all		3

D I feel as if I am slowed down....

Nearly all the time		3
Very often		2
Sometimes		1
Not at all		0

A I get a sort of frightened feeling like "butterflies" in The stomach...

Not at all		0
Occasionally		1
Quite often		2
Very often		3

D I have lost interest in my appearance...

Definitely		3
I don't take as much care as I should		2
I may not take quite as much care		1
I take just as much care as ever		0

A I feel restless as I have to be on the move.....

Very much indeed		3
Quite a lot		2
Not very much		1
Not at all		0

D I look forward with enjoyment to things.....

As much as I ever did		0
Rather less than I used to		1
Definitely less than I used to		2
Hardly at all		3

A I get sudden feelings of panic.....

Very often indeed		3
Quite often		2
Not very often		1
Not at all		0

D I can enjoy a good book or radio or TV program.....

Often		0
Sometimes		1
Not often		2
Very seldom		3

2) Food Frequency Questionnaire (FFQ)

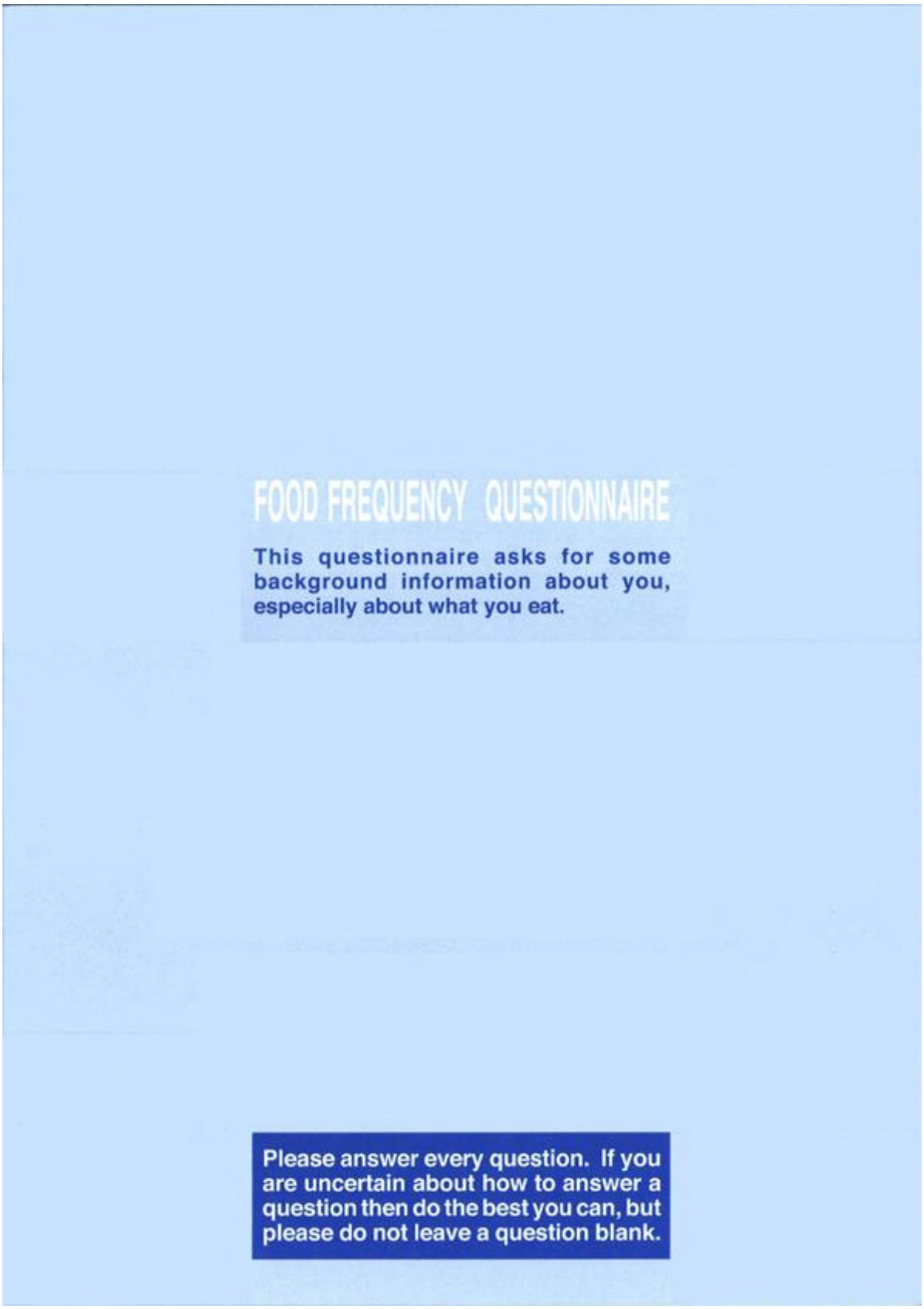

1. **YOUR DIET LAST YEAR**

For each food there is an amount shown, either a "medium serving" or a common household unit such as a slice or teaspoon. Please put a tick (✓) in the box to indicate how often, **on average**, you have eaten the specified amount of each food **during the past year**.

EXAMPLES:

For white bread the amount is one slice, so if you ate 4 or 5 slices a day, you should put a tick in the column headed "4-5 per day".

FOODS AND AMOUNTS	AVERAGE USE LAST YEAR								
BREAD AND SAVOURY BISCUITS (one slice or biscuit)	Never or less than once/month	1-3 per month	Once a week	2-4 per week	5-6 per week	Once a day	2-3 per day	4-5 per day	6+ per day
White bread and rolls								✓	

For chips, the amount is a "medium serving", so if you had a helping of chips twice a week you should put a tick in the column headed "2-4 per week".

FOODS AND AMOUNTS	AVERAGE USE LAST YEAR								
POTATOES, RICE AND PASTA (medium serving)	Never or less than once/month	1-3 per month	Once a week	2-4 per week	5-6 per week	Once a day	2-3 per day	4-5 per day	6+ per day
Chips				✓					

For very seasonal fruits such as strawberries and raspberries you should estimate your average use when the fruits are in season, so if you ate strawberries or raspberries about once a week when they were in season you should put a tick in the column headed "once a week"

FOODS AND AMOUNTS	AVERAGE USE LAST YEAR								
FRUIT (1 fruit or medium serving)	Never or less than once/month	1-3 per month	Once a week	2-4 per week	5-6 per week	Once a day	2-3 per day	4-5 per day	6+ per day
Strawberries, raspberries, kiwi fruit			✓						

Please estimate your average food use as best you can, and please answer every question - do not leave ANY lines blank. PLEASE PUT A TICK (✓) ON EVERY LINE

FOODS AND AMOUNTS	AVERAGE USE LAST YEAR								
MEAT AND FISH (medium serving)	Never or less than once/month	1-3 per month	Once a week	2-4 per week	5-6 per week	Once a day	2-3 per day	4-5 per day	6+ per day
Beef: roast, steak, mince, stew or casserole									
Beefburgers									
Pork: roast, chops, stew or slices									
Lamb: roast, chops or stew									
Chicken or other poultry eg. turkey									
Bacon									
Ham									
Corned beef, Spam, luncheon meats									
Sausages									
Savoury pies, eg. meat pie, pork pie, pasties, steak & kidney pie, sausage rolls									
Liver, liver paté, liver sausage									
Fried fish in batter, as in fish and chips									
Fish fingers, fish cakes									
Other white fish, fresh or frozen, eg. cod, haddock, plaice, sole, halibut									
Oily fish, fresh or canned, eg. mackerel, kippers, tuna, salmon, sardines, herring									
Shellfish, eg. crab, prawns, mussels									
Fish roe, taramasalata									
	Never or less than once/month	1-3 per month	Once a week	2-4 per week	5-6 per week	Once a day	2-3 per day	4-5 per day	6+ per day

Please check that you have a tick (✓) on EVERY line

PLEASE PUT A TICK (✓) ON EVERY LINE

FOODS AND AMOUNTS	AVERAGE USE LAST YEAR								
BREAD AND SAVOURY BISCUITS (one slice or biscuit)	Never or less than once/month	1-3 per month	Once a week	2-4 per week	5-6 per week	Once a day	2-3 per day	4-5 per day	6+ per day
White bread and rolls									
Brown bread and rolls									
Wholemeal bread and rolls									
Cream crackers, cheese biscuits									
Crispbread, eg. Ryvita									
CEREALS (one bowl)									
Porridge, Readybrek									
Breakfast cereal such as cornflakes, muesli etc.									
POTATOES, RICE AND PASTA (medium serving)									
Boiled, mashed, instant or jacket potatoes									
Chips									
Roast potatoes									
Potato salad									
White rice									
Brown rice									
White or green pasta, eg. spaghetti, macaroni, noodles									
Wholemeal pasta									
Lasagne, moussaka									
Pizza									
	Never or less than once/month	1-3 per month	Once a week	2-4 per week	5-6 per week	Once a day	2-3 per day	4-5 per day	6+ per day

Please check that you have a tick (✓) on EVERY line

PLEASE PUT A TICK (✓) ON EVERY LINE

FOODS AND AMOUNTS	AVERAGE USE LAST YEAR								
DAIRY PRODUCTS AND FATS	Never or less than once/month	1-3 per month	Once a week	2-4 per week	5-6 per week	Once a day	2-3 per day	4-5 per day	6+ per day
Single or sour cream (tablespoon)									
Double or clotted cream (tablespoon)									
Low fat yogurt, fromage frais (125g carton)									
Full fat or Greek yogurt (125g carton)									
Dairy desserts (125g carton)									
Cheese, eg. Cheddar, Brie, Edam (medium serving)									
Cottage cheese, low fat soft cheese (medium serving)									
Eggs as boiled, fried, scrambled, etc. (one)									
Quiche (medium serving)									
Low calorie, low fat salad cream(tablespoon)									
Salad cream, mayonnaise (tablespoon)									
French dressing (tablespoon)									
Other salad dressing (tablespoon)									
The following on bread or vegetables									
Butter (teaspoon)									
Block margarine, eg. Stork, Krona (teaspoon)									
Polyunsaturated margarine (tub), eg. Flora, sunflower (teaspoon)									
Other soft margarine,dairy spreads (tub), eg. Blue Band, Clover (teaspoon)									
Low fat spread (tub), eg. Outline, Gold (teaspoon)									
Very low fat spread (tub) (teaspoon)									
	Never or less than once/month	1-3 per month	Once a week	2-4 per week	5-6 per week	Once a day	2-3 per day	4-5 per day	6+ per day

Please check that you have a tick (✓) on EVERY line

PLEASE PUT A TICK (✓) ON EVERY LINE

FOODS AND AMOUNTS	AVERAGE USE LAST YEAR								
SWEETS AND SNACKS (medium serving)	Never or less than once/month	1-3 per month	Once a week	2-4 per week	5-6 per week	Once a day	2-3 per day	4-5 per day	6+ per day
Sweet biscuits, chocolate , eg. digestive (one)									
Sweet biscuits, plain, eg. Nice, ginger (one)									
Cakes eg. fruit, sponge, home baked									
Cakes eg. fruit, sponge, ready made									
Buns, pastries eg. scones, flapjacks, home baked									
Buns, pastries eg. croissants, doughnuts, ready made									
Fruit pies, tarts, crumbles, home baked									
Fruit pies, tarts, crumbles, ready made									
Sponge puddings, home baked									
Sponge puddings, ready made									
Milk puddings, eg. rice, custard, trifle									
Ice cream, choc ices									
Chocolates, single or squares									
Chocolate snack bars eg. Mars, Crunchie									
Sweets, toffees, mints									
Sugar added to tea, coffee, cereal (teaspoon)									
Crisps or other packet snacks, eg. Wotsits									
Peanuts or other nuts									
SOUPS, SAUCES, AND SPREADS									
Vegetable soups (bowl)									
Meat soups (bowl)									
Sauces, eg. white sauce, cheese sauce, gravy (tablespoon)									
Tomato ketchup (tablespoon)									
Pickles, chutney (tablespoon)									
Marmite, Bovril (teaspoon)									
Jam, marmalade, honey (teaspoon)									
Peanut butter (teaspoon)									
	Never or less than once/month	1-3 per month	Once a week	2-4 per week	5-6 per week	Once a day	2-3 per day	4-5 per day	6+ per day

Please check that you have a tick (✓) on EVERY line

PLEASE PUT A TICK (✓) ON EVERY LINE

FOODS AND AMOUNTS	AVERAGE USE LAST YEAR								
DRINKS	Never or less than once/month	1-3 per month	Once a week	2-4 per week	5-6 per week	Once a day	2-3 per day	4-5 per day	6+ per day
Tea (cup)									
Coffee, instant or ground (cup)									
Coffee, decaffeinated (cup)									
Coffee whitener, eg. Coffee-mate (teaspoon)									
Cocoa, hot chocolate (cup)									
Horlicks, Ovaltine (cup)									
Wine (glass)									
Beer, lager or cider (half pint)									
Port, sherry, vermouth, liqueurs (glass)									
Spirits, eg. gin, brandy, whisky, vodka (single)									
Low calorie or diet fizzy soft drinks (glass)									
Fizzy soft drinks, eg. Coca cola, lemonade (glass)									
Pure fruit juice (100%) eg. orange, apple juice (glass)									
Fruit squash or cordial (glass)									
FRUIT **For seasonal fruits marked *, please estimate your average use when the fruit is in season**									
Apples (1 fruit)									
Pears (1 fruit)									
Oranges, satsumas, mandarins (1 fruit)									
Grapefruit (half)									
Bananas (1 fruit)									
Grapes (medium serving)									
Melon (1 slice)									
* Peaches, plums, apricots (1 fruit)									
* Strawberries, raspberries, kiwi fruit (medium serving)									
Tinned fruit (medium serving)									
Dried fruit, eg. raisins, prunes (medium serving)									
	Never or less than once/month	1-3 per month	Once a week	2-4 per week	5-6 per week	Once a day	2-3 per day	4-5 per day	6+ per day

Please check that you have a tick (✓) on EVERY line

PLEASE PUT A TICK (✓) ON EVERY LINE

FOODS AND AMOUNTS	AVERAGE USE LAST YEAR								
VEGETABLES Fresh, frozen or tinned (medium serving)	Never or less than once/month	1-3 per month	Once a week	2-4 per week	5-6 per week	Once a day	2-3 per day	4-5 per day	6+ per day
Carrots									
Spinach									
Broccoli, spring greens, kale									
Brussels sprouts									
Cabbage									
Peas									
Green beans, broad beans, runner beans									
Marrow, courgettes									
Cauliflower									
Parsnips, turnips, swedes									
Leeks									
Onions									
Garlic									
Mushrooms									
Sweet peppers									
Beansprouts									
Green salad, lettuce, cucumber, celery									
Watercress									
Tomatoes									
Sweetcorn									
Beetroot									
Coleslaw									
Avocado									
Baked beans									
Dried lentils, beans, peas									
Tofu , soya meat, TVP, Vegeburger									
	Never or less than once/month	1-3 per month	Once a week	2-4 per week	5-6 per week	Once a day	2-3 per day	4-5 per day	6+ per day

Please check that you have a tick (✓) on EVERY line

YOUR DIET LAST YEAR, continued

2. Are there any **OTHER** foods which you ate more than once a week? Yes ☐ No ☐

If yes, please list below

Food	Usual serving size	Number of times eaten each week

3. What type of milk did you most often use?

Select one only

Full cream, silver ☐
Skimmed/blue ☐
Dried milk ☐
Other, *specify* ☐
Semi-skimmed, red/white ☐
Channel Islands, gold ☐
Soya ☐
None ☐

4. How much milk did you drink each day, including milk with tea, coffee, cereals etc?

None ☐
Quarter of a pint ☐
Half a pint ☐
Three quarters of a pint ☐
One pint ☐
More than one pint ☐

5. Did you usually eat breakfast cereal (excluding porridge and Ready Brek mentioned earlier)? Yes ☐ No ☐

If yes, which brand and type of breakfast cereal, including muesli, did you usually eat?

List the one or two types most often used

Brand *e.g. Kellogg's*	Type *e.g. cornflakes*

6. What kind of fat did you most often use for frying, roasting, grilling etc?

Select one only

Butter ☐
Lard/dripping ☐
Vegetable oil ☐
Solid vegetable fat ☐
Margarine ☐
None ☐

If you used vegetable oil, please give type eg. corn, sunflower ☐

7. What kind of fat did you most often use for baking cakes etc?

Select one only

Butter ☐
Lard/dripping ☐
Vegetable oil ☐
Solid vegetable fat ☐
Margarine ☐
None ☐

If you used margarine, please give name or type eg. Flora, Stork ☐

8. How often did you eat food that was fried at home?

Daily ☐ 1-3 times a week ☐ 4-6 times a week ☐
Less than once a week ☐ Never ☐

9. How often did you eat fried food away from home?

Daily ☐ 1-3 times a week ☐ 4-6 times a week ☐
Less than once a week ☐ Never ☐

10. What did you do with the visible fat on your meat?

Ate most of the fat ☐ Ate as little as possible ☐
Ate some of the fat ☐ Did not eat meat ☐

11. How often did you eat grilled or roast meat? ☐☐ times a week

12. How well cooked did you usually have grilled or roast meat?

Well done /dark brown ☐ Lightly cooked/rare ☐
Medium ☐ Did not eat meat ☐

13. How often did you add salt to food while cooking?

Always ☐ Rarely ☐
Usually ☐ Never ☐
Sometimes ☐

14. How often did you add salt to any food at the table?

Always ☐ Rarely ☐
Usually ☐ Never ☐
Sometimes ☐

15. Did you regularly use a salt substitute (eg LoSalt)? Yes ☐ No ☐

If yes, which brand? ☐

16. During the course of last year, on average, how many times a week did you eat the following foods?

Food type	**Times/week**	**Portion size**
Vegetables (not including potatoes)	☐☐	medium serving
Salads	☐☐	medium serving
Fruit and fruit products (not including fruit juice)	☐☐	medium serving or 1 fruit
Fish and fish products	☐☐	medium serving
Meat, meat products and meat dishes (including bacon, ham and chicken)	☐☐	medium serving

17. Have you taken any vitamins, minerals, fish oils, fibre or other food supplements during the past year? Yes ☐ No ☐ Don't know ☐

If yes, please complete the table below. If you have taken more than 5 types of supplement please put the most frequently consumed brands first.

Vitamin supplements	**Average frequency** Tick **one** box per line to show how often on average you consumed supplements									
Name and brand Please list full name, **brand** and strength	**Dose** Please state number of pills, capsules or teaspoons consumed	Never or less than once a month	1-3 per month	Once a week	2-4 per week	5-6 per week	Once a day	2-3 per day	4-5 per day	6+ per day

Thank you for your help

Appendix 2: 16S rRNA primer sequences

Primer name	Primer sequence (5'-3')	Length
515rcbc0	AATGATACGGCGACCACCGAGATCTACACGCTAGCCTTC GTCGCTATGGTAATTGTGTGYCAGCMGCCGCGGTAA	75
515rcbc1	AATGATACGGCGACCACCGAGATCTACACGCTTCCATAC CGGAATATGGTAATTGTGTGYCAGCMGCCGCGGTAA	75
515rcbc2	AATGATACGGCGACCACCGAGATCTACACGCTAGCCCT GCTACATATGGTAATTGTGTGYCAGCMGCCGCGGTAA	75
515rcbc3	AATGATACGGCGACCACCGAGATCTACACGCTCCTAAC GGTCCATATGGTAATTGTGTGYCAGCMGCCGCGGTAA	75
515rcbc4	AATGATACGGCGACCACCGAGATCTACACGCTCGCGCC TTAAACTATGGTAATTGTGTGYCAGCMGCCGCGGTAA	75
515rcbc5	AATGATACGGCGACCACCGAGATCTACACGCTTATGGTA CCCAGTATGGTAATTGTGTGYCAGCMGCCGCGGTAA	75
515rcbc6	AATGATACGGCGACCACCGAGATCTACACGCTTACAATA TCTGTTATGGTAATTGTGTGYCAGCMGCCGCGGTAA	75
515rcbc7	AATGATACGGCGACCACCGAGATCTACACGCTAATTTAG GTAGGTATGGTAATTGTGTGYCAGCMGCCGCGGTAA	75
515rcbc8	AATGATACGGCGACCACCGAGATCTACACGCTGACTCAA CCAGTTATGGTAATTGTGTGYCAGCMGCCGCGGTAA	75
515rcbc9	AATGATACGGCGACCACCGAGATCTACACGCTGCCTCTA CGTCGTATGGTAATTGTGTGYCAGCMGCCGCGGTAA	75
515rcbc10	AATGATACGGCGACCACCGAGATCTACACGCTACTACTG AGGATTATGGTAATTGTGTGYCAGCMGCCGCGGTAA	75
515rcbc11	AATGATACGGCGACCACCGAGATCTACACGCTAATTCAC CTCCTTATGGTAATTGTGTGYCAGCMGCCGCGGTAA	75
515rcbc12	AATGATACGGCGACCACCGAGATCTACACGCTCGTATAA ATGCGTATGGTAATTGTGTGYCAGCMGCCGCGGTAA	75
515rcbc13	AATGATACGGCGACCACCGAGATCTACACGCTATGCTG CAACACTATGGTAATTGTGTGYCAGCMGCCGCGGTAA	75
515rcbc14	AATGATACGGCGACCACCGAGATCTACACGCTACTCGCT CGCTGTATGGTAATTGTGTGYCAGCMGCCGCGGTAA	75
515rcbc15	AATGATACGGCGACCACCGAGATCTACACGCTTTCCTTA GTAGTTATGGTAATTGTGTGYCAGCMGCCGCGGTAA	75
515rcbc16	AATGATACGGCGACCACCGAGATCTACACGCTCGTCCG TATGAATATGGTAATTGTGTGYCAGCMGCCGCGGTAA	75
515rcbc17	AATGATACGGCGACCACCGAGATCTACACGCTACGTGA GGAACGTATGGTAATTGTGTGYCAGCMGCCGCGGTAA	75
515rcbc18	AATGATACGGCGACCACCGAGATCTACACGCTGGTTGC CCTGTATATGGTAATTGTGTGYCAGCMGCCGCGGTAA	75

515rcbc19	AATGATACGGCGACCACCGAGATCTACACGCTCATATAG CCCGATATGGTAATTGTGTGYCAGCMGCCGCGGTAA	75
515rcbc20	AATGATACGGCGACCACCGAGATCTACACGCTGCCTAT GAGATCTATGGTAATTGTGTGYCAGCMGCCGCGGTAA	75
515rcbc21	AATGATACGGCGACCACCGAGATCTACACGCTCAAGTG AAGGGATATGGTAATTGTGTGYCAGCMGCCGCGGTAA	75
515rcbc22	AATGATACGGCGACCACCGAGATCTACACGCTCACGTTT ATTCCTATGGTAATTGTGTGYCAGCMGCCGCGGTAA	75
515rcbc23	AATGATACGGCGACCACCGAGATCTACACGCTTAATCGG TGCCATATGGTAATTGTGTGYCAGCMGCCGCGGTAA	75
515rcbc24	AATGATACGGCGACCACCGAGATCTACACGCTTGACTAA TGGCCTATGGTAATTGTGTGYCAGCMGCCGCGGTAA	75
515rcbc25	AATGATACGGCGACCACCGAGATCTACACGCTCGGGAC ACCCGATATGGTAATTGTGTGYCAGCMGCCGCGGTAA	75
515rcbc26	AATGATACGGCGACCACCGAGATCTACACGCTCTGTCTA TACTATATGGTAATTGTGTGYCAGCMGCCGCGGTAA	75
515rcbc27	AATGATACGGCGACCACCGAGATCTACACGCTTATGCCA GAGATTATGGTAATTGTGTGYCAGCMGCCGCGGTAA	75
515rcbc28	AATGATACGGCGACCACCGAGATCTACACGCTCGTTTG GAATGATATGGTAATTGTGTGYCAGCMGCCGCGGTAA	75
515rcbc29	AATGATACGGCGACCACCGAGATCTACACGCTAAGAACT CATGATATGGTAATTGTGTGYCAGCMGCCGCGGTAA	75
515rcbc30	AATGATACGGCGACCACCGAGATCTACACGCTTGATATC GTCTTTATGGTAATTGTGTGYCAGCMGCCGCGGTAA	75
515rcbc31	AATGATACGGCGACCACCGAGATCTACACGCTCGGTGA CCTACTTATGGTAATTGTGTGYCAGCMGCCGCGGTAA	75
515rcbc32	AATGATACGGCGACCACCGAGATCTACACGCTAATGCG CGTATATATGGTAATTGTGTGYCAGCMGCCGCGGTAA	75
515rcbc33	AATGATACGGCGACCACCGAGATCTACACGCTCTTGATT CTTGATATGGTAATTGTGTGYCAGCMGCCGCGGTAA	75
515rcbc34	AATGATACGGCGACCACCGAGATCTACACGCTGAAATCT TGAAGTATGGTAATTGTGTGYCAGCMGCCGCGGTAA	75
515rcbc35	AATGATACGGCGACCACCGAGATCTACACGCTGAGATA CAGTTCTATGGTAATTGTGTGYCAGCMGCCGCGGTAA	75
515rcbc36	AATGATACGGCGACCACCGAGATCTACACGCTGTGGAG TCTCATTATGGTAATTGTGTGYCAGCMGCCGCGGTAA	75
515rcbc37	AATGATACGGCGACCACCGAGATCTACACGCTACCTTAC ACCTTTATGGTAATTGTGTGYCAGCMGCCGCGGTAA	75
515rcbc38	AATGATACGGCGACCACCGAGATCTACACGCTTAATCTC GCCGGTATGGTAATTGTGTGYCAGCMGCCGCGGTAA	75
515rcbc39	AATGATACGGCGACCACCGAGATCTACACGCTATCTAGT GGCAATATGGTAATTGTGTGYCAGCMGCCGCGGTAA	75

515rcbc40	AATGATACGGCGACCACCGAGATCTACACGCTACGCTTA ACGACTATGGTAATTGTGTGYCAGCMGCCGCGGTAA	75
515rcbc41	AATGATACGGCGACCACCGAGATCTACACGCTTACGGAT TATGGTATGGTAATTGTGTGYCAGCMGCCGCGGTAA	75
515rcbc42	AATGATACGGCGACCACCGAGATCTACACGCTATACATG CAAGATATGGTAATTGTGTGYCAGCMGCCGCGGTAA	75
515rcbc43	AATGATACGGCGACCACCGAGATCTACACGCTCTTAGTG CAGAATATGGTAATTGTGTGYCAGCMGCCGCGGTAA	75
515rcbc44	AATGATACGGCGACCACCGAGATCTACACGCTAATCTTG CGCCGTATGGTAATTGTGTGYCAGCMGCCGCGGTAA	75
515rcbc45	AATGATACGGCGACCACCGAGATCTACACGCTAGGATC AGGGAATATGGTAATTGTGTGYCAGCMGCCGCGGTAA	75
515rcbc46	AATGATACGGCGACCACCGAGATCTACACGCTAATAACT AGGGTTATGGTAATTGTGTGYCAGCMGCCGCGGTAA	75
515rcbc47	AATGATACGGCGACCACCGAGATCTACACGCTTATTGCA GCAGCTATGGTAATTGTGTGYCAGCMGCCGCGGTAA	75
515rcbc48	AATGATACGGCGACCACCGAGATCTACACGCTTGATGTG CTAAGTATGGTAATTGTGTGYCAGCMGCCGCGGTAA	75
515rcbc49	AATGATACGGCGACCACCGAGATCTACACGCTGTAGTA GACCATTATGGTAATTGTGTGYCAGCMGCCGCGGTAA	75
515rcbc50	AATGATACGGCGACCACCGAGATCTACACGCTAGTAAAG ATCGTTATGGTAATTGTGTGYCAGCMGCCGCGGTAA	75
515rcbc51	AATGATACGGCGACCACCGAGATCTACACGCTCTCGCC CTCGCCTATGGTAATTGTGTGYCAGCMGCCGCGGTAA	75
515rcbc52	AATGATACGGCGACCACCGAGATCTACACGCTTCTCTTT CGACATATGGTAATTGTGTGYCAGCMGCCGCGGTAA	75
515rcbc53	AATGATACGGCGACCACCGAGATCTACACGCTACATACT GAGCATATGGTAATTGTGTGYCAGCMGCCGCGGTAA	75
515rcbc54	AATGATACGGCGACCACCGAGATCTACACGCTGTTGATA CGATGTATGGTAATTGTGTGYCAGCMGCCGCGGTAA	75
515rcbc55	AATGATACGGCGACCACCGAGATCTACACGCTGTCAAC GCTGTCTATGGTAATTGTGTGYCAGCMGCCGCGGTAA	75
515rcbc56	AATGATACGGCGACCACCGAGATCTACACGCTTGAGAC CCTACATATGGTAATTGTGTGYCAGCMGCCGCGGTAA	75
515rcbc57	AATGATACGGCGACCACCGAGATCTACACGCTACTTGGT GTAAGTATGGTAATTGTGTGYCAGCMGCCGCGGTAA	75
515rcbc58	AATGATACGGCGACCACCGAGATCTACACGCTATTACGT ATCATTATGGTAATTGTGTGYCAGCMGCCGCGGTAA	75
515rcbc59	AATGATACGGCGACCACCGAGATCTACACGCTCACGCA GTCTACTATGGTAATTGTGTGYCAGCMGCCGCGGTAA	75
515rcbc60	AATGATACGGCGACCACCGAGATCTACACGCTTGTGCA CGCCATTATGGTAATTGTGTGYCAGCMGCCGCGGTAA	75

515rcbc61	AATGATACGGCGACCACCGAGATCTACACGCTCCGGAC AAGAAGTATGGTAATTGTGTGYCAGCMGCCGCGGTAA	75
515rcbc62	AATGATACGGCGACCACCGAGATCTACACGCTTTGCTG GACGCTTATGGTAATTGTGTGYCAGCMGCCGCGGTAA	75
515rcbc63	AATGATACGGCGACCACCGAGATCTACACGCTTACTAAC GCGGTTATGGTAATTGTGTGYCAGCMGCCGCGGTAA	75
515rcbc64	AATGATACGGCGACCACCGAGATCTACACGCTGCGATC ACACCTTATGGTAATTGTGTGYCAGCMGCCGCGGTAA	75
515rcbc65	AATGATACGGCGACCACCGAGATCTACACGCTCAAACG CACTAATATGGTAATTGTGTGYCAGCMGCCGCGGTAA	75
515rcbc66	AATGATACGGCGACCACCGAGATCTACACGCTGAAGAG GGTTGATATGGTAATTGTGTGYCAGCMGCCGCGGTAA	75
515rcbc67	AATGATACGGCGACCACCGAGATCTACACGCTTGAGTG GTCTGTTATGGTAATTGTGTGYCAGCMGCCGCGGTAA	75
515rcbc68	AATGATACGGCGACCACCGAGATCTACACGCTTTACACA AAGGCTATGGTAATTGTGTGYCAGCMGCCGCGGTAA	75
515rcbc69	AATGATACGGCGACCACCGAGATCTACACGCTACGACG CATTTGTATGGTAATTGTGTGYCAGCMGCCGCGGTAA	75
515rcbc70	AATGATACGGCGACCACCGAGATCTACACGCTTATCCAA GCGCATATGGTAATTGTGTGYCAGCMGCCGCGGTAA	75
515rcbc71	AATGATACGGCGACCACCGAGATCTACACGCTAGAGCC AAGAGCTATGGTAATTGTGTGYCAGCMGCCGCGGTAA	75
515rcbc72	AATGATACGGCGACCACCGAGATCTACACGCTGGTGAG CAAGCATATGGTAATTGTGTGYCAGCMGCCGCGGTAA	75
515rcbc73	AATGATACGGCGACCACCGAGATCTACACGCTTAAATAT ACCCTTATGGTAATTGTGTGYCAGCMGCCGCGGTAA	75
515rcbc74	AATGATACGGCGACCACCGAGATCTACACGCTTTGCGG ACCCTATATGGTAATTGTGTGYCAGCMGCCGCGGTAA	75
515rcbc75	AATGATACGGCGACCACCGAGATCTACACGCTGTCGTC CAAATGTATGGTAATTGTGTGYCAGCMGCCGCGGTAA	75
515rcbc76	AATGATACGGCGACCACCGAGATCTACACGCTTGCACA GTCGCTTATGGTAATTGTGTGYCAGCMGCCGCGGTAA	75
515rcbc77	AATGATACGGCGACCACCGAGATCTACACGCTTTACTGT GGCCGTATGGTAATTGTGTGYCAGCMGCCGCGGTAA	75
515rcbc78	AATGATACGGCGACCACCGAGATCTACACGCTGGTTCAT GAACATATGGTAATTGTGTGYCAGCMGCCGCGGTAA	75
515rcbc79	AATGATACGGCGACCACCGAGATCTACACGCTTAACAAT AATTCTATGGTAATTGTGTGYCAGCMGCCGCGGTAA	75
515rcbc80	AATGATACGGCGACCACCGAGATCTACACGCTCTTATTA AACGTTATGGTAATTGTGTGYCAGCMGCCGCGGTAA	75